Safety Formats for the Assessment of Concrete Bridges

with special focus on precast concrete

Dawid F. Wiśniewski

Doctoral Thesis

Department of Civil Engineering
School of Engineering - University of Minho
Guimarães, Portugal

March 2007

Acknowledgements

First of all, I would like to thank my supervisor, Prof. Paulo Cruz, for convincing me to make this thesis and for his help, interest and friendship during the period I have spent at the University of Minho. I would also like to thank my co-supervisor, Prof. Abel Henriques, for his involvement, encouragement and patience in explaining to me the intricacies of Structural Reliability. Without both of them this thesis would never has been possible.

Furthermore, I would like to express my gratitude to my second co-supervisor, Prof. Jan Biliszczuk. His lectures during my undergraduate study developed my special interests in bridges and were the beginning of my 'bridge adventure'.

I would like to take this opportunity to thank the following people who have shaped my interest and developed my understanding of various aspects of my academic route.

Prof. Jan Bien for being a mentor during all these years, for encouraging me to study abroad, for his attitude and many interesting discussions. His critical point of view has always been very creative.

Prof. Joan Ramon Casas for his involvement and friendship. The five months stage in the Technical University of Catalunya in Barcelona under his supervision has been the beginning of the end of this thesis.

Prof. Michel Ghosn for his help in the part of the work related to bridge redundancy and reliability of structural systems. I would never imagine that such complicated problems can be explained in such a simple way.

I remember also the help of many other people that provide data and materials used in this thesis. Among many others I would like to express my gratitude to: Prof. Angel Aparicio, Prof. Rui Simoes, Prof. Sven Thelandersson, Prof. Lennart Elfgren, Eng. Paulo Lopes, Eng. Jose Lello, Eng. Anibal Leite, Prof. Eugene O'Brien, Prof. Alfred Strauss, Prof. Marcello Ciampoli and Prof. Evan Bentz.

I would also like to thank all my friends that share with me free time and make this four years of my life cheerful and interesting. Unfortunately I cannot list all of them but al least I would like to mention: Michal, Ismael, Francisco, Riitta, Miguel, Nuno, Luis, Jorge, Isabel, Lupe, Cristina, Sabina, Lukasz, Gosia and Ola.

Last but not least, I would like to thank my parents, Irena and Ferdynand, and my sister, Patrycja. Their understanding and support has been very important for me. Without them I could never have come this far.

The research work presented in this thesis was carried out at the Department of Civil Engineering of the University of Minho between January 2003 and February 2007. The project was financed by the Portuguese Foundation of Science and Technology (*FCT*) through the grant SFRH/BD/11401/2002 which is gratefully acknowledged.

Abstract

Many bridges in Portugal and in other countries that are still in service are subjected to loads far higher than those for which they were designed. Also, due to insufficient investment in the bridge maintenance, many of existing bridges have significantly deteriorated over their years of service and thus their actual capacity has drastically reduced. Aiming to avoid unexpected bridge failures, it is of vital importance to verify that existing bridges can still provide adequate levels of safety under increased loads. These concerns can in many cases be addressed by using traditional bridge load capacity evaluation methods. However, existing load evaluation procedures are usually adopted from the design codes, which are meant for new bridges, and may not be adequate for the assessment of existing bridges.

This thesis deals with different topics related to the load capacity evaluation of existing concrete bridges. At the beginning the currently recommended procedures and methodologies for the assessment of existing bridges are presented and discussed. One of the presented procedures is selected as the most adequate for the Portuguese conditions. The procedure systematize the use of several assessment approaches, starting with the simplest semi-probabilistic approach, based on the current design code, and finishing with fully probabilistic assessment, based on the reliability theory.

Following the general introductory section, several probabilistic models of bridge geometry and mechanical properties of materials, used in the construction of concrete bridges, are shown. Also, some new models, developed within the program of this thesis, are presented. These models aim to be representative for the stock of existing concrete bridges in Portugal. Subsequently, the problem of bridge loading is discussed. Several probabilistic models of bridge permanent loads are shown. However, the major focus is placed on bridge traffic loads. Two simplified probabilistic traffic load models are presented as an alternative to the commonly used models from codes that were found to give inconsistent results. Afterwards, several probabilistic models of bending and shear resistance of concrete bridge elements are shown and discussed. Also, some new models developed within the program of this thesis are presented. The developed models can be considered representative for stock of precast concrete bridges in Portugal.

After the load and the resistance models, the safety requirements and safety formats applicable to bridge assessment are presented. Some of the presented semi-probabilistic and probabilistic formats are able to account for a bridge redundancy and the system effects that may significantly increase the evaluation of a bridge capacity. All the presented safety formats are then practically verified and compared by applying them to the assessment of reinforced concrete railway bridge.

Finally, the selected assessment procedure, the proposed resistance models, the presented models of traffic loads and some of the discussed safety formats are applied to the assessment of two precast prestressed concrete highway bridges. These examples show that the bridges which fail evaluation using traditional procedures may by rated as safe when using more advanced models and approaches developed and presented in this thesis.

Resumo

Em Portugal e noutros países, existe um número significativo de pontes em serviço que se encontram sujeitas a cargas muito superiores aquelas para as quais foram dimensionadas. Por outro lado, o investimento reduzido na conservação das pontes faz com que muitas dessas estruturas se deteriorem significativamente durante a sua vida útil e que a capacidade de carga esteja drasticamente reduzida. Para evitar um decréscimo acentuado do desempenho estrutural ou mesmo o colapso de algumas dessas pontes, é de crucial importância avaliar se ainda verificam os níveis de segurança adequados para esse maior nível de carregamento. Estas preocupações podem, em muitos casos, ser analisadas usando métodos tradicionais de avaliação da segurança. Porém, os procedimentos de avaliação da segurança existentes são, normalmente, baseados nos regulamentos para o dimensionamento de pontes novas e que podem não ser adequados para a avaliação de pontes existentes.

Nesta tese é abordado um vasto conjunto de aspectos relacionados com avaliação de segurança de pontes existentes de betão. Inicialmente, são apresentados e discutidos os procedimentos e as metodologias actualmente recomendadas para a avaliação das pontes existentes. De todos estes procedimentos, o mais adequado para as condições portuguesas preconiza a utilização de vários métodos de avaliação de segurança, começando pelo mais simples - avaliação semi-probabilística, baseada nos actuais regulamentos para dimensionamento - e termina com a avaliação totalmente probabilística, baseada na teoria de fiabilidade estrutural.

Após a secção geral introdutória, são apresentados os vários modelos probabilísticos para o estudo das incertezas associadas à geometria de elementos estruturais e de propriedades mecânicas de materiais, usados em pontes de betão. Apresenta-se também alguns modelos desenvolvidos no âmbito do programa desta tese. Estes modelos pretendem ser representativos da população de pontes de betão existentes em Portugal. Posteriormente, é analisado o problema das acções em pontes, propondo-se vários modelos probabilísticos para as acções permanentes e dando-se especial ênfase à modelação das acções variáveis devidas ao tráfego. Como alternativa aos modelos regulamentares correntemente utilizados, e que nem sempre conduzem a resultados consistentes, são apresentados dois modelos probabilísticos simplificados. De seguida, são analisados alguns modelos probabilísticos de resistência à flexão e ao corte de elementos de betão e alguns modelos novos, desenvolvidos dentro do programa desta tese, que podem ser considerados representativos das pontes pré-fabricadas em betão existentes em Portugal.

Descrevem-se ainda os níveis de segurança associados aos diferentes níveis de desempenho estrutural e os formatos de segurança aplicáveis. Alguns dos formatos, semi-probabilísticos e probabilísticos, podem ter em conta a redundância e o tipo de sistema estrutural, podendo resultar num aumento significativo da avaliação da capacidade duma ponte em relação àquela que se obteria se a avaliação fosse efectuada individualmente a cada elemento estrutural. Todos os formatos de segurança apresentados foram validados e comparados entre si, nomeadamente na avaliação de segurança duma ponte ferroviária.

Finalmente, o procedimento escolhido para a avaliação de segurança, os modelos da resistência desenvolvidos, os modelos das acções apresentados e alguns formatos de segurança discutidos, foram aplicados na avaliação de segurança de duas pontes rodoviárias pré-fabricadas em betão pré-esforçado. Esses exemplos tornaram evidente como pontes consideradas inseguras pelos procedimentos tradicionais podem vir a ser consideradas seguras, recorrendo, para o efeito, aos modelos e metodologias mais avançadas, desenvolvidas e apresentadas nesta tese.

Contents

Chapter 1

Introduction

1.1 Background and motivations

The transport network is extremely important to the World's economic and social development. It has been a crucial factor in spurring economic growth and prosperity and plays an important role in our daily lives, allowing the fast, easy, and safe movement of people and goods. Recent studies have shown that the movement of goods and people around the European Union is estimated to cost 500 billion Euros per annum, which is about 15 percent of the income of all European citizens (BRIME, 2001). A great majority of this mobility in Europe is provided by the roadway and railway infrastructures.

Bridges constitute a significant portion of the fixed assets of the roadway and railway transportation infrastructure. Due to the fact that the expansion of the road and railway networks in most of the European countries started in the XIX century, a significant part of the bridge stock was built more than 100 years ago and a number of masonry arch bridges date back to the Roman times (COST345, 2004). According to survey performed in countries of northern and central Europe (SAMARIS, 2005) most of the road bridges have been built within the period 1946-1965. However, many of Europe's railway bridges were built more than 50 years ago and 35% of the bridge stock is older than 100 years (Bell, 2004).

In Portugal the proportion of bridges at the age of around 50–60 years is not so significant as in the countries affected by the Second World War where all the transportation infrastructure had to be rebuild after war's destruction.

Nevertheless, within the national road network and within railway network there exists a lot of bridges that have been built more than 50 years ago. Furthermore, many bridges that have been built in last decades, were designed considering traffic load model which was developed in the fiftieths (RSA, 1983; RSEP, 1961).

Due to the above discussed facts, many bridges that are still in service are subjected to loads far higher than those for which they were designed. Also, due to insufficient investments in bridge maintenance, many of the existing bridges have significantly deteriorated over their years of service.

Moreover, due to the expansion of the European Community and due to the continuous growth of its economy, the traffic loads on European highways and railway lines have been increasing in recent years, a trend that is expected to continue into the foreseeable future. As a consequence, demands in terms of loads and robustness, on existing bridges will increase. Therefore, it is of vital importance to upgrade the highway and railway bridge networks and ensure that existing bridges can still provide adequate levels of safety under increased loads.

These concerns can in many cases be addressed by using traditional bridge load capacity evaluation methods. However, existing load evaluation procedures for existing structures are usually adopted from the design codes, which are meant for new bridges, and may not be adequate for the assessment of existing bridges.

The majority of methods presently used for the safety assessment of bridges are based on linear elastic analysis and the deterministic or semi-probabilistic evaluation of individual member strengths. In reality, a bridge consists of a system of interconnected members where the failure of any single member may not necessarily cause the collapse of the whole structure. Therefore, the reliability of the member may not be representative of the reliability of the whole bridge. Furthermore, most of the variables describing structure geometry, mechanical properties of materials and applied loads are not deterministic parameters and their design or characteristic values, which are often used during the assessment of existing bridges, do not always properly reflect their inherent uncertainties. Due to all the simplifications and conservative assumptions usually made during the design process, using the same standards for the assessment of existing bridges may lead to having many bridges that are in reality completely safe be rated as unsafe.

The benefits gained by performing a probability-based reliability analysis during the process of designing new bridges are usually quite low. Therefore, the significant computational effort necessary to perform system or even member reliability analysis is not usually justified at the design level. Alternatively, the explicit consideration of bridge redundancy and/or variability in the important parameters can be very important and could lead to significant economical benefits when assessing the safety of existing bridges. This is mostly the case when decisions have to be made regarding what appropriate maintenance actions to undertake including rehabilitation, strengthening or replacement of bridges that may not satisfy the deterministic single member criteria but are known to have significant levels of reserve strength. For this reason, the use of probability-based safety assessment methods for existing bridges is increasing in academical studies and in practical applications (Casas, 1999; Enevoldsen, 2001; Jeppsson, 2003; Lauridsen, 2004; Sobrino, 1993; Strauss, 2003). However, in many cases the probability-based methods are still applied to linear elastic models of the bridge, without taking full advantage of the bridge's redundancy and strength reserve in the non-linear range. Furthermore, the probabilistic models of bridge geometry, mechanical properties of materials and applied loads, used in the assessment, are based on the limited amount of data collected in North America and in some parts of Europe and are not necessarily representative of the variability of those parameters observed in bridges constructed in every European country or, particularly, in Portugal.

Due to the above mentioned facts there is a need to review and verify applicability of the various safety formats that can be used for the evaluation of load carrying capacity of existing bridges. The selected safety formats need to take into account the actual variability of parameters influencing bridge resistance and the variability of all the bridge loads. Some of them should also take into account bridge redundancy and mechanical and/or geometrical non-linearities. Furthermore, there is a need to review existing and develop some new probabilistic models of bridge loads, parameters influencing bridge's resistance and also the models of the shear and bending resistance of typical bridge sections itself. Moreover, it is also necessary to verify the applicability of all those models to the safety assessment of existing bridges and to the Portuguese conditions.

1.2 Objectives and scope

This thesis is concerned with selecting, refining and improving procedures, safety formats, and the load and resistance models employed in the load capacity evaluation of existing concrete bridges. In this regard the following objectives were defined to be accomplished within the planned work:

- Review procedures and methodologies currently recommended for the load capacity evaluation of existing bridges and check theirs applicability to Portuguese conditions.
- Propose a new or/and verify the adequacy of the existing probabilistic models of bridge geometry and mechanical properties of materials that can be used in the process of probability-based reliability assessment of existing concrete bridges, particularly bridges in Portugal.
- Verify the adequacy of existing, or if necessary develop new probabilistic models of bridge permanent and variable loads suitable for evaluation of existing bridges, which allow to take into account specifics of Portuguese traffic.
- Review existing probabilistic models of shear and bending resistance of typical concrete bridge sections and if necessary develop new ones that would be representative for Portuguese bridge stock.
- Select and verify adequacy of existing safety formats that can be used within the proposed procedures for evaluation of load carrying capacity of existing bridges.
- Develop examples that show how to assess existing concrete bridges using procedures, formats and models proposed.

The above presented objectives are quite ambitious and could not be fulfilled within the program of this thesis when all the bridge types would have to be covered. Therefore, only certain concrete bridge types were selected to be analysed in this work and all other bridge types and construction materials were omitted.

Furthermore, the problem of modelling bridge traffic loads was treated quite superficially and the probabilistic traffic load models just for certain bridge types and spans were decided to be presented. Moreover, all the common problems of existing bridges regarding deterioration of capacity due to corrosion, fatigue or other causes were decided to be neglected in this thesis. Finally, the problems related to functionality or serviceability of bridges were also omitted.

1.3 Outline of the thesis

The thesis is organised in ten chapters and four related appendices.

In Chapter 1 general introduction to the problem is provided and the objectives and scope of the current work are stated.

In Chapter 2 methodologies for the assessment of existing bridges are demonstrated and analysed. At first the difference between assessment of existing bridges and the design of new bridges are outlined. Then the concept of probability based assessment is introduced and it is compared with semi-probabilistic or deterministic capacity evaluation methods known from design codes. Afterwards several procedures and methodologies for safety assessment of existing bridges are presented based mainly on recent codes and guidelines, and finally one procedure is selected to be used for load capacity evaluation of bridges in Portugal.

In Chapter 3 basics of statistics and some principles and methods of reliability analysis are briefly introduced. The aim of this chapter was to provide theoretical background necessary to understand the following parts of the thesis. It has to be stressed that it was intended to give guidance to one who is not familiar with statistical analysis or with reliability analysis, and generally it can be skipped by everyone who has sufficient knowledge in those fields.

In Chapter 4 the probabilistic models of basic mechanical properties of concrete and reinforcing and prestressing steels are analysed. The probabilistic models of structure and structural member geometry are also presented and discussed. Besides the models available in the technical literature and in specialized codes or guidelines the probabilistic models developed within the program of this thesis are also presented.

In Chapter 5 the probabilistic models of bridge permanent loads are presented. The models of bridge variable loads due to roadway or railway traffic are also showed and analysed. Furthermore, probabilistic load models for load capacity evaluation of existing highway bridges are presented. The models are based on the results of traffic measurements using Weigh-in-Motion systems.

In Chapter 6 the probabilistic models of ultimate shear and bending responses of typical concrete bridge sections are presented and analysed. Besides some models proposed by other authors the probabilistic models developed within the program of this thesis are presented. The models developed aim to be representative for stock of concrete bridges in Portugal.

In Chapter 7 the requirements regarding bridge safety, necessary to set when assessing load carrying capacity of existing bridges, are showed. The theoretical backgrounds based on which the target reliabilities are usually selected are also discussed. Furthermore, several safety formats that can be used in the bridges evaluation are presented. The described safety formats were selected in such a way to form solid framework for the assessment of existing bridges based on 'step-level' philosophy.

In Chapter 8 several safety formats presented previously are applied to the reliability assessment of a reinforced concrete railway bridge. The assessment using various methods proposed is carried out for the intact bridge and for the bridge where the significant damaged is assumed in such a way that the bridge does not fulfil the safety requirements of the legal design code. The evaluation of bridge using the same basic material and geometrical parameters but different safety formats shows clearly advantages of using more sophisticated assessment methods in the process of bridge evaluation.

In Chapter 9 two examples that show how to assess existing concrete bridges using procedures, formats and models proposed in previous chapters are presented. The bridges chosen for this purpose are a one span simply supported precast prestressed concrete I girder bridge and a continuous two span concrete overpass constructed from precast prestressed U shape girders.

In Chapter 10 summary and conclusions of this study are presented and suggestions for future research are stated.

Chapter 2

Assessment of existing bridges

2.1 Introduction

The need for the safety assessment of an existing bridge may arise due to several reasons. One of the reasons is when there is a necessity to carry an exceptional heavy load that are normally not permitted. Other, when the bridge has been subjected to change such as deterioration, mechanical damage, repair or change of use, as for example introduction of new carriageways or introduction of a line of railway or tramway. Following, when a bridge was designed according to outdated design code and it have to be check against new code and new traffic load requirements, as for example in the case when it is going to be reused within a new roadway or railway link. Finally, when the maximum permit load on a road or railway network is going to be increased and there is a concern if this change not put in hazard existing bridges.

The question 'is the bridge still sufficiently safe?' is quite different to that commonly faced by engineers during the design process of a new bridge and may not be answered using traditional safety checking procedures known from design codes. One of the reasons is that the many 'design uncertainties' related to prediction of mechanical properties of materials, structure geometry and loads in the existing bridge can be eliminated since most of those parameters can be measured. This make significant difference between the two processes. Therefore, the procedures for assessment also differ from that known from the design.

This chapter introduces the concepts and procedures used in the safety and serviceability assessment of existing bridges. At first the difference between safety assessment of existing bridges and the design of new bridges are outlined. Then, the main stages of assessment are specified and the concepts of probability based assessment and experimental assessment are introduced. Afterwards several procedures and methodologies for safety assessment of existing bridges are presented based mainly on recent codes, guidelines and research projects reports. Finally one the most suitable procedure is selected to be used for load capacity evaluation of bridges in Portugal.

2.2 Principles of assessment

2.2.1 Assessment versus design of bridges

The standard procedure used in the design process of a new bridge is as follows. At first the road or railway line geometry is defined according to certain class of traffic. Afterwards the bridge typology is chosen and the span lengths are determined regarding required clearance. Then the static system is defined and the dimensions of the members cross-sections are assumed. The loads acting on the bridge are assumed according to information and models from design codes. In the next step the load effects in the structural elements are calculated and the the capacity of the bridge members is determined using values of the strength properties of materials and the design formulas provided in the codes. When the capacity of all the bridge members is greater than the calculated load effects the process may stop (eventually optimization may be performed). Otherwise the section geometry or class of material have to be adjusted to meet the safety criteria.

When evaluating load carrying capacity of an existing bridge the procedures are different due to the fact that the situation is totally different. At first, since the bridge exists its geometry is already determined and can be measured. Eventually it can be assumed according to as-built or design drawings (assuring that they corresponds to actual structure geometry). Furthermore, the strength properties of construction materials can be quantified using one of the available nondestructive or partially destructive methods. Alternatively they can be assumed based on design specifications and/or data obtained within quality control procedures. The loads acting on the bridge can also be obtained due to measurements. For example the self weight of the bridge (including pavement, railings, kerbs, etc.) can be determined by weighting the bridge with hydraulic jacks. However, the traffic loads can be measured using bridge Weigh-in-Motion system and then bridge-specific traffic load model can be developed using for example procedures applied for the calibration of traffic load models from design codes. Furthermore, the load effects in some bridge elements can be determined using for example strain gauges. Then, the numerical model of the bridge can be calibrated in order to predict distribution of internal forces between bridge members with greater accuracy. Finally, the capacity of the bridge members can be also predicted or updated based on measurements and load tests.

Due to all above mentioned facts it is evident that the amount of information available in the process of assessment of existing bridges is significantly higher than in the bridge design. Therefore, the uncertainty related to the assessment is generally lower than uncertainty characteristic for the design. Nevertheless, it have to be stated that in practical situations not all the information about an existing bridge will be available from measurements and some of the available measurement data may be of low quality. Thus, the uncertainty related to our limited knowledge of the actual state of the structure may be still significant.

2.2.2 Main stages of assessment

The assessment of load carrying capacity of a bridge usually starts with the evaluation of its condition. The condition evaluation consists of examining existing documents and visiting the bridge for a preliminary inspection. The aim of the inspection is to identify bridge particularities (e.g. delamination, material loses, cracking, etc.) which need to be investigated with more detail in order to determine their cause, extent and consequently their effect on structural behaviour and carrying capacity. Finally, all this information is used in structural assessment which consists of determining the bridge strength in relation to bridge loads.

Having in mind the above described usual procedure the following stages of bridge assessment can be identified (BRIME, 2001):

- Study of design and inspection documents and their correctness.
- Preliminary inspection in order to identify visually the structural system and possible damages.
- Supplementary investigations in order to refine information about the bridge.
- Structural assessment in order to evaluate load carrying capacity and safety of the bridge.

The last two stages of the assessment can be carried out using different levels of accuracy and complexity. For many bridges simple check based on information from existing documentation and visual inspection may be enough to proof their safety. However, for some bridges, named sometimes 'substandard bridges', more detailed investigation and sophisticated analysis (e.g. non-linear structural analysis, probabilistic safety analysis, etc.) would be necessary.

2.2.3 Deterministic and probabilistic approach

Traditionally the design and safety evaluation of bridges were performed using allowable stresses approach. In this method the maximum stresses calculated in any member of a structure under worst case loading had to be checked against a so-called allowable stress. The values of allowable stresses were set arbitrarily on the basis of the mechanical properties of the materials used. In order to rationalise the design and to consider observed variability in mechanical properties of material, geometry and loads, engineers have tried to approach the problem from a different point of view by defining safety by means of a probability threshold. This gives the beginning for the structural reliability theory and the use of probabilistic safety assessment methods in bridge design and assessment.

In a probabilistic approach the stress S applied to a structural element and the strength R of this element, due the fact that their values are not perfectly known, are considered to be random quantities described by some probability density functions (see Figure 2.1). The safety criterion remains very similar to that used in allowable stress methods and can be expressed by the following inequality:

$$S \leq R \tag{2.1}$$

The actual measure of the reliability level corresponding to the analysed element of the structure can be characterized by the probability P_f that stress (or generalized load) S applied to the analysed element exceed the strength (or generalized resistance) R of that element:

$$P_f = P(R \leq S) \tag{2.2}$$

This can be illustrated graphically as the shaded overlap area between two probability density functions as presented in Figure 2.1.

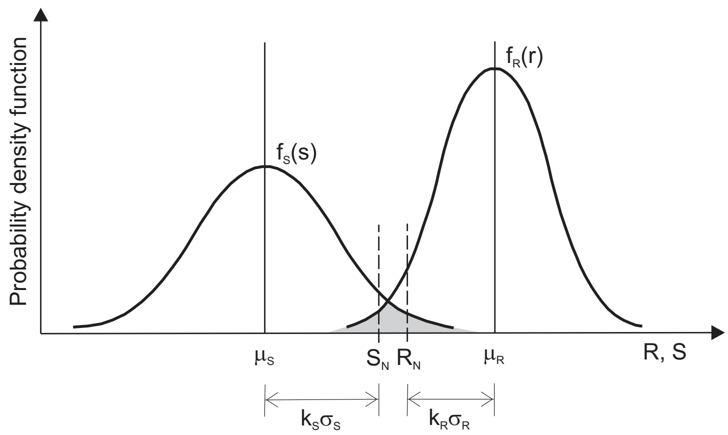

Figure 2.1: Fundamentals of risk evaluation, from Haldar & Mahadevan (2000a).

The semi-probabilistic approach currently used in most of the design and assessment codes replaces this probability calculation by the verification of a criterion involving nominal (or characteristic) values of R and S, denoted as R_N and S_N, and partial safety factors γ_R (or Φ_R) and γ_S which may be represented in the following form:

$$\gamma_S S_N \leq \frac{R_N}{\gamma_R} = \Phi_R R_N \tag{2.3}$$

The nominal (or characteristic) generalized resistance R_N is usually a conservative value, perhaps one, two or three standard deviations σ_R below the mean

μ_R (see Figure 2.1). The nominal (or characteristic) load S_N is also a conservative value, however, it is several standard deviations σ_S above the mean μ_S (see Figure 2.1). The partial safety factors for resistance γ_R (or Φ_R) and loads γ_S are usually conservatively chosen based on past experience, engineering judgement or calibration.

The partial safety factor method is noted as semi-probabilistic, considering the application of statistics and probability in the evaluation of the input data, the formulation of assessment criteria and the determination of load and resistance factors. However, from the point of view of the engineer performing assessment, the application of this method is still completely deterministic and it not allowed to assess the actual risk or reserves in carrying capacity of structural members.

In the process of bridge design the use of semi-probabilistic format is very practical since it allows to provide relatively uniform level of safety in the designed structural elements and it is very simple in application. In the process of bridge assessment it could be also practical and sufficiently accurate. However, in some situations it can be too conservative and could lead to unnecessary strengthening or replacement of the bridge. Therefore, the direct use of probabilistic safety evaluation method may be required.

2.2.4 Experimental approach

Alternatively to the analytical methods, the safety of a bridge may be assessed using bridge load tests. Basically, there are two types of load tests: diagnostic tests and proof tests. Diagnostic tests serve to verify and adjust the predictions of analytical methods and structural models used in the assessment. Proof tests are used to verify component and/or system performance and provide an alternative evaluation methodology to analytically computing the load rating of a bridge.

Successful proof test shows directly that the bridge can safely resist the load as big as that applied during the test. Therefore using simple deterministic (or semi-probabilistic) safety concept one can assume that applying loads on the bridge up to a value equivalent to the assessment loads factored for the ultimate limit state gives the proof of sufficient bridge safety (Ryall, 2001). The problem is that if full design factors are used the bridge would theoretically have collapsed. According to Ryall (2001), if it suspected that exist some hidden reserves of strength then a test can be sanctioned. If not, then lower load factor will have to be assumed and the safe load capacity will have to be calculated from the maximum test load reduced by an appropriate factor.

A more rational way of dealing with the information from proof test is using probabilistic framework. Based on the survival of proof load testing the reliability of a bridge may be updated in accordance with the pattern and intensity of the proof load applied (Faber *et al.*, 2000).

Several approaches can be used to incorporate the information of successful prove load test in reliability assessment. In the simplest one the probability distribution function (PDF) of the bridge resistance, or the resistance of one of its members, can be updated by truncating the lower tail of corresponding theoretical distribution at the value which is equal to the load effect induced by the applied proof load (see Figure 2.2).

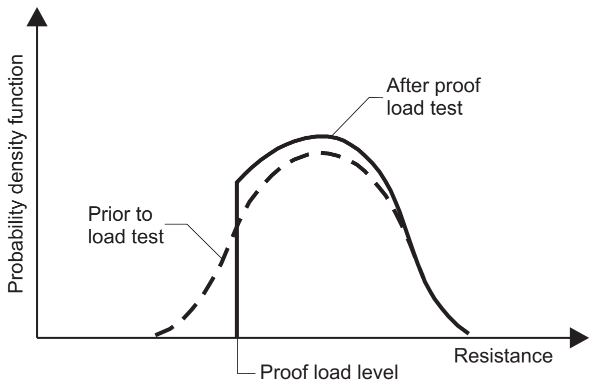

Figure 2.2: Truncation of PDF of bridge resistance after application of proof load.

It has to be stated that the truncation of the probability density function of resistance is not very effective when a low variability of resistance is adopted in the initial assessment (Faber *et al.*, 2000). This occurs because the lower tail of the distribution of resistance is less sensitive to truncation at lower proof loads.

Proof load testing update information on bridge resistance and consequently improve the assessment of bridge reliability. However, there is always a risk of bridge failure during a proof load test. Furthermore, the risk increases when the required proof load level increases. Therefore some balance has to be found between the risk of failure under the test load and the updated risk of bridge failure.

2.3 Procedures and methods of assessment

2.3.1 General

According to Schneider (1997) and JCSS (2001b) the process of assessment of existing structures should be break down into three phases presented schematically in a flowchart showed in Figure 2.3. Each of these phases should be complete in itself and should gives results allowing the bridge owner to make decision regarding conditions of its further exploitation or eventual demolition.

In other references slightly different approaches are recommended. For example in BRIME (2001) and COST345 (2004) five levels of assessment with increasing levels of complexity are proposed. However, in AASHTO LRFR (2003) and CAN/CSA-S6-00 (2000) the levels of assessment are not clearly identified. Nevertheless, all the assessment procedures can be generally embedded in the scheme similar to that presented in Figure 2.3. In the following section short overview of the assessment procedures and methods proposed in some national codes, guidelines and research project reports is presented based mostly on the information from SAMARIS (2005).

2.3.2 Approaches proposed in European research projects

BRIME and COST 345. In the European research projects BRIME and COST345 the assessment of existing highway bridges is proposed to be handled using 'step-level' philosophy. In the reports BRIME (2001) and COST345 (2004) five levels of assessment are proposed with increasing level of complexity and decreasing level of conservatism.

Level 1 is the simplest level of assessment, giving a conservative estimate of load capacity. At this stage, only simple analysis methods are necessary and partial safety factors from the design or assessment (if available) standards are used.

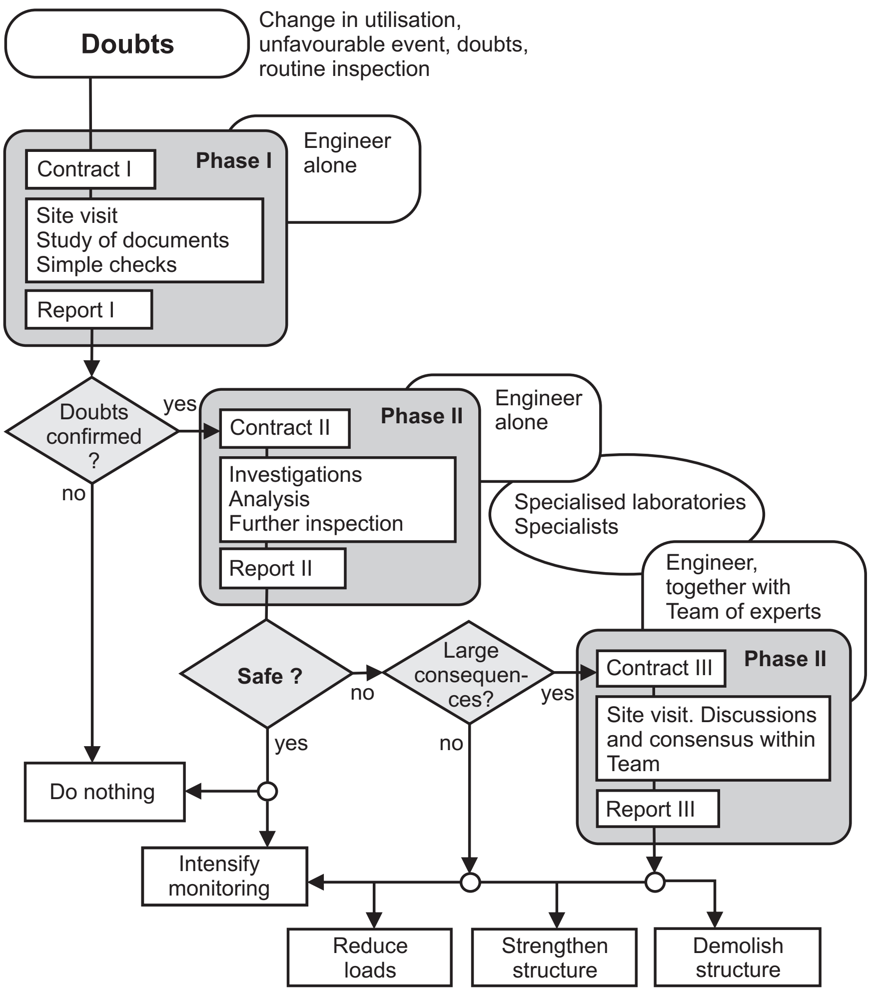

Figure 2.3: Illustration of the three phases approach, from Schneider (1997).

Level 2 assessment involves the use of more refined analysis (grillage, FEM, eventually non-linear FEM or plastic) and better structural idealisation (refined mesh, more adequate FEM types of elements). Furthermore, it allows for determination of characteristic strengths of materials based on available data (existing certificates or recent tests on similar structure).

Level 3 assessment allows to use in the safety evaluation bridge-specific loading (traffic load model developed based on WIM data collected on bridge in cause). Moreover, it allows for material testing in order to determine characteristic material strength properties. At this level assessment again partial safety factors from the design or assessment codes are recommended to be applied.

Level 4 assessments allows for any additional safety characteristic (member importance in global safety of the structure, past performance and service proven safety, failure consequences, etc.) of structure in cause and corresponding refine of the assessment criteria. Any changes to the criteria used may be determined through rigorous reliability analysis, or by judgemental changes to the partial safety factors. It have to be stressed that special care should be taken not to double count bridge specific benefits which have already been taken into account.

Level 5 assessment make use of reliability theory in the process of load carrying capacity evaluation. Such analyses require statistical data for all the variables defined in the loading and resistance equations. Assessment at that level provides greater flexibility but it should be noted that the results are very sensitive to the statistical parameters and the methods of structural analysis used. Generally the assessment at that level requires special knowledge and expertise.

Sustainable Bridges The 'step-level' philosophy has been also assumed in the European Guideline for the load capacity and safety assessment of existing railway bridges (Sustainable Bridges, 2006). In this document the assessment is proposed to be carried out using three-steps approach and the procedure similar to that presented in Figure 2.3. The phases can be generally characterized as follows:

- Purely heuristic experience based statements (phase 1).
- Application of deterministic safety formats (phase 2).
- Instrumentation, testing and/or probabilistic analyses (phase 3).

An assessment is proposed to be carried out within the framework of these phases, however, the levels of detail within each phase may vary. In this way it is possible to tailor a reassessment for different purposes. The level of detail of the assessment is recommended to be chosen for the analysed bridge considering its specifics.

In the highest level assessment, when relevant, the 'Guideline' recommends to use: the information regarding observed behaviour (records from testing and monitoring), measured material properties, refined structural model, non-linear or plastic analysis, probabilistic analysis, bridge specific loads, etc..

Furthermore, in Sustainable Bridges (2006) several safety formats for the assessment are proposed, starting from deterministic up to fully probabilistic. The several safety formats are clearly associated to each of the proposed assessment phases.

2.3.3 Approaches in national codes and guidelines

According to surveys performed (BRIME, 2001; SAMARIS, 2005) the bridge assessment in most of the European countries is still performed based on current design standards. This is also the common practice in Portugal. In some countries some small adjustment in partial safety factors (France) or in traffic loads (Norway) are allowed. Nevertheless, the procedures and basis for the assessment remains the same as in the design.

In the United States and in Canada the specific procedures for assessment of existing bridge have been developed during last decades and nowadays they are already quite well established. Recently, also in some European countries, as for example United Kingdom, Switzerland, Denmark, new codes or guidelines were developed dealing with the problem of the assessment of existing bridges. In the following paragraph the procedures and methods proposed in those documents are briefly described.

Canadian code (CAN/CSA-S6-00). In the Canadian code for design of bridges, CAN/CSA-S6-00 (2000), special section is dedicated to the assessment of existing bridges. According to the procedure presented in the mentioned section, bridge safety can be assessed using one of the three proposed methods.

The first method is based on the concept of partial safety factors known from the design codes. However, in this case the partial safety factors are calibrated for the assessment purposes. The specified factors are calculated using reliability procedures to provide target safety level defined in the code.

The alternative method, so called Mean Load Method, may be also used in the assessment when for example the structure fails the assessment using previously described method. The Mean Load Method is a probability based method and requires knowledge about the statistics of all variables. In the commentary to the code CAN/CSA-S6-00 (2000) some of the necessary informations regarding stochastic modelling are presented. Alternatively, they can be obtained from technical publications or from field measurements.

The third proposed method of an assessment is bridge load test. However, this method is considered as a part or complement of the evaluation procedure and have to be proceed by the theoretical evaluation.

American code (AASHTO LRFR). In the United States the procedures and methods required for the assessment of existing bridges are defined in a manual AASHTO LRFR (2003) specifically dedicated to this problem. This code provides three methods for evaluating maximum live load capacity of bridges or for assessing the safety under particular loading condition.

The first method named as Load and Resistance Factor Rating (LRFR) is equivalent to partial safety factor method known from the design codes. In the manual the rating is proposed to be performed at first for design load. In this level two different partial safety factors for traffic load are proposed. One for inventory level (safety factor equal to that from design) and second for operating level (reduced safety factor). Bridges that pass check at the inventory level have adequate capacity for all AASHTO and State legal loads. Bridges that pass the check at operating level have adequate capacity for AASHTO legal loads. When bridge fails the rating at the design loads it may be rated for legal loads in order to establish the need for load posting or strengthening. In this level the safety factor for traffic load has to be calculated using provided formula that take into account actual traffic conditions on the bridge.

In all the mentioned situations, the safety factors for bridge permanent loads remains as that used for the design, except the factor for wearing surface which can be decreased if its thickness is measured on the field. However, the partial safety factor for resistance has to be calculated according to the provided formula that accounts for bridge redundancy and its condition.

The second method of safety evaluation proposed in AASHTO LRFR (2003) is due to bridge load tests. Two types of bridge load test are available for bridge evaluation, diagnostic and proof test. Diagnostic tests allows to check certain bridge response characteristics whereas proof test allows to check directly load capacity of a bridge.

The third possible method of safety evaluation proposed in the code is using direct structural reliability analysis. The first order reliability format (FORM) of analysis and the 'a priori' probabilistic models of variables specified in AASHTO LRFD (1994) are recommended. This method of assessment is suggested to be used in some exceptional situations when for example the load characteristics, material properties, levels of deterioration or economic consequences differs significantly form those considered in the manual.

British guidelines. In the UK, the set of assessment codes have been developed by modifying the design standards. The modifications provide more realistic formulae for calculating member resistance, allowances for non-conforming details and imperfections, methods for incorporating field tested material strengths in calculations and also provides specific load model for assessment.

Five levels of assessment of increasing sophistication are proposed. They may be applied when a simple assessment (Level 1) indicates that the bridge is substandard. The first level uses a basic load model, codified resistance models and simple analysis. If this does not prove the structure satisfactory, the analysis and data are refined eventually up to the fully probabilistic analysis.

Among many others recommendations specific for bridge assessment the manuals BD21/01 (2001) and BD44/95 (1995) are the most relevant for the assessment of concrete bridges. The first uses bridge specific loading which allows reduction in traffic loads for low traffic flow and good surface condition. It also defines partial safety factors to be used in the assessment and proposes some methods of calculating member resistance considering its condition. The second manual introduces the safety factors for materials different from those used in the design based on the concept of 'worst credible strength'. The worst credible strength is the lowest value of the strength that could be obtained according to the engineer belief based on the prior experience and knowledge.

In opposite to the Canadian and American codes the BD21/01 (2001) clearly states that the bridge load test may not be used for direct safety evaluation. However, they can be used as complementary to the analytical assessment.

Swiss guideline (SIA 462). In Switzerland the assessment of existing structures is at first performed using current design code. When the structure fails that 'first level' assessment, the procedures proposed in SIA 462 (1994) have to be applied. This guideline allows for the reduction of partial safety factors for actions assuring that supplementary safety measures are taken. The safety measures may for example contain continuous or periodic monitoring of the structural performance and/or serviceability level. When the additional safety measures are envisaged the structure has to be inspected at least every 5 years.

The guideline SIA 462 (1994) also allows for more refined methods of analysis when they are justified by new developments or adequately based on the solid theory or reliable experiments. Therefore, all the advanced structural analysis methods (plastic, non-linear, etc.) and probabilistic safety evaluation methods may be applied in the assessment.

Danish guidelines. In Denmark all the bridges have to be at first evaluated using deterministic analysis and procedures presented in the guideline Vejdirectoratet (1996) specific for assessment of existing bridges. When any particular structure or structure element fails the deterministic assessment the probabilistic assessment according to Vejdirectoratet (2004) may be performed. Since in the deterministic analysis the critical (i.e. governing) ultimate and serviceability limit states are already determined, in the probabilistic assessment just those critical limit states are analysed.

The guideline Vejdirectoratet (2004) provides all the necessary information required in the probabilistic assessment including probabilistic models of bridge traffic loads and probabilistic models of resistance variables. It also gives some guidance how to deal with supplementary information as for example some test results.

2.4 Proposed methodology

As it can be observed in all the codes and guidelines described in previous section, it has been recognized and recommended that efficient structural assessment strategies be based on the application of new and increasingly sophisticated analysis levels. This 'step-level' philosophy seems also to be the most appropriate for the assessment of existing bridges in Portugal.

Concerning that the assessment strategies in all the European countries should be similar and should be based on the recommendations of European scientific bodies, organizations or research groups the procedures proposed in BRIME (2001) and COST345 (2004) are suggested to be applied for assessment of existing bridges in Portugal. Therefore, five levels of assessment with increasing levels of complexity are proposed as presented in Table 2.1, with Level 1 being the simplest and Level 5 the most sophisticated. The recommendation to go forward to the next level is made only if the bridge fails to pass the previous assessment level.

Table 2.1: General scheme of the 5 assessment levels.

<table>
<tr><th>Level</th><th>Strength & Load Models</th><th>Calculation Models</th><th>Assessment Methodology</th></tr>
<tr><td>1</td><td rowspan="2">Strength and load models as in design code. Material properties based on design documentation and standards.</td><td>Simple, linear-elastic calculation.</td><td rowspan="3">LRFD-based analysis. Load combinations and partial factors as in design code.</td></tr>
<tr><td>2</td><td rowspan="4">Refined, load redistribution is allowed, provided that the ductility requirements are fulfilled.</td></tr>
<tr><td>3</td><td rowspan="2">Material properties and loads can be updated on the basis of in-situ testing and observations.</td></tr>
<tr><td>4</td><td>LRFD-based analysis.
Modified partial factors are allowed.</td></tr>
<tr><td>5</td><td>Strength model including probability distribution for all variables.</td><td>Probabilistic analysis.</td></tr>
</table>

As it can be seen in Table 2.1, the most advanced assessment method combines load redistribution analysis (non-linear analysis) with a probabilistic analysis and this level can be applied as the last resort to save the bridge from unnecessary repair/strengthening or replacement. Because this level reflects more accurately the real structural behaviour of the bridge, many bridges that are declared unsafe based on the four previous levels, may show enough reserve strength to safely support the applied loads when analysed at this fifth assessment level.

Chapter 3

Concepts of statistics and the introduction to reliability analysis

3.1 Introduction

Engineers are responsible for proportioning the elements of the structure in such a way that satisfy the design criteria related to performance, safety, serviceability or durability under various demands. Handling this responsibility, in everyday practice they have to deal with uncertainties. The sources of uncertainty are various. Most of them are related to the uncertain mechanical parameters of constructional materials, uncertain geometry of the structure and uncertain loads. The models describing behaviour of the structure or the structural element are also uncertain. The most rational way to deal with this problem is to treat all the uncertain parameters as random variables (described by their probability distribution function PDF) and perform reliability analysis which is basically a probabilistic analysis of the assurance of system performance.

In this chapter basics of statistics and some principles and methods of reliability analysis are briefly introduced based mainly on books of Melchers (1999), Nowak & Collins (2000), Schneider (1997) and Haldar & Mahadevan (2000a).

3.2 Fundamental statistics

3.2.1 Random variables

Most of the physical phenomena are not able to be predicted with certainty. The observations and measurement of those phenomena gives multiple outcome among which some are more frequent than others. The occurrence of multiple outcomes without any pattern is often called 'uncertainty', 'randomness' or 'stochasticity'.

Definition of random variables. Any quantity that is uncertain is a random quantity and is often called 'random variable'. In general, most of the parameters in engineering problems are uncertain and should be considered as random variables. Random variables are discrete or continuous, however, in structural engineering problems most of them are continuous.

The variation of a random variable is generally described by its cumulative distribution function, CDF, $F_X(x)$ (see Figure 3.1), which defines the probability, P, that a variable X is equal or less than a certain value x:

$$F_X(x) = P(X \leq x) \tag{3.1}$$

Very often instead of cumulative distribution function probability density function, PDF, $f_X(x)$ (see Figure 3.1), is used to describe variation of the parameter X. For continuous random variables the PDF is related to its CDF as follows:

$$f_X(x) = \frac{dF_X(x)}{dx} \tag{3.2}$$

Parameters of random variables. For any random variable X there is possible to define certain 'parameters' that help to describe the properties of the variable. Those parameters of random variables are often called 'statistical moments'.

Mean or expected value (First Moment). The mean of X is denoted by μ_X and for continuous random variable is defined as:

$$E(X) = \mu_X = \int_{-\infty}^{+\infty} x f_X(x) dx \tag{3.3}$$

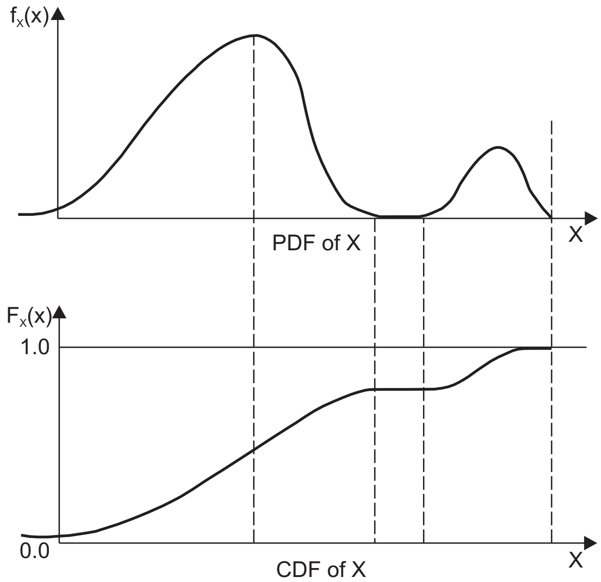

Figure 3.1: PDF and CDF of a continuous random variable, from Haldar & Mahadevan (2000a).

Variance and standard deviation (Second Moment). The variance of X is denoted by σ_X^2 and for continuous random variable is defined as:

$$E(X - \mu_X)^2 = \sigma_X^2 = \int_{-\infty}^{+\infty} (x - \mu_X)^2 f_X(x) dx \tag{3.4}$$

The standard deviation of X, σ_X, can be defined as follows:

$$\sigma_X = \sqrt{\sigma_X^2} \tag{3.5}$$

The coefficient of variation, COV, denoted often as V_X is defined as:

$$V_X = \frac{\sigma_X}{\mu_X} \tag{3.6}$$

Skewness (Third Moment). The skewness, also known as third central moment, gives a measure of lack of symmetry of the distribution and is defined as follows:

$$E(X - \mu_X)^3 = \int_{-\infty}^{+\infty} (x - \mu_X)^3 f_X(x) dx \tag{3.7}$$

The dimensionless 'skewness coefficient', γ_1, can be introduced as:

$$\gamma_1 = \frac{E(X - \mu_X)^3}{\sigma_X^3} \tag{3.8}$$

If γ_1 is zero, the randomness is symmetric, if γ_1 is positive, the dispersion is more above the mean, and if it is negative the the dispersion is more below the mean.

Kurtosis (Fourth Moment). The kurtosis, also known as fourth central moment, gives a measure of flatness of the distribution and is defined as follows:

$$E(X - \mu_X)^4 = \int_{-\infty}^{+\infty} (x - \mu_X)^4 f_X(x) dx \tag{3.9}$$

The dimensionless 'kurtosis coefficient', γ_2, can be introduced as:

$$\gamma_2 = \frac{E(X - \mu_X)^4}{\sigma_X^4} \tag{3.10}$$

If γ_1 is positive, the distribution is relatively peaked, and if it is negative the distribution is relatively flat.

Common probability distributions. The common distribution types used in the structural reliability analysis are as follows: uniform, triangular, normal, lognormal, exponential, gamma, beta, extreme Type I (Gumbel), extreme Type II (Frechet), extreme Type III (Weilbull), and Poisson. Nevertheless, the most commonly used are normal and lognormal distributions and just they are described in this paragraph. Detailed information about all the remaining distributions can be found in Melchers (1999), Nowak & Collins (2000), Schneider (1997) and Haldar & Mahadevan (2000a).

Normal or Gaussian distribution. The normal distribution is probably the most widely used distribution in structural reliability. The PDF of the distribution can be expressed as:

$$f_X(x) = \frac{1}{\sigma_X \sqrt{2\pi}} \exp\left[-\frac{1}{2}\left(\frac{x - \mu_X}{\sigma_X}\right)^2\right] \tag{3.11}$$

where μ_X and σ_X are the mean and standard deviation respectively. The corresponding CDF can be expressed as:

$$F_X(x) = \int_{-\infty}^{x} \frac{1}{\sigma_X\sqrt{2\pi}} \exp\left[-\frac{1}{2}\left(\frac{x-\mu_X}{\sigma_X}\right)^2\right] dx \tag{3.12}$$

The normal distribution, denoted often as $N(\mu, \sigma)$, is symmetric about the mean and it is applicable for any value of random variable from $-\infty$ to $+\infty$. Figure 3.2 shows the shapes of PDF of normal distributions with mean 0 and standard deviation 0.5, 1.0 and 2.0 respectively.

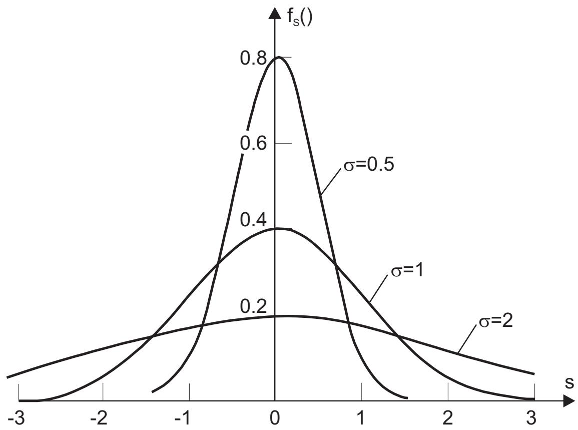

Figure 3.2: Normal probability density function, from Melchers (1999).

The normal distribution with zero mean and unit standard deviation, denoted as $N(0, 1)$, it is called standard normal distribution and its CDF is denoted as $F_S(s) = \Phi_S$. The CDF of standard normal distribution is widely available in tabulated form. Any normal variable X can be transformed to standard normal variable as:

$$S = \frac{X - \mu_X}{\sigma_X} \tag{3.13}$$

Performing transformation the PDF and CDF of S can be expressed as follows:

$$f_S(s) = \frac{1}{\sqrt{2\pi}} \exp\left[-\frac{1}{2}s^2\right] \tag{3.14}$$

$$F_S(s) = \int_{-\infty}^{s} \frac{1}{\sqrt{2\pi}} \exp\left[-\frac{1}{2}s^2\right] ds \tag{3.15}$$

Lognormal distribution. The lognormal distribution is the widely used distribution in structural reliability when a random variable cannot have negative values. If a random variable has a lognormal distribution, then its natural logarithm has a normal distribution. The PDF of the lognormal distribution can be expressed as:

$$f_X(x) = \frac{1}{\zeta_X\sqrt{2\pi}} \exp\left[-\frac{1}{2}\left(\frac{\ln x - \lambda_X}{\zeta_X}\right)^2\right] \tag{3.16}$$

where λ_X and ζ_X are the parameters of the distribution. The corresponding CDF can be expressed as:

$$F_X(x) = \int_0^x \frac{1}{\zeta_X\sqrt{2\pi}} \exp\left[-\frac{1}{2}\left(\frac{\ln x - \lambda_X}{\zeta_X}\right)^2\right] dx \tag{3.17}$$

The lognormal distribution is unsymmetrical and it is applicable for any value of random variable from 0 to $+\infty$. Figure 3.3 shows the shapes of PDF of lognormal distributions with λ equal to 0 and ζ of 0.5, 1.0 and 2.0 respectively.

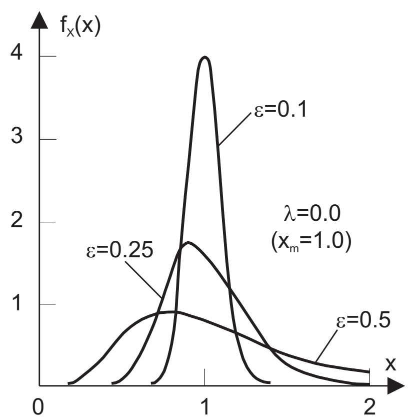

Figure 3.3: Lognormal probability density function, from Melchers (1999).

The distribution parameters λ_X and ζ_X are related to the mean value μ_X and the standard deviation σ_X as follows:

$$\mu_X = \exp\left(\lambda_X + \frac{\zeta_X^2}{2}\right) \tag{3.18}$$

$$\sigma_X = \mu_X\sqrt{\exp\left(\zeta_X^2\right) - 1} \tag{3.19}$$

3.2.2 Determination of distribution and moments from observation

In engineering problems very often the distribution type and its parameters describing some random property are unknown and have to be selected based on available experimental data. Furthermore, even when the distribution type can be prescribed to some property arbitrary based on past experience there is necessity to check if the experimental data fit well to the prescribed distribution.

Determination of probability distribution. Exist many procedures to determine type of the probability distribution function for any sample data. They can be subdivided into two groups, visual (histograms, cumulative histograms, P-P plots, probability papers, etc.) and analytical known also as goodness of fit tests (chi-square test and Kolmogorov-Smirnov test). In the following paragraphs just histograms, P-P plots and Kolmogorov-Smirnov test are introduced since they are further used in this thesis.

Histograms. Histogram is a bar diagram where each bar shows the relative frequency of the data points in predefined interval. By looking at the bar graph it can be observed trends in the data and visually can be determined the theoretical distribution that fits to the data. As an example Figure 3.4 shows typical histogram for compressive strength of concrete.

P-P plots. P-P plot shows the correspondence of the experimental results to the theoretical distribution function. It is basically a plot of the cumulative curve of deflection against the cumulative normal distribution. As an example Figure 3.5 shows typical P-P plot for compressive strength of concrete.

Kolmogorov-Smirnov (K-S) test. The K-S test compares the observed cumulative frequency with CDF of assumed theoretical distribution. It is based on the maximum difference between the two cumulative distributions defined as:

$$D_n = \max \Big| F_X(x_i) - S_n(x_i) \Big| \tag{3.20}$$

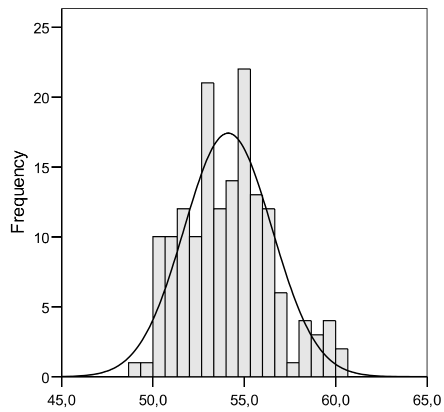

Figure 3.4: Typical histogram.

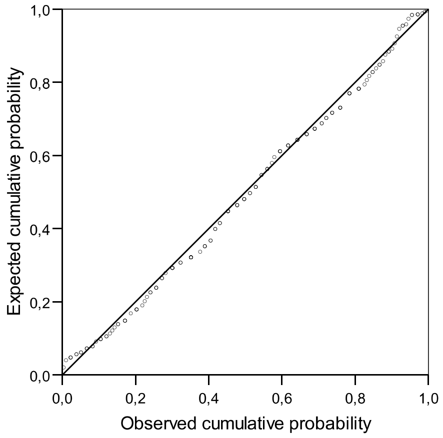

Figure 3.5: Typical P-P plot.

where $F_X(x_i)$ is the theoretical CDF at the i-th observation of ordered samples x_i and $S_n(x_i)$ is the corresponding observed CDF of ordered samples. D_n is also a random variable which distribution depends on the sample size n. The cumulative distribution of D_n is related to the significance level α as follows:

$$P(D_n \leq D_n^\alpha) = 1 - \alpha \tag{3.21}$$

D_n^α at various significance levels are tabulated. According to K-S test, if the maximum difference D_n is less than or equal to D_n^α, the assumed distribution is acceptable at the significance level α.

Estimation of parameters of a distribution. For a given sample of a random variable the parameters of its distribution can be estimated using the 'method of moments' or 'method of maximum likelihood'. In the following text just the method of moment is presented since it is further used in this thesis. The basic concept behind this method is that all the parameters of a distribution can be estimated using the information on its moments.

Mean or expected value (First Moment). The mean or expected value of a random sample X, μ_X, can be estimated as:

$$\overline{x} = \frac{1}{n} \cdot \sum_{i=1}^{n} x_i \tag{3.22}$$

Variance (Second Moment). The variance of a random sample X, σ_X^2, can be estimated as:

$$s_X^2 = \frac{1}{n-1} \cdot \sum_{i=1}^{n} (x_i - \mu_X)^2 \tag{3.23}$$

Skewness and kurtosis coefficients (Third and Fourth Moments). The skewness coefficient, γ_1, and the kurtosis coefficient, γ_2 , of a random sample X can be estimated as:

$$\widehat{\gamma_1} = \frac{n}{(n-1)(n-2)\sigma_X^3} \cdot \sum_{i=1}^{n} (x_i - \mu_X)^3 \tag{3.24}$$

$$\widehat{\gamma_2} = \frac{n^2}{(n-1)(n-2)(n-3)\sigma_X^4} \cdot \sum_{i=1}^{n} (x_i - \mu_X)^4 \tag{3.25}$$

3.2.3 Jointly distributed random variables.

Sometimes it is of interest to observe simultaneously two or more properties each of them being random. The question that can be asked whether there exist any interdependence between those properties an how important it is. To deal with this problem the concepts of joint distribution and correlation have to be introduced.

Joint and marginal probabilities. If some observed property is the result of two (or more) random variables its CDF can be described as:

$$F_{X_1 X_2}(x_1, x_2) = P\Big[(X_1 \leq x_1) \cap (X_2 \leq x_2)\Big] \geq 0 \tag{3.26}$$

The corresponding joint PDF can be expressed as follows:

$$f_{X_1 X_2}(x_1, x_2) = \frac{\delta^2 F_{X_1 X_2}(x_1, x_2)}{\delta x_1 \delta x_2} \tag{3.27}$$

However, a marginal probability density function may be obtained from the joint density function by integrating over the other variables:

$$f_{X_1}(x_1) = \int_{-\infty}^{+\infty} f_{X_1 X_2}(x_1, x_2) dx_2 \tag{3.28}$$

Bivariate joint probability density function and marginal probability density functions are shows in Figure 3.6.

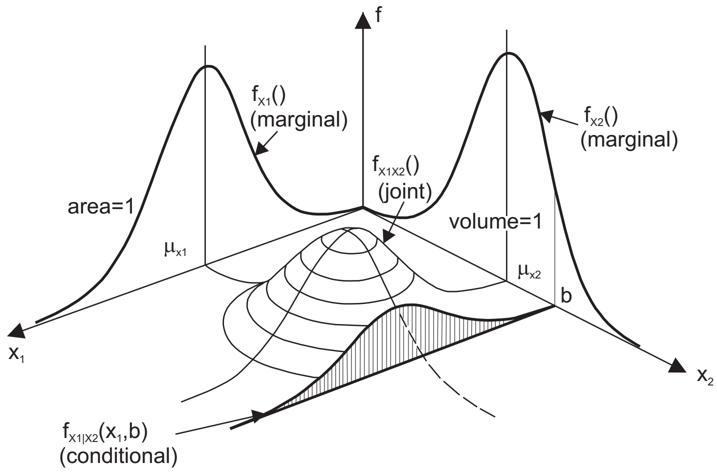

Figure 3.6: Joint and marginal PDFs, from Melchers (1999).

Correlation between variables. The interdependence between any two variables can be checked plotting each pair of the variable (x_1, x_2) as points in the corresponding coordinate system. Figure 3.7 shows several possible outputs of such graphical representation. The covariance, denoted as $\text{cov}(X_1, X_2)$, is a mea-

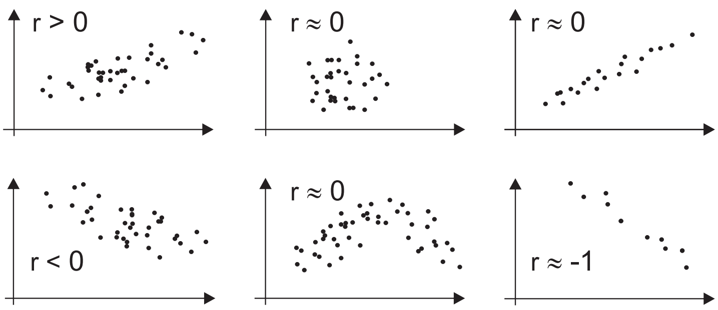

Figure 3.7: Correlation plots and corresponding correlation coefficients, from Schneider (1997).

sure of the interdependence of two random quantities and for continuous random variables it is defined as:

$$\text{cov}(X_1, X_2) = \int_{-\infty}^{+\infty} \int_{-\infty}^{+\infty} (x_1 - \mu_{X_1})(x_2 - \mu_{X_2}) f_{X_1 X_2}(x_1, x_2) dx_1 dx_2 \tag{3.29}$$

The estimation of the covariance, $\text{cov}(X_1, X_2)$, can be obtained as follows:

$$\text{cov}(X_1, X_2) = \frac{1}{n-1} \cdot \sum_{i=1}^{n} (x_{1,i} - \mu_{X_1})(x_{2,i} - \mu_{X_2}) \tag{3.30}$$

The dimensionless correlation coefficient, $\rho_{X_1 X_2}$, is defined as:

$$\rho_{X_1 X_2} = \frac{\text{cov}(X_1, X_2)}{\sigma_{X_1} \sigma_{X_2}} \tag{3.31}$$

The correlation coefficient takes values from -1 to 1 and its correspondence to the type of interdependency is illustrated in Figure 3.7.

3.2.4 Functions of random variables

When the response variable (e.g. bending resistance of reinforced concrete section) is a function of several random variables (e.g. section depth, reinforcement area, reinforcement and concrete strengths), its uncertainty analysis is quite complicated. However, for some exceptional cases exist some simple, closed-form solutions. This is the case of sums and differences of independent normal variables and products and quotients of independent lognormal variables.

Sum of independent normal variables. When a random variable Y is a sum (or difference) of independent normal random variables X_i, with mean μ_{X_i} and standard deviation σ_{X_i}, expressed as:

$$Y = a_1 X_1 + a_2 X_2 + \ldots + a_i X_i + \ldots + a_n X_n \tag{3.32}$$

where a_i's are constants, it can be shown that Y is also normal random variable with mean and variance defined as follows:

$$\mu_Y = \sum_{i=1}^{n} a_i \mu_{X_i} \tag{3.33}$$

$$\sigma_Y^2 = \sum_{i=1}^{n} a_i^2 \mu_{X_i}^2 \tag{3.34}$$

Product of independent lognormal variables. When a random variable Y is a product (or quotient) of independent lognormal random variables X_i, with parameters λ_{X_i} and ζ_{X_i}, expressed as:

$$Y = X_1 \cdot X_2 \cdot \ldots \cdot X_i \cdot \ldots \cdot X_n \tag{3.35}$$

it can be shown that Y is also lognormal random variable with the following parameters:

$$\lambda_Y = \sum_{i=1}^{n} \lambda_{X_i} \tag{3.36}$$

$$\zeta_Y^2 = \sum_{i=1}^{n} \zeta_{X_i}^2 \tag{3.37}$$

Central limit theorem. According to central limit theorem the sum of large number of variables, where none of them dominates the sum, tends to the normal distribution (regardless to their initial distributions) as the number of variables increase. Similarly for product of a large number of random variables, where none of them dominates the product, tends to the lognormal distribution (regardless to their initial distribution) as the number of variables increase.

3.3 Introduction to structural reliability

3.3.1 Limit states and definition of reliability

According to Nowak & Collins (2000) the limit state is defined as the boundary between the desired and undesired performance of the structure and is mathematically represented by the so called limit state function or performance function $g(X_i)$. Particularly in bridge structures, failure (or limit state violation) could be defined as the inability to carry traffic. This undesired performance can have several sources such as cracking, excessive deformation, insufficient bending or shear strength to carry traffic and many others. Traditionally each of that sources (or failure modes) is considered separately and for each the limit state function is defined.

Generally in the structural reliability analysis two kinds of limit states can be distinguished, Ultimate Limit States ULS and Serviceability Limit States SLS. Some authors separate the third kind of limit state, namely Fatigue Limit State FLS, considered traditionally as one of the ultimate limit states. Recently the fourth group of limit states was distinguished that is related to the structural durability.

The ultimate limit states are mostly related to loss of load-carrying capacity. However the serviceability limit states are related to gradual deterioration, comfort of the users, maintenance issues among others. In bridge engineering the common ultimate limit states are due to bending, shear, punching, loss of stability. The serviceability limit states in bridges are due to excessive deformations or vibrations, cracking, excessive stresses (leading to permanent deformations).

As it was already shown each limit state can be represented by the limit state function $g(X_i)$, where X_i represents the vector of random variables, which describe both the problem and the requirements for a particular problem. Violation of the limit state function can be defined by the following expression (failure condition):

$$g(X_i) < 0 \tag{3.38}$$

The probability of limit state violation (probability of failure) can be written as follows:

$$P_f = P\{g(X_i) < 0\} \tag{3.39}$$

Knowing already the probability of failure we can define the reliability (probability of the complement of the adverse event):

$$R = 1 - P_f \tag{3.40}$$

The practical methods of quantitative evaluation of probability of failure or reliability are the subject of reliability theory.

3.3.2 Fundamental case

In the simplest case the limit state function $g(X_i)$ can be the function of just two basic variables R and S, where the first is the generalized structural resistance and the second is the generalized action or action effect. When the generalized action or action effect is bigger than generalized resistance the failure occur. Therefore, the probability of failure can be defined as follows:

$$P_f = P(R < S) = P(R - S < 0) = P\left(\frac{R}{S} < 1\right) \tag{3.41}$$

or more generally:

$$P_f = P\{g(R, S) < 0\} \tag{3.42}$$

The problem can be also illustrated graphically, as it is presented in Figure 3.8, where marginal density functions $f_R(r)$ and $f_S(s)$ together with the joint density function $f_{R,S}(r, s)$ of two random variables are showed. The shaded area represents the failure domain D. For such illustrated problem the probability of failure becomes:

$$P_f = P(R - S < 0) = \int_D \int f_{R,S}(r, s) dr ds \tag{3.43}$$

When the basic variables R and S are independent (there is no any statistical correlation between them) Equation 3.43 can be rewritten as follows:

$$P_f = P(R - S < 0) = \int_{-\infty}^{\infty} F_R(x) f_S(x) dx \tag{3.44}$$

where $F_R(x)$ is the probability that $R \leq x$ and $f_S(x)$ represents the probability that load effects S takes the value between x and $x + \Delta x$ ($\Delta x \to 0$). The integral over all possible x gives the total probability of failure.

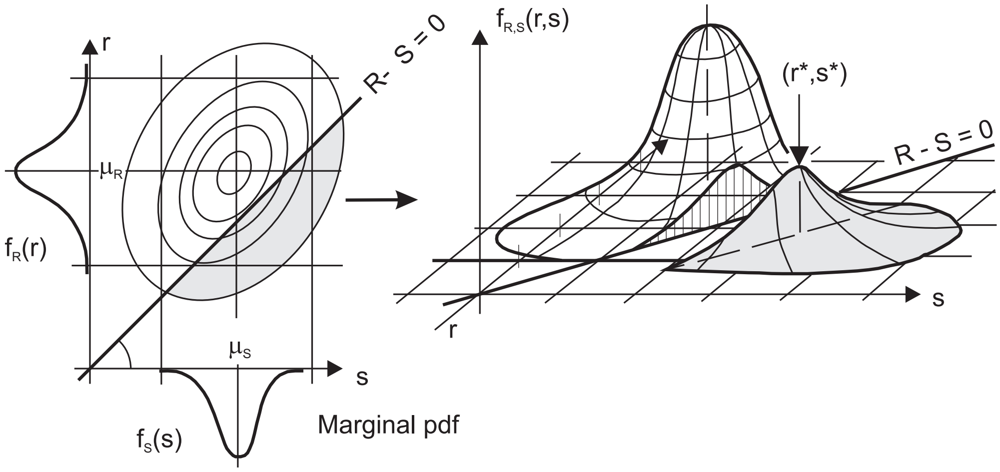

Figure 3.8: Two random variable joint density function $f_{R,S}(r, s)$, marginal density functions $f_R(r)$ and $f_S(s)$ and as shaded failure domain, from Schneider (1997).

3.3.3 Definition of the Reliability Index

In some particular cases it is possible to solve Equation 3.44 analytically, for example when variables R and S are normally distributed with mean values μ_R and μ_S and standard deviations of σ_R and σ_S respectively. Defining the new variable called 'safety margin' as:

$$Z = R - S \tag{3.45}$$

and using theorem saying that the sum/difference of normal random variables is also a normal variable with a mean μ_Z and a standard deviation σ_Z defined as:

$$\mu_Z = \mu_R - \mu_S \tag{3.46}$$

$$\sigma_Z = \sqrt{\sigma_R^2 + \sigma_S^2} \tag{3.47}$$

the probability of failure p_f can be expressed by following equation:

$$P_f = P(R - S < 0) = P(Z < 0) = \Phi\left(\frac{0 - \mu_Z}{\sigma_Z}\right) = \Phi(-\beta) \tag{3.48}$$

In Equation 3.48 Φ is the standard normal distribution function with zero mean and unit standard deviation and β is so called 'reliability index' often referred as

Cornell reliability index. The Cornell reliability index can be interpreted as the number of standard deviations σ_Z necessary to subtract from the mean value μ_Z to exceed zero (see Figure 3.9).

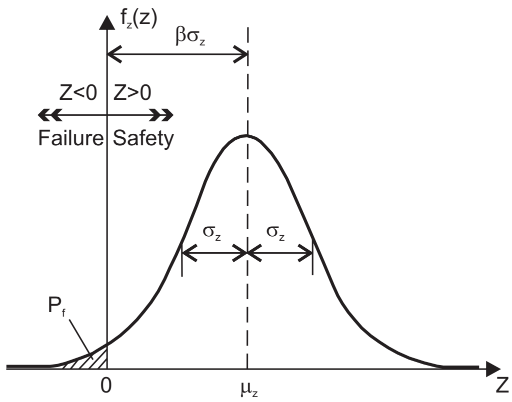

Figure 3.9: Distribution of safety margin $Z = R - S$, from Melchers (1999).

Substituting the μ_Z and σ_Z by the Equations 3.46 and 3.47, and subtracting the definition of β from Equation 3.48 the Cornell reliability index can be rewritten as follows:

$$\beta_C = \frac{\mu_R - \mu_S}{\sqrt{\sigma_R^2 + \sigma_S^2}} \tag{3.49}$$

The definition of the reliability index proposed by Cornell (see Equation 3.49) is valid for normal random variables. However, in structural reliability it is often more convenient to use lognormal distributions for modelling random variables due to the fact that they do not allow for negative values. In those situations the reliability index can be defined as follows:

$$\beta_{RE} = \frac{\ln \frac{\mu_R}{\mu_S}}{\sqrt{V_R^2 + V_S^2}} \tag{3.50}$$

where V_R and V_S are the coefficient of variations COV of R and S. The reliability index defined by Equation 3.50 is often called Rosenbluth-Esteva reliability index.

The estimation of the Cornell reliability index depends on the formulation of the limit state function and consequently it is not invariant. The formulation of the reliability index known as the Hasofer-Lind reliability index allows to overpass this invariance problem.

The Hasofer-Lind reliability index is formulated based on the limit state function transformed into so-called standard normal space. The equations 3.51 and 3.52 show the transformation of normally distributed variables R and S into standardized normally distributed variables U_1 and U_2 with mean zero and unit standard deviation.

$$U_1 = \frac{R - \mu_R}{\sigma_R} \tag{3.51}$$

$$U_2 = \frac{S - \mu_S}{\sigma_S} \tag{3.52}$$

After transformation the limit state function becomes:

$$g(R, S) = \mu_R - \mu_S + U_1\sigma_R - U_2\sigma_S \tag{3.53}$$

The reliability index β_{HL} according to the Hasofer-Lind formulation is a minimum distance between the origin and the limit state function (see Figure 3.10). The limit state function $g(R, S)$ after transformation no more passes through the origin (compare with Figure 3.8). However, the so-called design point $[u_1^*, u_2^*]$ still lies at the highest elevation of the joint PDF above the straight line $g(R, S) = 0$ (compare with the design point $[r^*, s^*]$ in Figure 3.8).

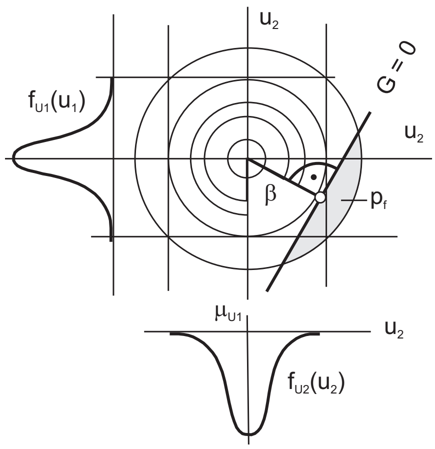

Figure 3.10: Bivariate standardized joint density function $f_{U_1,U_2}(u_1, u_2)$, marginal standardized density functions $f_{U_1}(u_1)$ and $f_{U_1}(u_2)$ and as shaded failure domain, from Schneider (1997).

The advantage of the Hasofer-Lind definition of the reliability index, compare to other definitions presented previously, is that it allows for further extension to more general situations as it will be explained in following section.

3.4 Methods of reliability analysis

The definitions of the reliability index presented in previous section are valid for the case of two independent normal (eventually lognormal, Rosenbluth-Esteva definition) random variables R and S, and linear limit state function $g(R, S) = R - S = 0$ (eventually $g(R, S) = R/S = 1$, Rosenbluth-Esteva definition). In the real situations the limit state functions $g()$ are often non-linear and dependent on many, sometimes correlated, arbitrary distributed random variables X_i.

$$g(x_1, x_2, \ldots, x_n) = g(X_i) = 0 \tag{3.54}$$

The methods that allow to estimate the probability of failure or the reliability index for more complicated limit state functions and arbitrary distributed variables are called 'reliability analysis methods'.

3.4.1 First and second order reliability method (FORM and SORM)

The first and second order reliability method, FORM and SORM, are based on the extended definition of the Hasofer-Lind reliability index. In FORM and SORM all the n random variables X_i are transformed into standardized normally distributed variables U_i similarly as showed by Equations 3.51 and 3.52. Subsequently the limit state function $g(X_i)$ is redefined to be expressed in terms of the reduced variables. Afterwards the reliability index is calculated as the shortest distance from the origin of n-dimensional space of reduced variables to the curve described by limit state function $g(U_1, U_2, \ldots, U_n) = 0$.

In case the limit state function is non-linear it have to be approximated in the vicinity of the design point $[U_i^*]$ by some simpler function. It is done using Taylor's expansion series. When just the first order terms of Taylor's series are used the approximation function is linear and the method is then called FORM. When the second order terms are used in the Taylor's series the limit state function is approximated by a tangent hypersurface and the method is named SORM. The design point on the failure surface is normally unknown, therefore, it has to be found interactively minimizing β (see e.g. Melchers, 1999; Nowak & Collins, 2000).

If the random variables are not normal, they are approximated near the design point by normally distributed variables using for example the so-called 'tail approximation' method. However, when the random variables are correlated they are transformed to independent variables using Rosenblatt or Nataf transformation. Detailed information about those algorithms can be found in specialized literature (Melchers, 1999; Nowak & Collins, 2000).

3.4.2 Monte-Carlo method

The alternative procedure to calculate the probability of failure or the reliability index for any limit state function of arbitrary distributed variables is the Monte-Carlo method. In this method the probability of failure or reliability index is calculated based on the results of the large number, z, of the individual evaluation of the limit state function $g(X_i)$. Each individual evaluation, k, of the limit state function is obtained using random realisations x_{ik} of the underlining variables' distributions X_i.

In the simplest approach the probability of failure can be approximated as follows:

$$p_f \approx \frac{z_0}{z} \tag{3.55}$$

where z is total number of realisation of $g(X_i)$ and z_0 is the number of realisation for which $g(X_i) < 0$. The greater the number of z the more accurate is the approximation of p_f. Unfortunately for low probability of failures huge number of realisation is required to obtain reliable estimate of p_f.

Alternatively to counting z_0 and z, all the realisation of the limit state function could be analysed statistically in order to determine the corresponding probability distribution function, the mean value μ_g and the standard deviation σ_g. Subsequently, assuming that the realisations of $g(X_i)$ are normally distributed, the reliability index can be estimated as:

$$\beta \approx \frac{\mu_g}{\sigma g} \tag{3.56}$$

and the corresponding probability of failure p_f can be calculated according to Equation 3.48.

The 'crude' Monte Carlo method introduced above is very simple and intuitive, however, it requires significant computational effort. The derivatives of this method, so-called Importance Sampling methods, allow to reduce the minimum required number of realisation. Further information about those methods can be found, for example, in Melchers (1999).

3.5 Reliability of structural systems

The methods for estimating probability of failure p_f presented in previous section generally characterize the reliability of single element of the structure. However, the real structures are usually composed by several structural elements composing structural system where individual element failure not necessary leads to the failure of the whole system. For example, in statically indeterminate structures usually only combinations of failing elements cause the system failure but in statically determinate structures the failure of one element it is enough to cause total collapse.

3.5.1 Series system

In a series system the elements of the systems are connected in series and the failure of any of the elements causes the failure of the whole system (see Figure 3.11). The series system is often calls weakest link system due to its correspon-

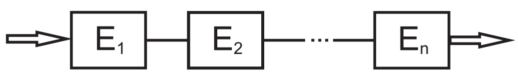

Figure 3.11: Series system.

dence to the chain which breaks when the weakest link brakes. The probability of failure of the series system is defined as follows:

$$P_f = 1 - \prod_{i=1}^{n}(1 - p_{fi}) \approx \sum_{i=1}^{n} p_{fi} \tag{3.57}$$

where p_{fi} are the probabilities of failure of the system's elements. The summation approximation is valid for small probabilities of failure p_{fi}. The probability of failure of the series system increase with the number of system's elements and is usually conditioned by the most failure prone element.

Equation 3.57 for calculation P_{fi} is valid only when all the elements of the system are statistically independent. The correlation between the elements of the series system reduce the probability of its failure. For perfectly correlated elements the probability of failure can be expressed as:

$$P_f = max[p_{fi}] \tag{3.58}$$

For partially correlated elements P_{fi} lays between the values defined by Equations 3.58 and 3.57.

3.5.2 Parallel system

In a parallel system the elements of the system are connected in parallel and just the failure of all the elements causes the failure of the whole system (see Figure 3.12). The probability of failure of the parallel system is defined as follows:

$$P_f = \prod_{i=1}^{n} p_{fi} \tag{3.59}$$

where p_{fi} are the probabilities of failure of the system's elements.

Again, Equation 3.59 for calculation P_{fi} is valid only when all the elements of the system are statistically independent. However, the correlation between the elements of the parallel system increase the probability of its failure. For perfectly correlated elements the probability of failure can be expressed as:

$$P_f = min[p_{fi}] \tag{3.60}$$

For partially correlated elements P_{fi} lays within the limits defined by Equations 3.59 and 3.60.

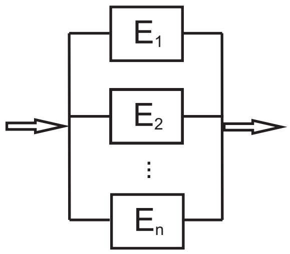

Figure 3.12: Parallel system.

3.5.3 Mixed system

In a mixed systems the elements of the system are connected in more complex way. However, usually they can be simplified to series or parallel system composed by several subsystems which can be either connected in series, parallel or some mixed way. The probability of failure of the mixed systems can be determined by a stepwise reduction to simple systems (see Figure 3.13). The probabilities of subsystems are calculated according to rules given in previous section.

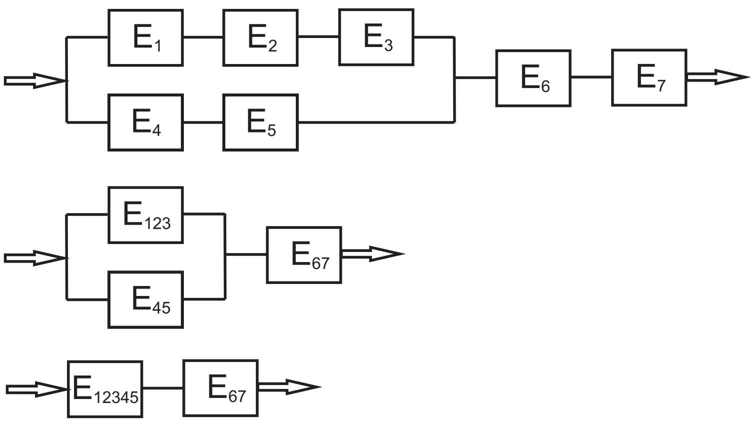

Figure 3.13: Mixed system.

3.6 Computational approaches for advanced reliability problems

3.6.1 General

The safety assessment of existing concrete bridges requires, in the process of structural analysis, the utilization of the most appropriate models allowing to describe the real behaviour under certain load condition (Casas *et al.*, 2005). In many cases there are used simple models that in the reliability analysis can be expressed by explicit limit state function $g(X)$. However, in some situations, where the imposed load or other conditions (e.g. corrosion of reinforcement, delamination of concrete, cracks etc.) may lead to the excursion of the structure into the non-linear behaviour in situations close to failure, more advanced theoretical models are needed. In those cases the performance function $g(X)$ is not available in an explicit form. It has to be computed through a numerical procedure such as finite element analysis (including non-linearities) or other numerical methods. This brings another level of complexity to the reliability analysis that is not possible to solve using analytical or traditional methods described in previous sections.

In the last decades, many computational approaches allowing to perform reliability analysis for the implicit performance function (e.g. available only due to non-linear FEM) were proposed. According to Haldar & Mahadevan (2000a) these can be broadly divided into three categories, based on their essential philosophy: Monte Carlo simulation (including efficient sampling method and variance reduction techniques), the Response Surface approach and a sensitivity based analysis (including Stochastic Finite Element Method). All those methods are briefly described in the following subsections.

3.6.2 Monte Carlo simulation

The most intuitive and probably the most commonly used method of structural reliability analysis is the Monte Carlo simulation technique. Using this technique it is possible to calculate the probability of failure or limit state violation for implicit and also explicit limit state function g(x) using the most basic background in probability and statistics.

The Monte Carlo simulation technique is based on the concept of random sampling in order to simulate artificially a large number of experiments and to observe the results. The availability of personal computers and software makes the process very simple even for a significant number of simulations (trials, runs) that are required to obtain reliable results. The Monte Carlo simulation method allows to evaluate even very complicated problems defined by complicated implicit functions as long as an algorithm (e.g. non-linear Finite Element code or non-linear sectional analysis code) is available to compute the structural response, given the values of the input variables. The method can easily evaluate $g(X)$ for each deterministic analysis and therefore compute the failure probability after performing several deterministic analyses.

The simplest Monte Carlo simulation technique, sometimes called 'crude' Monte Carlo, can be explained by the following six essential steps (Haldar & Mahadevan, 2000b):

- Define the problem in terms of all the random variables.
- Quantify the probabilistic properties of all the random variables in terms of their probability density functions and correlations.
- Randomly generate values for each random variable.
- Evaluate the problem deterministically for each set of realizations of all the random variables.
- Extract the required probabilistic information from N such realizations (e.g. determine how many sets from the total N evaluated sets lead to failure).
- Determine the accuracy and efficiency of simulation by increasing N and verifying that the final conclusion is robust and meets a certain level of accuracy.

The concept behind the Monte Carlo simulation is very simple, but its application in engineering reliability analysis and its acceptance as an alternative reliability evaluation method depends mainly on the efficiency of the simulation. Since the 'crude' Monte Carlo simulation requires a significant number of runs, it may not be practical when the deterministic analysis requires considerable computational effort as is the case when non-linear models are used with a very fine Finite Element mesh.

To improve the efficiency, the number of simulation cycles needs to be greatly reduced. More advanced simulation techniques such as the importance sampling method, the Latin Hypercube method or the directional sampling technique (Melchers, 1999) are often used. These advanced methods are based on the same principles as the 'crude' Monte Carlo method but employ some theoretical modifications, which would allow the reduction of the variance of the error of the estimated output variable without affecting the mean value and without increasing the sample size.

Latin Hypercube method is a special type of Monte Carlo numerical simulation described which uses the stratification of the theoretical probability distribution function of input random variables. In this method the range of possible values of each random input variable is partitioned into 'strata', and a value from each stratum is randomly selected as a representative value (Nowak & Collins, 2000). The representative values for each random variable are then combined in a way that they are used only once in the simulation. This procedure guarantees that all the input variables have been equally represented in the simulation.

The basic steps in Latin Hypercube sampling are as follows (Crespo, 1996; Nowak & Collins, 2000):

- Divide the range of each variable X_i into N intervals preferably of equal probability (probability of a value X_i occurring in each interval is 1/N).
- For each variable X_i and each of its N intervals select representative value for the interval (for large number of intervals the central point of each interval can be used, for small number of intervals centroid of the interval will be more appropriate).
- Shuffle the sets of the vector containing representative N values of each of the variable X_i.

- From the shuffled vectors create a fictitious matrix R with N rows and K columns, where K is the number of input random variables.
- Evaluate the problem deterministically for each N sets of realizations of all the random variables ordered in N rows of the matrix R.
- Based on the output obtained in previous step estimate the desired parameters and extract the required probabilistic information.

The algorithm has proved to be more efficient than the 'crude' Monte Carlo, reducing substantially the variance of the final estimates of the output parameters. It is very efficient for the estimation of the first two or three statistical moments of structural response and requires a relatively small number of simulations. However, in its original form the method may lead to the final matrix R with the accidental correlations between variables, especially when variables are divided into few intervals. On the other hand, in some situations statistical correlation between random variables defined by a prescribed correlation matrix have to be introduced. To solve that problems some modifications to the algorithm can be introduced (Florian, 1992; Iman & Conover, 1982).

3.6.3 Response Surface method

The Response Surface method provides an approach that can be used for the structural reliability analysis when a non-linear solution for the structural response is required. RSM constructs a polynomial closed-form approximation (usually a first order or second order polynomial is used) for the limit state function $g(X)$ through a few selected deterministic analyses. A regression analysis (or other curve fitting techniques) of the results provides an approximate closed-form expression that is used to search for the design point (the point on the limit state function closest to the origin in the normalized standard space of the random variables), and the failure probability is computed using first order (FORM) or second order (SORM) reliability methods as described in previous sections. A Monte Carlo simulation may also be used with the closed form approximation to estimate the failure probability. Clearly, the polynomial function needs to represent the structural response most accurately in the area around the design point with lower accuracy elsewhere. Provided the approximating response surface fits the point responses reasonably well, a fairly good estimate of the probability of structural failure would be expected

The implementation of the response surface concept may proceed along the following steps (Haldar & Mahadevan, 2000b):

- Select sets of values of the random variables to evaluate the performance function $g(X)$.

- Evaluate the performance function $g(X)$ at discrete values of x_i using a deterministic non-linear finite element analysis of the structure for all the sets of the values of the random variables selected in step 1.

- Construct a first-order (or higher) model of $g(X)$ using a regression analysis with the data collected in step 2.

- Use either FORM/SORM or Monte Carlo simulations with the closed form expression developed in step 3 to estimate the probability of failure or probability of limit state violation and extract the corresponding reliability index β.

The selection of the sets of the random variables could be preceded by the elimination of the variables which variability is not important, so, in further analysis can be considered as deterministic. After this pre-selection, which could reduce the size of the problem significantly, the selection of characteristic values (samples) has to be performed. Usually two or three values of each variable are used. If two values are used they are commonly selected as a low and a high value (e.g. $\mu \pm k\sigma$, where μ is the mean value, σ is the standard deviation and k is an integer). If three values are used they are commonly selected as a low, medium and a high value (e.g. $\mu + k\sigma$, μ , and $\mu + k\sigma$). In the case of the incorporation of the response surface method to the non-linear Finite Element analysis or other non-linear problems three or more values should be used to construct regression model of higher order which allows to better capture the possible non-linearity of the performance function.

It is noted that the response surface method is quite practical and effective in most common situations. However its application for highly non-linear performance functions, even when using its more advanced variants such as as the adaptive methods (Rajashekhar & Ellingwood, 1993) or DARS, Directional Adaptive Response Surface sampling method (Waarts, 2000), could be inefficient in some cases. Also, as a general rule, the closed-form approximation to $g(X)$ is valid only within the range of the values considered for the random variables and the extrapolation beyond that range may not be accurate. Thus, occasionally the method may lead to the evaluation of the safety for the less critical modes of failure.

Although the method described above is the most commonly used variant of response surface technique, some modifications and refinements to that method are continuously being introduced to improve its efficiency or accuracy. For example instead of using polynomial function and the regression analysis the suggestions have been made to approximate the performance function using Taylor series expansion (Ghosn & Frangopol, 1999) or advanced interpolation techniques with Splines or Kriging interpolations (Kaymaz, 2005; Schueremans & Van Gemert, 2005).

3.6.4 Sensitivity based analysis and probabilistic FEM

Other possible approach of structural reliability analysis applicable to non-linear problems e.g. non-linear FEM consists of methods based on sensitivity analysis. In this approach, the sensitivity of the structural response to the input variables is computed and used in FORM or SORM methods. The fundamental concept of the FORM and SORM method, the search for the design point or checking point, requires only the value and gradient of the limit state function at a number of selected points. The value of the performance function is available from deterministic structural analysis. The gradient is computed using a sensitivity analysis.

Since the performance function is implicit (can only be obtained at discrete points e.g. using finite element analysis) the gradient cannot be computed analytically by the numerical differentiation of the performance function. Thus, approximate methods such as finite difference methods and perturbation methods can be used to compute the gradient of the performance function (Haldar & Mahadevan, 2000b).

Once the derivatives of the performance function with respect to the random variables are computed and the value of the performance function is defined $g(X)$, this information can be used directly in FORM or SORM algorithms to estimate the reliability of the structure. Detailed information about these concepts can be found in Teigen *et al.* (1991), Val *et al.* (1996) and Val *et al.* (1997).

The sensitivity based reliability analysis is more elegant and more efficient than the Monte Carlo simulation and are more formally integrated into the theoretical formulation of the Finite Element solution as compared to the response surface method. Sensitivity based methods use information about actual value and the actual gradient of the performance function at each iteration during the search for the design point and use an optimization scheme to converge to the minimum distance point. The method however requires specialized programs that are not yet widely available or easily adaptable for practical applications.

3.7 Stochastic processes and return periods

3.7.1 Stochastic processes

Many of the loads acting on the structures are variable in time, for example: traffic loads, wind actions, snow, seismic actions. For this type of loads not only the individual values (point in time) are of interest but also their chronological sequence. Such loads can be described by the stochastic processes in time. For example, they can be recorded in regular time intervals and reproduced on the graph representing the process by plotting the recorded values and connecting them by straight lines (see Figure 3.14).

The stochastic process characterized by constant mean, variance and higher moments and by the constant correlation between the consecutive process realisations is called stationary.

Describing some type of load defined by the stationary stochastic process two types of histograms are usually useful. First is the histogram of average point in

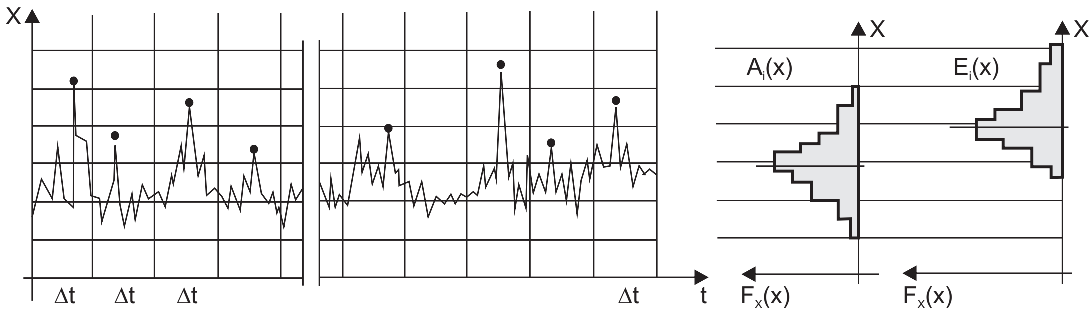

Figure 3.14: Stochastic process, from Schneider (1997).

time values $A_i(x)$ and second is the histogram of extreme values $E_i(x)$ in chosen time intervals Δt so-called reference periods (see Figure 3.14). The histogram of average point in time values is created from all the recorded data. However, the histogram of extreme values is created from the extreme values recorded within each of the time intervals for which the time is divided (often a period of one year is chosen).

3.7.2 Return periods

Sometimes the magnitude of the maximum load is not important and just the fact that the load cross some threshold value within some predefined period of time (e.g. lifetime of the structure) are of interest. The return period T is defined as the average time between two successive statistically independent events, for example exceedance of x, and is given by:

$$T = \frac{1}{1 - F_X(x)} \tag{3.61}$$

where $F_X(x)$ is the cumulative probability distribution function of the maximum of a random variable X within the reference period.

For example, when the annual probability that traffic load exceed some value x is equal to 0.02 (F(x)=1-0.02=0.98), the return period calculated according to Equation 3.61 will be 50 years. Using other words, the average time between two consecutive exceedence of value x characterized by annual probability 0.02 will be 50 years.

Chapter 4

Probabilistic models of material properties and geometry

4.1 Introduction

The theoretical models describing structural behaviour of reinforced or prestressed concrete structures requires basic information about the structure geometry (dimensions of the cross-section, position of the reinforcement, eccentricities, etc.) and about mechanical properties of the materials (compression strength of concrete, yielding strength of reinforcing steel, proportionality limits of prestressing steel, etc.). Therefore, in order to analyse the capacity of a structure or some of their member, it is required at first to define those parameters. However, the structure geometry as well as mechanical properties of materials composing the structure have a random nature and they should be treated as random variables. Consequently, in order to describe accurately the structural behaviour of the reinforced or prestressed concrete structure the complete probabilistic models (probability distribution function and basic statistics) of those variables are indispensable.

In this chapter the probabilistic models of basic mechanical properties of concretes (precast and cast-on-site) and steels (reinforcing and prestressing) are analysed. The probabilistic models of structure and structural member geometry are also presented and discussed. Besides the models available in the technical literature and in specialized codes or guidelines the probabilistic models developed within the program of this thesis are also presented. The original models were proposed for concrete ultimate strength (separately for precast and cast-in-place concretes) for precast bridge girders geometry, for proportionality limit and ultimate strength of prestressing steel and for yield and ultimate strength of reinforcing steel.

The original models of the mentioned mechanical and geometrical parameters were mainly developed to verify the applicability of the probabilistic models already available in the literature to the Portuguese conditions. However, the statistical analysis of data collected in the bridge girder precast plants and in the bridge sites also allows to validate the assumption of higher quality of precast bridges execution comparing to bridges constructed on-site.

4.2 Material models for concrete

4.2.1 Basics

Concrete is a composite material consisting of cement paste and aggregates. Due to its heterogeneity is characterized by strong non-linear and rheological behaviour. Normally, the mechanical behaviour of concrete is defined by few separate theoretical models. One, for the short-term loading (where long-term effects are neglected) describes standard stress-strain relationship. Others, for the long-term loading (where the rheology is crucial) describe the development of stresses and strains in time.

Under short-term monotonic quasi-static uniaxial loading the mechanical behaviour of concrete can be described by the schematic stress-strain relationship presented in Figure 4.1.

Although the probabilistic models of strength properties of concrete were an object of intensive study for many years, they often have much smaller influence on structural strength and ultimate behaviour than do reinforcement properties (Melchers, 1999). This is due to the commonly used philosophy of designing structures characterized by high level of ductility. Nevertheless, some mechanical

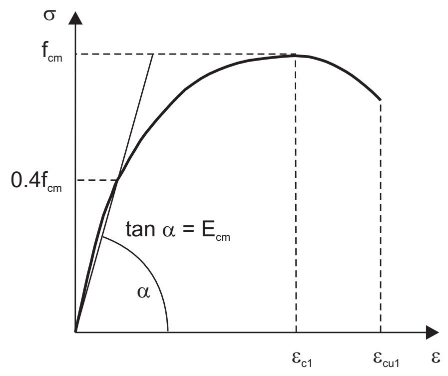

Figure 4.1: Typical stress-strain diagram for concrete.

properties of concrete are important for the structure serviceability and durability and for the ultimate strength of reinforced concrete columns.

The variability of the mechanical properties of concrete depends mostly on the following factors:

- material properties (cements, aggregates, etc.);
- concrete composition (water-cement ratio, cement quantity, etc.);
- execution (mixing, transporting, placing, curing and hardening, etc.);
- testing procedure (type and dimensions of specimens, velocity of the load application, etc.);
- concrete being in the structure rather in a control specimens;
- maintenance, material degradation, etc.;

The parameter of concrete which is investigated with higher frequency is the compressive strength f_c. This parameter serve commonly to control quality of concrete during structure execution and is used by the legal codes to define the acceptance/rejection criteria. Other mechanical properties, namely tensile strength f_{ct}, elasticity modulus E_c, ultimate strain ϵ_{cu}, etc., are sometimes also defined during experimental tests. However, due to high correlation with the concrete compressive strength they are usually defined via some empirical relations.

The rheological properties of concrete, namely ageing, creep and shrinkage, are also sometimes tested experimentally and exist reported statistical data on those properties. However, they are very sensitive to environment conditions and existing data is not sufficient to establish reliable probabilistic models.

In the following points the probabilistic models of most important material properties of concrete found in specialized codes and in the technical literature are resumed. Besides that the probabilistic models of concrete compressive strengths, for precast and cast-in-place concretes, developed within the program of this thesis are also presented.

4.2.2 Codes approach

Model proposed in Probabilistic Model Code. According to JCSS (2001) the strength of concrete at the particular point i in a given structure j as a function of standard strength f_{c0} is given by Equations 4.1 and 4.2.

$$f_{c,ij} = \alpha(t,\tau) f_{c0,ij}^{\lambda} Y_{1j} \tag{4.1}$$

$$f_{c0,ij} = \exp(U_{ij}\Sigma_j + M_j) \tag{4.2}$$

where:
$f_{c0,ij}$ is the lognormal variable, independent of Y_{1j}, with distribution parameters M_j and σ_j;
M_j is the logarithmic mean at job j;
σ_j is the logarithmic standard deviation at job j;
Y_{1j} is a lognormal variable representing additional variations due to the placing, curing and hardening conditions of in-situ concrete at job j (see Table 4.1);
U_{ij} is a standard normal variable representing variability within one structure;
λ is a lognormal variable with mean 0.96 and coefficient of variation 0.005 (generally it is possible to consider λ as deterministic parameter);
The remaining concrete properties as tensile strength, elasticity modulus and ultimate strain in compression are given by Equations 4.3, 4.4 and 4.5 respectively.

$$f_{ct,ij} = 0.3 f_{c,ij}^{2/3} Y_{2j} \tag{4.3}$$

$$E_{c,ij} = 10.5 f_{c,ij}^{1/3} Y_{3j} (1 + \beta_d \phi(t,\tau))^{-1} \tag{4.4}$$

$$\epsilon_{u,ij} = 6 \cdot 10^{-3} f_{c,ij}^{-1/6} Y_{4j} (1 + \beta_d \phi(t, \tau)) \tag{4.5}$$

where the variables Y_{2j}, Y_{3j} and Y_{4j} reflects variations due to factors not well accounted for by concrete compressive strength (gravel type and size, type of cement, etc.) and can be taken according to the Table 4.1.

Table 4.1: Data for parameters Y_i (JCSS, 2001).

Related to the parameter	Variable	Distr. type	Mean	Coef. of Var. [%]
compression	Y_{1j}	lognormal	1.0	6
tension	Y_{2j}	lognormal	1.0	30
elasticity modulus	Y_{3j}	lognormal	1.0	15
ultimate strain	Y_{4j}	lognormal	1.0	15

Note: if the direct measurements are available the parameters in table can be taken as parameters of equivalent prior sample with size n'=10

The distribution of $x_{ij} = \ln(f_{c0,ij})$ is normal if its parameters M and Σ are obtained from an infinitely large sample, but because the concrete production varies from production unit, site, construction period, etc. and the sample sizes are limited the parameters M and Σ must be treated as random variables. Then, x_{ij} has a Student distribution according to the Equation 4.6.

$$F_x(x) = F_{t_{v''}} \left[\frac{\ln(x/m'')}{s''} \left(1 + \frac{1}{n''}\right)^{-0.5} \right] \tag{4.6}$$

where $F_{t_{v''}}$ is the Student distribution for v'' degrees of freedom. $f_{c0,ij}$ can be represented by the Equation 4.7.

$$f_{c0,ij} = \exp \left[m'' + t_{v''} s'' \left(1 + \frac{1}{n''}\right)^{0.5} \right] \tag{4.7}$$

The values of m'', n'', s'' and v'' depends on the amount of specific information. Table 4.2 gives the values if no specific information is available (prior information). If $n''f'' > 10$ a good approximation of the concrete strength distribution is the lognormal distribution with mean m" and standard deviation $s''\sqrt{\frac{n''}{n''-1}\frac{v''}{v''-2}}$.

The spatial variability of the concrete properties in the member is considered assuming that the variables U_{ij} and U_{kj} are correlated by the correlation

Table 4.2: Prior parameters for concrete strength distribution (JCSS, 2001).

Conc. type	Conc. grade	Param. m'	Param. n'	Param. s'	Param. v'
Ready mixed	C15	3.40	3.0	0.14	10
	C25	3.65	3.0	0.12	10
	C35	3.85	3.0	0.09	10
	C45	3.98	3.0	0.07	10
	C55	—	—	—	—
Plant cast	C15	—	—	—	—
	C25	3.80	3.0	0.09	10
	C35	3.95	3.0	0.08	10
	C45	4.08	4.0	0.07	10
	C55	4.15	4.0	0.05	10

Note: f_{c0} in MPa; the prior parameters may depend on the geographical area and the technology with which concrete is produced

coefficient defined as follows (see Equation 4.8):

$$\rho(U_{ji}, U_{kj}) = \rho + (1-\rho)\exp\left[\frac{(r_{ij}-r_{kj})^2}{d_c^2}\right] \tag{4.8}$$

where $d_c = 5m$ and $\rho = 0.5$. For different jobs U_{ij} and U_{kj} are uncorrelated.

4.2.3 Existing probabilistic models

Concrete compressive strength. One of the first comprehensive probabilistic model of this parameter was proposed by Mirza *et al.* (1979). The model bases on the observations and analysis of experimental data collected by various authors in the United States, Canada and Europe. The model can be expressed by the following Equation 4.9:

$$f_{c,real} = f_{c,nominal} MFL \tag{4.9}$$

where $f_{c,real}$ is the real concrete compressive strength in the structure; $f_{c,nominal}$ is nominal concrete compressive strength; M is random variable relating real cylinder strength to nominal compressive strength; F is random variable relating in-situ strength to real cylinder strength; and L is random variable relating strengths obtained at different test conditions (e.g. velocity of load application).

In their work Mirza *et al.* (1979) concluded that the variable F relating the in-situ strength to the real cylinder strength has a normal distribution with a mean value varied from 0.74–0.96 and a coefficient of variation around 10%. Based on the works of other authors he also deduced that the mean value of the concrete cilinder compresive strength is about 5–7 MPa greater than the nominal value. However, the probability distribution functions describing properly the concrete cylinder compressive strength are normal or lognormal (for low strength concretes).

Considering those observations and neglecting the effect of the test conditions Mirza *et al.* (1979) suggest the following expression for the mean value of concrete compressive strength (see Equation 4.10):

$$\bar{f}_{c,real} = 0.675 f_{c,nominal} + 7.7 \leq 1.15 f_{c,nominal} \text{ [MPa]} \tag{4.10}$$

The coefficient of variation of real concrete compressive strength, proposed by Mirza *et al.* (1979), can be calculated due to Equation 4.11.

$$V_{c,real}^2 = V_M^2 + V_F^2 + V_L^2 \tag{4.11}$$

where V_M, V_F and V_L are coefficients of variation of variables M, F and L respectively.

Neglecting the effect of test condition, $V_L = 0\%$, assuming variation of concrete strength in a structure with a respect to the compressive strength of control cilinder, V_F, of 10% and considering that the strength of concrete measured by control cilinders includes variations in the "real" concrete strength and and the so-called "in-test" variations due to testing procedure, $V_M^2 = V_{c,cyl}^2 - V_{test}^2$ (where the variation within cilinder test $V_{test}^2 = 4\%$), the expression 4.11 can be simplified to the following Equation 4.12:

$$V_{c,real}^2 = V_{c,cyl}^2 + 0.0084 \tag{4.12}$$

where $V_{c,cyl}$ is the coefficient of variation for results for control cylinders taken on-site.

Based on the observations of other authors Mirza *et al.* (1979) also concluded that in general the coefficient of variation of compression strength of in-situ concrete test cylinders for high quality control oscillate around 7–10% and for normal quality control around 12–20%. This values refers to the test speciments from the same batch. When the test speciments are taken from different batches the additional dispersion are observed. For high quality control the additional coefficent of variation oscilate around 4–5% and for the normal control quality is close to 6%.

In the 90-ties Stewart (1995) proposed a probabilistic model which define the real in-situ concrete strength as a function of curing and compaction of concrete (see Equation 4.13):

$$f_{c,real} = f_{c,nominal} F k_{cr} k_{cp} \tag{4.13}$$

where $f_{c,real}$ is the real concrete compressive strength in the structure; $f_{c,nominal}$ is nominal concrete compressive strength; F is random variable relating real cylinder strength to nominal compressive strength; (k_{cr}) is random variable describing curing conditions and (k_{cp}) is random variable describing compaction.

Based on the collected data Stewart (1995) suggested to model k_{cp} by normal or lognormal probability distribution function with mean value oscillating between 0.8 and 1.0 for poor and good concretes respectively. However, for the k_{cr} he proposed to use the same distribution types as previously with mean value between 0.66 for poor concretes and 1.0 for concretes of good quality. The coefficient of variation of $f_{c,real}$ can be calculated assuming that the coefficient of variation of k_{cp} takes values between 6% and 0% for poor and good compaction respectively and the coefficient of variation of k_{cr} varies between 5% for poor concrets and 0% for concretes of good quality. However the variable F in Equation 4.13, relating in-situ strength to real cylinder strength, can be considered as in the previously described model.

Another comprehensive and relatively simple model was proposed by Bartlett & MacGregor (1996). It was developed based on the already described work of Mirza *et al.* (1979). The model can be expressed by the following Equation 4.14:

$$f_{c,real} = F_1 F_2 f_{c,nominal} \tag{4.14}$$

where $f_{c,real}$ is the real concrete compressive strength in the structure; $f_{c,nominal}$ is nominal concrete compressive strength; F_1 is random variable relating real cylinder strength to nominal compressive strength and F_2 is random variable relating in-situ strength to real cylinder strength.

The coefficient of variation of real concrete compressive strength, proposed by Bartlett & MacGregor (1996), can be calculated due to Equation 4.15.

$$V_{c,real}^2 = V_{F_1}^2 + V_{F_2}^2 \tag{4.15}$$

where V_{F_1} is the coefficient of variation of F_1 and V_{F_2} is the coefficient of variation of F_2.

Based on the experimental results performed in Canada Bartlett & MacGregor (1996) concluded that F_1 can be described by the normal or lognormal probability distribution function with the mean value of 1.25 and a standard deviation of 0.13 for concretes produced for cast-in-place constructions or a mean value of 1.19 and a standard deviation of 0.06 for concretes produced for precast production. However, F_2 at 28-days can be expressed by the lognormal distribution function with the mean value oscillating between 0.95 and 1.03 (depending on the element height) and the coefficient of variation of 14%. Bartlett & MacGregor (1996) suggest that the in-place strength for a given specified strength is uncertain due to the inherent randomness of factors F_1 and F_2 and also due to the variation in strength within the structure (spatial variability). The coefficient of variation due to spatial variability was assessed to vary between 7% for one member cast form one batch and 13% for many members casted from many batches.

Besides the already described models of concrete compressive strength in structures many others works characterizing statistically variations of concrete strength in the test cylinders exist. Sobrino (1993) proposed models based on the results collected on the bridge construction sites in Spain. Henriques (1998) studied the variability of strength of concretes used in the constructions of two viaducts in Portugal. In the Project Report PCSF (2002) authors present result of the study of the variability of strength of concretes used for production of precast elements (obtained due to test campaign in 20 Europeans precast plants). Moreover, Nowak & Szerszen (2003) published the results obtained for ordinary ready mix, high strength and plant cats concretes collected in the United States and used for the calibration of ACI Design Code for Buildings. The resume of all the results obtained by various authors in all the mentioned works and also some not mentioned in the text are presented in Tables 4.3 and 4.4.

Table 4.3: Statistical parameters of site-cast concrete.

Origin (*Reference*)	Nominal f_{ck} [MPa]	Bias λ_c	St. Dev. σ_c [MPa]	COV CV_c [%]
US, Canada and Europe, (*Mirza* et al., *1979*)	< 27 ≥ 27	— —	— 2.7 – 5.4	10 – 20 —
Sweden, (*see Thelandersson, 2004*)	35	1.24	—	8.5
Former Czechoslovakia, (*see Sobrino, 1993*)	20 – 25	1.17 – 1.33	2.8 – 4.6	9 – 14
Germany, (*see Sobrino, 1993*)	25 – 45	—	—	9 – 20
Spain, (*Sobrino, 1993*)	25 – 40	1.09 – 1.39	2.6 – 4.2	6 – 11
Canada, (*Bartlett & MacGregor, 1996*)	≤ 55	1.25	—	10
Portugal, (*Henriques, 1998*)	20 – 35	1.23 – 1.55	3.9 – 6.6	9 – 17
Austria, (*Strauss, 2003*)	25 – 50	1.02 – 2.04	1.0 – 2.7	2 – 6
United States, (*Nowak & Szerszen, 2003*)	21 – 41 48 – 83	1.12 – 1.35 1.04 – 1.19	1.5 – 4.9 5.4 – 9.0	4 – 15 9 – 12

Note: in general the lower values of bias factors, standard deviations and coefficient of variations corresponds to concretes of higher resistance

Table 4.4: Statistical parameters of plant-cast concrete.

Origin (*Reference*)	Nominal f_{ck} [MPa]	Bias λ_c	St. Dev. σ_c [MPa]	COV CV_c [%]
Germany, (*see Sobrino, 1993*)	50 – 65	—	—	6
Canada, (*Bartlett & MacGregor, 1996*)	≤ 55	1.19	—	5
Europa, (*PCSF, 2002*)	40 – 90	—	2.0 – 6.0	3 – 11
United States, (*Nowak & Szerszen, 2003*)	34 – 45	1.14 – 1.38	4.1 – 5.7	8 – 12

Note: in general the lower values of bias factors, standard deviations and coefficient of variations corresponds to concretes of higher resistance

As it was already mentioned before the concrete strength in the structure is usually somehow smaller than the strength of the concrete test cylinders. In the literature exist some models which allowed to relate the compressive strength of the standard test cylinder with the compressive strength of cores drilled from the structure. Besides the already described works of Mirza *et al.* (1979) and Bartlett & MacGregor (1996) the study performed by Gonçalves (1987) and the study performed within European Research Project "Precast Concrete Safety Factors" (PCSF, 2002) are examples of significant importance. In Table 4.5 the models proposed by various authors are presented.

Table 4.5: In-situ concrete compressive strength versus test cylinder strength.

Origin *(Reference)*	Type of Distrib.	Mean μ	Coef. of Var. CV [%]
US, Canada and Europe, *(Mirza* et al.*, 1979)*	Not specified	0.74 – 0.96	10
Portugal, *(Gonçalves, 1987)*	Not specified	0.69 – 1.02	3 – 14[(a)]
Canada, *(Bartlett & MacGregor, 1996)*	Lognormal	0.95 – 1.03	14
Europa, *(PCSF, 2002)*	Deterministic	0.86	—

[(a)] depending on the element type (slab, beam, etc.) and curing and compaction condition

Other mechanical properties of concrete. Besides compressive strength the properties of concrete that are of interest are: tensile strength, f_{ct}; elasticity modulus, E_c; and ultimate strain in compression, ϵ_{cu}. Unfortunately there are not many publications where some probabilistic models of those parameters are presented. However, in references (Mirza *et al.*, 1979; Spaethe, 1992) some models can be found.

The concrete uniaxial splitting tensile strength, according to Mirza *et al.* (1979), can be modelled by the normal distribution with the mean value calculated by the Equation 4.16 (where f_c is the concrete compressive strength) and with the coefficient of variation equal to 13%.

$$f_{cts} = 0.53 f_c^{1/2} \text{ [MPa]} \tag{4.16}$$

The concrete uniaxial flexural tensile strength can be modelled by the normal distribution with the mean value calculated by the Equation 4.17 and with the coefficient of variation equal to 20%.

$$f_{ctf} = 0.69 f_c^{1/2} \text{ [MPa]} \tag{4.17}$$

However Spaethe (1992) suggests to model the uniaxial splitting tensile strength by the normal or lognormal distribution function with the mean value defined by the Equation 4.18 (where f_c is the concrete compressive strength) and with the coefficient of variation of 18–20%.

$$f_{cts} = 0.30 f_{ck}^{2/3} \text{ [MPa]} \tag{4.18}$$

For the high strength concretes (>C50/60), according to EC-2 (2004), the following relation should be used 4.19:

$$f_{cts} = 2.12 \ln\left(1 + \frac{f_{cm}}{10}\right) \text{ [MPa]} \tag{4.19}$$

The concrete initial tangent elasticity modulus, according to Mirza *et al.* (1979), can be modelled by the normal distribution with the mean value calculated by the Equation 4.20 (where f_c is the concrete compressive strength) and with the coefficient of variation equal to 8%.

$$E_{ci} = 5015 f_c^{1/2} \text{ [MPa]} \tag{4.20}$$

The concrete secant elasticity modulus (at 30% of maximum stress) can be modelled by the normal distribution with the mean value defined by the equation 4.21 and the coefficient of variation of 12%.

$$E_{cs} = 4600 f_c^{1/2} \text{ [MPa]} \tag{4.21}$$

However, according to EC-2 (2004), the following relation should be used to model secant elasticity modulus up to 40% of maximum stress (see Equation 4.22):

$$E_{cs} = 22000 f_c^{0.3} \text{ [MPa]} \tag{4.22}$$

The Equation 4.22 refers to the concretes with quartzite aggregates. For limestone and sandstone aggregates the value should be reduced by 10% and 30% respectively. For basalt aggregates the value should be increased by 20%.

4.2.4 Obtained experimental results

In order to verify the correspondence between the probabilistic models of the most important concrete properties presented in previous section and variability of those properties observed in the precast concrete bridges in Portugal a significant amount of data was collected and analysed statistically within the program of this thesis. The analysed data was made available for this study by the concrete laboratories of one civil engineering contractor and two precast concrete companies from north of Portugal.

The statistical evaluation of data confirmed that normal and lognormal probability distribution functions describes accurately variability of concrete compressive strength. The basic statistics of that property obtained in the analysis are showed in Tables 4.6 and 4.7. The results presented in tables correspond to concrete compressive strength at 28 days tested on the standard specimens used for the purpose of the quality control.

The complete outcome of the performed statistical analysis is presented in the report Wiśniewski *et al.* (2006c) and its resume can be find in the Appendix A.

Table 4.6: Statistical parameters of site-cast concrete.

Origin, *(Reference)*	Nominal f_{ck} [MPa]	Bias fact. λ_c	St. Dev. σ_c [MPa]	Var. coef. CV_c [%]
Portugal, *(see Appendix A)*	25	1.26	2.9	7.7
	30	1.18	3.3	7.5
	40	1.18	3.4	5.8

Table 4.7: Statistical parameters of plant-cast concrete.

Origin, *(Reference)*	Nominal f_{ck} [MPa]	Bias fact. λ_c	St. Dev. σ_c [MPa]	Var. coef. CV_c [%]
Portugal, *(see Appendix A)*	35	1.08	2.3	4.7
	40	1.08	2.4	4.5
	45	1.00	2.2	3.9
	30	1.23	4.0	8.8
	45	1.02	2.9	5.2

4.2.5 Proposed probabilistic models

Despite the fact that the analysed amount of data, regarding concrete compressive strength at 28 days, was quite significant and corresponds to the production of concrete of several producers during significant period of time the results presented in previous section are not exhaustive. However, comparing the results showed in Tables 4.6 and 4.7 with those presented in Tables 4.3 and 4.4 it can be observed that they are very similar, especially when comparing them with just the most recent data. Therefore, it can be assumed that the results obtained in the performed study and presented in Tables 4.6 and 4.7 are representative for the concrete compressive strength in the test specimens of site-cast and plant-cast concretes used for the construction of bridges in Portugal.

In order to define compressive strength of concrete in structure one of the models described previously in this chapter may be used. In particular the model proposed by Bartlett & MacGregor (1996) (defined by Equations 4.14 and 4.15) can be recommended as relatively simple and sufficiently comprehensive. The distribution function recommended to use are normal and lognormal.

Considering above mentioned model and using somehow averaged values of the parameters presented in Tables 4.6 and 4.7 the following statistical parameters of 28 days concrete compressive strength in structures were obtained:

- for site-cast concrete: $f_{c,real} = 1.0 \times f_{c,nominal}$ considering $F_1 = 1.20$ and $F_2 = 0.85$; $V_{c,real} = 12\%$ considering $V_{F_1} = 7\%$ and $V_{F_2} = 10\%$.
- for plant-cast concrete: $f_{c,real} = 1.0 \times f_{c,nominal}$ considering $F_1 = 1.10$ and $F_2 = 0.90$; $V_{c,real} = 9\%$ considering $V_{F_1} = 5\%$ and $V_{F_2} = 8\%$.

Lower value of F_2 and a bit bigger V_{F_2} were chosen for site-cast concrete due to the fact that the level of concrete compaction in those structures is usually not as good as in plant-cast structures.

Regarding probabilistic models of other concrete properties, the tensile strength can be modelled by normal or lognormal distribution with the mean value calculated using Equation 4.18 and with the coefficient of variation of 20%. The elasticity modulus can be modeled by normal distribution with the mean value defined by the Equation 4.22 and with the coefficient of variation of 8%.

4.3 Material models for reinforcing steel

4.3.1 Basics

The mechanical behaviour of the reinforcing steel is characterized by the ultimate tensile strength, by the yielding strength and by the ductility or deformation capacity. Knowing all those parameters it is possible to define unambiguously the reinforcing steel behaviour expressed by the stress-strain curves. In Figure 4.2 the typical stress-strain curve for hot rolled steel is presented.

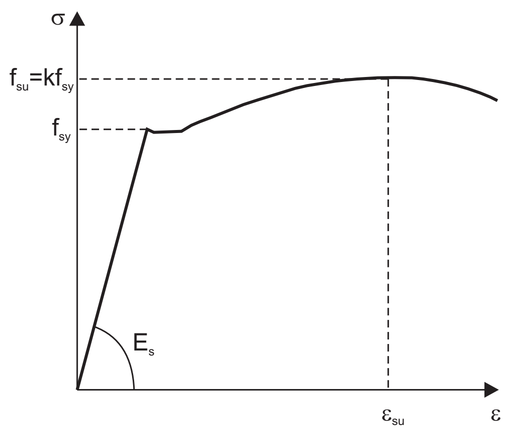

Figure 4.2: Typical stress-strain diagram for reinforcing steel.

The variability of mechanical properties of reinforcing steel is generally lower than variability of parameters describing concrete. This is mostly due to higher industrialization of the production and higher level of the quality control. According to Sobrino (1993) the principal factors that influence the variability of mechanical behaviour of reinforcing steel bars are as follows:

- variability of the material strength (which depends of material itself, fabrication process, producer, etc.);
- variability of bar's geometry;
- material degradation (e.g. corrosion);
- load history (fatigue phenomena);

- method of definition of the conventional strength parameters f_{sy} and f_{su} and their's experimental evaluation (type of the test, velocity of the load application, etc.);

Several mechanical properties of the reinforcing steel can be defined during experimental tests, namely yielding strength f_{sy}, ultimate strength f_{su}, ultimate strain ϵ_{su}, etc. However, the property which is tested most often is the yielding strength. Remaining parameters describing steel behaviour are investigated with lower frequency. Even so the existing results allow to define the probabilistic models of those properties and allow to check the correlations between them. Some data about variation in the bar diameters and related with it bar area A_s are also collected and probabilistic models are proposed.

In the following points the probabilistic models of most important material and geometrical properties of the reinforcing steel found in specialized codes and in the technical literature are resumed. Besides that the probabilistic models developed within the program of this thesis are also presented.

4.3.2 Codes approach

Model proposed in Probabilistic Model Code. According to JCSS (2001), the yield stress of the reinforcing steel bar can be defined as the sum of three independent Gaussian variables (see Equation 4.23)

$$X_1(d) = X_{11} + X_{12} + X_{13} \tag{4.23}$$

where:
$X_{11} = N(\mu_{11}(d), \sigma_{11})$ represents the variations related to different steel producers,
$X_{12} = N(0, \sigma_{12})$ represent the batch to batch variation,
$X_{13} = N(0, \sigma_{13})$ represent the variation within the single batch and
d is the nominal bar diameter.

For a steel production of good quality the following values of standard deviations can be used: $\sigma_{11} = 19$ MPa, $\sigma_{12} = 22$ MPa and $\sigma_{13} = 8$ MPa resulting in an overall standard deviation $\sigma_1 = 30$ MPa. The mean value of the yield strength is defined by the Equation 4.24.

$$\mu_1 = S_{nom} + 2\sigma_1 \tag{4.24}$$

The Table 4.8 shows remaining steel parameters as defined in JCSS (2001). However Table 4.9 shows the correlations between all the parameters. For all the quantities presented in the Table 4.8 normal distribution can be adopted.

Table 4.8: Statistical parameters of reinforcing steel (JCSS, 2001).

Steel Property	Mean value X_{mean}	Standard dev. σ_X	Coef. of Var. CV
Bar area A_s	$A_{s,nom}$	—	2.0%
Yield strength f_{sy}	$f_{sy,nom} + 2\sigma$	30 MPa	—
Ultimate strength f_{su}	—	40 MPa	—
Ultimate strain ϵ_{su}	—	—	9.0%

Table 4.9: Correlations between parameters of reinforcing steel (JCSS, 2001).

	Bar area A_s	Yield strength f_{sy}	Ult. strength f_{su}	Ult. strain ϵ_{su}
Bar area	1.00	0.50	0.35	0.00
Yield strength	0.50	1.00	0.85	−0.50
Ult. strength	0.35	0.85	1.00	−0.55
Ult. strain	0.00	−0.50	−0.55	1.00

4.3.3 Existing probabilistic models

Yield strength of reinforcing steel. The probabilistic model of this parameter was already proposed in the end of the 70-ties by Mirza & MacGregor (1979a) when the first generation of partial safety factor design codes were under development. The proposed model bases on the experimental data collected in the United States, Canada and Europe mostly in the 50-ties and 60-ties.

In the last decades also some probabilistic models were defined based on the more recent data collected in Europe. Among others, the works of Sobrino (1993) and Pipa (1995) should be mentioned here as the examples of great relevance.

Aiming to verify hypothesis about higher quality of ordinary reinforcing steel produced nowadays in comparison to the steels produced in past decades numerous data of yielding tensile strength were collected recently in the United States.

Based on those data probabilistic models were developed by Nowak & Szerszen (2003) and they where used in the calibration of the latest version of the ACI design code for buildings.

In Europe also new campaign of data collection was recently performed and the probabilistic models for produced reinforcing steels bars were proposed by Strauss (2003).

In Table 4.10 the resume of the experimental results obtained by various authors is presented. Table shows the nominal values, the bias factors and the coefficients of variations of the steel yield strength. It is important to notice that the coefficients of variation presented in the table are affected by all the sources of uncertainty as: variation in the strength of material itself, variation in the area of the cross-section, effect of bar diameter on properties of bars and effect of strain at which yield is defined.

Table 4.10: Experimental results of steel yielding strength.

Origin *(Reference)*	Nominal value f_{syk} [MPa]	Bias fact. λ_{sy}	Coef. of Var. CV_{sy} [%]
Denmark, *(see Sobrino, 1993)*	370 – 420	—	4 – 5$^{(a)}$; 10$^{(b)}$
Sweden, *(see Sobrino, 1993)*	—	—	8$^{(b)}$
US, Canada and Europe, *(Mirza & MacGregor, 1979a)*	280 410	1.20 1.20	10.7$^{(b)}$ 9.3$^{(b)}$
France, *(see Henriques, 1998)*	—	—	4$^{(a)}$; 10$^{(b)}$
Spain, *(Sobrino, 1993)*	500	1.20	8.1$^{(b)}$
Europe, *(Pipa, 1995)*	400 500	1.24 1.17	4.7$^{(b)}$ 5.2$^{(b)}$
Europe, *(Strauss, 2003)*	500	1.156	2.3$^{(b)}$
US, *(Nowak & Szerszen, 2003)*	420	1.145	5.0$^{(b)}$

$^{(a)}$ samples derived from one batch; $^{(b)}$ samples derived from different batches or sources

As can be observed the bias factor which relates the mean value obtained from the experimental test with the nominal or expected value, regardless to the steel grade, oscillate around value 1.20 except two last cases when it is close to 1.15. The coefficients of variation obtained for the specimens taken from the same batch or from the same producer are taking values around 4–5%. However the coefficients of variations obtained for the speciments taken from different sources are oscilating around 8–10% except the cases of the most recent results when the coefficients of variation are between 2.5% and 5%. Observed significant difference in the coefficient of variation between data collected in the past decades and that collected recently could be explained by the improvements of the fabrication process and by more stricted requirements related to the control of quality.

Regarding the types of the probability distribution functions, various authors suggest different theoretical models. Nowak & Szerszen (2003) use the normal probability distribution function to model the yield strength of reinforcing steel. However, other authors recommend lognormal distribution (Sobrino, 1993) or Beta distribution (Mirza & MacGregor, 1979a) as more appropriate.

Other properties of reinforcing steel. Besides the yield strength of steel some other properties were also observed by several authors. Tables 4.11, 4.12 and 4.13 show the results of experimental test gathered and statistically treated by Sobrino (1993) and Pipa (1995). The results correspond to steel grades S500 and S400 produced in Europe.

Table 4.11: Experimental results obtained by Sobrino (1993) for S500 steel grade.

Steel Property	Mean value X_{mean}	Min. value X_{min}	Max. value X_{max}	Coef. of Var. CV
Ultimate strength f_{su}	690 MPa	614 MPa	856 MPa	7.8%
Yield strength f_{sy}	602 MPa	511 MPa	770 MPa	8.1%
Ratio f_{su}/f_{sy}	1.147	1.055	1.250	4.0%
Ultimate strain ϵ_{su}	23.3%	12.6%	30.3%	12.7%
Ratio $A_{s,real}/A_{s,nom}$	1.005	0.965	1.055	2.1%

Analysing the results presented in those tables, it can be observed that for the reinforcing steel bars produced in Europe the ultimate strength is 15 to 20% higer than yield strength. Results obtained by Strauss (2003) are nearly the same. However, based on data collected in US, Canada and Europe Mirza & MacGregor (1979a) concluded, that ultimate strength of reinforcing bars is aproximatelly 55% higher than yield strength.

Table 4.12: Experimental results obtained by Pipa (1995) for S400 steel grade.

Steel Property	Mean value X_{mean}	Min. value X_{min}	Max. value X_{max}	Coef. of Var. CV
Ultimate strength f_{su}	598 MPa	552 MPa	646 MPa	3.3%
Yield strength f_{sy}	496 MPa	431 MPa	544 MPa	4.7%
Ultimate strain ϵ_{su}	11.8%	7.5%	16.0%	14.3%
Inic. of hard. ϵ_{sh}	2.2%	1.6%	3.1%	20.0%
Modul. of hard. E_{sh}	3.00 GPa	2.17 GPa	5.02 GPa	22.0%

Table 4.13: Experimental results obtained by Pipa (1995) for S500 steel grade.

Steel Property	Mean value X_{mean}	Min. value X_{min}	Max. value X_{max}	Coef. of Var. CV
Ultimate strength f_{su}	680 MPa	613 MPa	752 MPa	4.2%
Yield strength f_{sy}	585 MPa	519 MPa	656 MPa	5.2%
Ultimate strain ϵ_{su}	9.4%	6.0%	13.0%	14.9%
Inic. of hard. ϵ_{sh}	1.4%	0.7%	2.3%	31.0%
Modul. of hard. E_{sh}	3.51 GPa	2.72 GPa	5.33 GPa	15.0%

Mirza & MacGregor (1979a) observed as well that the coefficients of variation of the ultimate strength is very similar to the coefficient of variation of the yield strength. It can be explained by the fact of the same sources of variation for this two parameters. The results obtained by Sobrino (1993) and Strauss (2003) confirm this observation. However, analysing result of Pipa (1995) it can be noticed that coefficient of variation of ultimate strength is slightly lower than this corresponding to the yield strength.

Regarding the probability density functions, various authors suggest different types. However, in general they recommend to be consistent and use the same distribution for ultimate and yield strength.

In their work, besides the already discussed ultimate and yield strengths of steel, Mirza & MacGregor (1979a) analysed also the ratio of the real to notional reinforcing bar area. They concluded that the mean value of this parameter oscillate between 0.96 and 1.20. However the coefficient of variation takes the values between 0.2% and 9%. Sobrino (1993) obtained results of 1.005 for mean value of the ratio and 2.1% for its coefficient of variation. The type of the probability distribution function considered by both authors most appropriate for modeling this parameter is the Gaussian distribution.

Mirza & MacGregor (1979a) proposed also the probabilistic models of steel elasticity modulus. The recommended distribution type is the normal distribution with the mean value of 201 GPa and coefficient of variation 3.3%.

As it can be observed in Tables 4.11, 4.12 and 4.13, the ultimate strain of reinforcing steel is characterized by relatively high coefficient of variation oscillating between 12-15%. The mean values of the ultimate strain are taking values between 9 and 24%. Similar results of the mean ultimate strains were obtained by Strauss (2003). However, the coeficients of variation were smaller, around 8%.

4.3.4 Obtained experimental results

In order to verify the correspondence between the probabilistic models of the properties of reinforcing steel bars presented in previous section and variability of these properties observed on construction-sites in Portugal the significant amount of data were collected and analysed statistically. The analysed data were made available for this study by the Department of Civil Engineering of the University of Coimbra. The data were collected for reinforcing bars of various diameters (10–25 mm) and for steels S500 of normal (NR) and special (NRSD) ductility.

The statistical evaluation of data confirmed that normal and lognormal probability distribution functions describes accurately variability of most of the properties of reinforcing steel bars. The basic statistics of all the parameters obtained in the analysis are showed in Tables 4.14 and 4.15. The results presented in Tables correspond to properties tested on the standard specimens. The complete outcome of the performed statistical analysis is presented in the Appendix B.

4.3.5 Proposed probabilistic models

Although the analysed amount of data, regarding properties of reinforcing steel bars, was quite significant the results presented in previous section are not sufficient to propose reliable probabilistic models. However, comparing the results showed in Tables 4.14 and 4.15 with those presented in Tables 4.10, 4.11, 4.12

Table 4.14: Experimental results of reinforcing steel strength.

Origin *(Reference)*	Str.	Nominal val. [MPa]	Bias fact. λ	Coef. of Var. CV [%]
Portugal, *(see Appendix B)*	f_{sy}	500	1.21	6.0
	f_{su}	550	1.28	5.9
	f_{sy}	500	1.16	5.5
	f_{su}	575	1.20	4.9

Table 4.15: Experimental results of other properties of reinforcing steel.

Origin *(Reference)*	Param.	Nominal value	Bias λ	Var. Coef. CV [%]
Portugal, *(see Appendix B)*	f_{us}/f_{ys}	1.10 (1.15)	1.06 (1.04)	3.3 (2.8)
	E_s	200 GPa	1.01 – 1.03	1.0 – 4.9
	ϵ_s	5% (8%)	2.7 (1.64)	24.5 (19.2)
	A_s	10–25 mm^2	0.92 – 0.94	4.3 – 4.4

Values in the parenthesis corresponds to steel bars of special ductility.

and 4.13 it can be observed that they are quite similar especially when comparing them to the most recent data. Therefore, it can be assumed that the results obtained in the performed study are representative for the reinforcing steel bars used in the construction of bridges in Portugal.

Based on the results presented mostly in Tables 4.14 and 4.15 but also in Tables 4.8–4.15 the following statistical parameters of strength properties of reinforcing steel are recommended for using in the probabilistic analysis:

- yield strength: for older steels λ=1.20 and CV=10%; for modern steels λ=1.15 and CV=5%.
- ultimate strength: 15-20% higher than yield strength; CV=10% and CV=5% for older and modern steels respectively.

Both properties can be modelled by lognormal or normal probability distribution function.

Regarding probabilistic models of other properties of reinforcing steel, the ultimate strain can be modelled by lognormal or normal distribution function with mean value equal to 10% and the coefficient of variation equal to 15%. Steel elasticity modulus can be modelled by normal distribution with the mean value equal to 202 GPa and the coeficient of variation of 4%. The area of reinforcement can also be modelled by normal distribution with coeficient of variation of 2% and the mean value equal to nominal.

4.4 Material models for prestressing steel

4.4.1 Basics

The mechanical behaviour of the prestressing steel is characterized by the ultimate tensile strength, by the proportionality limits and by the ductility or deformation capacity. In Figure 4.3 the typical stress-strain diagram of prestressing steel in uniaxial tension is presented.

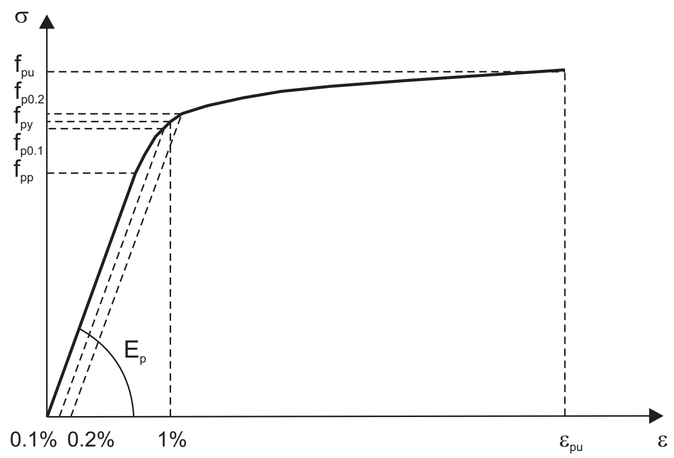

Figure 4.3: Typical stress-strain diagram for prestressing steel.

As in the case of reinforcing steel the variability of mechanical behaviour of prestressing steel bars, strands or wires depends on the following factors:

- variability of the material strength (which depends of material itself, fabrication process, producer, etc.);
- variability of wire, strand or bar geometry;

- material degradation (e.g. corrosion);
- load history (fatigue phenomena);
- method of definition of the conventional strength parameters f_{py} and f_{pu} and their's experimental evaluation (type of the test, velocity of the load application, etc.);

Due to the fact that prestressing steel do not have a distinct yield point their yield stress is determined according to strain criteria. Depending on the standard, the yield stress f_{py} can be defined as the stress at 0.1% offset, $f_{p0.1}$, as the stress at 0.2% offset, $f_{p0.2}$ or as the stress that corresponds to total strain of 1% for wires and strands and of 0.75% for prestressing bars. Besides those parameters defining proportionality limits for prestressing steel, other mechanical properties as ultimate tensile strength f_{pu}, modulus of elasticity E_p, ultimate strain ϵ_{pu}, are also of interest.

In the following points the probabilistic models of most important material properties of the prestressing steel found in codes and in the specialized literature are resumed. The probabilistic models developed based on data collected in Portugal are also presented.

4.4.2 Codes approach

Model proposed in Probabilistic Model Code. According to JCSS (2001), the variability of mechanical properties of prestressing steel can be described by the following independent Gaussian variables: f_{pu}, E_p and ϵ_{pu}. Statistical parameters of these variables are presented in Table 4.16, where f_{pk} is the characteristic (nominal) tensile strength of prestressing steel which usually denotes the steel grade.

According to JCSS (2001), due to the strong correlations between the ultimate tensile strength f_{pu} and other stresses that characterize the stress-strain diagram (f_{pp}, $f_{p0.1}$, $f_{p0.2}$, f_{py}), these stresses can be expressed via ultimate tensile strength f_{pu}. Table 4.17 shows the relations between the stresses and f_{pu} which can be adopted when the steel supplier does not provide more adequate informations.

Table 4.16: Statistical parameters of properties of prestressing steel (JCSS, 2001).

Steel Property	Mean value X_{mean}	Stand. dev. σ_X	Coef. of Var. CV
Ultimate strength f_{pu}	$1.04 f_{pk}$	—	2.5%
	$f_{pk} + 66$ MPa	40 MPa	—
Elasticity modulus E_p	200 GPa$^{(a)}$, 195 GPa$^{(b)}$	—	2.0%
Ultimate strain ϵ_{pu}	0.05	0.0035	—

$^{(a)}$ for bars and wires; $^{(b)}$ for strands

Table 4.17: Relations between f_{pu} and proof stresses (JCSS, 2001).

Steel type	Stress f_{pp} (proportional)	Stress $f_{p0.1}$ (0.1% offset)	Stress $f_{p0.2}$ (0.2% offset)	Stress f_{py} (1% strain)
Wire	$0.70 f_p$	$0.86 f_p$	$0.90 f_p$	$0.85 f_p$
Strand	$0.65 f_p$	$0.85 f_p$	$0.90 f_p$	$0.85 f_p$
Bar	—	—	—	$0.85 f_p$

4.4.3 Existing probabilistic models

Strength of prestressing steel. The statistical parameters of the prestressing steel mechanical properties were not so well reported before the middle of the 90-ties. However, some probabilistic models based on data from United States were already proposed by Mirza *et al.* (1980) two decades ago.

In the beginning of the 90-ties some results of experimental tests performed in the United States were published (Devalapura & Tadros, 1992). However, the number of tested samples was relatively low and the probabilistic models proposed based on those results were not sufficiently reliable.

The important step on the definition of probabilistic models of prestressing steel mechanical properties was done by Sobrino (1993). He proposed model based on data from more than 800 results of strength test performed in Spain.

Recently significant amount of data was gathered in United States and in Europe in order to upgrade the existing probabilistic models of prestressing steel strength parameters. The upgraded models corresponding to North American production were proposed by Nowak & Szerszen (2003). However, Strauss (2003) proposed models based on European data.

In Table 4.18 the resume of the experimental results obtained by various authors is presented. Table shows the nominal values, the bias factors and the coefficients of variations of the prestressing steel ultimate and theoretical yield strengths. The theoretical yield was considered, in the most cases presented in the table, as the stress corresponding to 1% strain.

Table 4.18: Experimental results of prestressing steel strength.

Origin *(Reference)*	Str.	Nominal val. [MPa]	Bias λ	Coef. of Var. CV [%]
US, *(Mirza et al., 1980)*	f_{pu}	—	—	2.5
France,	f_{py}	—	—	2.0 – 5.5
(see Sobrino, 1993)	f_{pu}	—	—	1.5 – 4.5
United States,	f_{py}	—	—	3.0
(see Sobrino, 1993)	f_{pu}	—	—	1.0
United States,	f_{py}	1670	1.06	1.3
(Devalapura & Tadros, 1992)	f_{pu}	1860	1.02	1.1
Spain,	f_{py}	1670	1.04 – 1.06	1.7 – 2.5
(Sobrino, 1993)	f_{pu}	1860	1.04 – 1.06	1.8 – 2.0
Europe,	$f_{p0.2}$	1570	1.07 – 1.14	0.6 – 2.3
(Strauss, 2003)	f_{pu}	1770	1.03 – 1.08	0.5 – 2.2
United States,	f_{pu}	1720	1.07 – 1.14	1.0 – 3.0
(Nowak & Szerszen, 2003)	f_{pu}	1860	1.04 – 1.06	1.0 – 3.0

As can be observed the bias factor which relates the mean value obtained from the experimental test with the nominal or expected value take values between 1.02 and 1.08 for the ultimate strength. However, the values of the bias factor for the theoretical yield are slightly higher. The coefficient of variation of the ultimate steel strength oscillates around 0.5–3.0%. The coefficients of variations obtained for yield strength are on the same order.

In opposite to ordinary reinforcing steel it was not possible to observe significant improvements in the quality of prestressing steels produced nowadays in comparison to steels produced some decades ago. It can be explained by the fact that the quality of the production of prestressing steel was always very high.

Regarding the types of the probability distribution functions, Nowak & Szerszen (2003) propose to use Gaussian distribution function to model the ultimate strength of prestressing steel. Sobrino (1993) recommends to use lognormal distribution. However, Strauss (2003) concludes that either normal, lognormal or gamma distributions types can be applied.

Other properties of reinforcing steel. Besides the statistical distribution of the ultimate tensile strength and the yield strength the probabilistic models of some other prestressing steel properties were proposed by Sobrino (1993) based on collected experimental data. Tables 4.19 and 4.20 show the results obtained for strands of 0.5" and 0.6" diameter with the characteristic (nominal) ultimate strength equal to 1860 MPa. However, the results were originally presented as the loads registered by the strength machine, in the tables they are presented in stress convention. The stresses in the specimens corresponding to certain level of load were calculated assuming nominal strand area equal to $0.987cm^2$ and $1.40cm^2$ for 0.5" and 0.6" strands respectively.

Table 4.19: Experimental results obtained by Sobrino (1993) for strands 0.5".

Steel Property	Mean value X_{mean}	Min. value X_{min}	Max. value X_{max}	Coef. of Var. CV
0.1% proof stress $f_{p0.1}$	1766 MPa	1660 MPa	1925 MPa	3.2%
0.2% proof stress $f_{p0.2}$	1823 MPa	1677 MPa	1987 MPa	2.9%
1% proof stress f_{py}	1778 MPa	1671 MPa	1903 MPa	2.5%
Ultimate strength f_{pu}	1973 MPa	1874 MPa	2091 MPa	2.0%
Elasticity modulus E_p	197.2 GPa	189.3 GPa	205.1 GPa	1.8%
Ultimate strain ϵ_p	5.07%	4.01%	5.58%	4.2%

Note: All the stresses were calculated considering strand area $A_p = 0.987\ cm^2$.

Analysing the results presented in those tables, it can be observed that the coefficients of variation of the 0.1%, 0.2% and 1% proof stresses are slightly higher than the coefficient of variation of the ultimate strength. The results obtained by Strauss (2003) confirm this observation. Due to this fact the probabilistic models of those parameters proposed by both authors recomend higher values of the coeficient of variation for proof stresses than for ultimate strength. Regarding

Table 4.20: Experimental results obtained by Sobrino (1993) for strands 0.6".

Steel Property	Mean value X_{mean}	Min. value X_{min}	Max. value X_{max}	Coef. of Var. CV
0.2% proof stress $f_{p0.2}$	1766 MPa	1660 MPa	1907 MPa	2.2%
1% proof stress f_{py}	1734 MPa	1682 MPa	1855 MPa	1.7%
Ultimate strength f_{pu}	1942 MPa	1864 MPa	2077 MPa	1.8%
Elasticity modulus E_p	196.5 GPa	186.7 GPa	208.3 GPa	1.9%

Note: All the stresses were calculated considering strand area $A_p = 1.40\ cm^2$.

the type of probability distribution function, both authors recomend to use the same functions as in the case of ultimate strength.

Besides strength parameters Sobrino (1993) proposes also the probabilistic models for ultimate strain and for elasticity modulus of prestressing steel. In Tables 4.19 and 4.20, the values obtained and suggested by him as representative for whole population are presented. The values proposed by Strauss (2003) are nearly the same. The probability distribution function recommended to model those parameters are normal, lognormal and gamma.

Regarding the statistical parameters of the prestressing steel area, there is almost no data. This is due to the fact, that normally variability of this property is included in the total variability of the specimen strength. The only found data were presented in Mirza *et al.* (1980) where the coefficient of variation of the prestressing steel area is reported to be around 1.25%.

4.4.4 Obtained experimental results

In order to verify the correspondence between the probabilistic models of the properties of prestressing steels presented in previous section and variability of those properties observed in Portugal the significant amount of data was analysed statistically within the program of this thesis. The analysed data was made available for this study by the Department of Civil Engineering of the University of Coimbra. The data was obtained for 7 wires prestressing strands of two different grades, 1770 and 1860, and two different diameters, 15.2 and 16 mm.

The statistical evaluation of data confirmed that normal and lognormal probability distribution functions describes accurately variability of most of the prestressing steel properties. The basic statistics of all the parameters obtained in the analysis are showed in Tables 4.21 and 4.22. The results presented in tables correspond to properties tested on the standard specimens used for the purpose of the quality control. The complete outcome of the performed statistical analysis is presented in the Appendix C.

Table 4.21: Experimental results of prestressing steel strength.

Origin *(Reference)*	Str.	Nominal val. [MPa]	Bias λ	Coef. of Var. CV [%]
Portugal, *(see Appendix C)*	f_{py}	1520	1.05	1.7
	f_{pu}	1770	1.02	1.2
	f_{py}	1670	1.03 – 1.04	2.6 – 2.9
	f_{pu}	1860	1.03 – 1.04	2.2 – 2.3

Table 4.22: Experimental results of other properties of prestressing steel.

Origin *(Reference)*	Par.	Nominal value	Bias λ	Var. Coef. CV [%]
Portugal, *(see Appendix C)*	E_p	195 GPa	1.00 – 1.02	1.7 – 2.1
	ϵ_p	3.5 %	1.10 – 1.19	8.7 – 13.8
	A_p	140/150 mm^2	1.00 – 1.01	0.4 – 1.3

4.4.5 Proposed probabilistic models

Despite the fact that the analysed amount of data, regarding properties of prestressing steel, was quite significant and corresponds to the production of prestressing strands of various producers during several years the results presented in previous section can not be considered as representative for whole population of prestressing steels used in the construction of bridges in Portugal. However, comparing the results showed in Tables 4.21 and 4.22 with those presented in Tables 4.16, 4.18,4.19 and 4.20 it can be observed that they are very similar.

Therefore, it can be assumed that the results obtained in the performed study are of rather good quality and may represent properties of the prestressing steel strands with sufficient accuracy.

Based on the results presented mostly in Tables 4.21 and 4.22 but also in Tables 4.16–4.20 the following statistical parameters of strength properties of prestressing steel are recommended for using in the probabilistic analysis:

- ultimate strength: λ=1.04 and CV=2.5%.
- proof stress: 10-15% lower than yield strength; CV=3.0%.

Both properties can be modelled by lognormal or normal probability distribution function.

Regarding probabilistic models of other properties of prestressing steel, the ultimate strain can be modelled by lognormal or normal distribution function with mean value equal to 5% and the coefficient of variation equal to 8%. Steel elasticity modulus can be modelled by normal distribution with the mean value equal to 197 GPa and the coeficient of variation of 2%. The area of reinforcement can also be modelled by normal distribution with coefficient of variation of 1.3% and the mean value equal to nominal.

4.5 Models of geometry

4.5.1 Basics

Geometric imperfections in concrete elements are caused by deviations from the specified values of the cross-sectional shape and dimensions, the position of active and passive reinforcement, the horizontality and verticality of concrete lines, the alignment of columns and beams and the grades and surfaces of constructed structure (Mirza & MacGregor, 1979b).

Obviously the geometric imperfections affects both, actions on the structure (structure self weight) and the structure response (ultimate resistance, stiffness, etc.). Besides this it could also affects the structure durability (e.g. due to reduced reinforcement cover).

The geometrical imperfections are strictly related to the execution quality and to the tolerances permissible by the legal codes or norms for structure execution. The following factors affects the basic statistical characteristics (bias factor, coefficient of variation, correlations, etc.) of structure geometric imperfections:

- structural type (slab bridge, voided slab bridge, I girder bridge, box girder bridge, etc.);
- construction process and applied technology (precast, in-situ, launching method, cantilever method, etc.);
- execution quality;
  - constructor, workmen, experience in the same types of construction;
  - site location;
  - size, type and quality of formworks;
  - easiness of concreting and compaction operations;
  - easiness of reinforcement placement;
  - control and speed of execution;
  - construction season and weather conditions (winter, summer, extreme temperatures, precipitations, etc.);

The geometrical imperfections are in many cases very particular to some type of structures, construction methods or execution technologies and they require individual models (Sobrino, 1993). Consequently the probabilistic models or experimental data obtained on some certain structures should be used with special concern when trying to adopt them to different cases.

In the following points the probabilistic models of the most important dimensions of typical reinforced and prestressed concrete sections found in the literature are presented. Also the models proposed by the codes are discussed and some results of measurements performed within the program of this thesis are showed.

4.5.2 Codes approach

Model proposed in Probabilistic Model Code. According to JCSS (2001), the dimensional deviations of a dimension X can be described by the statistical characteristics of its deviations Y from the nominal value X_{nom} (see Equation 4.25):

$$Y = X - X_{nom} \tag{4.25}$$

The deviations of the external dimensions of precast and cast in-situ concrete components, for the nominal dimensions X_{nom} up to 1000 mm, can be modelled by the normal distribution with the mean value and standard deviation defined by the Equations 4.26 and 4.27 respectively.

$$0 \leq \mu_Y = 0.003 X_{nom} \leq 3 \text{ [mm]} \tag{4.26}$$

$$\sigma_Y = 4 + 0.006 X_{nom} \leq 10 \text{ [mm]} \tag{4.27}$$

The deviations of the concrete cover in the reinforced and prestressed concrete elements can be generally modelled by the normal distribution with the mean and standard deviation as defined in Table 4.23. However, in some cases other types of distribution, namely one or two side limited distributions (e.g. beta, gamma, shifted lognormal, etc.) can be more appropriate.

Table 4.23: Statistical parameters of concrete cover (JCSS, 2001).

Element and cover type	Mean value μ_Y [mm]	Stand. dev. σ_Y [mm]
column and wall	$0 - 5$	5 - 10
slab bottom steel	$0 - 10$	$5 - 10$
beam bottom steel	$-10 - 0$	$5 - 10$
slab and beam top steel	$0 - 10$	$10 - 15$

The deviations of the effective depth of the concrete cross-sections can be calculated from the external dimensions and concrete cover (remembering that the depth and concrete cover could be highly correlated). However, when better estimates do not exist, they could be assumed as normally distributed with mean value $\mu_Y \cong 10$ mm and with the standard deviation $\sigma_Y \cong 10$ mm.

4.5.3 Existing probabilistic models

As in the case of probabilistic models of reinforcing steel and concrete mechanical properties, one of the first comprehensive probabilistic models of the geometric deviations in reinforced concrete members were proposed by Mirza & MacGregor (1979b). The models base on the measurement results obtained by other authors on buildings and bridges (precast and cast in-situ) constructed in Europe and in North America. The values of basic statistical parameters proposed by Mirza & MacGregor (1979b) to model geometric deviations in slabs, beams and columns are presented in Tables 4.24, 4.25 and 4.26 respectively.

Table 4.24: Variability of slab dimensions (Mirza & MacGregor, 1979b).

Dimension description	Technology of execution	Nominal range [mm]	Dev. from Nominal [mm]	Standard dev. [mm]
Thickness	In-situ	100 – 230	0.8	12
	Precast	100 – 230	0.0	5
Effective depth (top reinforcement)	In-situ	100 – 200	±20	15 – 20
	Precast	100 – 200	±20	3 – 6
Effective depth (bottom reinf.)	In-situ	100 – 200	−8 – 9	10 – 15
	Precast	100 – 200	0	3 – 6

Table 4.25: Variability of beam dimensions (Mirza & MacGregor, 1979b).

Dimension description	Technology of execution	Nominal range [mm]	Dev. from Nominal [mm]	Standard dev. [mm]
Overall depth	In-situ	460 – 690	2.5	5
	Precast	530 – 990	3.2	4
Rib width	In-situ	280 – 305	2.8	4.8
	Precast	480 – 610	4	6.5
Flange width	Precast	280 – 305	2.8	4.8
Concrete cover (bottom reinf.)	In-situ	12 – 25	−3 – 6	16 – 18
	Precast	50 – 60	3	8 – 9
Concrete cover (top reinforcement)	In-situ	19 – 25	−5 – 2	11 – 13
	Precast	19	3	8 – 9

Table 4.26: Variability of column dimensions (Mirza & MacGregor, 1979b).

Dimension description	Technology of execution	Nominal range [mm]	Dev. from Nominal [mm]	Standard dev. [mm]
Rectangular	In-situ	280 – 760	1.6	6.4
(width, thickness)	Precast	180 – 410	0.8	3.2
Circular	In-situ	280 – 330	0	4.8
(diameter)	Precast	280 – 330	0	2.4

Regarding the types of distribution functions, Mirza & MacGregor (1979b) recommended Gaussian distribution for all dimensions except concrete cover where normal truncated distribution is suggested in order to avoid negative values.

Based on data obtained in United States Siriaksorn (1980) proposed to use also normal probability distribution function for modelling geometric variability of bridge sections. However, he recommends to consider the mean value of every geometric parameter equal to the nominal and the standard deviation as defined by the Equations 4.28 and 4.29 respectively for section effective depth and remaining dimensions (height, width, thickness, etc.) respectively.

$$\sigma_D = 17.8/D \text{ [mm]} \tag{4.28}$$

$$\sigma_A = 10.2/A \text{ [mm]} \tag{4.29}$$

Melchers (1999) suggests, based on the observation that the actual thickness of slabs is greater then the nominal thickness, to use mean thickness about 6% greater than nominal (bias factor 1.06) and consider the coefficient of variation up to about 8%. For precast slabs and in-situ high quality bridge decks he recommends to use mean thickness of 0.5% greater than nominal (bias factor 1.005) and coeffcient of variation equal to 2%.

Another study related to probabilistic description of bridge section geometric variations was performed by Sobrino (1993). During the years 1990–1993 he collected data on several bridges (precast and cast in-situ) in Spain. Based on that data he proposed mean values and standard deviation of distribution functions which can be used in modelling characteristic dimensions of the bridge sections (see Tables 4.27 and 4.28). Sobrino (1993) also recommends to use normal distribution function for the modelling of geometric variations.

Table 4.27: Variability of bridge sections dimensions (Sobrino, 1993).

Dimension description	Technology of execution	Nominal range [mm]	Dev. from Nominal [mm]	Standard dev. [mm]
Horizontal	In-situ	< 600	—	—
		≥ 600	0.2	3
	Precast	≤ 250	-2 $(0)^{(b)}$	5 $(2)^{(b)}$
		250 – 600	10 $(-4\text{–}5)^{(b)}$	12 $(2\text{–}3.5)^{(b)}$
		≥ 600	-2–1	—
Vertical	In-situ	≤ 250	0–2 $(-13\text{–}34)^{(a)}$	2–3 $(10\text{–}12)^{(a)}$
		250 – 600	-2	8–10 $(10\text{–}18)^{(a)}$
		≥ 600	40–20	15–22
	Precast	≤ 250	5 $(2.5)^{(b)}$	5–9 $(2\text{–}4)^{(b)}$
		250 – 600	12 $(6)^{(b)}$	5 $(2\text{–}3.5)^{(b)}$
		≥ 600	—	—

Note: Normal execution quality; $^{(a)}$ low execution quality; $^{(b)}$ high execution quality;

Table 4.28: Variability of reinforcement position in bridges (Sobrino, 1993).

Dimension description	Nominal range [mm]	Dev. from Nominal [mm]	Standard dev. [mm]
Concrete cover (top reinforcement)	$H \leq 200$	5–10 $(15)^{(a)}$	10–12 $(10\text{–}15)^{(a)}$
	$H \geq 200$	5–30 $(50\text{–}70)^{(a)}$	7–10 $(10\text{–}15)^{(a)}$
Effective depth (bottom reinforcement)	$D \leq 200$	2.5	6 $(12)^{(a)}$
	$D \geq 200$	-7–10	6 $(12)^{(a)}$
Effective depth (cable)	$D \geq 1000$	-30–0	16.3
Transversal spacing	150 – 200	1–4	13–36

Note: Normal and high execution quality; $^{(a)}$ low execution quality;

During the European Research project "Precast Concrete Safety Factors" (PCSF, 2002) the measurements campaign has been performed on precast structural elements representative of the production of several European countries. The measurements were taken on reinforced and prestressed beams, columns and slabs produced in 20 different precasting factories. Most of the measurements were performed on the structural elements of the buildings rather than bridges. However, some measurements were also taken on the prestressed concrete I bridge girders. Based on the data from this campaign the probabilistic models as presented in Table 4.29 were proposed. For all the dimensions presented in the table normal distribution were recommended.

Table 4.29: Geometric variability of precast concrete (PCSF, 2002).

Dimension description	Level of quality control	Dev. from Nominal [mm]	Standard dev. [mm]
Reinforcement position	Standard	0	6.1
	Enhanced	0	3.0
Effective depth	Standard	0	7.89
	Enhanced	0	3.61
Section depth	Standard	0.85	5.0
	Enhanced	0	2.0
Section width	Standard	0.23	5.0
	Enhanced	0	1.5
Section thickness	Standard	2.6	3.7
	Enhanced	0	1.6

4.5.4 Obtained experimental results

Aiming to verify the correspondence between the probabilistic models of geometry of concrete bridges presented in previous section and variability of bridge geometry observed in Portugal the dimensions of few types of precast concrete beams were collected and analysed statistically within the program of this thesis. The analysed data were collected on the casting plants of two Portuguese precasters - Maprel and Civibral.

The basic statistics of girders' geometry obtained in the analysis are showed in Tables 4.30 and 4.31. The results presented in tables correspond to dimensions of U-shape and I-shape precast prestressed concrete bridge girders measured on the executed elements.

The complete outcome of the performed statistical analysis is presented in the Appendix D.

Table 4.30: Variability of the dimensions of precast U-shape girders.

Dimension description	Nominal range [mm]	Dev. from Nominal [mm]	Standard dev. [mm]	Bias fact. λ	Var. coef. CV [%]
Height	900 – 1900	14 – 18	4.3 – 6.9	1.008	0.55
Width	2800 – 3500	-10 – 18	0 – 8	0.999	0.20
Thickness	200	6 – 22	5.3 – 14.1	1.061	4.69

Table 4.31: Variability of the dimensions of precast I-shape girders.

Dimension description	Nominal range [mm]	Dev. from Nominal [mm]	Standard dev. [mm]	Bias fact. λ	Var. coef. CV [%]
Height	600 – 1200	-1 – 12	3.4 – 4.2	1.005	0.69
Width	350 – 440	0 – 2	3.3 – 4.4	1.007	0.95
	450 – 800	1 – 5	1.6 – 2.5	1.002	0.56
Thickness	75 – 100	-1 – 2	2.0	1.009	1.98
	100 – 150	1 – 8	2.2 – 2.4	1.036	2.10

4.5.5 Proposed probabilistic models

The amount of data about bridge girders geometry collected within the program of this thesis was relatively small and does not allow for defining reliable probabilistic models. Furthermore, the collected data corresponds to precast presctressed concrete girders and are not representative for other types of bridge girders and bridge secondary members. Nevertheless, based on data collected by other authors and presented in Tables 4.25, 4.27 and 4.29 and comparing them with results presented in Tables 4.30 and 4.31 some proposal of probabilistic models of precast bridge girder geometry can be made. For other types of bridge members results from Tables 4.24–4.29 can be used.

The effective depth and the overall height of precast prestressed concrete U-shape and I-shape bridge girders may be modelled by normal distribution with the mean value 0.5% higer then the nominal (bias factor λ=1.005) and a standard deviation σ=5mm. The section width in this type of elements can be modelled also by normal distribution with the following paramaters: bias factor λ=1.00; standard deviation σ=5mm. The thickness of a bottom slab (U-shape girders) may be assumed as normally distributed with bias λ=1.05 and standard deviation σ=10mm.

The effective depth and overall height of precast reinforced concrete bridge slabs may be modelled by normal distribution with a mean value 0.5% higher than nominal (bias factor λ=1.005) and a standard deviation σ=5mm.

The effective depth and overall height of cast in-situ reinforced concrete slabs may be modelled as normally distributed with following distribution parameters: bias factor λ=1.00; standard deviation σ=10–15mm.

Chapter 5

Probabilistic models of bridge loads

5.1 Introduction

The safety assessment of a bridge structure involves the verification if the effects of loads applied to the structure do not exceed its capacity or the capacity of one of its members. As already mentioned in previous chapters, the determination of structure capacities and the effects of loads applied to the structure is a quite complex task associated with high level of uncertainty. Particularly, the loads due to highway or railway traffic are the main cause of uncertainty and usually the governing variables in the reliability analysis of short and medium span bridges. Nevertheless, the permanent loads are also relatively important in the safety assessment, especially for the case of concrete bridges.

In this chapter the probabilistic models of bridge permanent loads are presented. The models of bridge variable loads due to railway traffic are also showed. However, the major emphasis is placed on the models of highway traffic loads. Furthermore, site-specific load models for load capacity evaluation of existing highway bridges are discussed. The model are based on results of traffic measurements using Weigh-in-Motion systems.

Due to the fact that effects of other loads (e.g. wind, snow, temperature, etc.) are usually insignificant for short and medium span bridges, they are not discussed in this thesis. Furthermore, the accidental loads due to earthquake or collision are also omitted, because of their exceptional character.

5.2 Types and general models of bridge loads

5.2.1 Basis

The loads applied on a bridge may arise from the self-weight of the structure, man-made sources, and environmental phenomena (Ghosn, 1999). Man-made sources include variable loads due to vehicular and pedestrian traffic, collision forces and additional permanent loads (asphalt wearing surface, rail truck, ballast, bridge equipment, etc.). Environmental loads are due to snow, wind, temperature gradients, earthquakes, etc. Loads on bridges are usually classified based on their variability in magnitude and position in time (i.e. permanent or transient, moving or fixed), and based on the type of structural response (i.e. static or dynamic). All above mentioned load types are random variables, including permanent loads which do not change with time nor create dynamic oscillation. This is explained because their magnitudes and their effects on the structure are not precisely known.

The modelling of bridge loads is quite a complex task due to the fact that, it requires long term data (which is often not available) and it requires the prediction of future loads (which can only be based on subjective engineering judgement). According to Melchers (1999), due to above mentioned difficulties, perfect models are not possible. Therefore, the objective of load modelling is rather to represent most important features of the loading phenomenon than to come up with exact mathematical formulation (Ghosn, 1999).

The process of developing a probabilistic load model for the purpose of the reliability assessment of bridges may be resumed in the following three steps (Melchers, 1999):

- identification and definition of variables which can be used to represent the uncertainties in loading description (this requires a real understanding of loading phenomenon and the physical factors affecting the loading process);

- selection of appropriate probability distribution for each random variable identified in previous step;
- estimation of the distribution parameters required to determine unambiguously the probability distribution identified in the previous step (the statistical parameters should be based on available data and prior knowledge).

5.2.2 General load models and modelling uncertainty

In the structural reliability assessment it is often convenient to express the magnitude of the generalized load Q_i as follows (Nowak & Collins, 2000):

$$Q_i = A_i B_i C_i \tag{5.1}$$

where A_i is the load itself, B_i is the variation due to the mode in which the load is assumed to act, and C_i is the variation due to the method of structural analysis. The variable C_i accounts for the simplifications and the idealization made in the creation of the structural analysis model (e.g. two dimensional idealisation of three-dimensional structure, support assumption, etc.). The variable B_i take into account the assumption about how the loading is applied to the structure (e.g. uniformly distributed load instead of the group of concentrated loads and non-uniform distributed loads, etc.).

Unfortunately, according to Ghosn (1999), do not exists any reliable statistical data about modelling uncertainties, $B_i C_i$, that one can use in the reliability assessment of bridges. One possible approach, to define such uncertainties, would be by comparing the results of the structural analysis with the measured response of bridges subjected to known loads. So far, the modelling uncertainties, $B_i C_i$, that are available in literature, are defined based basically on the engineering judgement. For example, in Vejdirectoratet (2004), the model uncertainty for permanent loads is suggested to be introduced into the computational model by adding to the relevant basic variables an independent normally distributed random variable with mean value 0.0 and a standard deviation of 5% of the mean value of the permanent load. However, the model uncertainty for variable loads is suggested to be introduced into the computational model by multiplying the basic parameters by normally distributed random variable with mean value 1.0 and variation coefficient of 10%, 15% and 20% depending on the loading situation.

5.3 Models of permanent loads

5.3.1 Models of permanent loads due to self-weight

For bridges, the primary permanent loads are due to the self-weight of the bridge deck and the weight of non-structural elements permanently installed on the bridge. The uncertainty in predicting the magnitude of the permanent load are due to variations in the density of the materials used as well as the variations in dimensions of the elements (Ghosn, 1999). The variations in the dimensions of structural elements have been already discussed in Section 4.5. The variations in the density of the materials can be assumed as presented in Table 5.1.

Table 5.1: Weight density statistics (JCSS, 2001).

Construction material	Mean value [kN/m^3]	Coefficient of Variation
Steel	77	1%
Ordinary concrete [(a)]	24	4%
High strength concrete	24-26 [(b)]	3%
Lightweight concrete	[(b)]	4–8%

Note: All the values refer to large populations; [(a)] valid for concrete without reinforcement and with stable moisture content; [(b)] depends on mix, composition and treatment.

The permanent loads due to the weight of structural and non-structural elements are usually modelled by normal distribution with the mean equal to the nominal load and the coefficient of variation of 5–10% (Melchers, 1999). However, some researchers observed that often there is a tendency on part of designers to underestimate the total permanent load (Nowak & Collins, 2000). Therefore, to account for this, the use of the mean load somehow bigger than the nominal may be recommended.

In the Project Report PCSF (2002) authors define the bias factor and the coefficient of variation of the self-weight of precast concrete elements. Based on the results of the measurement campaign they observed that the mean weight of precast concrete elements is usually higher than nominal (calculated considering nominal dimensions and volume weight of concrete equal to 2500 kg/m^3) up to 7%. The observed coefficient of variation oscillates around 2.5%.

In Vejdirectoratet (2004) the permanent loads are suggested to be modelled by normally distributed random variable with mean value equal to the nominal and with the coefficient of variation of 5% and 10%, respectively for load of the structure itself and for the superimposed permanent loads. In addition to the given variations, the uncertainty of the model has also to be taken into account (see Section 5.2.2).

Because of different degrees of variation in different structural and non-structural elements, Nowak & Szerszen (1998) and Nowak & Collins (2000) propose to break up the total permanent bridge load into following components:

- weight of factory-made elements (steel and precast concrete elements);
- weight of cast-on-site concrete members;
- weight of the wearing surface (asphalt);
- weight of the bridge installations and equipment (railing, luminaries, etc.)

Nowak & Szerszen (1998) recommend to model each of the above listed component by independent normally distributed random variable with the statistics presented in Table 5.2.

Table 5.2: Statistics of permanent loads (Nowak & Szerszen, 1998).

Component	Bias factor	Coefficient of Variation
Factory-made members	1.03	8%
Cast-on-site members	1.05	10%
Asphalt	75 mm	25%
Other	1.03–1.05	8–10%

In the case of railway bridges, the permanent loads due to ballast and rail track can be modelled according to the information presented in Sustainable Bridges (2006). Concerning the variability in the geometry and in the density of the track components the total coefficient of variation proposed are 3%, 8% and 15%

respectively for steel elements, pre-cast concrete sleepers and timber sleepers. For ballast, the mean weight is proposed to be calculated assuming actual depth and density of 1600-2000 kg/m^3. No specific value is presented in Sustainable Bridges (2006) for the coefficient of variation of the ballast weight. However, in normal circumstances it might be considered in the order of 10–15%.

5.3.2 Models of permanent loads due to prestress

In the concrete structures the effect of prestress is usually considered as a prestressing force applied to the structure. A prestressing force $P(x, t)$ at a distance x from the active end (jacking end) at a time t can be expressed as follows (JCSS, 2001):

$$P(x, t) = P_0 - \Delta P(x, t) \tag{5.2}$$

where P_0 is the jacking force and $\Delta P(x, t)$ are losses of prestress. In practical applications it is usually sufficient to assess prestressing losses at two times: immediately after prestress transfer $t = t_0$, and after losses have stabilised $t = \infty$.

Due to the multiplicity of the factors affecting prestress losses and due to the existing interrelations between some of them, does not exist analytical models allowing to predict $\Delta P(x, t)$ with high accuracy. Therefore, different codes provide different empirical models to estimate the losses.

The uncertainty of the prestressing force applied to the structure depends on the uncertainty of the models used to estimate the prestress losses and variability of parameters employed in these models. According to JCSS (2001), currently do not exist sufficient data to quantify uncertainties of the prestress losses models and of the parameters associated with the models. However, for typical situations JCSS (2001) recommends to estimate the mean value of losses using models provided in design codes and consider the coefficient of variation as presented in Table 5.3. Considering the typical magnitudes of prestress losses the corresponding coefficients of variations of actual prestressing force are estimated to be as showed in Table 5.3.

According to JCSS (2001) for the group (bundle) of prestressing tendons, prestress losses in different tendons of the group can be assumed fully correlated.

Table 5.3: COV of prestress losses and prestressing force (JCSS, 2001).

Parameter	Coefficient of variation	
	Immediate, $t = t_0$	Long-term, $t = \infty$
Prestress losses, $\Delta P(x, t)$	30%	30%
Prestressing force, $P(x, t)$	4–6%	6-9%

The prestress losses in different location of the same tendon group can be also assumed fully correlated.

In other sources slightly different values may be found than those presented in Table 5.3. For example, for prestressing force at transfer (considering immediate losses) Mirza *et al.* (1980) suggest to use a normal distribution with the coefficient of variation of 1.5% and 2% for pretensioned and post-tensioned beams respectively. However, for the prestressing force, after considering all long-term losses (with corresponding coefficient of variation 15–20%), they suggest normal distribution with the coefficient of variation of 3.8% for stress relived strands and 3.3% for stabilized strands.

5.4 Models of variable loads on bridges

5.4.1 General

There is a number of variable loads that are normally acting on a bridge structure (vehicular and pedestrian traffic, temperature, wind, snow, etc.). However, for typical short and medium span bridges, the most important loads are due to moving vehicular traffic including their static and dynamic effects (Ghosn, 1999). The static and dynamic effects occur simultaneously as vehicles move across the bridge. However, traditionally, in some countries, the dynamic effects are separated from the static effects in the bridge analysis. In such approach the bridge is analysed statically considering static vehicle load factored by dynamic amplification factor which accounts for bridge vibrations due to the moving vehicles.

The effect of vehicular variable load on the bridge depends on following parameters: bridge span, total vehicle weight, axle loads, axle configuration, position of the vehicle on the bridge (transverse and longitudinal), number of vehicles on the bridge (multiple presence), girder spacing and stiffness of bridge members (Nowak & Collins, 2000). In practical analysis of a bridge, it is also convenient to characterize the distribution of the load to the bridge girders.

Due to the fact that the effect of the vehicular load on the bridge depends on so many factors and, furthermore, most of these factors are stochastic random variables (changing in time), the modelling of the effect of a bridge traffic load is a very complex task. In common bridge design and assessment practice this problem is overcome by using load models defined in codes (composed usually by a group of concentrated forces and uniformly distributed loads). These models are aimed to produce load effects in bridge members similar to that the bridge will experience during its lifetime under regular traffic and under special passage situations (passages of very heavy vehicles). Since these load models have to cover a wide range of bridge locations, spans, typologies, materials, etc., they are usually very conservative. However, some of them may not be conservative at all, especially when they have been developed some decades ago. Such models may not reflect appropriately the actual heavy traffic.

In the bridge analysis it is necessary to distinguish between two different phenomena that may lead to the bridge failure (Ghosn, 1999). First phenomenon is the occurrence of the set of loads that causes stresses in the bridge component that exceed the stress capacity of the component. This problem is known as the barrier crossing problem or the first passage problem. Second phenomenon is when the accumulated damage due to repeated crossing of a large number of vehicles produce a brittle fracture in the component. This is known as the fatigue fracture problem. The traffic load models used for assessment of these two phenomena are quite different. Traffic load models for barrier crossing problems need to focus only on the maximum load that may occur during the lifetime of the bridge. However, the load models for fatigue problems need to represent all load history during the bridge entire life of the bridge. In this thesis just the load models for barrier crossing problem are going to be presented in more details.

In the following sections some selected aspects related to the modelling of bridge traffic loads are discussed. They are presented aiming to give some general overview, allowing to understand the following parts of this thesis, rather than to give complete information regarding modelling of bridge traffic loads.

5.4.2 Traffic regulations and measured loads

The bridge load models defined in design or assessment codes should reflect the actual loading conditions on bridges. Therefore, they should be somehow related to the traffic regulations, defining the dimensions, maximum axle loads and maximum gross weights of vehicles allowed to circulate freely, or with some restriction (special permited vehicles, e.g. mobile cranes, military vehicles, etc.), within the highway network. Furthermore, they should account for possible exceed of the legal weight limits since overloading of the vehicles is profitable for transportation companies and it is actually quite commonly practised.

In Portugal, the current load regulations for vehicles are defined in document Portaria n.1092/97 (1997). The maximum gross weight of the rigid vehicles is limited to 190 kN, 260 kN and 320 kN for two, three and four (or more) axle vehicles respectively. The maximum gross weight of the semi-trailer vehicles is limited to 290 kN, 380 kN and 400 kN for three, four and five (or more) axle vehicles respectively. For five (or more) axle vehicles transporting containers ISO 40', the maximum gross weight is limited to 440 kN. For the rigid vehicles with trailers, the maximum gross weight is limited to 290 kN, 370 kN and 400 kN for three, four and five (or more) axle trailer vehicles respectively. The maximum gross weight per axle is 75–120 kN for single axle, 120–200 kN for tandem axle and 210–240 kN for tridem axle.

Tables 5.4 and 5.5 compare the current Portuguese traffic load regulations with former Portuguese regulations and with the regulations in other European countries as they are presented in COST323 (1997) and SAMARIS (2005). As it can be observed, the legal gross weight limits for heavy vehicles varies between the countries. The limits for maximum axle load are more uniform but small differences can also be observed. Nevertheless, in recent years there is a tendency to standardize the maximum axle loadss and weights of vehicles in Europe and the new regulations usually follows the requirements set by European Union.

The growing problem on the highway network in many countries is the commonly practised overloading of the vehicles. This fact has been confirmed by the extensive campaign of measurement of real traffic performed in several EU member states (Carlson, 2006; COST323, 1997; O'Brien & O'Connor, 1998; SAMARIS,

Table 5.4: Allowed axle load in selected countries (COST323, 1997).

Country	Allowed axle load [kN]		
	Single axle	Double axle axle dist. 1–1.8 m	Triple axle axle dist. 2–3.6 m
Austria	115	160–200	210–240
Belgium	120	160–200	200–240
Czech Republic	100 (115*)	180	240
Denmark	100 (115*)	160–200	210–240
Spain	115	160–200	210–270
Finland	115	160–200	210–240
France	130	210	240
Great Britain	105	160–200	210–225
Hungary	100 (110*)	160	220–240
Netherlands	115	160–200	240
Norway	100 (115*)	180	240
Poland	80 (115*)	180	240
Portugal-new	100 (120*)	170–200	210–240
Slovenia	100 (115*)	160–200	210–240
European Union	115	160–200	210–240

Note: (*) corresponds to driving axle.

2005). The measurements have been performed using Weigh-in-Motion (WIM) systems allowing weighing the vehicles without stopping. For example, during the campaign of measurements of real traffic loads, performed for the purpose of calibration of the bridge traffic load model in Eurocode (O'Connor *et al.*, 1998), it has been observed that the daily maximum gross weight of the vehicles exceed 650 kN. The daily maximum single, tandem and tridem axle load exceed 190 kN, 300 kN and 380 kN respectively.

This tendency of overloading heavy vehicles has also been observed in Portugal. Figure 5.1 shows the histograms of gross vehicle weights (GVW), for vehicles over 3.5 t, registered on one of the highways belonging to 'SCUTVIAS - Autoestradas de Beira Interior' located in the centre of Portugal. The data have been collected during 24 hours on 22-nd of July 2005. All three histograms (cor-

Table 5.5: Allowed gross weight [kN] of vehicles (COST323, 1997).

	R_2	R_3	R_4	S_{21}	S_{22}	S_{23}	S_{32}	S_{33}	T_{22}	T_{23}	T_{33}	T_{44}
AT	180	250	320	280	360	380	380	380	360	380	380	380
BE	190	260	360	320	390	430	440	440		440	440	
CH	160	190	280	260	280	280	280	280	280	280	280	280
DE	160	220		260	360	380	380	380	320	380	380	380
DK	180	240	320	280	340	420	400	480	380	420	480	480
SP	180	250	310	280	360	400	400	400	360	400	400	400
FI	180	250	310	280	360	420	440	440	360	440	530	600
FR	190	260	320	260	400	400	400	400	380	400	400	400
GB	170	260	320	260	350	380	380	380	350	380	380	380
HU	200	240	300	280	360	400	400	400	360	400	400	400
IE	160	220	280	220	320	320	320	320	320	320	320	320
LU	190	260	360	320	380	380	400	440	380	400	440	
NL	200	300	400	300	400	410	500	500	400	500	500	500
PT	160	220		260	320	380	380	380	320	320	320	320
PT*	190	260	320	290	380	400	400	400	370	400	400	400
SL	180	250	320	280	380	400	400	400	360	400	400	400
EU						400	400	400		400	400	

Note: R, S and T corresponds to rigid vehicles, semi-trailers and vehicles with trailer respectively; the subscript numbers after the letter defining the type of the vehicle corresponds to the number of axles in the vehicle and in the trailer respectively; (*) corresponds to new regulations presented in Portaria n.1092/97 (1997).

responding to the registered data for both traffic directions and separately for the direction South-North and North-South) have a two peak shape, more or less visible, typical for GVW histograms. The first peak corresponds to the fully loaded small trucks and unloaded or partially loaded large trucks. The second peak corresponds to fully loaded large trucks.

The data presented in Figure 5.1 corresponds to rather light traffic, with the average intensity of heavy vehicles per day around 1000 in each direction. Despite the fact that the highway, where the WIM measurements have been performed, is located far away from the industrial regions of the country, significant number of overloaded vehicles, with weight exceeding 400–440 kN, has been observed. There are also some records of the vehicles with weight approaching 600 kN, however, they might be erroneous. The collected data is rather of poor quality and the individual records are neither precise nor very reliable. Nevertheless, the general trends presented in histograms should not deviate much from the reality.

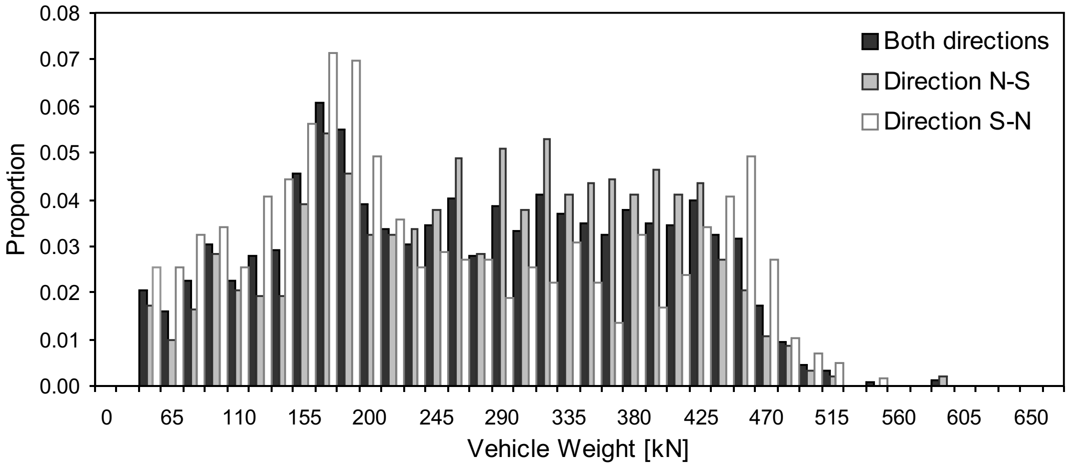

Figure 5.1: Gross vehicle weight histogram for one day data - Beira Interior.

It should be kept in mind that performing the measurements close to the busy industrial areas can significantly affect the registered maximum (i.e. higher value will be observed). Furthermore, the extension of the measuring period (e.g. 1 week instead of 1 day) will also increase the value of the maximum observed vehicle weight.

5.4.3 Traffic load models in bridge codes

The traffic load models defined in current bridge design codes consist of a number concentrated loads, representing heavy axles of trucks (or locomotive), and a uniformly distributed load representing light vehicles (or wagons). As it was already mentioned, the load intensities are selected by the code authors in a way to produce effects similar to that the bridge is going to experience during its lifetime. The bridge load models of railway and highway traffic, commonly used in the design and assessment of bridges in Portugal, are presented in the following sections.

RSA load model for railway traffic. The load model that is used for the design of railway Bridges in Portugal is shown in Figure 5.2. The characteristic values of load intensities for this load model are presented in Table 5.6 (RSA, 1983). This load model has been developed by National Union of Railways (UIC) and is meant to represent normal railway traffic on international lines.

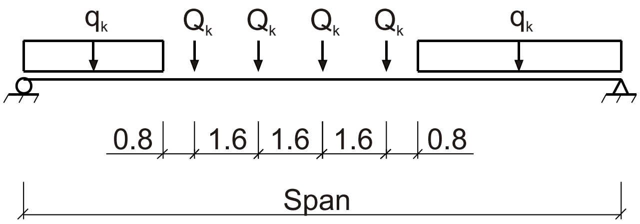

Figure 5.2: Description of UIC model of railway traffic loads.

Table 5.6: Intensities of load in UIC railway traffic load model.

Type of track	Concentrated loads Q_k	Distributed loads q_k
Normal track	250 kN	80 kN/m
Narrow track	180 kN	50 kN/m

The load should be placed at the most unfavourable position for the structural component and local effect in question. It does not take into account the dynamic effects. Therefore, in order to obtain design value, the effects produced by this load have to be multiplied by the partial safety factor for load (γ_S=1.5) and by the dynamic amplification factor defined as follows (RSA, 1983):

$$\phi = 1 + \left(\frac{2.16}{\sqrt{l} - 0.2} - 0.27 \right) \tag{5.3}$$

where l is the reference length (span length for simply supported bridges, average span length multiplied by $(1 + 0.1n)$ for continuous bridges, where n is the number of spans, and half of span length for frames and arches). The dynamic amplification factor should never be considered lower than 1.1 and higher than 2.0 (or 1.5 for continuous bridges).

For multiple track bridges the most unfavourable of the two possibilities should be considered. The load placed on one or two trucks and other tracks unloaded, or load placed on all trucks but with intensity reduced by 25%.

EC1 load model for railway traffic. The principal railway load model 'Load Model 71' defined in EC-1b (2002) is basically the same as that shown in Figure 5.2. The characteristic values of the basic load intensity for this load model is also the same (see the first row of Table 5.6). However, EC-1b (2002) allows for adjusting the load intensity, according to the railway line classification, by multiplying it by a factor α taking one of the following values: 0.75; 0.83; 0.91; 1.00; 1.10; 1.21; 1.33; 1.46. In EC-1b (2002), the dynamic amplification factor for normally maintained tracks is equal to that from RSA (1983) (see Equation 5.3). However, for carefully maintained tracks it is defined as follows:

$$\phi = 1 + \left(\frac{2.16}{\sqrt{l} - 0.2} - 0.18 \right) \tag{5.4}$$

The reference length l in EC-1b (2002) is defined in a more complex way, depending on many bridge features. According to EC-1b (2002), the dynamic amplification factor should never be considered lower than 1.0 and higher than 2.0.

RSA load model for highway traffic. The load models, 'Vehicle' and 'Knife', that are used for the design of highway bridges in Portugal are shown in Figures 5.3 and 5.4. The characteristic values of load intensities for these load models are presented in Table 5.7 (RSA, 1983). The characteristic load intensities presented in table take into account the dynamic effects.

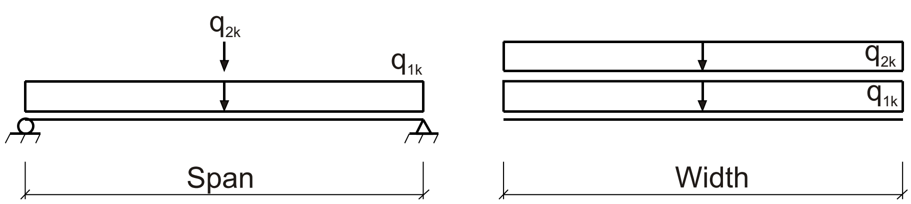

Figure 5.3: Description of RSA model (Knife) of highway traffic loads.

The load should be placed on the bridge deck, longitudinally or transversally, at the most unfavourable position for the structural component and local effect in question. For bridges with dual carriageway, supporting traffic in two opposite directions, the vehicle should be placed in each of the carriageway or in both of

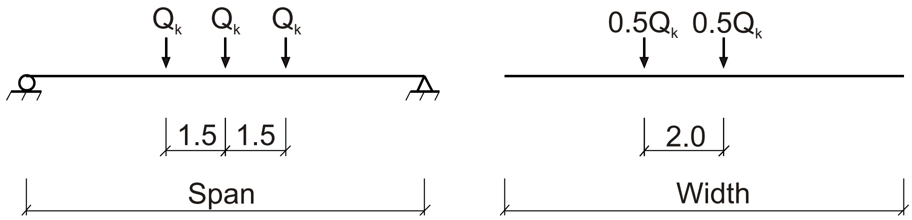

Figure 5.4: Description of RSA model (Vehicle) of highway traffic loads.

Table 5.7: Intensities of load in RSA highway traffic load model.

Bridge class	Conc. load Q_k	Distr. load q_{1k}	Distr. load q_{2k}
Class 1	200 kN	4 kN/m^2	50 kN/m
Class 2	100 kN	3 kN/m^2	30 kN/m

them simultaneously, provided that each of the carriageway supports two or more traffic lines.

These load models have been developed in the beginning of 60-ties (RSEP, 1961) and, almost unchanged, are used until now. The only changes involve the increase of the intensity of the q_{1k} for class 1 (formerly it was 3 kN/m^2) and the definition of lower load classes (three classes for vehicle and only one class for distributed load).

EC1 load model for highway traffic. The principal highway load model 'LM1' defined in EC-1b (2002) is shown in Figure 5.5. The load model LM1 can be used for both local and global verification of bridge elements. The characteristic values of load intensities for this load model, defined as 95-th percentile of a maximum distribution for a return period of 50 years, are presented in Table 5.8.

The load should be placed at the most unfavourable position for the structural component and local effect in question. However, at first it is necessary to identify notional lanes. Generally, a carriageway is divided into an integer number of 3 meters wide notional lanes. Among these lanes, the one causing the most unfavourable effect is termed Lane 1, with the second most unfavourable Lane 2, etc. These lanes do not have to correspond to intended lane markings on the bridge. Furthermore, a demountable central safety barrier is ignored in locating

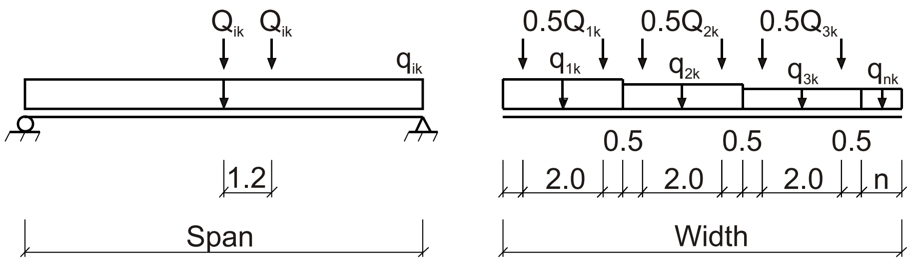

Figure 5.5: Description of EC1 principal model (LM1) of highway traffic loads.

Table 5.8: Intensities of load in EC1 highway traffic load model.

Lane	Concentrated loads Q_{ik}	Distributed loads q_{ik}
Lane 1	300 kN	9 kN/m^2
Lane 2	200 kN	2.5 kN/m^2
Lane 3	100 kN	2.5 kN/m^2
Other lanes, n	0	2.5 kN/m^2
Remaining area	0	2.5 kN/m^2

the notional lines. Space not occupied by the lanes is named remaining area.

The additional load model, LM2, is specified to cover the dynamic effects of the normal traffic on short structural members. This model consist of a single axle load of 400kN (or 200kN per wheel).

The load intensities specified for load models LM1 and LM2 can be multiplied by a national adjustment factor α. The factor α is meant to cover all the differences between the highway traffic characteristics in different EU member countries and different road classes. The load models LM1 and LM2 already takes into account the dynamic effects. The code EC-1b (2002) also specifies a specialized load model, LM3, that is intended to be used in special situations (e.g. heavy industrial transport).

5.4.4 Comparison of traffic load models in EC1 and RSA

The two railway traffic load models (i.e. RSA and EC1) presented in previous section are both based on the UIC recommendations and are almost the same (the only difference is in the intensity of load for the rail line classes different than standard). Consequently, the load effects produced by these models are also the same and there is probably no much sense to analyse these models in more detail. In contrast, the EC1 and RSA highway traffic load models are quite different and they are expected to produce significantly different traffic load effects. Considering the fact that the traffic load model defined in RSA (1983), which has been used for design and assessment of bridges in Portugal since 60-ties, soon it is going to be replaced by the load model from EC-1b (2002), it might be interesting to compare the traffic load effects produced by these two models in most common bridge configurations.

Figures 5.6 and 5.7 show the maximum bending moment, as a function of a bridge span, in the simply supported bridges with two and three traffic lanes. As it can be observed, the bending moment produced by the EC1 load model in two lane bridges is around two times higher than the maximum moments produced by the conditioning RSA load model (i.e. 'knife' in this case). For three lane bridges this difference is lower, however, the EC1 load model still produces bending moments around 1.6–1.8 times higher than the RSA-knife. Quite similar results can be observed for the maximum shear force presented in Figures 5.8 and 5.9. The difference between the maximum shear force produced by the EC1 load model and the shear force produced by conditioning RSA load model (i.e. 'vehicle' or 'knife') exceeds 70–100%.

The difference in the load effects produced by EC1 and RSA load models is not surprising. However, the magnitude of this difference is kind of scaring, especially when having in mind that the safety formats (checking equations, partial safety factors, definition of characteristic and design values, etc.) in both codes are nearly the same. This difference basically means that most of the bridges designed according to Portuguese codes will probably fail the assessment performed using Eurocodes. Of course, it does not mean that all the bridges designed using RSA load model are unsafe. However, the safety margin for all these bridges is lower than that provided when using EC1 load model for design. In this situation one may ask 'which load model provide more rational safety margin'? The answer to this question depends very much on that which load model reflects better the actual traffic loading conditions in a country, region or even in a specific site.

As it has been already mentioned, the bridge traffic load model defined in current Portuguese code, RSA (1983), has been developed in 60-ties for the purpose of former bridge load regulations, RSEP (1961). Therefore, nowadays it can be considered rather obsolete. The traffic intensity, the maximum gross weight of the heavy vehicles and the maximum pressures of axle loads (single, tandem or tridem) increased brutally during last 40 years. In 60-ties Portugal has been rather undeveloped country with almost no industry and with quite poor road network limiting the transportation of goods to other regions of the country and abroad. Today the situation is totally different. Portugal has very well developed network of highways. It is much more industrialized and it is commercially connected with other countries. This of course reflects in the traffic loads and theirs effects on bridges.

On the other hand, the bridge traffic load model defined in Eurocode, EC-1b (2002), has been developed in the late 80-ties based on real traffic data recorded in some EU member states. Furthermore, it has been verified against new traffic data in the late 90-ties (O'Connor, 2001). Therefore, it is expected to represents the actual traffic loads in Europe reasonably well. Nevertheless, the EC1 load model LM1 has been developed based on traffic records from very busy highways connecting the industrial regions of France, Germany, Netherlands, Belgium, Spain and Italy. Consequently, this load model is more representative for a very heavy traffic in strongly industrialized countries of Europe rather than for the normal traffic in Portugal or other countries on the boundaries of Europe, as for example Ireland or Greece. The study performed in Ireland, in order to calibrate the national adjustment factor α, shows that considering actual traffic records from Irish highways, the load effects in common bridge typologies can be significantly lower (O'Brien & O'Connor, 1998). This calibration study has been performed using exactly the same simulation and extrapolation procedures as that used for the development of the EC1 load model.

The selected results of the simulations performed by O'Brien & O'Connor (1998) are presented in Figures 5.6, 5.7, 5.8 and 5.9. They are showed together with the load effects produced by EC1 and RSA load models to facilitate the verification of the adequacy of the code models against the real data. Besides the fact that the simulation results presented in O'Brien & O'Connor (1998) are

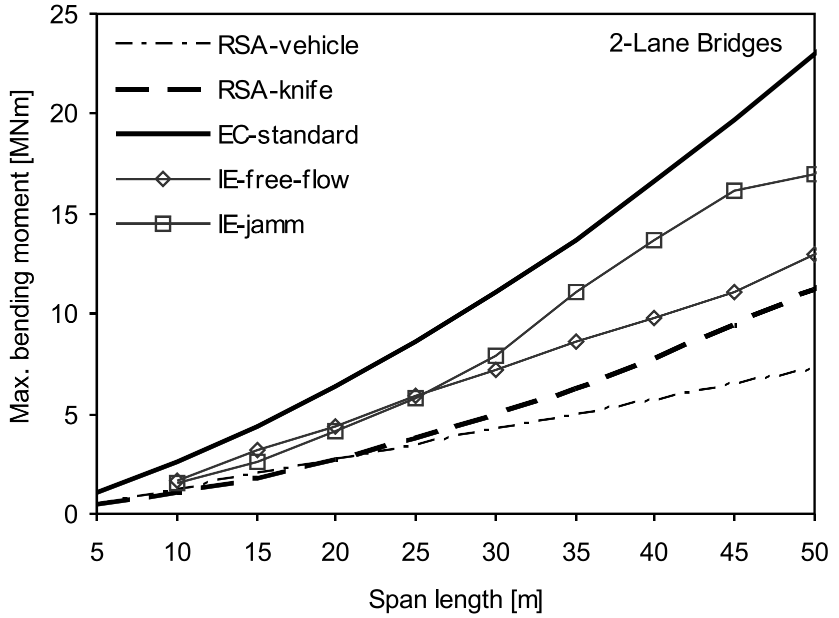

Figure 5.6: Comparison of maximum bending moments for 2-lane bridges.

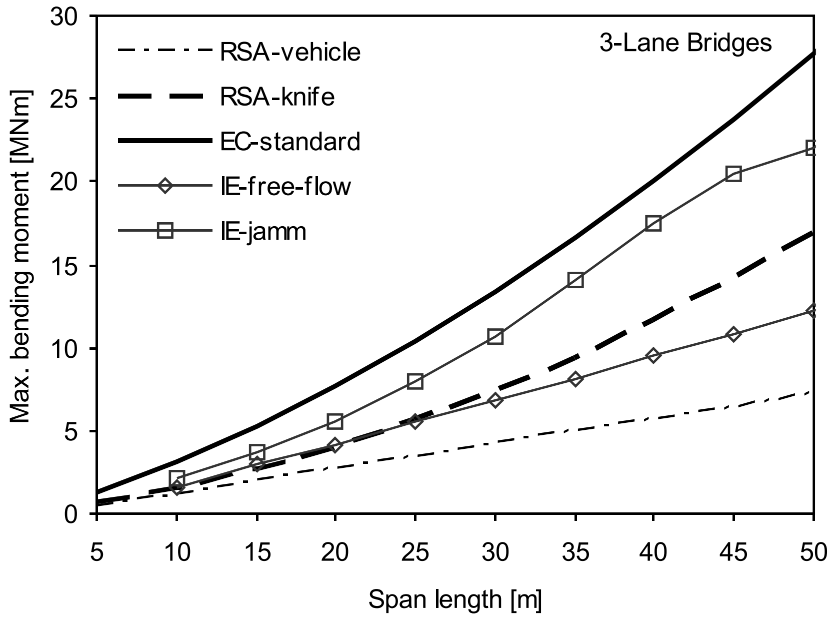

Figure 5.7: Comparison of maximum bending moments for 3-lane bridges.

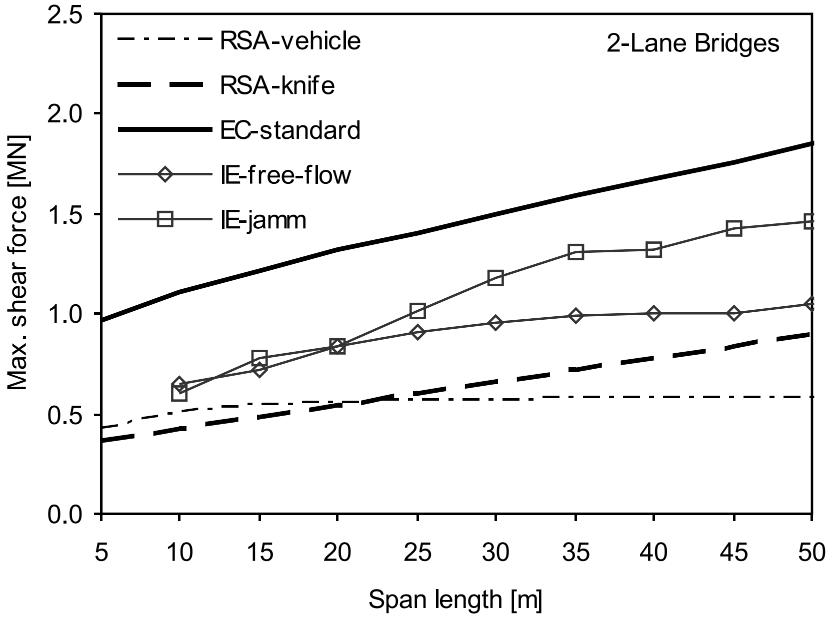

Figure 5.8: Comparison of maximum shear force for 2-lane bridges.

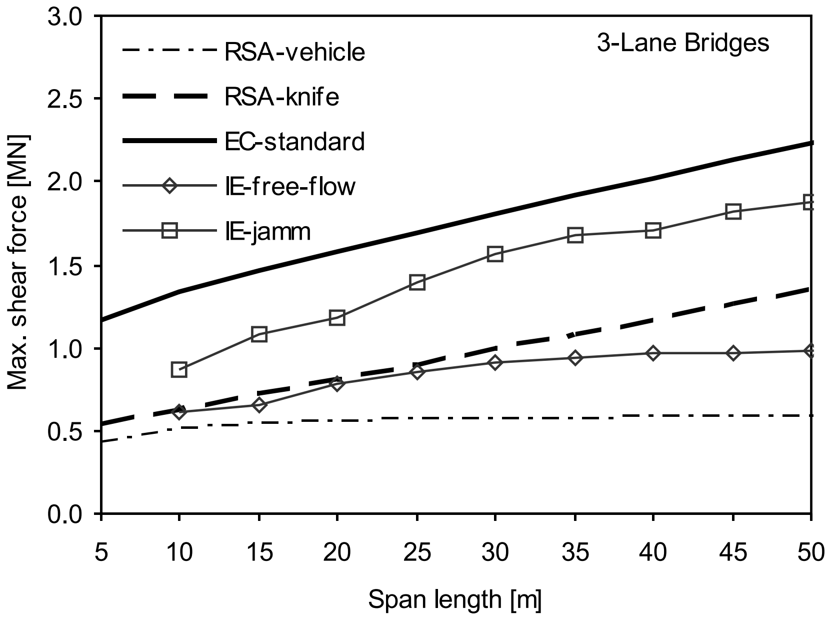

Figure 5.9: Comparison of maximum shear force for 3-lane bridges.

corresponding to Irish traffic they are believed to be more representative for the Portuguese conditions than the results produced be EC1 traffic load model, which has been calibrated against traffic data mainly from French highway with very heavy traffic.

When comparing the load effects presented in Figures 5.6, 5.7, 5.8 and 5.9 one have to keep in mind that those corresponding to EC1 load model are values with the probability of exceedance of 5% in 50 years (or 1000 year return period) (EC-1b, 2002). The load effects obtained due to simulations (considering Irish data and free flow and jammed scenario) are the values with the probability of exceedance of 5% in 100 years (or 2000 year return period). According to O'Brien & O'Connor (1998) this difference in the reference period (50 to 100 years) will affect the results only by 1–2%. Regarding the load effects produced by 'vehicle' or 'knife', RSA (1983) do not specify any reference period characteristic for these models. All the load effects presented in Figures 5.6, 5.7, 5.8 and 5.9 take into account the dynamic effects when relevant (e.g. in the jammed situations the dynamic effects are not included).

5.4.5 Probabilistic bridge traffic load models

The use of probabilistic framework for the modelling of bridge traffic loads has been a subject for research during last few decades. Consequently, most of the load models present in recent bridge codes (e.g. AASHTO LRFD, 1994; CAN/CSA-S6-00, 2000; EC-1b, 2002), have been developed using probabilistic methods and are based on real traffic records. Therefore, behind deterministic values of the load intensities, characteristic for each of these load models, the fully probabilistic bridge traffic load models are hidden. Usually, the load intensity in the models corresponds to 95-th or 98-th percentile of the probability distribution function of the load (or the effect of the load). Due to the fact that the traffic load model has to represent the maximum load which a bridge is going to experience during its lifetime, the extreme value distributions (e.g. type I - Gumbel distribution; type II - Fréchet distribution) are commonly used (Vejdirectoratet, 2004). However, for a sake of simplicity, some authors describe bridge loads using also normal or lognormal distributions.

The traffic load effects on bridges can be modelled using several different probability based approaches. Generally they can be divided into the four following groups (Ghosn, 1999; Melchers, 1999):

- methods based on the simulation of real traffic flow;
- methods based on the simulation of static traffic configuration;
- methods based on the convolution or numerical integration;
- methods based on the theory of stochastic processes, including Markov models.

The first group of methods for modelling traffic load effects involves the simulation of real traffic flow over bridges (Carlson, 2006; Crespo, 1996; Getachew, 2003; James, 2003; O'Connor, 2001). In this method the sequences of random loads passing the bridge are generated using Monte Carlo simulation technique. All the characteristics of the traffic (composition of traffic, headway distance, traffic intensity, vehicles velocity, etc.) and the vehicles (vehicle gross weight, axle loads, axle configuration) are assumed according to the records of real data (collected using bridge Weigh-in-Motion systems). The methods allow to define histograms of load effects in any bridge section. Then, the theoretical probability distribution function may be fitted to the histogram and the extrapolation may be performed to obtain a prediction of the maximum value within certain reference period. These real flow simulations algorithms are the most complete models. They are applicable to the complete range of bridge spans and static configurations. Furthermore, besides the maximum load effects required for ultimate limit state analysis, they are also able to estimate the complete spectrum of load effects for fatigue or serviceability analysis.

The second group of 'simulation based' methods analyses two traffic situations, namely congested and free (Bez & Hirt, 1991; Nowak & Hong, 1991). The method uses real traffic data to describe the basic parameters (i.e. vehicle length and weight, axle configuration, axle loads, probabilities of the vehicles to take certain location of the bridge, correlations between the vehicles at certain locations, etc.) and to define the distribution between free and congested situations within the bridge service life. The results from the basic load situations (i.e. one truck on the bridge, two tracks following each other, two side-by-side trucks, etc.) are combined and extrapolated to give the maximum load effects for a certain reference period. In the present form, these models are valid only for short and medium span bridges. This is because they are based upon simplified assumptions of multiple presence of the heavy vehicles on the bridge (usually up to four heavy vehicles are considered). Furthermore, since they are focused only on maximum load effects, they are not suitable for the fatigue analysis.

The third group consists of convolution or numerical integration approaches (Moses & Ghosn, 1985). The calculation of the distribution of the maximum moment in a bridge over a period of time using convolution approach involves two stages: first, a probability distribution for the moment due to a single event is determined; then, the distribution of the maximum response over the lifetime of the structure is projected given the number of the events for that period of time (Moses & Ghosn, 1985). For a given bridge influence line, the probability of the event is defined as the product of the probability of the placement of the trucks on the bridge, the probability of the weight of the truck and the probability of axle spacing or truck type. The same as the methods described in the previous section, the convolution approaches are suitable for ultimate analysis of short and medium span bridges only.

The methods within the fourth group are based on the theory of stochastic processes as Poisson process or Markov renewal models (Ghosn, 1999; Ghosn & Moses, 1985). These models assume that the trucks arrive on a bridge following one of these process and that the bridge acts as a filter represented by its moments influence line at a given location. Consequently, the bridge response is a filtered Poisson (or Markov renewal) process. The theories provide a set of equations, which under certain assumptions allow to obtain the probability distribution function of the bridge response. Then, the mean upcrossing rate is calculated according to the Rice's formula. These methods are usually more efficient than the convolution method and can model all load effects. They can also be used for studying the fatigue problems.

Most of the above discussed approaches require quite advanced theoretical backgrounds (e.g. extreme value theory, theory of stochastic processes, etc.).

Furthermore, some of them (i.e. simulation based methods) require significant computational effort. Therefore, they are not very practical for standard engineering application. Nevertheless, they are usually used for calibration of traffic load models in codes or as a basis for some other simplified models.

5.4.6 Simplified probabilistic traffic load models for assessment of highway bridges

The simplified probabilistic traffic load models have been developed in order to assess the bridge traffic loads without the necessity of performing numerous simulations or complicated theoretical analysis. They are usually based on some simplified assumptions (regarding composition of traffic, multiple presence of heavy vehicles, position of the heavy vehicles on a bridge, etc.). The simplified models are very practical in the modelling of traffic loads (or load effects) characteristic for a specific bridge location and are especially suitable for reliability based load capacity evaluation of existing bridges.

Model of Moses and Ghosn. One of the first simplified probabilistic models of bridge traffic loads, for short and medium span bridges, has been proposed in Moses & Ghosn (1985). In this report it is assumed that the maximum traffic load is due to the occurrence of several heavy trucks simultaneously on the bridge. Just two types of trucks (single unit trucks and semi-trailer trucks) are considered, with random weight and a limited number of possible locations of the trucks on a bridge.

Performing analysis for a wide range of bridge spans and bridge locations Moses & Ghosn (1985) observed that a good representation of the tail of the gross vehicle weight histogram at a given site can be obtained from the gross weight value corresponding to the 95-th percentile value of all the gross weights recorded at that site. Also, they observed that 50-th percentile (i.e. median) value of the maximum moment distribution is a good representation of the maximum lifetime response.

Based on the above mentioned observations it is proposed to approximate the median of the total response of the maximum load, M, for a general truck traffic at a given site by the following relation (Moses & Ghosn, 1985):

$$M = amW_{95}H \tag{5.5}$$

where: a is a deterministic value relating the load effect to a reference loading scheme; m is a factor reflecting the variations of load effects of random heavy vehicles, compared to the standard, reference vehicle; W_{95} is a characteristic vehicle weight, defined as 95-th percentile of the weight probability function; H is a headway factor, describing the multiple presence of the vehicles on the bridge, it depends on the truck volume and span length. All parameters except a are random variables. Table 5.9 shows the parameters of the Equation 5.5 calibrated based on WIM data from nine different sites in United States (Moses & Ghosn, 1985).

Table 5.9: Model parameters (Moses & Ghosn, 1985).

Bridge span	Parameter a	Parameter m		Parameter H	
[m]	[kNm/kN]	Mean	COV	Mean	COV
9.1	1.85	0.92	15%	2.63	10%
12.2	2.61	0.93	12%	2.69	10%
18.3	4.14	0.94	6%	2.75	10%
24.4	4.08	0.93	9%	2.78	7%
30.5	5.61	0.95	7%	2.80	7%
38.1	7.44	0.96	6%	2.86	7%
45.7	9.42	0.96	5%	2.87	7%
53.3	11.25	0.97	4%	2.98	7%
61.0	13.23	0.97	4%	3.05	7%

The statistics of the parameter H presented in Table 5.9 have been obtained assuming 75-years projection, average truck volume of 2000 trucks per day and considering traffic moving in the same direction of two lane highways. For different traffic volumes, for different projection (reference) period, for opposing traffic or for one/three lane highways the parameter H may require some adjustment. Table 5.9 may give an idea about the necessary adjustments for different traffic volumes and different projection.

Table 5.10: Model parameters H for different volumes and projection periods (Moses & Ghosn, 1985).

Bridge span	Truck volume per day			Projection period		
[m]	200 t/d	2000 t/d	10000 t/d	1 year	5 years	50 years
12.2	2.41	2.69	2.79	2.35	2.42	2.58
30.5	2.51	2.80	2.93	2.48	2.55	2.68
61.0	2.54	3.05	3.57	2.65	2.80	3.01

The parameters a presented in Table 5.9 are corresponding to maximum (mid-span) moment effect. For the bending moment in a different location than mid-span, or for the shear force, the corresponding values of a have to be calculated separately. They can be easily obtained by comparing the weight of the reference vehicle with the corresponding load effect (moment or shear) caused by this vehicle (i.e. dividing the load effect by the load).

The parameters m presented in Table 5.9 are corresponding to the statistics of axle configuration of random truck traffic obtained from WIM measurements in United States. For European conditions and for some specific sites this parameter may take different values. Factor m is calculated as a ratio of the maximum response of a random truck to the maximum response of a reference truck (single unit or semi-trailer) of the same gross weight.

The characteristic vehicle weight W_{95} in Equation 5.5, for a specific bridge location, may take two different values depending on the bridge span. For spans less than 18.3 m the single unit trucks produce the critical loads, however, for spans longer than 18.3 m, semi-trailers control the loading. Based on the WIM data from nine different sites in United States Moses & Ghosn (1985) estimated the average value of W_{95} as 209 kN and 334 kN for the single unit and the semi-trailer trucks respectively. The corresponding coefficients of variation are 15% and 10%.

Equation 5.5 corresponds to the maximum total static traffic load applied on the bridge within its lifetime (considered usually as 50, 75 or 100 years). Furthermore, it considers that the traffic characteristics (vehicle weights and traffic volume) do not change with time during entire bridge life. To account for the possible traffic growth, for the dynamic effects and to take into consideration the distribution of load to the girders, Moses & Ghosn (1985) propose to modify the Equation 5.5 to the following form:

$$L = amW_{95}HIgG_r \tag{5.6}$$

where: I is a impact factor (dynamic amplification factor) taking into account dynamic effects; g is a girder distribution factor and G_r is traffic growth factor.

The impact factor I is dependent on the surface roughness. As suggested in Ghosn (1999) it can be considered equal to 1.1, 1.2 and 1.3 for smooth, medium and rough surfaces respectively. The corresponding coefficient of variation can be taken as 10%. However, Nowak (1999) suggests for prestressed concrete bridges the dynamic amplification factor of 1.09 with the coefficient of variation equal to 5%

According to Ghosn (1999), the girder distribution factor g calculated using the following relation:

$$g = \frac{S}{D} \tag{5.7}$$

is characterized by the bias factor 1.01 and 0.96 for reinforced concrete T-beams and prestressed concrete I girders respectively. The corresponding coefficient of variations are 5% and 8%. In the Equation 5.7 S is a girder spacing (in meters) and D is the factor depending on girder types (D=5.5 for prestressed concrete girders).

The mean value of the parameter G_r assumed by Moses & Ghosn (1985) is 1.15 with the corresponding coefficient of variation of 10%.

Model of Flint and Neill Partnership. The FNP (Flint and Neill Partnership) traffic load model (Cooper, 1997) has been created to help in checking the United Kingdom bridge stock for adequacy of carrying current (at the time) and future heavy vehicle (i.e. 40 tonne vehicles that were not allowed in UK before 1999). The model has been developed using full simulation performed based on WIM records collected during two weeks on the motorway carrying heavy intercity traffic in UK. Then, it has been verified against the WIM traffic data from some rural motorway. The model provide a set of modification factors on a general traffic load model which is similar to that presented in Eurocode (see Section

5.4.3). The model comprises statistically defined factors that, applied to the load effects produced by the basic deterministic load model, provide the probabilistic effects.

The basic deterministic static load model is very similar to the load model in EC-1b (2002). The only difference is that the tandem load on the Lane 2 in this model is considered to has the same intensity as the tandem load on the Lane 1 (axle load 300 kN). The additional lanes are loaded with tandem load equal to that defied for the Lane 3 in EC1 (axle load 100 kN). The area outside the notional lines are considered to be unloaded.

The probabilistic model assumes that the maximum load effects in a bridge element in question are well described by the type I extreme value distribution (Gumbel distribution). The probability density function of this distribution (PDF) is defined as follows (Cooper, 1997):

$$f_X(x) = \alpha \exp\left(-\alpha(x-U) - \exp\left(-\alpha(x-U)\right)\right) \tag{5.8}$$

The cumulative distribution function (CDF) is given by:

$$F_X(x) = \exp\left(-\exp\left(-\alpha(x-U)\right)\right) \tag{5.9}$$

where U is the mode of the distribution and α is an inverse measure of dispersion.

In order to obtain the probabilistic load effect, the deterministic load effect have to be multiplied by the above defined distribution function considering the distribution parameters U and α as presented in Tables 5.11 and 5.12.

The values of the parameter U, presented in Tables 5.11 and 5.12, correspond to annual maxima. The mode of the distribution for the maxima within N years would be (Cooper, 1997):

$$U_N = U - \frac{\ln(-\ln(1-1/N))}{\alpha} \tag{5.10}$$

which for large N can be simplified to:

$$U_N = U + \frac{\ln(N)}{\alpha} \tag{5.11}$$

The parameters of the probabilistic distribution presented in Tables 5.11 and 5.12 are applicable only for simply supported spans. Furthermore, they do not

Table 5.11: Lane 1 load effect factors (Cooper, 1997).

Bridge span [m]	Moment U 50000[(a)]	Moment U 10000[(b)]	Moment U 2000[(c)]	Moment α	Shear U 50000[(a)]	Shear U 10000[(b)]	Shear U 2000[(c)]	Shear α
5	0.423	0.383	0.354	56	0.443	0.400	0.370	53
10	0.387	0.350	0.324	62	0.407	0.368	0.340	58
16	0.444	0.399	0.368	52	0.490	0.435	0.396	42
20	0.411	0.381	0.360	77	0.421	0.381	0.354	58
40	0.373	0.351	0.335	102	0.382	0.347	0.323	67

Note: [(a)] trucks per direction per day (motorway); [(b)] trucks per direction per day (main road); [(c)] trucks per direction per day (minor road).

Table 5.12: All lanes load effect factors (Cooper, 1997).

Bridge span [m]	Moment U 50000[(a)]	Moment U 10000[(b)]	Moment U 2000[(c)]	Moment α	Shear U 50000[(a)]	Shear U 10000[(b)]	Shear U 2000[(c)]	Shear α
5	0.311	0.275	0.250	64	0.307	0.271	0.246	64
10	0.341	0.302	0.275	58	0.334	0.294	0.265	56
16	0.388	0.344	0.313	52	0.389	0.349	0.322	58
20	0.386	0.341	0.310	52	0.386	0.344	0.315	55
40	0.376	0.332	0.301	52	0.353	0.315	0.289	61

Note: [(a)] trucks per direction per day (motorway); [(b)] trucks per direction per day (main road); [(c)] trucks per direction per day (minor road).

Table 5.13: Dynamic amplification factors (Cooper, 1997).

Bridge span [m]	Bridge Frequency [Hz]	Road surface roughness	1 lane Mean	1 lane St. Dev.	1+2 lanes Mean	1+2 lanes St. Dev.
<25	>5	Good	1.08	0.10	1.08	0.07
		Medium/Poor	1.13	0.15	1.13	0.10
>40	< 3	Good	1.20	0.15	1.20	0.10
		Medium/Poor	1.27	0.20	1.27	0.14

consider the dynamic effects. To account for them, the load effects have to be multiplied by the normally distributed random variable with the distribution parameters presented in Table 5.13.

Chapter 6

Probabilistic response of typical concrete bridge sections

6.1 Introduction

The verification of a load carrying capacity of a bridge or other structures in accordance with the existing design or assessment codes is usually performed on the sectional level. In this approach the structure safety is checked comparing load effects in each particular component obtained from global structural analysis with its resistance calculated separately using sectional analysis. The resistance of a component is typically a function of the mechanical properties of materials and cross-sectional geometry. As it was already discussed in Chapter 4 all these quantities are uncertain and should be considered as random variables. Consequently, the resistance of a component is also a random variable.

In this chapter the probabilistic models of ultimate shear and bending responses of typical concrete bridge sections are presented and analysed. Besides some models proposed by other authors the original probabilistic models developed within the program of this thesis are presented. The models developed aims to be representative for stock of concrete highway bridges in Portugal with spans ranging from 3 to 35 meters. The developed models are focused on precast concrete bridges as they became quite common in Portugal and there is a lack of reliable models for this bridge typologies available in literature.

6.2 Methods of analysis and uncertainties of the analytical models

6.2.1 Basics

As it was already stated the resistance of a bridge component, commonly denoted by R, is a random variable. Theoretically the overall uncertainty in R could be determined based on results of extensive full scale tests. However, the possibility of performing a significant number of such test is rather limited because of significant costs. Therefore, the behaviour of structure components are usually analysed using some theoretical models and numerical simulations.

According to Nowak & Collins (2000) the possible sources of uncertainty in the resistance of a structural element can be divided into the following categories:

- Material properties (uncertainty in the material strength, the modulus of elasticity, cracking stress, ultimate strain, etc.);
- Fabrication (uncertainty in overall dimension of a component affecting cross-section area, inertia, section modulus, etc.);
- Analysis (uncertainty resulting from approximate methods of analysis and idealized models of material behaviour).

Therefore the resistance R may be considered as a function of nominal resistance R_n (as determined from a code rule) and three factors: material properties M, fabrication (geometry) F, and analysis (professional) P (Schneider, 1997).

$$R = R_n \cdot M \cdot F \cdot P \tag{6.1}$$

Factors P, M and F are ratios of actual to nominal values and have their own distribution properties. Considering that they are normally distributed and statistically independent it is possible to express the mean value of the variable R as:

$$\mu_R = R_n \cdot \mu_M \cdot \mu_F \cdot \mu_P \tag{6.2}$$

and its coefficient of variation as:

$$V_R = \sqrt{V_M^2 + V_F^2 + V_P^2} \tag{6.3}$$

where μ_M, μ_F and μ_P are the mean values and V_M, V_F and V_P are the coefficient of variations of factors M, F and P respectively.

6.2.2 Simulations

Many times the dimensional and material properties used for the derivation of some member property are non-normal. Furthermore, the relationship between them, describing the response of the component, are quite complex. Thus, the Equations 6.2 and 6.3 can not be directly applied and simulation may be required. The simulation procedure is presented schematically in Figure 6.1. Detailed information about 'crude' Monte Carlo simulation technique and about Latin Hypercube sampling method, two procedures commonly used to obtain statistical properties of member strength, is presented in Section 3.6.

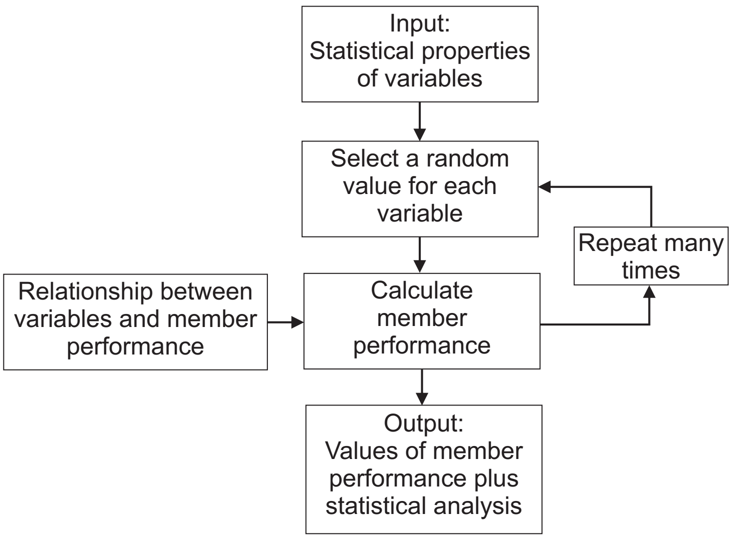

Figure 6.1: General scheme of simulation procedure, from Melchers (1999).

Since the distribution of the resistance is desired with most of the interest over the whole region rather than just the tails (an objective is to define mean and standard deviation of the response), relatively few simulations are required to obtain reasonable results (Melchers, 1999). For 'crude' Monte Carlo simulations it would be typically 100–500 and for Latin Hypercube 10–50.

The results of simulations, although take into account variability in geometrical (fabrication), F, and material, M, parameters (see Equation 6.1) already discussed in Chapter 4, may not reflect results of experimental tests. This can be explained by the fact that mathematical models used in the simulation algorithm do not predict the actual strength of the structure component with perfect accuracy. The expected deviations between analysis and tests may be taken into account by introducing a model (professional) variable P, the same as explained in previous section. This parameter theoretically can be also incorporated into the simulation algorithm. However, most of the authors prefer to consider it in the analysis separately (Casas, 2005; Nowak *et al.*, 1994; Tabsh & Nowak, 1991).

6.2.3 Model uncertainties

The probabilistic model of the professional factor P, known also as a model uncertainty, can be obtained by comparing the results of experimental tests R_e with values predicted by the analytical model $\widehat{R}_n$ considering the real geometry and mechanical properties of materials (Schneider, 1997):

$$P = \frac{R_e}{\widehat{R}_n} \tag{6.4}$$

From a number of experimental data a histogram for professional factor P can be obtained together with the mean value μ_P and the standard deviation σ_P. Then, some theoretical probability distribution function can be fitted to this sample of experimental results.

In general for good resistance prediction models $\mu_P \approx 1$ and the coefficient of variation is around few percent. For poor models, typically very conservative, $\mu_P > 1$ and the coefficient of variation is about 10–20%.

As discussed in Melchers (1999) the model of the professional factor defined by the Equation 6.4 is not dependent just on the quality of the mathematical model itself but also contains errors due to testing procedure and in-batch variations. These errors should to be excluded in order to obtain strictly modelling uncertainty. According to Melchers (1999) the mean values for both type of errors can be considered equal to 1.00 and the coefficients of variation can be taken as 2–4% and 4% for testing errors and in-batch variations respectively.

Since the full size test of structural components are relatively expensive, do not exist many information about the statistics of professional factor P. However, in the literature and in some codes it is possible to find several proposed values to be used in the reliability analysis and in the development of probabilistic models of components resistance.

Bending resistance of concrete elements. Mathematical models of bending capacity of reinforced and prestressed concrete sections gives generally good results when compared to the experimental data. This reflects in the statistics of the professional factor related to this property.

According to Melchers (1999), for the bending response of the reinforced and prestressed concrete elements calculated considering the non-linear behaviour of materials and the real stress-strain relations, the mean value, μ_P, of the model uncertainty can be considered equal to 1.02 and the corresponding coefficient of variation, V_P, equal to 3–4.6%.

Similar values for the same model of the bending response have been used by Nowak *et al.* (1994) and Nowak (1999) in the development of the resistance models of typical concrete bridge sections. For the resistance of reinforced concrete elements Nowak *et al.* (1994) and Nowak (1999) used μ_P=1.02 and V_P=6% and for prestressed concrete μ_P=1.01 and V_P=6%.

Quite different values, namely μ_P=1.20 and V_P=15%, are recommended in JCSS (2001). However, they corresponds to simple bending models based on linear behaviour of material and simplified stress-strain relations.

Generally, in order to avoid negative values, all authors recommend to use lognormal or normal truncated distribution function to model uncertainty of the analytical models of the bending response.

Shear resistance of concrete elements. As it is illustrated in Table 6.1, where statistics of the ratio R_T/R_P (tested/predicted resistance) obtained by Bohigas (2002) are presented, the existing models of shear capacity of reinforced and prestressed concrete elements are generally not very accurate. Therefore, the professional factors are characterized typically by higher mean and bigger scatter than in case of bending resistance models.

Table 6.1: Uncertainty of models of shear response R_T/R_P (Bohigas, 2002).

Shear model	Without shear reinf.		With shear reinf.	
	Mean value	COV [%]	Mean value	COV [%]
EHE - Spanish code	1.23	23.61	1.64	26.26
EC-2 - Eurocode	1.02	22.03	1.83	40.29
LRFD - AASHTO code	1.28	16.80	1.18	19.23
ACI 11-5 - ACI code	1.28	26.36	1.36	24.60
ACI 11-3 - ACI code	1.29	31.21	1.41	26.70
MCFT	1.13	20.00	1.07	17.39

Note: Presented statistics are based on the results of 316 experimental shear tests of high-strength concrete beams; MCTF - Modified Compression Fields Theory.

Nowak *et al.* (1994) and Nowak (1999) for relatively accurate model of shear response of reinforced and prestressed concrete elements, known as MCTF - Modified Compression Fields Theory (Vecchio & Collins, 1986), use the professional factor with mean μ_P=1.075 and the coefficient of variation V_P=10%. However, for concrete elements without shear reinforcement they used μ_P=1.20 and V_P=10%.

Similar values were observed by Bentz (2000). He compared results of 534 experimental tests with the values predicted using Modified Compression Field Theory. The statistics obtained for the professional factor are: μ_P=1.05 and V_P=12%. When the coefficients of variation of in-batch uncertainty, 4%, and testing error, 2%, would be subtracted from the overall value V_P, as suggested in Melchers (1999), the coefficient of variation of the model uncertainty would be reduced to 11%.

Significantly different values, namely μ_P=1.40 and V_P=25%, are recommended in JCSS (2001). However, they corresponds to very simple shear models as present in design codes.

Comparing results of the already mentioned 534 tests with values calculated using relatively simple shear model present in ACI code Bentz (2000) obtained the following statistics of the professional factor μ_P=1.20 and V_P=32.2%.

The same as in previous case, in order to avoid negative values, all authors recommend to use lognormal or normal truncated distribution function to model uncertainty of the analytical models of the shear response.

6.3 Models of flexural response

6.3.1 Basics

The behaviour of the reinforced or prestressed concrete elements subjected to bending is usually described by a moment-curvature relationship. In the case of reinforced concrete member the moment-curvature diagram is characterized by the cracking moment, M_{cr}, by the moment corresponding to steel yielding, M_y, by the ultimate bending resistance, M_u, and by the rotation capacity, Θ_u. As an example, the typical moment-curvature relationship for reinforced concrete element is showed in Figure 6.2.

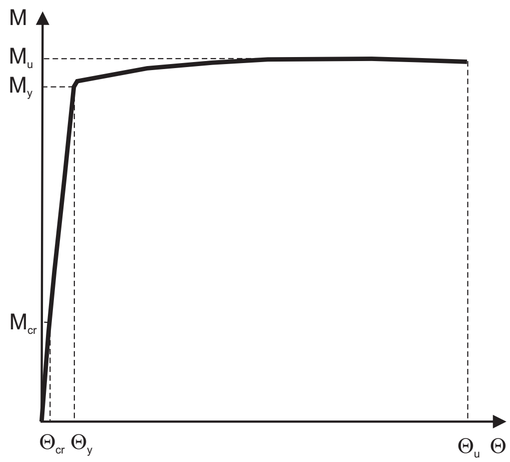

Figure 6.2: Typical moment-curvature diagram for reinforced concrete elements.

For prestressed concrete members, besides already mentioned points characteristic for reinforced concrete, on the moment-curvature diagram the decompression moment, M_d, may be also distinguished as a point of relevance. The typical moment-curvature relationship for a prestressed concrete element is shown in Figure 6.3.

The variability in the flexural response of reinforced and prestressed concrete elements depends on the following factors:

- variability of the mechanical properties of concrete and steel (concrete compressive strength, strength of reinforcing and prestressing steel, etc.);

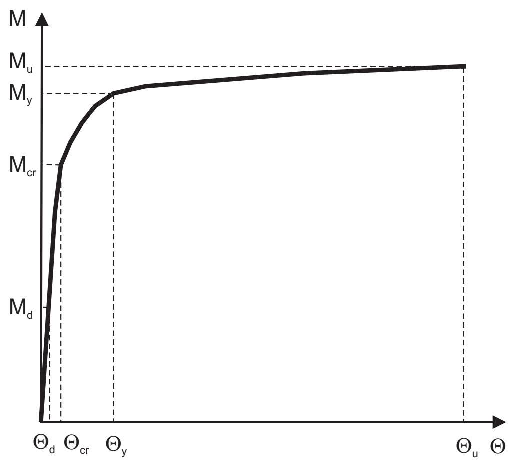

Figure 6.3: Typical moment-curvature diagram for prestressed concrete elements.

- variability in element geometry (effective depth, flange dimensions, etc.);
- materials degradation (e.g. corrosion);
- load history (fatigue phenomena);
- method of definition of the structural response.

Neglecting the effects of material degradation and load history, which are not a subject of this thesis, the causes of uncertainty about structural resistance can be put into three categories, already discussed in previous sections: material M, fabrication F and analysis P.

Although the decompression moment, the cracking moment and the moment corresponding to steel yielding, may be important from the serviceability point of view, in the capacity evaluation the ultimate bending resistance is the key parameter. Therefore, its variability has been studied more than variability of other characteristic properties of concrete members what is reflected on the availability of probabilistic models.

In the following points the probabilistic models of cracking moment and ultimate bending capacity of the reinforced and prestressed concrete bridge sections found in literature are discussed. Besides that, the probabilistic models developed within the program of this thesis are also presented.

6.3.2 Existing probabilistic models

Models for US highway bridges. The statistical parameters of bending resistance for typical reinforced and prestressed concrete bridge sections in United States were derived by Tabsh & Nowak (1991), Nowak *et al.* (1994) and Nowak (1999). They have analysed three reinforced concrete T-beams (depth 0.90–1.20m) and three prestressed concrete AASHTO-type girders (depth 1.13–1.58m), all of different depths corresponding to different spans. Considering probabilistic models of the basic variables representative for bridges in United States (for details see Nowak, 1999; Nowak *et al.*, 1994; Tabsh & Nowak, 1991) and using numerical procedure allowing for non-linear behaviour of concrete and steel they obtain results presented in the column assigned FM in Table 6.2. After taking into consideration the model uncertainty P the final values shown in the last two columns (R) of the Table 6.2 have been obtained.

Table 6.2: Statistical parameters of bending resistance (Nowak, 1999).

Type of structure	FM		P		R	
	Bias	COV	Bias	COV	Bias	COV
Reinforced concrete - T-beams	1.12	12%	1.02	6%	1.14	13%
Prestressed concrete - I-girders	1.04	4%	1.01	6%	1.05	7.5%

In general, the major parameters which determine the flexural performance of reinforced concrete elements with the defined geometry are the amount of reinforcement, steel yield stress and concrete strength. However, Nowak *et al.* (1994) observed that for ductile members (designed to fail by steel) the most important parameter is the steel yield stress. Therefore, the bias factor and the coefficient of variation of the member resistance FM, obtained from simulations (see Table 6.2), are similar to the bias and coefficient of variation of the steel yield strength, considered in the analysis as λ=1.12 and V=10% respectively.

In the prestressed concrete members designed to fail in a ductile manner, the ultimate flexural response is governed by the strength of prestressing steel (Nowak *et al.*, 1994). This happens because precast prestressed concrete girders are usually under reinforced (the amount of traditional reinforcing steel is very small). Therefore, the bias factor of the member resistance FM obtained from simulations (see Table 6.2) is equal to the bias of the ultimate strength of prestressing steel considered in the analysis as λ=1.04. However, the coefficient of variation of the ultimate bending capacity (see Table 6.2) is just slightly higher than the coefficient of variation of the ultimate strength of prestressing steel taken as V=2.5%.

Tabsh & Nowak (1991), Nowak *et al.* (1994) and Nowak (1999) use normal distributions to model ultimate bending capacity of reinforced and prestressed concrete sections.

Models for Spanish highway bridges. Sobrino (1993) developed probabilistic models for bending capacity of some bridge typologies common in Spain. He studied the performance of reinforced concrete solid slab (depth 0.65m), prestressed (post-tensioned) concrete voided slab (depth 1.50m), designed to fail in ductile manner, and prestressed (post-tensioned) concrete voided slab (depth 0.90m), designed to fail by concrete crushing. Considering probabilistic models of material properties and geometrical variations representative for bridge constructions in Spain (for details see Sobrino, 1993) and using professional factor P with unit mean and coefficient of variation of 4% he obtained the results presented in Table 6.3.

Table 6.3: Statistical parameters of bending resistance (Sobrino, 1993).

Type of structure	Cracking moment		Ultimate moment	
	COV	Distrib.	COV	Distrib.
Reinforced concrete slab	12.9%	Normal	8.3%	Normal
Prestressed concrete slab (ductile)	8.1%	Lognor.	5.5%	Lognor.
Prestressed concrete slab (n/ductile)	8.2%	Lognor.	7.4%	Normal

Sobrino (1993) similarly to Nowak *et al.* (1994) observed that the coefficient of variation of the ultimate bending response of reinforced concrete slab (see Table 6.3) is nearly the same as the coefficient of variation of yielding stress of steel (in this case assumed as $V \approx 8\%$). Nevertheless, the coefficient of variation of the ultimate bending response of prestress concrete slabs obtained by Sobrino (1993) is significantly higher than the coefficient of variation of yielding stress of steel (taken as $V \approx 2\%$). For the case of slab designed to fail by steel, this can be explained by the fact that in opposite to prestressed sections analysed by Nowak *et al.* (1994) the slabs analysed by Sobrino (1993) are strongly reinforced with ordinary reinforcement. However, for the case of slab designed to fail by concrete, it can be explained by the fact that the ultimate response of the section is governed more by concrete strength and geometry rather than by prestressing steel strength.

Regarding cracking moment capacity of reinforced and prestressed concrete bridge sections, based on the results presented in Table 6.3 it can be observed that the coefficient of variation describing this property is higher than the coefficient of variation corresponding to ultimate bending capacity. This can be explained by the fact that the cracking capacity is usually governed by concrete strength properties that are characterized by higher coefficient of variation than steel properties.

Sobrino (1993) recommends to use normal or lognormal distributions to model cracking moment and ultimate bending capacity of reinforced and prestressed concrete sections.

Models for European railway bridges. The statistical parameters of bending resistance for reinforced and prestressed concrete elements representative for European railway bridges were derived by Casas (2005). He analysed reinforced concrete rectangular beams (depth 1.2–1.8m), reinforced concrete T-beams (depth 0.8–1.5m), prestressed (post-tensioned) concrete rectangular beams (depth 1.0–1.8m) and prestressed (post-tensioned) massive slabs (depth 1.0m). Besides the influence of section geometry (different section of the same typology) Casas (2005) analysed the influence of several other parameters. For reinforced concrete rectangular beams and reinforced concrete T-shape beams he investigated the influence of variability of steel yielding strength on the mean value and the coefficient of variation of the ultimate flexural response. For the post-tensioned concrete rectangular beam and the post-tensioned massive slab he investigated the influence of variability of reinforcing and prestressing steel strengths and variability of concrete strength on the mean value and the coefficient of variation of the ultimate bending resistance.

Based on the results of several analysis performed, Casas (2005) proposed probabilistic models resumed in the column assigned FM in Tables 6.4 and 6.5. After taking into consideration the model uncertainty P the values shown in last two columns (R) of Tables 6.4 and 6.5 have been obtained. These values can be directly used in the reliability analysis.

Table 6.4: Statistics of bending resistance for RC and PC members (Casas, 2005).

Type of structure	COV of f_{sy}	FM		P		R	
		Bias	COV	Bias	COV	Bias	COV
RC beams and slabs	5%	1.15	5.5%	1.02	6%	1.17	8%
	10%	1.15	10%	1.02	6%	1.17	12%
	15%	1.15	15%	1.02	6%	1.17	16%
PC slabs, $A_s/A_p < 1.2$	5-15%	1.11	5%	1.01	6%	1.12	8%
PC slabs, $A_s/A_p > 1.2$	5%	1.11	4%	1.01	6%	1.12	7%
	10%	1.11	5%	1.01	6%	1.12	8%
	15%	1.11	6%	1.01	6%	1.12	8.5%

Note: A_s and A_p are the area of reinforcing and prestressing steel respectively: f_{sy} is the steel yielding strength.

The study performed by Casas (2005) confirm the observation of other authors that for reinforced concrete ductile members (designed to fail by steel) the most important parameter in the ultimate flexural response is the steel yield stress. Therefore, the bias factor and the coefficient of variation of the member resistance FM obtained from simulations (see Table 6.4) are similar to the bias and the coefficient of variation of the steel yield strength considered in the analysis as λ=1.15 and V=5–15% respectively.

In the prestressed concrete beams, depending on the ratio A_p/A_c (area of prestressing steel to area of concrete) the ultimate flexural response is governed by the strength of prestressing steel and/or strength of concrete (Casas, 2005). The influence of the traditional reinforcing steel is quite small. It could be expected since the prestressed concrete beams are usually reinforced with minimum amount of traditional reinforcement. Owing to the fact that the response is governed by more than one variable there is not possible to correlate statistics of ultimate bending resistance with the statistics corresponding to one only variable.

Table 6.5: Statistics of bending resistance for PC rect. beams (Casas, 2005).

Type of structure	COV of f_c	FM		P		R	
		Bias	COV	Bias	COV	Bias	COV
PC beams, $A_p/A_c \approx 0.3\%$	5-15%	1.10	3%[(a)]	1.01	6%	1.11	7%
	5-15%	1.10	5%[(b)]	1.01	6%	1.11	8%
PC beams, $A_p/A_c \approx 0.5\%$	5%	1.06	3%	1.01	6%	1.07	6.5%
	10%	1.06	4%	1.01	6%	1.07	7%
	15%	1.06	6%	1.01	6%	1.07	8.5%
PC beams, $A_p/A_c \approx 0.7\%$	5%	1.00	3%	1.01	6%	1.01	6.5%
	10%	1.00	4%	1.01	6%	1.01	7%
	15%	1.00	6%	1.01	6%	1.01	8.5%

Note: A_p is the area of prestressing steel and A_c is the area of concrete; f_c is the concrete strength; [(a)] and [(b)] corresponds to COV of ultimate strength of prestressing steel, f_{pu}, equal to 2% and 5% respectively.

In the prestressed concrete massive slabs, depending on the ratio A_s/A_p (area of reinforcing steel to area of prestressing steel), the ultimate flexural response is governed by the strength of reinforcing steel and/or strength of prestressing steel (Casas, 2005). The influence of concrete strength is quite small due to the fact that prestressed concrete massive slabs have very large area of concrete that can work in compression and change in concrete strength does not influence significantly the section capacity. The same as previously, in this case the response is governed by more than one variable. Therefore, it is not possible to correlate easily the statistics of ultimate bending resistance with the statistics of any single variable.

Casas (2005) suggest to use normal distributions to model ultimate bending capacity of reinforced and prestressed concrete elements.

6.3.3 Selection of representative examples

In recent years, precast concrete solutions for highway bridges become really common in Portugal (Cruz & Wiśniewski, 2004; Lopes & Wiśniewski, 2004). The national programs of the development of the railway and highway network, which starts in the last decade, cause huge progress on the area of civil engineering. Very harsh requirements related to the time of contract execution forced engineers and contractors to use efficient technologies of constructing small and medium span bridges. In many cases the precast solutions have been found the most competitive. Therefore, at the moment precast concrete bridges make up a significant part of the stock of existing bridges in Portugal.

Considering the above mentioned facts and assuming that for older, cast in-situ concrete bridges, the models proposed by Nowak *et al.* (1994), Sobrino (1993) and Casas (2005), and described in previous section may be used, it has been decided to develop probabilistic models of flexural response just for typical precast concrete sections representative of the stock of bridges in Portugal.

Very short span bridges in Portugal (spans ranging from 3 to 10 meters) are commonly constructed from reinforced concrete elements (Lopes & Wiśniewski, 2004; Wiśniewski *et al.*, 2005). The longitudinal sections are usually closed boxes, two legs frames or vaults. However, their cross-sections are normally in a form of a massive slab with depth ranging between 0.25 m and 0.55 m. Therefore, in the development of the probabilistic models of ultimate flexural response of bridge slab elements (see Figure 6.4), several different depths have been considered (see Table 6.6). Furthermore, for each depth three different cases, corresponding to different amount of reinforcement (A - minimum; B - moderate; C - high), have been analysed. The slab depth and area of reinforcement have been designed for each considered bridge span according to REBAP (1985) and assuming bridge traffic loads from RSA (1983).

Short and medium span bridges in Portugal (spans ranging from 10 to 40 meters) are commonly constructed as cast in-situ reinforced concrete slabs on precast prestressed concrete I-shape and U-shape girders (Lopes & Wiśniewski, 2004; Wiśniewski *et al.*, 2004a). In the longitudinal configuration they can be simply supported or continuous (with partial or full continuity provided between adjacent spans). However, their cross-sections are normally composed by 0.25–0.30 m thick reinforced concrete slab cast on several precast prestressed concrete girders, with depth ranging from 0.75 m to 2.40 m, spaced by 1.5–8.0 m (depending on girder type and depth). Therefore, in the development of probabilistic models of ultimate flexural response of precast prestressed concrete bridge sections (see Figures 6.5 and 6.6), several different sections dimensions have been considered (see Tables 6.7 and 6.8). Furthermore, for each section three different cases, corresponding to different amount of prestressing steel (A - minimum; B - moderate; C - high), have been analysed. The principal dimensions of the section (girder depth, girder spacing, etc.) have been assumed according to tables developed by girder producer. However, the area of prestressing steel have been designed for each considered bridge span according to REBAP (1985) and assuming bridge traffic loads from RSA (1983).

Reinforced concrete slabs - bridges with spans between 3 m and 10 m.

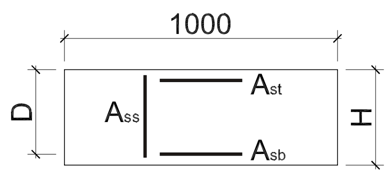

Figure 6.4: Cross-section of reinforced concrete slab (dimensions [mm]).

Table 6.6: Parameters of RC slab elements for flexural analysis.

Type of structure	Designation	Span L [m]	Height H [mm]	Depth D [mm]	Steel area $A_{sb/t}$ [mm^2]
Box culvert	S-250-A	3.0	250	220	251
	S-250-B	3.0	250	220	565
	S-250-C	3.0	250	220	1571
	S-350-A	5.0	350	320	393
	S-350-B	5.0	350	320	565
	S-350-C	5.0	350	320	3142
Optimized frame	S-450-A	7.5	450	410	565
	S-450-B	7.5	450	410	1571
	S-450-C	7.5	450	410	2199
	S-550-A	10.0	550	510	792
	S-550-B	10.0	550	510	2199
	S-550-C	10.0	550	510	3142

Prestressed concrete I-shape girders - bridges with spans 15–30 m.

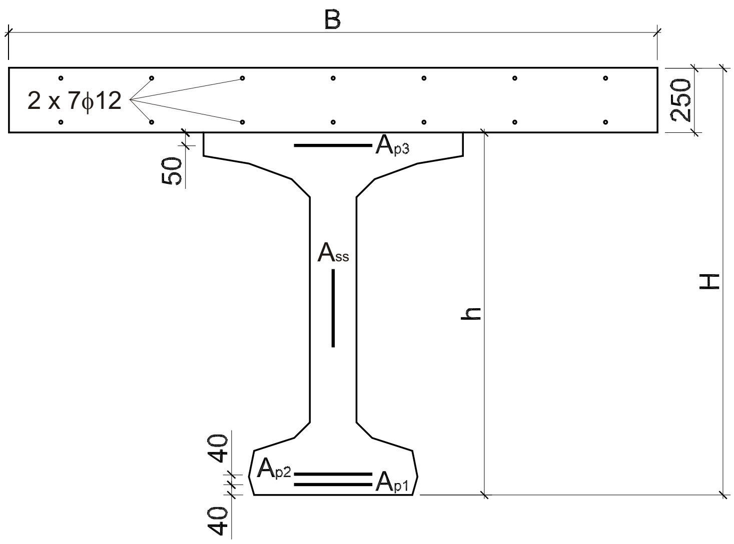

Figure 6.5: Cross-section of prestressed concrete I-shape girder (dim. [mm]).

Table 6.7: Parameters of I-shape girders for flexural analysis.

Designation	Span	Height	Tot. heig.	Width	Strands area [mm^2]		
	L [m]	h [mm]	H [mm]	B [mm]	A_{p1}	A_{p2}	A_{p3}
I-750-A	–	750	1000	2000	292.8	–	–
I-750-B	–	750	1000	2000	878.4	–	198
I-750-C	15.0	750	1000	2000	1464	585.6	585.6
I-1000-A	–	1000	1250	2000	292.8	–	–
I-1000-B	–	1000	1250	2000	1171.2	–	198
I-1000-C	20.0	1000	1250	2000	1464	1171.2	396
I-1400-A	–	1400	1650	2500	439.2	–	–
I-1400-B	–	1400	1650	2500	1464	–	198
I-1400-C	25.0	1400	1650	2500	1610.4	1464	396
I-1800-A	–	1800	2050	2500	585.6	–	–
I-1800-B	–	1800	2050	2500	1464	–	198
I-1800-C	30.0	1800	2050	2500	1756.8	1610.4	396

Prestressed concrete U-shape girders - bridges with spans 20–35 m.

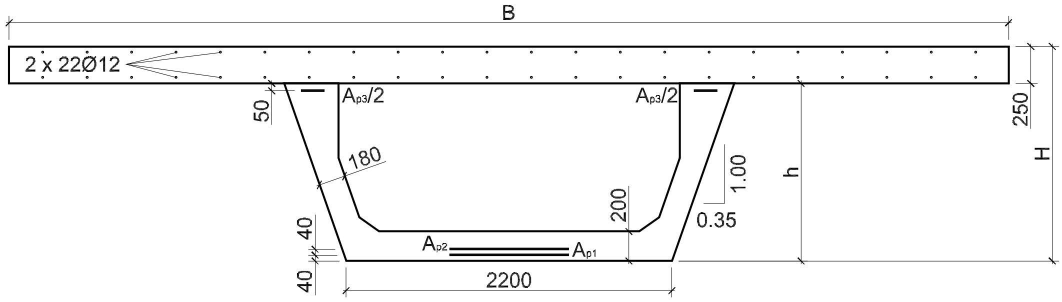

Figure 6.6: Cross-section of prestressed concrete U-shape girder (dim. [mm]).

Table 6.8: Parameters of U-shape girders for flexural analysis.

Designation	Span	Height	Tot. heig.	Width	Strands area [mm^2]		
	L [m]	h [mm]	H [mm]	B [mm]	A_{p1}	A_{p2}	A_{p3}
U-1000-A	–	1000	1250	6750	1024.8	–	–
U-1000-B	–	1000	1250	6750	2928	–	198
U-1000-C	20.0	1000	1250	6750	5856	585.6	396
U-1200-A	–	1200	1450	6750	1171.2	–	–
U-1200-B	–	1200	1450	6750	3806.4	–	198
U-1200-C	25.0	1200	1450	6750	5856	2049.6	198
U-1500-A	–	1500	1750	8000	1317.6	–	–
U-1500-B	–	1500	1750	8000	4392	–	198
U-1500-C	30.0	1500	1750	8000	5856	3220.8	198
U-2000-A	–	2000	2250	8000	1610.4	–	–
U-2000-B	–	2000	2250	8000	4684.8	–	198
U-2000-C	35.0	2000	2250	8000	5856	3513.6	396

6.3.4 Models and parameters used in the simulations

The analysis of the flexural response of concrete bridge sections, selected in previous paragraph, have been performed using special numerical code 'Seccao' (Henriques, 2002). The code allows to determine the moment-curvature relationship corresponding to the given material properties and the geometry of any kind of reinforced and/or prestressed concrete section. The program assumes that strains are linearly distributed within a given cross-section. The cross-section is modelled by a number of trapezoidal horizontal thin strips. For a given strain stage, the corresponding stresses are calculated using the apropriate material constitutive models. The bending moment correspondent to given curvature is calculated by integrating the internal stresses.

The models of the material behaviour considered in the analysis have been adopted from EC-2 (2004). Figures 6.7 and 6.8 show the constitutive models used for concrete and reinforcing and/or prestressing steel respectively.

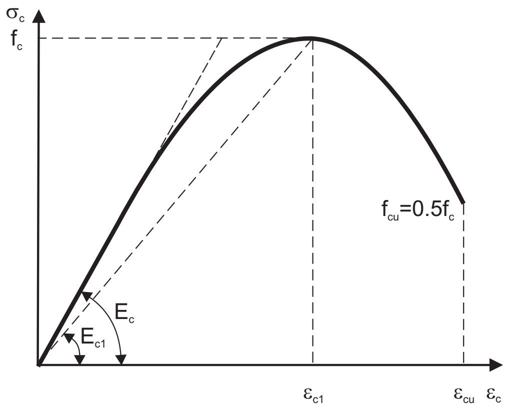

Figure 6.7: Stress-strain diagram for concrete.

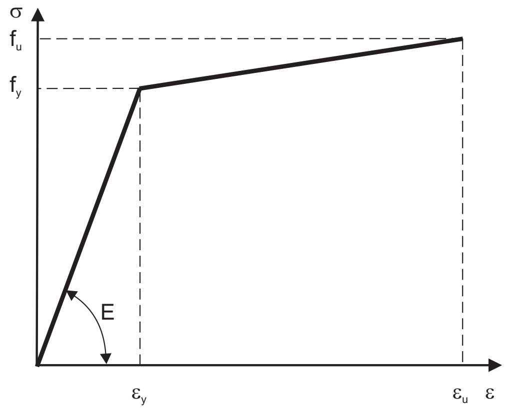

Figure 6.8: Stress-strain diagram for reinforcing and/or prestressing steel.

The statistics of the material and geometrical parameters considered in the analysis as random are shown in Table 6.9. They have been assumed based on the information presented in Chapter 4. All random variables presented in Table 6.9 have been considered normally distributed. Remaining parameters have been considered deterministic and their representative values have been taken from EC-2 (2004), Figures 6.4, 6.5, 6.6, and Tables 6.6, 6.7, 6.8. The representative values of the elasticity modulus of the reinforcing and prestressing steels have been taken as 200 GPa and 195 GPa respectively.

Table 6.9: Statistical parameters of material properties and dimensions.

Variable	Notation	Nominal	Bias	COV
Concrete compressive strength	f_c	30 MPa	1.0	$9\%^{(a)}$; $12\%^{(b)}$
Concrete elasticity modulus	E_c	33 GPa	1.0	$8\%^{(c)}$
Concrete tensile strength	f_{ct}	2.0 MPa	1.45	$20\%^{(d)}$
Concrete compressive strength	f_c	50 MPa	1.0	$9\%^{(a)}$
Concrete elasticity modulus	E_c	37 GPa	1.0	$8\%^{(c)}$
Concrete tensile strength	f_{ct}	2.85 MPa	1.45	$20\%^{(d)}$
Steel yielding strength	f_{sy}	500 MPa	1.15	5%
Steel ultimate strength	f_{su}	575 MPa	1.15	$5\%^{(e)}$
Strain at ultimate load	ϵ_{su}	7.5%	1.33	15%
Strands yielding strength	f_{py}	1670 MPa	1.04	2.5%
Strands ultimate strength	f_{pu}	1860 MPa	1.04	$2.5\%^{(f)}$
Strain at ultimate load	ϵ_{pu}	3.5%	1.43	8%
Reinforcement area	A_s	nominal	1.0	2.0%
Prestressing strands area	A_p	nominal	1.0	1.3%
Section depth	h	nominal	1.0	$500/h\%^{(g)}$
Effective depth	d	nominal	1.0	$500/h\%^{(g)}$
In-situ slab thickness	t	250 mm	1.0	4%
Stirrups spacing	s	nominal	1.0	$500/h\%^{(g)}$
Prestressing strain	P	0.537%	1.0	6%

Note: $^{(a)}$ for plant cast concrete; $^{(b)}$ for concrete cast in-situ; $^{(c)}$ correlated with f_c, correl. coef. C=0.9; $^{(d)}$ correlated with f_c, correl. coef. C=0.7; $^{(e)}$ correlated with f_{sy}, correl. coef. C=0.85; $^{(f)}$ correlated with f_{py}, correl. coef. C=0.80; $^{(g)}$ h in [mm].

6.3.5 Results obtained from simulation

The numerical analysis performed allows to define moment-curvature relationships for each of 36 selected examples. Firstly, the analysis has been carried out for each case considering all the variables at their characteristic or nominal value. Then, the analysis has been executed for all variables taken as their mean value. After that, simulations have been performed using 'crude' Monte Carlo method. In each case analysis has been executed 250 times for the set of variables generated randomly according to the corresponding probability distribution function. In the next step the characteristic points of the response, yielding moment and ultimate moment, have been evaluated statistically. The histograms have been created and basic statistics of the distribution (mean, standard deviation and coefficient of variation) have been calculated. Then, the K-S Lilliefors goodness-of-fit test has been performed to check if the obtained response can be modelled by normal distribution.

Figures 6.9 and 6.10 show the moment-curvature relationships obtained for reinforced concrete elements S-250-A and S-550-C. In referred figures, besides moment-curvature diagrams the histograms of yielding and ultimate moments are also presented. In general, the moment-curvature relationships and histograms of the yielding and ultimate moments obtained for all the analysed reinforced concrete sections are very similar to those presented in Figure 6.10. The only exception is the case of the section S-250-A characterized by very low reinforcement area which cause that in certain simulations the cracking moment was higher than the moment sustained by reinforcement after cracking. Therefore, two different failure modes have been observed which can be seen in the histogram of the ultimate moment where two peaks are visible.

Figures 6.11 and 6.12 show the moment-curvature relationships obtained for prestressed concrete bridge sections I-1800-C and U-2000-C. As previously, in referred figures the histograms of yielding and ultimate moments are also presented. Generally, the moment-curvature relationships and histograms of the yielding and ultimate moments obtained for all the analysed prestressed concrete sections are very similar to those presented in Figures 6.11 and 6.12.

In Tables 6.10 6.11 and 6.12 all the results of the simulations are resumed. For every analysed section the nominal values, bias factors (ratio of mean to nominal value) and coefficients of variation for yielding and ultimate moments are presented. As it can be seen there is a clear tendency in the obtained results.

For all the reinforced concrete sections, except S-250-A, the bias factor for ultimate moment is oscillating between 1.09 and 1.15 and the coefficient of variation takes values between 5% and 6%. Those values are very similar to that corresponding to the yielding strength and the ultimate strength of reinforcing steel. For yielding moment the bias factors and coefficients of variation are slightly higher.

Looking to the sensitivity plot presented in Figure 6.13 it can be seen that strength properties of reinforcing steel have actually the highest influence on the yielding and ultimate response of the analysed sections. Thus the observed relation between the bias factors and the coefficients of variation of steel strength properties and ultimate flexural response can be understood. Furthermore, it can be seen that besides strength properties of reinforcing steel the reinforcement area and the section effective depth shows significant correlation with the yielding and ultimate moments. Influence of the remaining variables is almost negligible. An exception is the case of the section S-250-A where, due to already explained reasons, the tensile strength of concrete is an important parameter.

In case of prestressed concrete sections, the bias factor and the coefficient of variation for the ultimate moment are 1.01–1.05 and 3.1–3.8% respectively. Those values are very similar to that corresponding to the yielding strength and the ultimate strength of prestressing steel. For yielding moment the statistics are nearly the same.

Analysing the sensitivity plots presented in Figures 6.14 and 6.15 similar conclusions can be drawn as in the previous case. The variables that have the highest influence on the yielding and the ultimate response of the analysed sections are the strength properties of the prestressing steel. The girder depth, the slab thickness and the area of bottom prestressing strands are also quite important. Remaining variables have negligible influence on the results.

For all the analysed cases the lognormal and normal distributions have been found appropriate to model the yielding moment and the ultimate moment.

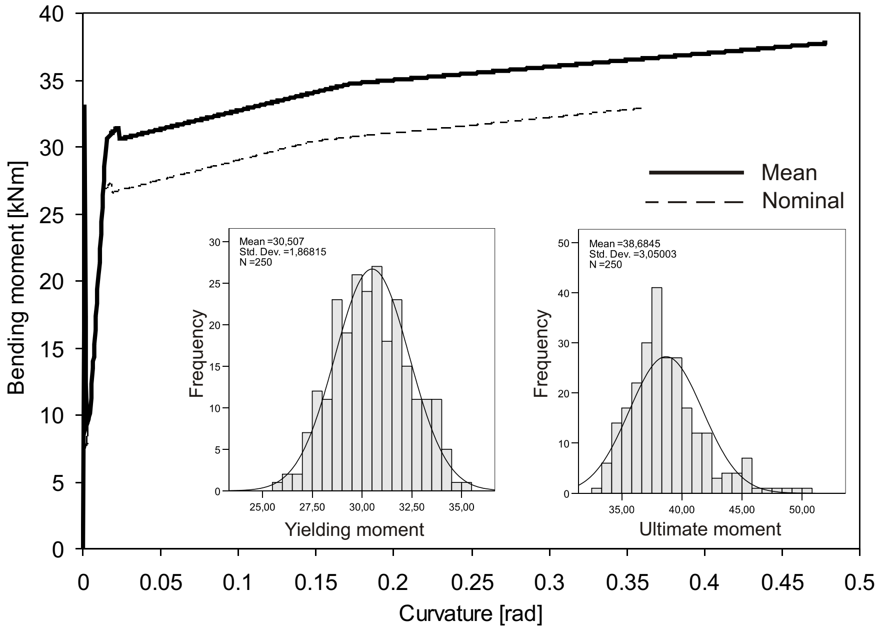

Figure 6.9: Moment-curvature diagrams for section S-250-A.

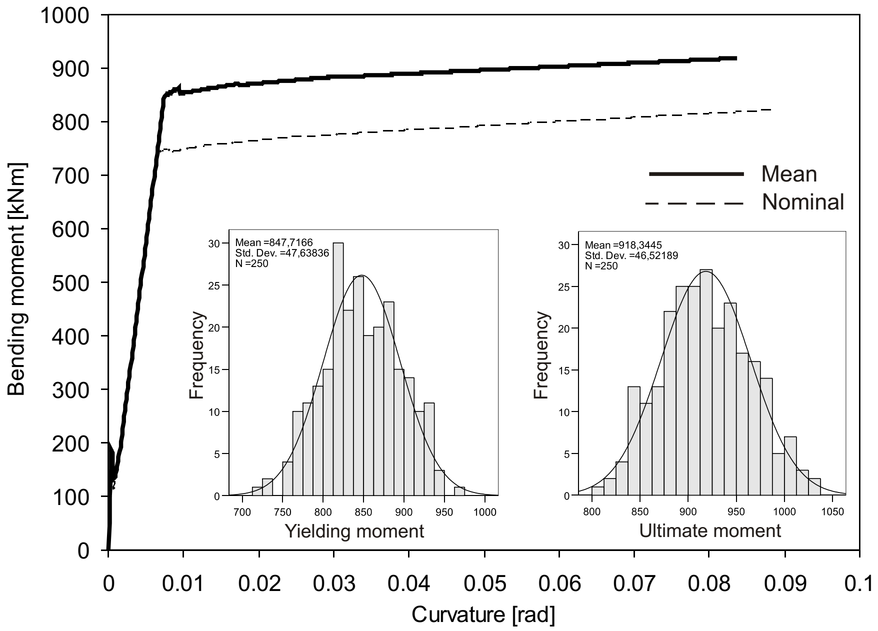

Figure 6.10: Moment-curvature diagrams for section S-550-C.

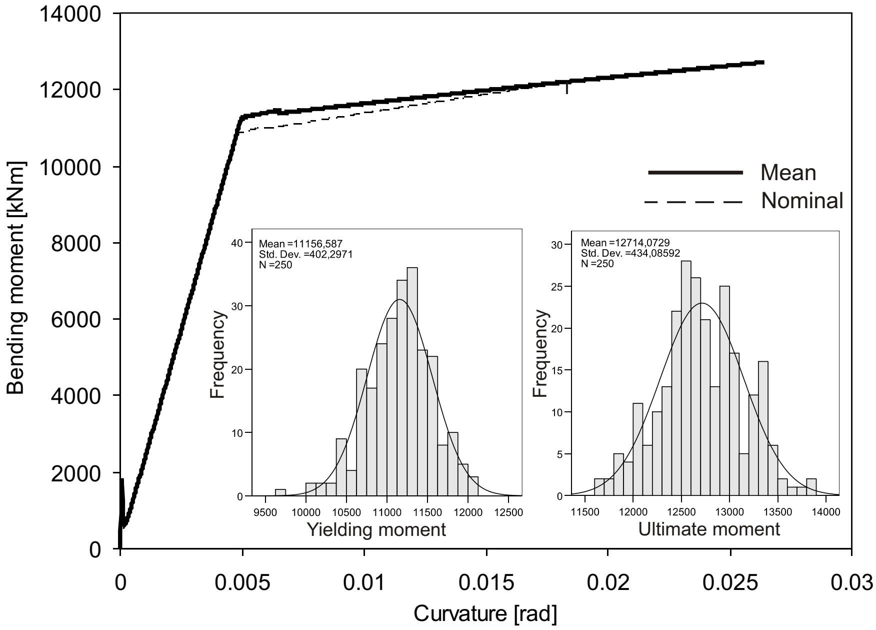

Figure 6.11: Moment-curvature diagrams for section I-1800-C.

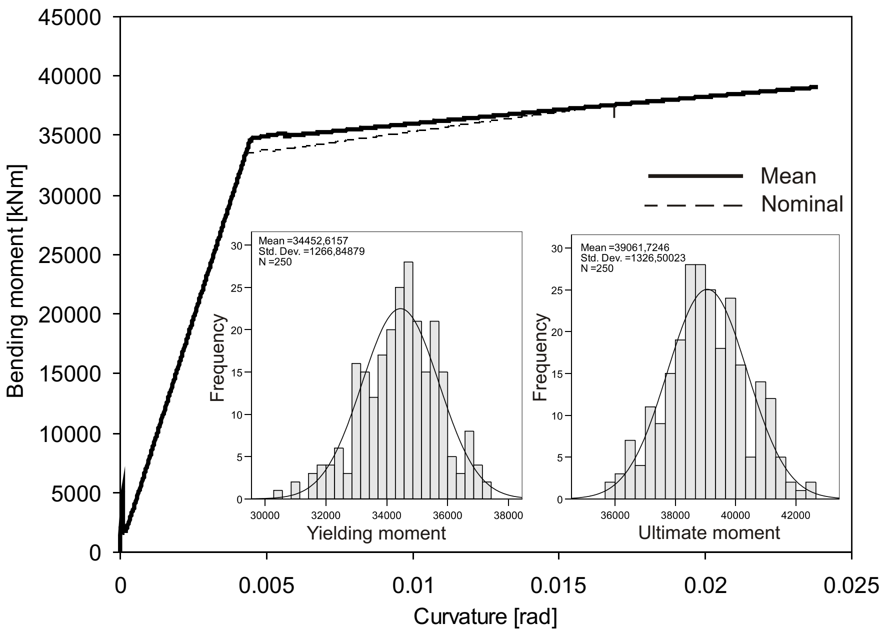

Figure 6.12: Moment-curvature diagrams for section U-2000-C.

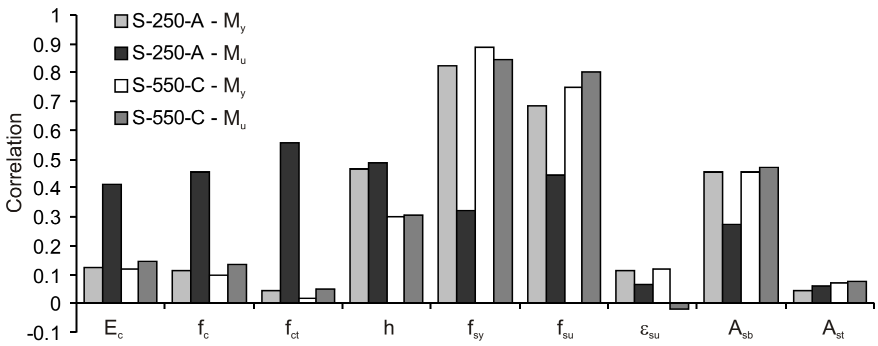

Figure 6.13: Sensitivity plot for sections S-250-A and S-550-C.

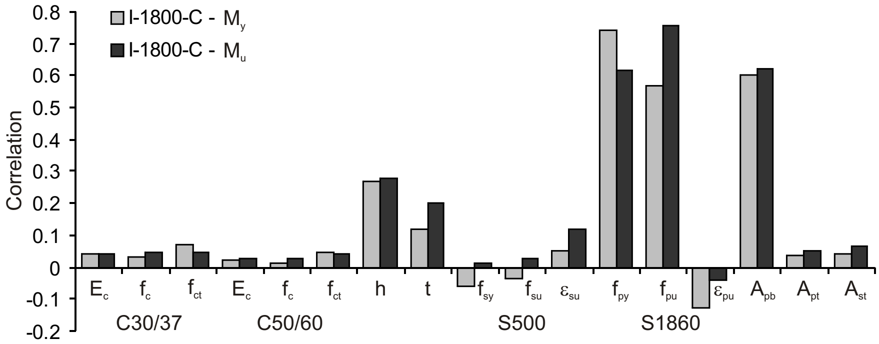

Figure 6.14: Sensitivity plot for section I-1800-C.

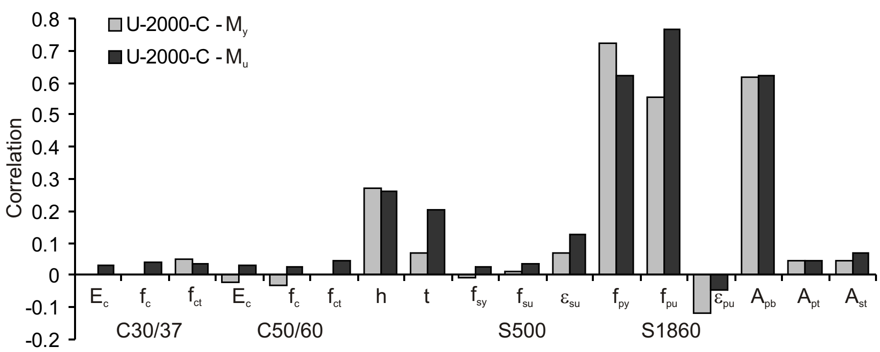

Figure 6.15: Sensitivity plot for section U-2000-C.

Table 6.10: Statistical parameters of M_y and M_u for RC slab elements.

Designation	Yielding moment M_y			Ultimate moment M_u		
	Nominal	Bias	COV	Nominal	Bias	COV
S-250-A	26.60 kNm	1.147	6.1%	34.00 kNm	1.138	7.9%
S-250-B	51.10 kNm	1.271	7.4%	72.47 kNm	1.089	5.7%
S-250-C	155.06 kNm	1.143	6.5%	169.88 kNm	1.119	5.8%
S-350-A	61.17 kNm	1.137	6.4%	73.99 kNm	1.151	5.6%
S-350-B	86.02 kNm	1.151	5.6%	106.22 kNm	1.110	5.2%
S-350-C	453.05 kNm	1.146	5.8%	498.44 kNm	1.120	5.4%
S-450-A	112.49 kNm	1.068	6.8%	138.21 kNm	1.092	5.1%
S-450-B	300.06 kNm	1.445	5.9%	340.78 kNm	1.112	5.1%
S-450-C	413.59 kNm	1.117	5.7%	462.50 kNm	1.088	5.1%
S-550-A	184.30 kNm	1.120	6.4%	232.84 kNm	1.107	5.1%
S-550-B	530.00 kNm	1.104	7.3%	592.47 kNm	1.111	5.0%
S-550-C	738.91 kNm	1.147	5.6%	820.87 kNm	1.118	5.1%

Table 6.11: Statistical parameters of M_y and M_u for prestressed I girders.

Designation	Yielding moment M_y			Ultimate moment M_u		
	Nominal	Bias	COV	Nominal	Bias	COV
I-750-A	501 kNm	1.045	3.9%	584 kNm	1.054	3.1%
I-750-B	1435 kNm	1.035	4.0%	1692 kNm	1.040	3.6%
I-750-C	3101 kNm	1.040	3.7%	3702 kNm	1.007	3.7%
I-1000-A	613 kNm	1.053	3.8%	719 kNm	1.052	3.4%
I-1000-B	2324 kNm	1.041	3.6%	2753 kNm	1.033	3.5%
I-1000-C	4933 kNm	1.040	3.5%	5724 kNm	1.027	3.5%
I-1400-A	1216 kNm	1.029	4.2%	1368 kNm	1.046	3.3%
I-1400-B	3844 kNm	1.041	3.5%	4447 kNm	1.037	3.5%
I-1400-C	7767 kNm	1.042	3.5%	8914 kNm	1.043	3.4%
I-1800-A	1963 kNm	1.042	3.6%	2235 kNm	1.048	3.7%
I-1800-B	4803 kNm	1.041	3.5%	5520 kNm	1.042	3.5%
I-1800-C	10728 kNm	1.040	3.6%	12197 kNm	1.042	3.4%

Table 6.12: Statistical parameters of M_y and M_u for prestressed U girders.

Designation	Yielding moment M_y			Ultimate moment M_u		
	Nominal	Bias	COV	Nominal	Bias	COV
U-1000-A	2132 kNm	1.053	3.8%	2491 kNm	1.055	3.8%
U-1000-B	5878 kNm	1.040	3.7%	6760 kNm	1.045	3.4%
U-1000-C	12434 kNm	1.040	3.5%	14301 kNm	1.036	3.6%
U-1200-A	2898 kNm	1.015	3.9%	3248 kNm	1.049	3.5%
U-1200-B	8759 kNm	1.041	3.6%	10094 kNm	1.043	3.5%
U-1200-C	417584 kNm	1.041	3.5%	20079 kNm	1.040	3.5%
U-1500-A	3868 kNm	1.033	4.0%	4359 kNm	1.047	3.4%
U-1500-B	12248 kNm	1.041	3.5%	14148 kNm	1.035	3.5%
U-1500-C	24579 kNm	1.040	3.7%	27999 kNm	1.041	3.4%
U-2000-A	5948 kNm	1.041	3.5%	6773 kNm	1.044	3.4%
U-2000-B	16898 kNm	1.040	3.5%	19283 kNm	1.041	3.4%
U-2000-C	33189 kNm	1.038	3.7%	37494 kNm	1.042	3.4%

6.3.6 Proposed probabilistic models

Based on the results of performed simulations (see Tables 6.10, 6.11 and 6.12) and assuming the modelling errors as presented in Section 6.2.3, the final statistics of the bending resistance have been obtained as showed in Table 6.13. The values presented are representative for a range of precast concrete bridges in Portugal. They may be also used for bridges in other countries that have similar material and geometrical characteristics. It have to be noted that the models may not be appropriate for sections with significantly different geometry and characteristics.

Table 6.13: Statistics of bending resistance for precast concrete bridges.

Type of structure	Response	FM		P		R	
		Bias	COV	Bias	COV	Bias	COV
Reinforced concrete	M_y	1.17	6.5%	1.02	6%	1.19	9%
	M_u	1.11	5.5%	1.02	6%	1.13	8%
Prestressed concrete	M_y	1.04	4%	1.01	6%	1.05	7%
	M_u	1.04	3.5%	1.01	6%	1.05	7%

6.4 Models of shear response

6.4.1 Basics

The behaviour of the reinforced or prestressed concrete elements subjected to shear may be described by the relationship between the shear force and the shear strain. For reinforced concrete members the shear force-shear strain diagram is characterized by the cracking shear, V_{cr}, by the shear corresponding to stirrups yielding, V_y, by the ultimate shear resistance, V_u, and by the ultimate deformation capacity, τ_u. As an example, the typical shear force-shear strain relationship for reinforced concrete T-section with web reinforcement is showed in Figure 6.16.

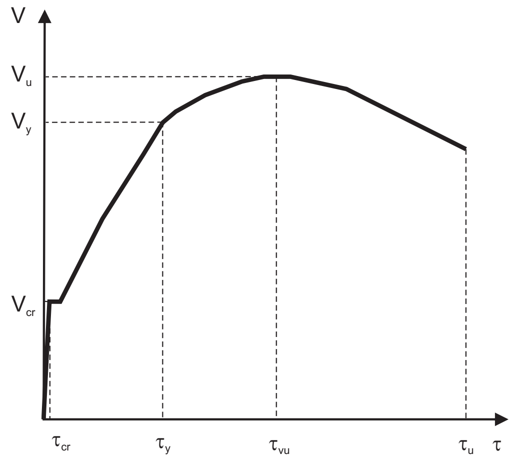

Figure 6.16: Typical shear force-shear strain diagram for reinforced concrete elements.

For prestressed concrete members the shape of shear force-shear strain curve is usually different than the curve typical for reinforced concrete. However, the characteristic point describing the curve are the same. Figure 6.17 shows typical shear force-shear strain relationship for prestressed concrete I-shape girder.

The variability in the shear response of reinforced and prestressed concrete elements depends on the similar factors as already discussed variability of flexural response, namely:

- variability of the mechanical properties of concrete and steel (concrete compressive and tensile strength, stirrups strength, etc.);

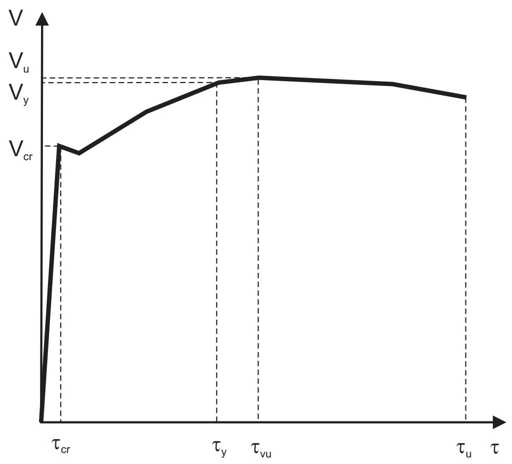

Figure 6.17: Typical shear force-shear strain diagram for prestressed concrete elements.

- variability in element geometry (stirrups spacing, effective section depth, web thickness, etc.);
- materials degradation (e.g. corrosion);
- load history (fatigue phenomena);
- method of definition of the structural response.

Neglecting the effects of the material degradation and load history, which are not a subject of this thesis, the causes of uncertainty about structural resistance can be put into three categories, already discussed in previous sections: material M, fabrication F and analysis P.

In the capacity evaluation of structures, the ultimate shear resistance is the most relevant parameter. Therefore, its variability has been studied more than the variability of other characteristic properties of concrete members subjected to shear force. This fact is also reflected on the availability of probabilistic models.

In the following points the probabilistic models of ultimate shear capacity of the reinforced and prestressed concrete bridge sections found in literature are resumed. Besides that the probabilistic models developed within the program of this thesis are also presented.

6.4.2 Existing probabilistic models

Models for US highway bridges. The statistical parameters of shear resistance for reinforced and prestressed concrete bridge sections common in United States have been derived by Nowak *et al.* (1994) and Nowak (1999). Three reinforced concrete T-beams (depth 0.90–1.20m) and three prestressed concrete AASHTO-type girders (depth 1.13–1.58m) have been analysed. Considering probabilistic models of the basic variables representative for bridges in US (see Nowak, 1999; Nowak *et al.*, 1994) and using numerical procedure based on Modified Compression Fields Theory (Vecchio & Collins, 1986) they obtained results resumed in the column assigned FM in Table 6.14. After taking into consideration the model uncertainty P, the final values showed in last two columns (R) of the Table 6.14 have been achieved.

Table 6.14: Statistical parameters of shear resistance (Nowak, 1999).

Type of structure	FM		P		R	
	Bias	COV	Bias	COV	Bias	COV
Reinforced concr. - w/stirrups	1.13	12%	1.075	10%	1.20	15.5%
Reinforced concr. - no stirrups	1.165	13.5%	1.20	10%	1.40	17%
Prestressed concr. - w/stirrups	1.07	10%	1.075	10%	1.15	14%

For members designed to have shear failure by stirrups yielding, the most important parameter is the steel yield stress. Therefore, the bias factor and the coefficient of variation of the member resistance FM obtained from simulations (see Table 6.14) are similar to the bias and coefficient of variation of the steel yield strength (considered in the analysis as λ=1.125 and V=12% respectively).

In the reinforced concrete elements without shear reinforcement, concrete tensile strength governs the ultimate capacity. Therefore the statistics of the member resistance FM obtained from simulations (see Table 6.14) are characterized by quite large scatter.

In the prestressed concrete members with shear reinforcement, the ultimate shear response is governed by several parameters where yielding strength of stirrups is probably the most important. Therefore, the bias factor and the coefficient of variation of the member resistance FM obtained from simulations (see Table

6.14) are quite similar to the bias and coefficient of variation of the stirrups yield strength (considered in the analysis as λ=1.125 and V=12% respectively). However, due to the influence of other parameters this relation is not very clear.

Plotting the results of simulations on normal probability papers, Nowak *et al.* (1994) and Nowak (1999) concluded that normal distribution may be used to model the ultimate shear capacity of reinforced and prestressed concrete sections.

Model for Spanish highway bridges. Sobrino (1993) studied the performance of precast prestressed concrete I-type girders (depth 1.5m) common in Spain. Considering probabilistic models of material properties and geometrical variations representative for bridges in Spain (for details see Sobrino, 1993) and using professional factor P with mean equal to 1.05 and coefficient of variation of 10% he obtained the coefficient of variation of shear resistance equal to 9.2%. As previously observed this value is very similar to the variability of yielding strength of stirrups.

Sobrino (1993) recommends to use translated lognormal distributions to model ultimate shear capacity of prestressed concrete section. However, he observed that normal and lognormal distributions are also appropriate to model this property of prestressed concrete elements.

Models for European railway bridges. The statistical parameters of shear resistance for reinforced and prestressed concrete elements representative for European railway bridges have been derived by Casas (2005). He analysed reinforced concrete rectangular beams (depth 1.5m) and prestressed (post-tensioned) concrete rectangular beams (depth 1.3m). Besides the influence of the amount of longitudinal and transverse reinforcement Casas (2005) analysed the importance of several other parameters. For reinforced concrete rectangular beams he investigated the effect of the variability of steel yielding strength and concrete compressive strength on the mean value and the coefficient of variation of the ultimate shear response. However, in the case of post-tensioned concrete rectangular beam he investigated the influence of the variability of reinforcing and prestressing steel strengths and the variability of concrete strength.

Based on the results of several analysis performed, Casas (2005) proposed probabilistic models resumed in the column assigned FM in Table 6.15. After taking into consideration the model uncertainty P the values shown in last column (R) of the Table 6.15 have been obtained.

Table 6.15: Statistical parameters of shear resistance (Casas, 2005).

Type of structure	COV of f_{ys}	FM		P		R	
		Bias	COV	Bias	COV	Bias	COV
RC beams w/stirrups	5%	–	5.5%	1.075	10%	–	11.5%
	10%	–	10%	1.075	10%	–	14%
	15%	–	15%	1.075	10%	–	18%
RC beams no stirrups	5-15%	–	7.5%$^{(*)}$	1.20	10%	–	12.5%
PC beams w/stirrups	5%	–	3%$^{(*)}$	1.075	10%	–	10.5%
	10%	–	4%$^{(*)}$	1.075	10%	–	11%
	15%	–	7.5%$^{(*)}$	1.075	10%	–	12.5%

Note: $^{(*)}$ values obtained considering perfect correlation between f_{ct} and f_c ($f_{ct} = 0.45(f_c)^{0.4}$); with this assumption the COV of f_{ct} is ≈7% for COV of f_c considered equal to 15%.

In Table 6.15 the values of the bias factor (nominal/mean ratio) are omitted due to the fact that it varies significantly dependent on the amount of longitudinal and transverse reinforcement. Furthermore, it depends very much on the mathematical model used for calculating the nominal values. The values of the bias factor corresponding to the nominal values calculated according to several national and European codes, reported in Casas (2005), varies between 0.7 and 2.3.

The study performed by Casas (2005) confirm the observation of other authors that for reinforced concrete members, designed to fail by shear reinforcement, the most important parameter in the ultimate shear response is the strength of stirrups. Therefore, the coefficient of variation of the member resistance FM obtained from simulations (see Table 6.15) is similar to the coefficient of variation of the steel yield strength considered in the analysis.

The most important parameter in the ultimate shear response of concrete members without stirrups is the concrete strength. Therefore, the coefficient of variation of the member resistance obtained from simulations corresponds to coefficient of variation of concrete tensile strength considered in the analysis (see Table 6.15).

In the prestressed concrete members with shear reinforcement, the ultimate shear response is governed by several parameters where yielding strength of stirrups and concrete strength are probably the most important. However, due to influence of other parameters this relation is not very clear.

Casas (2005) suggested to use normal distributions to model ultimate shear capacity of reinforced and prestressed concrete elements.

6.4.3 Selection of representative examples

Having in mind the fact, already discussed in Section 6.3.3, that the precast concrete bridges compose a significant part of the stock of existing bridges in Portugal and assuming that for older, cast in-situ concrete bridges, the models proposed by Nowak *et al.* (1994) and Casas (2005), and described in the previous section may be used, it has been decided to develop probabilistic models of shear response just for selected types of precast concrete bridge sections.

Generally, similar sections have been selected as for the case of bending analysis, namely reinforced concrete slab (see Figure 6.4) with depth ranging between 0.25 m and 0.55 m and cast in-situ reinforced concrete slab on precast prestressed concrete I-shape girders (see Figure 6.5) with depth ranging from 0.75 m to 1.80 m. The bridge sections with precast prestressed U-shape girders, analysed in bending, have been omitted in this case due to the fact that they have been found to behave similarly to the prestressed I-shape girders (half of the U-shape girder has similar dimensions to the I-shape girder and behaves nearly the same when subjected to shear).

In case of the reinforced concrete slabs, for each considered depth (see Table 6.16) four different situations, corresponding to different amount of longitudinal and shear reinforcement, have been analysed (D - minimum longitudinal and no shear; E - minimum longitudinal and minimum shear; F - high longitudinal and minimum shear; G - high longitudinal and high shear). The slab depth and the area of shear and longitudinal reinforcement have been designed according to REBAP (1985) and RSA (1983).

In the case of cast in-situ reinforced concrete slab on precast prestressed concrete I-shape girders for each section dimensions considered (see Tables 6.17) several different cases, corresponding to different amount of shear and prestressing reinforcement have been analysed (D - minimum prestress and high shear; E - moderate prestress and high shear; F - moderate prestress and minimum shear; G - high prestress and minimum shear). The principal dimensions of the section have been assumed according to design tables. However, the area of the reinforcing and prestressing steel have been designed according to REBAP (1985) and RSA (1983).

Reinforced concrete slabs - bridges with spans between 3 m and 10 m.

Table 6.16: Parameters of RC slab elements for shear analysis.

Designation	Bridge span L [m]	Total height H [mm]	Effect. depth D [mm]	Longitud. reinf. area $A_{sb/t}$ [mm^2]	Stirrups area A_{ss} [mm^2]	Stirrups spacing s [mm]
S-250-D	3.0	250	220	251	–	–
S-250-E	3.0	250	220	251	84	100
S-250-F	3.0	250	220	1571	84	100
S-250-G	3.0	250	220	1571	237	100
S-350-D	5.0	350	320	393	–	–
S-350-E	5.0	350	320	393	150	150
S-350-F	5.0	350	320	1571	150	150
S-350-G	5.0	350	320	1571	339	150
S-450-D	7.5	450	410	565	–	–
S-450-E	7.5	450	410	565	150	200
S-450-F	7.5	450	410	2199	150	200
S-450-G	7.5	450	410	2199	565	200
S-550-D	10.0	550	510	792	–	–
S-550-E	10.0	550	510	792	237	300
S-550-F	10.0	550	510	3142	237	300
S-550-G	10.0	550	510	3142	565	200

Prestressed concrete I-shape girders - bridges with spans 15–30 m.

Table 6.17: Parameters of I-shape girders for shear analysis.

Desig-nation	Bridge span L [m]	Total height H [mm]	Slab width B [mm]	Strands area [mm^2] $A_{p1/2}$	Strands area [mm^2] A_{p3}	Stirrups area A_{ss} [mm^2]	Stirrups spacing s [mm]
I-750-D	15.0	1000	2000	292.8	–	226	100
I-750-E	15.0	1000	2000	878.4	198	226	100
I-750-F	15.0	1000	2000	878.4	198	158	300
I-750-G	15.0	1000	2000	2049.6	585.6	158	300
I-1000-D	20.0	1250	2000	292.8	–	226	100
I-1000-E	20.0	1250	2000	1171.2	198	226	100
I-1000-F	20.0	1250	2000	1171.2	198	158	300
I-1000-G	20.0	1250	2000	2635.2	396	158	300
I-1400-D	25.0	1650	2500	439.2	–	226	150
I-1400-E	25.0	1650	2500	1464	198	226	150
I-1400-F	25.0	1650	2500	1464	198	158	300
I-1400-G	25.0	1650	2500	3074.4	396	158	300
I-1800-D	30.0	2050	2500	585.6	–	226	150
I-1800-E	30.0	2050	2500	1464	198	226	150
I-1800-F	30.0	2050	2500	1464	198	158	300
I-1800-G	30.0	2050	2500	3367.2	396	158	300

6.4.4 Models and parameters used in the simulations

The analysis of the shear response of concrete bridge sections, selected in the previous paragraph, have been performed using the Modified Compression Field Theory (Vecchio & Collins, 1986) and a special numerical code 'Response 2000' (Bentz, 2000). The code allows to determine shear force-shear strain relationship corresponding to given material properties and geometry of any kind of reinforced and/or prestressed concrete section.

The Modified Compression Field Theory is based on the truss analogy concept. After the stresses in concrete reach the concrete tensile strength and the first cracks forms, the reinforced concrete beam behaves as a truss with parallel longitudinal chords composed of longitudinal reinforcement embedded in concrete. The web is composed of transverse steel ties and diagonal concrete struts. The shear force applied to such truss causes tension in the chords and ties and compression in the struts.

The most important assumption in the Modified Compression Field Theory is that the cracked concrete in reinforced concrete members, when taken over areas or distances large enough to include several cracks, can be treated as a new material with its own stress-strain behaviour. The strains used for these stress-strain relationships are average strains that covers the combined effects of local strains at cracks, strains between cracks, bond slip and crack slip. The calculated stresses are also average stresses and they implicitly include stresses between cracks, interface shear on cracks and dowel action (Bentz, 2000).

In this theory equilibrium, compatibility and constitutive relationships are formulated in terms of already explained average stresses and strains. The theory takes into account strain-softening effects in concrete and allows for variability in the angle of inclination of the struts. Besides already explained assumption about averages stresses and strains the theory assumes that concrete and reinforcing bars are perfectly bonded together and that longitudinal and transverse reinforcing bars are uniformly distributed over the element. Furthermore, it imposes for each strain state only one corresponding stress state.

The analyses of the shear response have been carried out considering the constitutive relations for the material behaviour as suggested in Bentz (2000) and implemented in the 'Response 2000'. The basic relations considered for concrete and steel are generally similar to that presented in Figures 6.7 and 6.8.

The statistics of the material and geometrical parameters considered in the analysis as random are the same as used for the flexural analysis and are shown in Table 6.9. The only exception is the elasticity modulus of concrete which due to software restrictions have been assumed as totally dependent on concrete strength. All the random variables presented in Table 6.9 have been considered to be normally distributed. Remaining parameters necessary to perform analysis have been considered deterministic and their representative values have been taken from EC-2 (2004), Figures 6.4, 6.5, and Tables 6.16, 6.17.

6.4.5 Results obtained from simulations

The numerical analysis performed allows to define shear force-shear strain relationships for each of 32 selected examples. For each case, at first the analysis has been carried out considering all the variables at their characteristic or nominal value. Then, the analysis has been executed for all variables taken as their mean value. After that, simulations have been performed using Latin Hypercube method. In each case, analysis has been executed 25 times for the set of variables defined according to the corresponding probability distribution function and selected and shuffled using Latin Hypercube concept. In the next step the characteristic points of the response, cracking shear and ultimate shear, have been evaluated statistically. The P-P plots have been created and basic statistics of the distribution (mean, standard deviation and coefficient of variation) have been calculated. Then, the K-S Lilliefors goodness-of-fit test has been performed to check if the obtained response can be modelled by normal distribution.

Figures 6.18, 6.19, 6.21 and 6.20 show the shear force-shear strain relationship obtained for reinforced concrete elements S-550-D, S-550-E, S-550-F and S-550-G respectively. In referred figures, besides two shear force-shear strain diagrams obtained considering the characteristic values (dashed bold line) and the mean values (continuous bold line) for all parameters, the curves obtained from 25 simulations performed using Latin Hypercube sampling are also presented (grey thin lines). In general, the shear strain-shear force relationships and scatters of the cracking and ultimate shears obtained for all the analysed reinforced concrete sections are similar to those presented in Figures 6.18–6.20.

In Table 6.18 the results of simulations performed for reinforced concrete slabs are resumed. For every analysed section the nominal values, bias factors and coefficient of variation for cracking and ultimate shear are presented. The ultimate shear has been defined as the maximum shear capacity of the section after formation of cracks. Despite the fact that the results obtained for different sections are quite different some tendency can be observed.

For all the sections without shear reinforcement the bias factor for the cracking shear is close to 1.53 and the corresponding coefficient of variation is oscillating around 20.5%. Those values are very similar to the values of the bias factor and the coefficient of variation assumed for concrete tensile strength which is the governing parameter in this case. This can be confirmed on the sensitivity plot presented in Figure 6.22 where the correlations between the section shear capacity and the basic variables are shown. Despite the fact that the sections without shear reinforcement due to the presence of longitudinal reinforcement usually show some ductility after formation of the first shear cracks, the cracking capacity should be considered the ultimate shear capacity.

For remaining sections analysed within this study the cracking shear is also governed mostly by concrete tensile strength. This can be observed in the sensitivity plots presented in Figures 6.22 and 6.23. The statistics of the cracking capacity of the sections with shear reinforcement are as follows: bias factor 1.55–1.65 and coefficient of variation 20.5–21.5%.

For the slab sections with the area of longitudinal reinforcement close to minimum and with the low percentage of shear reinforcement the statistics of the ultimate shear response obtained by simulations do not show any reasonable trend. The bias factor for sections of different depth vary between 0.95–1.497 and the corresponding coefficient of variation oscillate between 26.4–40.5%. This happens because for this kind of sections the ultimate shear response, or the behaviour at failure, may be governed by different parameters leading to completely different failure modes (e.g. failure by stirrups, failure by longitudinal reinforcement, lack of equilibrium after cracking). This can be observed in Figure 6.19 where few shear strain-shear force diagrams are completely separated from the others. Furthermore, this can also be confirmed on the sensitivity plot presented in Figure 6.22 where the importance of the strength properties of the reinforcing steel on the ultimate shear capacity may be observed.

Slabs with the high amount of longitudinal reinforcement and with shear reinforcement close to minimum show more uniform behaviour. Except the case of section S-250-F where the statistics of the ultimate shear response are slightly different, the bias factor and the coefficient of variation for the ultimate shear capacity are around 1.11 and 9.5% respectively. However, looking to the shear strain-shear force relationships presented in Figure 6.20 it can be observed that for some simulations the failure occur in a different mode than for the others. By coincidence in the analysed cases (except section S-250-F) the different failure modes are characterized by mean values and the coefficients of variation relatively similar to each other. This results have similar bias and relatively low scatter. However, for other configurations these modes can be separated resulting in non-uniform bias and higher scatter (e.g. the case of section S-250-F).

Properly reinforced concrete slabs, namely the slabs with relatively high percentage of longitudinal and shear reinforcement, behaves similarly regardless the section dimensions. The bias factor and the coefficient of variation of the ultimate shear capacity obtained by the simulations for this type of section are oscillating around 1.07 and 4.5% respectively. Looking to the shear strain-shear force relationships presented in Figure 6.21 it can be observed that this kind of sections fails normally in a single mode. The analysis of the sensitivity plot presented in Figure 6.23 allows to distinguish this mode. Since the parameters governing the ultimate shear capacity in this case are the stirrups yielding strength and the concrete compressive strength, the failure occurs by stirrups yielding which after certain deformation lead to the crushing of concrete. This hypothesis has been confirmed by detailed analysis of all the results produced by the 'Response 2000'.

For the reinforced concrete sections with the area of shear reinforcement close to the minimum it has also been observed that, very often, the real shear cracking capacity, described by the mean value and the coefficient of variation, is higher than the shear capacity after the formation of the first cracks. Therefore, it can be considered that the shear capacity for such sections is the cracking capacity. This sometimes can not be noticed on the shear strain-shear force relationship obtained with the analysis performed considering the characteristic values of all the parameters.

For most of the analysed cases the lognormal and normal distribution have been found appropriate to model the cracking shear and the ultimate shear capacity of the reinforced concrete slabs. The cases where none of these probability distribution functions fit properly to the obtained results are the cases of sections with minimum longitudinal and shear reinforcement where distinct failure modes have been observed.

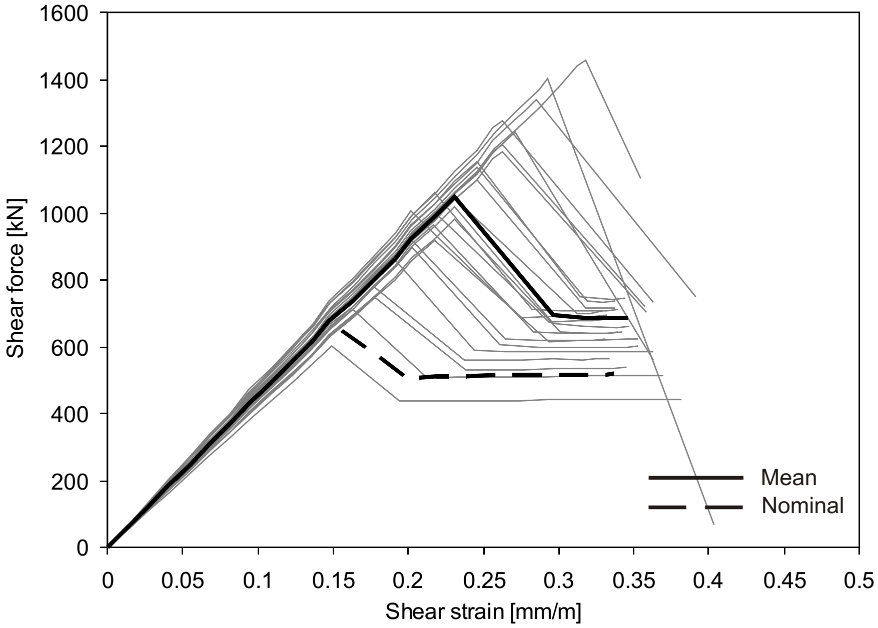

Figure 6.18: Shear force-shear strain diagrams obtained for section S-550-D.

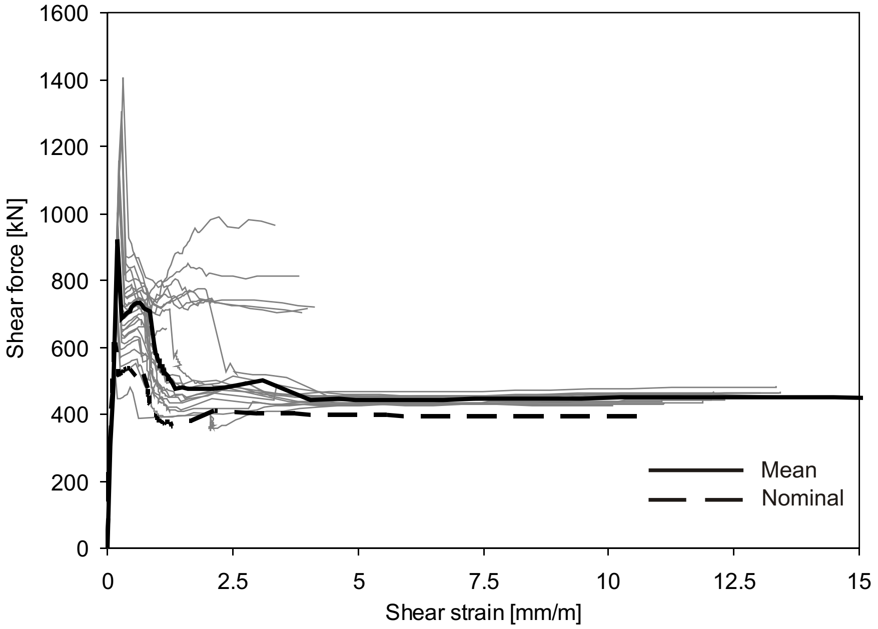

Figure 6.19: Shear force-shear strain diagrams obtained for section S-550-E.

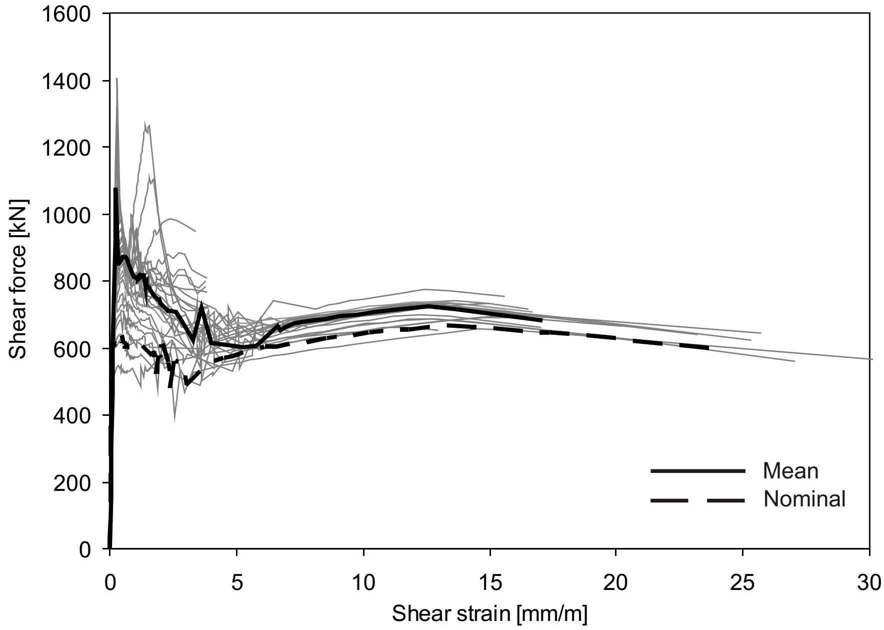

Figure 6.20: Shear force-shear strain diagrams obtained for section S-550-F.

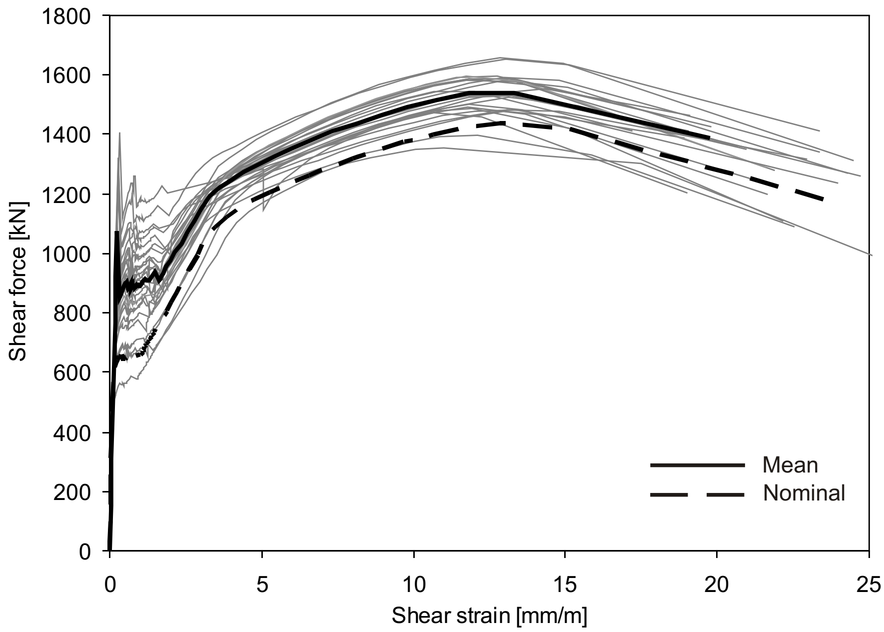

Figure 6.21: Shear force-shear strain diagrams obtained for section S-550-G.

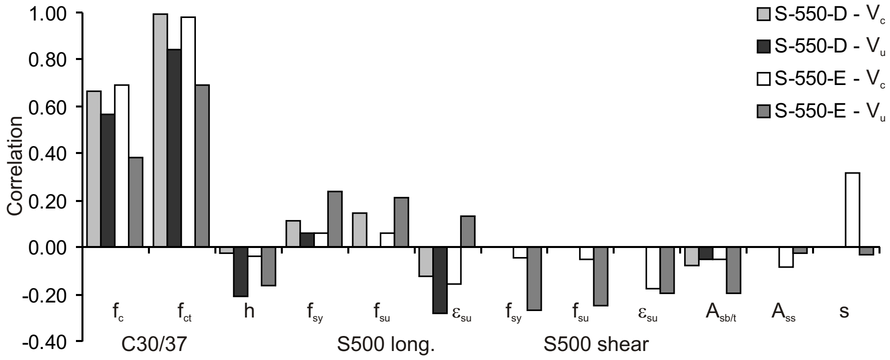

Figure 6.22: Sensitivity plot for sections S-550-D and S-550-E.

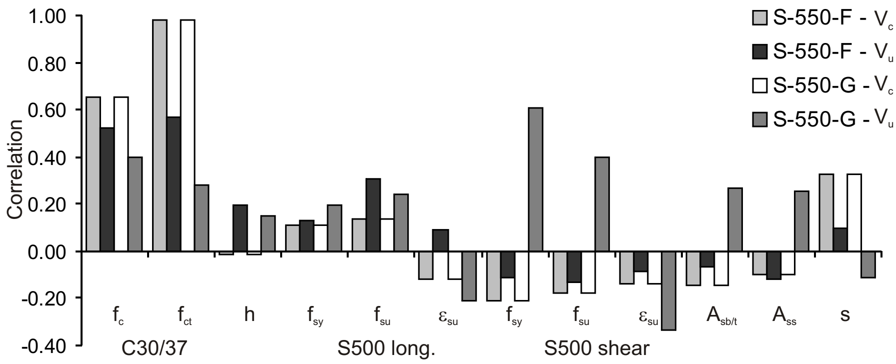

Figure 6.23: Sensitivity plot for sections S-550-F and S-550-G.

Table 6.18: Statistical parameters of V_{cr} and V_u for RC slab elements.

Designation	Cracking shear V_{cr}			Ultimate shear V_u		
	Nominal	Bias	COV	Nominal	Bias	COV
S-250-D	307.3 kN	1.528	20.3%	–	–	–
S-250-E	280.1 kN	1.596	21.8%	245.4 kN	0.950	40.5%
S-250-F	293.0 kN	1.544	20.4%	287.6 kN	1.162	14.6%
S-250-G	279.5 kN	1.618	20.4%	540.6 kN	1.077	4.8%
S-350-D	431.4 kN	1.525	20.5%	–	–	–
S-350-E	391.2 kN	1.609	20.7%	247.5 kN	1.320	26.8%
S-350-F	391.2 kN	1.649	21.7%	462.5 kN	1.104	9.4%
S-350-G	391.2 kN	1.649	21.7%	748.6 kN	1.075	3.9%
S-450-D	554.6 kN	1.529	20.6%	–	–	–
S-450-E	503.0 kN	1.609	20.8%	287.6 kN	1.497	31.7%
S-450-F	507.9 kN	1.633	21.7%	501.7 kN	1.106	10.2%
S-450-G	503.0 kN	1.649	21.7%	1107.3 kN	1.076	3.8%
S-550-D	678.0 kN	1.535	20.7%	–	–	–
S-550-E	614.8 kN	1.610	20.8%	392.7 kN	1.485	26.4%
S-550-F	614.8 kN	1.650	21.7%	663.5 kN	1.112	8.7%
S-550-G	614.8 kN	1.649	21.7%	1437.2 kN	1.067	4.6%

The behaviour of typical prestressed concrete bridge sections subjected to shear is even more complicated than the already described behaviour of reinforced concrete slabs. Figures 6.24, 6.25, 6.26 and 6.27 show the shear force-shear strain relationship obtained for prestressed sections I-1800-D, I-1800-E, I-1800-F and I-1800-G respectively. As previously, in the referred figures, besides the two shear force-shear strain diagrams obtained considering the characteristic values (dashed bold line) and the mean values (continuous bold line) for all parameters, the curves obtained from 25 simulations performed using Latin Hypercube sampling are also presented (grey thin lines). In general, the shear strain-shear force relationships and scatters of the cracking and ultimate shears obtained for all the analysed prestressed concrete sections are similar to those presented in Figures 6.24–6.27.

In Table 6.19 the results of simulations performed for prestressed concrete bridge sections are resumed. For every analysed sections the nominal values, bias factors and coefficients of variation for cracking and ultimate shear are presented. The ultimate shear has been defined as the maximum shear capacity of the section after formation of first diagonal cracks. Looking to Table 6.19 it can be seen that the results obtained for different sections are somehow different. However, some trends in the results may also be observed.

For all sections with minimum prestress the bias factor for the cracking shear is oscillating around 1.50–1.65 and the corresponding coefficient of variation is close to 20–21%. Those values are very similar to the values of the bias factor and the coefficient of variation assumed for concrete tensile strength which is the governing parameter in this case. This can be confirmed on the sensitivity plot presented in Figure 6.28 where the correlations between the section shear capacity (cracking and ultimate) and the basic variables are showed.

Increasing amount of prestressing reinforcement reduces the bias factor and the coefficient of variation for the cracking shear. For the section with moderate amount of the prestressing reinforcement the bias factor is in a range of 1.38–1.50 and the corresponding coefficient of variation is close to 17-18%. However, for sections strongly prestressed the bias factor oscillates around 1.24–1.42 and the coefficient of variation takes values between 14.6–17.4%. This reduction in the bias and in the coefficient of variation can be explained by the fact that, with the increase of prestress in the section, the importance of the concrete tensile strength on the cracking shear capacity slightly reduces. Simultaneously, the importance of the parameters related to amount of prestressing force applied slightly increases. This minor change in the response is almost not visible in the sensitivity plots presented in Figures 6.28, 6.29, 6.30 and 6.31. Nevertheless, it has been observed in sections I-1000-G and I-1400-G.

The response of prestressed concrete sections after formation of the first diagonal cracks is quite complex which is reflected on the statistics of the ultimate shear capacity. As it can be observed in Table 6.19 the bias factors for different sections vary between 1.06 and 1.43. The corresponding coefficient of variation oscillates between 3.6–13.3%. Nevertheless, when analysing the sections with similar percentage of prestressing steel and with similar amount of shear reinforcement some trends are observed.

For all sections with high amount of shear reinforcement and with minimum area of prestressing strands, the shear response is similar to that presented in Figure 6.24, where on the shear strain-shear force relationships three picks are easily visible. First corresponds to formation of the diagonal cracks in a web, second corresponds to the formation of transversal cracks in bottom flange and the third corresponds to the formation of transversal cracks in the top flange. When the section is already completely cracked the section fails by steel. Depending on the situation, the ultimate shear capacity may be reached in one of four different modes. However in the analysed examples the maximum shear capacity has been usually obtained before formation of the transversal cracks in the bottom flange. This can be confirmed on the sensitivity plot presented in Figure 6.28 where the high correlation of the tensile strength of concrete of the girder with ultimate shear capacity can be observed. The bias factor of the ultimate shear capacity for this kind of sections is varying significantly and takes values between 1.15 and 1.43. However, the corresponding coefficient of variation oscillates between 9.5% and 13.3%.

The increase of the prestress in the sections with the same geometry and with the same high amount of shear reinforcement changes the shear strain-shear force relationships. This can be observed in Figure 6.25 where just two peaks on the shear strain-shear force relationship are visible. The same as previously, the first corresponds to the formation of diagonal cracks. However, the second corresponds to the formation of the transversal cracks in the top flange. The third peak visible previously does not exist in this situation. This can be explained by the fact that the high prestress applied to the bottom flange of the girder effectively prevent from its cracking. After the development of the diagonal and transversal cracks, the sections fails by reinforcing steel or by concrete crushing preceded by plastic deformation of reinforcement. Therefore, in this case the ultimate shear capacity may be also reached in one of few different modes. In the analysed examples the maximum shear capacity has been usually obtained before the formation of the transversal cracks in the top flange. This can be confirmed on the sensitivity plot presented in Figure 6.29 where, besides the importance of concrete strength of the girder, the high correlation of the tensile strength of concrete of the top flange with ultimate shear capacity of the section can be observed. The bias factor of the ultimate shear capacity for this kind of sections takes values between 1.03–1.24. The corresponding coefficient of variation oscillates between 5.2% and 7.7%.

All sections with moderate amount of prestress and with amount of shear reinforcement close to minimum behave similarly, regardless the section dimensions. The bias factor and the coefficient of variation of the ultimate shear capacity, obtained by the simulations for this type of sections, are oscillating around 1.10 and 4.5% respectively. Looking to the shear strain-shear force relationships presented in Figure 6.26 it can be observed that this kind of sections fails normally in a single mode that may be identified analysing the sensitivity plot presented in Figure 6.30. Since the parameters governing the ultimate shear capacity in this case are the stirrups yielding strength and the concrete compressive strength of the girder, the failure occurs by stirrups yielding, which after certain deformation lead to the crushing of concrete struts. This hypothesis has been confirmed by detailed analysis of the results produced by the 'Response 2000'.

Further increase of the prestress in the sections with the shear reinforcement close to the minimum does not change the section behaviour significantly. However, the bias factor and the coefficient of variation of the ultimate shear capacity obtained by the simulations for this type of section are slightly different than in the previous case and are oscillating around 1.15 and 4.5% respectively. Looking to the shear strain-shear force relationships presented in Figure 6.27 it can be observed that, except few cases, this kind of sections fails generally also in a single mode, similar to that characteristic for the previously described case. Analysing the sensitivity plot presented in Figure 6.31 it can be observed that the increase in the prestress causes the increase of the importance of the concrete tensile strength of the top flange on the ultimate shear capacity of the section. Therefore, the few cases, when the different failure mode has been observed are probably governed by cracking capacity of the top flange.

For most of the analysed cases the lognormal and normal distribution have been found appropriate to model the cracking shear and the ultimate shear capacity of the prestressed concrete bridge sections. The cases where none of these probability distribution functions fit properly to the obtained results are the cases of sections with minimum prestress and with high percentage of shear reinforcement where distinct failure modes have been observed.

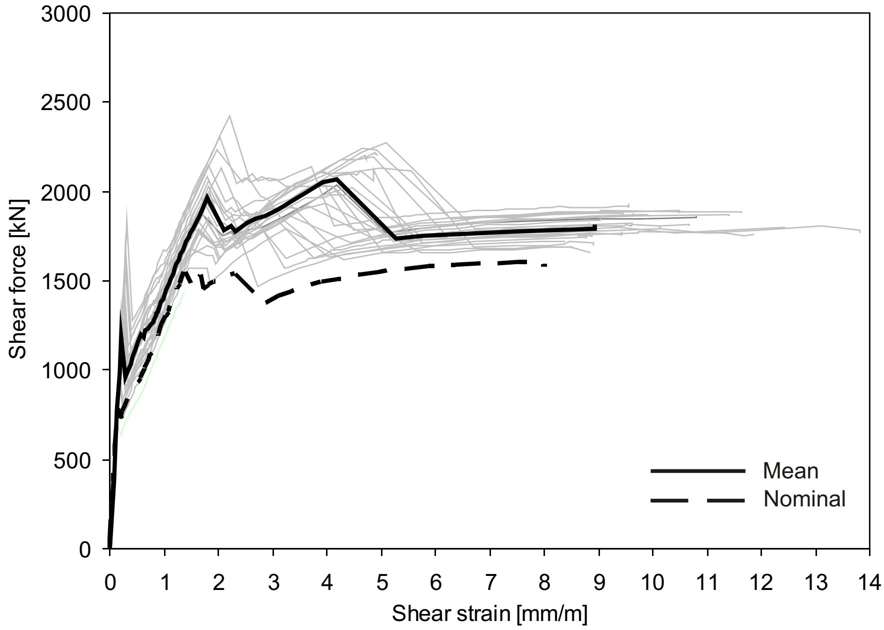

Figure 6.24: Shear force-shear strain diagrams obtained for section I-1800-D.

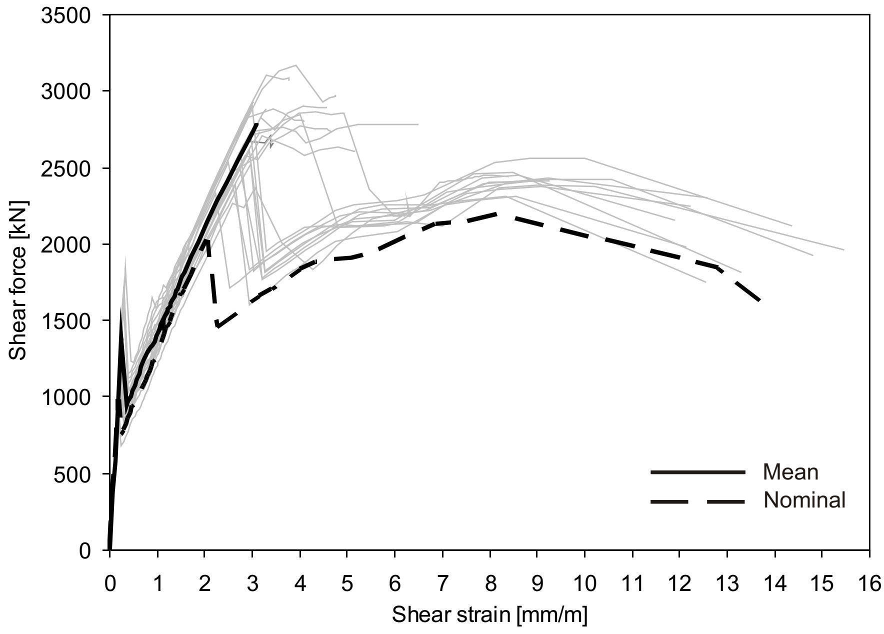

Figure 6.25: Shear force-shear strain diagrams obtained for section I-1800-E.

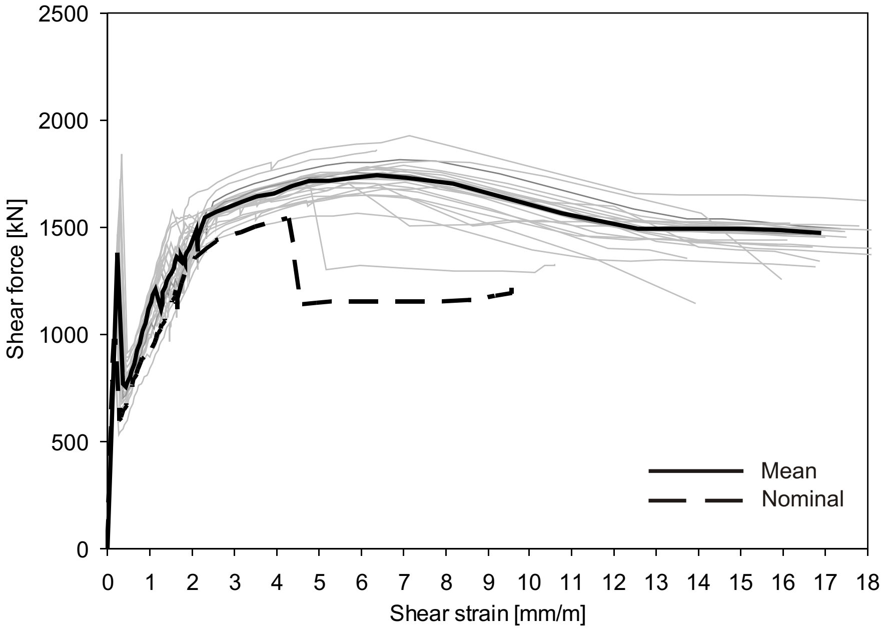

Figure 6.26: Shear force-shear strain diagrams obtained for section I-1800-F.

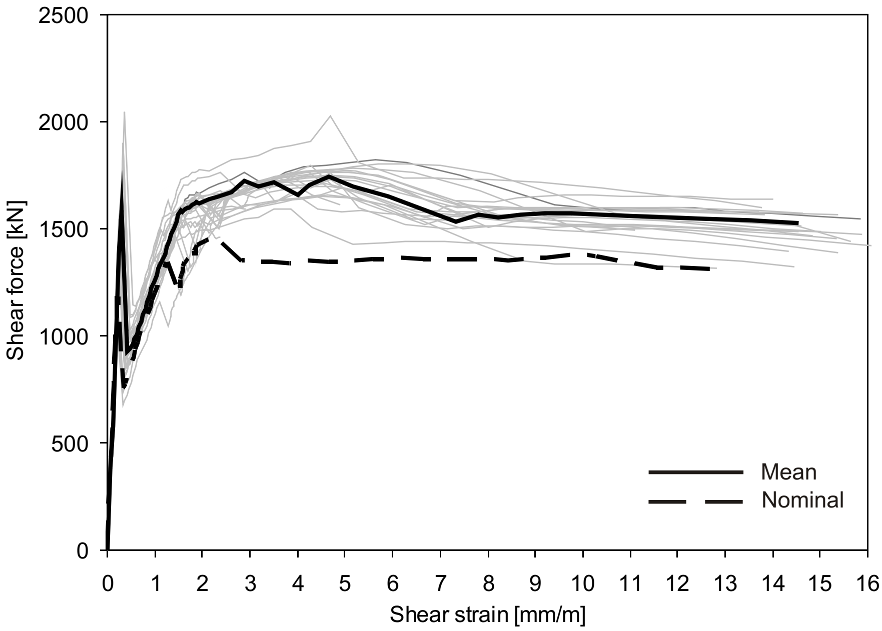

Figure 6.27: Shear force-shear strain diagrams obtained for section I-1800-G.

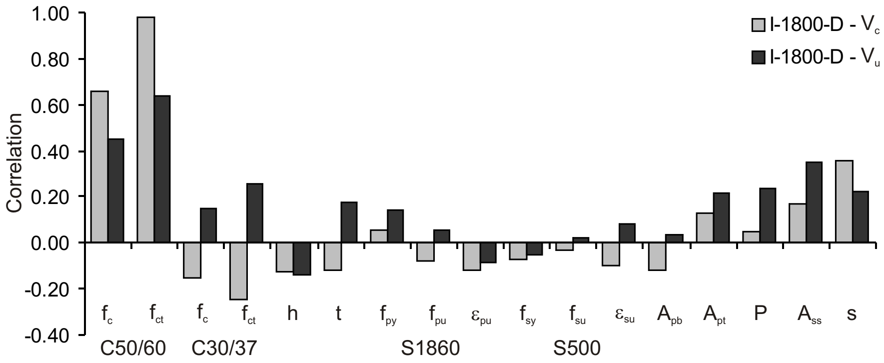

Figure 6.28: Sensitivity plot for section I-1800-D.

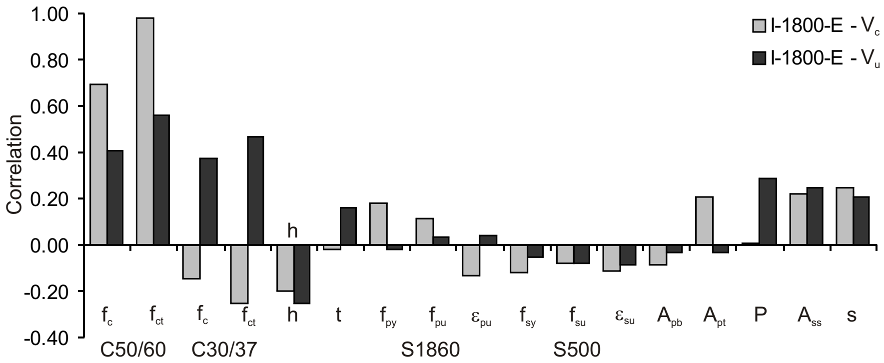

Figure 6.29: Sensitivity plot for section I-1800-E.

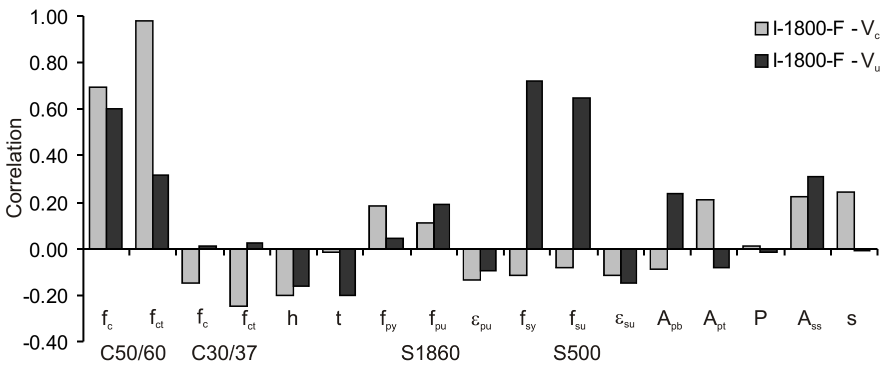

Figure 6.30: Sensitivity plot for section I-1800-F.

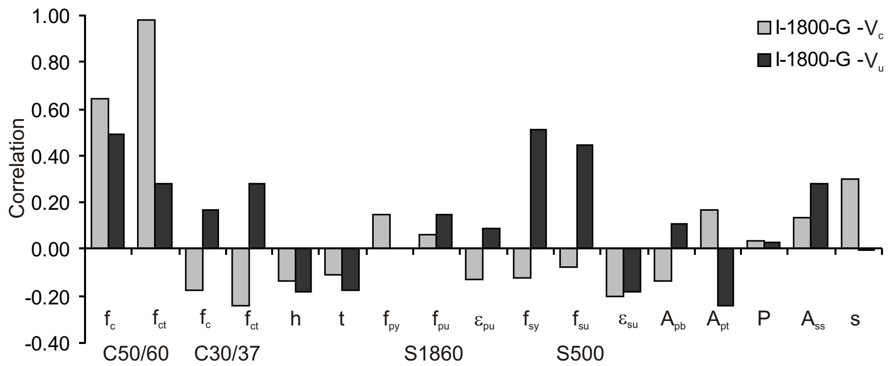

Figure 6.31: Sensitivity plot for section I-1800-G.

Table 6.19: Statistical parameters of V_{cr} and V_u for prestressed I girders.

Designation	Cracking shear V_{cr}			Ultimate shear V_u		
	Nominal	Bias	COV	Nominal	Bias	COV
I-750-D	255.4 kN	1.547	20.0%	907.4 kN	1.427	13.3%
I-750-E	343.7 kN	1.417	17.7%	1543.5 kN	1.028	6.7%
I-750-F	343.7 kN	1.417	17.7%	660.8 kN	1.116	4.1%
I-750-G	430.9 kN	1.420	15.1%	690.2 kN	1.100	3.6%
I-1000-D	334.4 kN	1.631	20.7%	1260.7 kN	1.154	10.7%
I-1000-E	450.5 kN	1.498	18.2%	1900.9 kN	1.140	5.6%
I-1000-F	450.5 kN	1.498	18.2%	866.6 kN	1.095	4.5%
I-1000-G	665.4 kN	1.244	14.6%	843.7 kN	1.152	4.1%
I-1400-D	595.8 kN	1.501	20.1%	1172.3 kN	1.381	12.6%
I-1400-E	749.7 kN	1.380	17.2%	1993.5 kN	1.242	5.2%
I-1400-F	749.7 kN	1.380	17.2%	1264.9 kN	1.060	4.2%
I-1400-G	902.2 kN	1.315	15.4%	1150.5 kN	1.171	3.8%
I-1800-D	780.8 kN	1.644	21.0%	1601.6 kN	1.288	9.5%
I-1800-E	981.4 kN	1.397	17.8%	2187.9 kN	1.244	7.7%
I-1800-F	981.4 kN	1.397	17.8%	1539.2 kN	1.130	4.2%
I-1800-G	1181.9 kN	1.289	17.4%	1464.4 kN	1.186	5.4%

6.4.6 Proposed probabilistic models

Based on the results of the performed simulations (see Tables 6.18 and 6.19) and assuming the modelling errors as presented in Section 6.2.3, the final statistics of the shear resistance have been obtained as showed in Table 6.20. The values presented are representative for a range of precast concrete bridges in Portugal. They may be also used for bridges in other countries that are characterized by the similar variability in the material properties and in the section geometry. It have to be noted that the models may not be appropriate for sections with significantly different geometry and executed from different materials.

The values presented in Table 6.20 are valid for precast reinforced and prestressed concrete bridge sections that are properly reinforced. It means that they have sufficient area of longitudinal and shear reinforcement (except the case of the slab without shear reinforcement). Furthermore, the bias factor presented in the last group of columns R relates the mean shear capacity with the characteristic capacity calculated using Modified Compression Field Theory.

Table 6.20: Statistics of shear resistance for precast concrete bridges.

Type of structure	Resp.	FM		P		R	
		Bias	COV	Bias	COV	Bias	COV
RC slabs - no stirrups	V_c	1.53	20.5%	1.20	10%	1.80	23%
Reinforced concrete	V_c	1.60	21.0%	1.20	10%	1.90	23%
slabs	$V_u^{(a)}$	1.11	9.5%	1.075	10%	1.20	15%
with stirrups	$V_u^{(b)}$	1.07	4.5%	1.075	10%	1.15	12.5%
Poorly prestressed	V_c	1.60	21.0%	1.20	10%	1.90	23%
concrete - w/stirrups	$V_u^{(b)}$	1.15	10.0%	1.075	10%	1.23	15%
Prestressed concrete	V_c	1.45	18.0%	1.20	10%	1.70	21%
girders - w/stirrups	$V_u^{(b)}$	1.10	7.5%	1.075	10%	1.18	12.5%
moderately prestressed	$V_u^{(a)}$	1.10	4.5%	1.075	10%	1.18	11%
Strongly prestressed	V_c	1.30	16.0%	1.20	10%	1.55	19%
concrete - w/stirrups	$V_u^{(a)}$	1.15	4.5%	1.075	10%	1.23	11%

Note: $^{(a)}$ low shear reinforcement area; $^{(b)}$ high shear reinforcement area.

Chapter 7

Safety requirements and formats for assessment of bridges

7.1 Introduction

In this chapter the requirements regarding bridges safety, necessary to set when assessing load carrying capacity of existing bridges, are showed. They were mostly collected from the existing national and international codes and guidelines. The theoretical backgrounds based on which the target reliabilities are usually selected are also discussed. Furthermore, several safety formats that can be used in the bridges evaluation are presented. The described safety formats were adopted from works of many authors and they were selected in such a way to form solid framework for the assessment of existing bridges based on 'step-level' philosophy. In this philosophy, discussed in more detail in the Chapter 2 of this thesis, the application of new and increasingly sophisticated analysis levels is made only if the bridge fails to pass the previous assessment level.

The requirements regarding bridges safety and the safety formats presented in the following sections were partially selected and described for the purpose of 'Sustainable Bridges' European Project and are also presented in Casas & Wiśniewski (2005). Furthermore, some of them are discussed in Wiśniewski *et al.* (2006a,b), Wiśniewski & Casas (2006) and Wiśniewski *et al.* (2007).

7.2 Safety requirements

7.2.1 General

One of the key issues when assessing an existing structure or bridge is to set the required minimum safety level that this structure should have in order not only to guarantee the security of the users and the surrounding infrastructure, but also to take a right decision on the future of the structure: leave as it is, strengthen, renew (Casas & Wiśniewski, 2005).

In the following section the problems related to the acceptability of a risk of a bridge collapse are discussed. Subsequently the concept of the nominal target probability is presented. Afterwards the cost-benefit issues in setting target reliabilities are discussed and finally target values of minimum reliability indices proposed in some national and international codes and guidelines are showed.

7.2.2 Risk acceptability

The acceptability of risk in general is affected by many factors such as the nature of hazard, the voluntary or involuntary nature of exposure to risk, the possible consequences and the benefits associated. In particular, the acceptability of risk of deaths and a social reaction to bridge collapse depends on (Menzies, 1997):

- The size of the bridge and its public profile.
- The class of road carried.
- The cause of collapse.

In defining acceptable risk criteria, it is possible to take into account acceptable or tolerable risk levels for other risk in society (Melchers, 1999). As an example Table 7.1 shows the indicative estimates of selected risk in society including structural failures.

Another approach is the concept of ALARP (as low as reasonably practical) (Melchers, 1999). Defining an upper limit to the risk, where greater risk can not be tolerated and a lower limit below which is of no practical interest and reducing

Table 7.1: Selected risk in society (Melchers, 1999).

Activity	Approximate death rate [x10^{-9} deaths/h exp.]	Typical exposure [h/year]	Typical risk of death [x10^{-6}/year round.]
Alpine climbing	30000–40000	50	1500–2000
Boating	1500	80	120
Swimming	3500	50	170
Cigarette smoking	2500	400	1000
Air travel	1200	20	24
Car travel	700	300	200
Construction work	70–200	2200	150–440
Manufacturing	20	2000	40
Building fires	1–3	8000	8–24
Structural failures	0.02	6000	0.1

(e.g. through spending money) the limit of the risk between these two limits the optimum value (as low as reasonably practical) can be found.

Considering these two approaches Menzies (1997) estimate that a maximum socially acceptable annual risk of loss of life associated with bridge collapse would be 1 in 10^6 for single life and 1 in 10^7 for many lives. This rate is actually bigger than the observed rate of bridge collapses in most of the countries.

For example in United Kingdom the observed failure rate of bridges is about one collapse every 1–2 years (Menzies, 1997). More than half of collapses are due to accidental impact or scour. The rate of bridge collapse due to structural deficiencies is about one collapse every five years. Therefore, the per annum fatality risk for the total UK population of bridges is about 1 in 5×10^8 which is lower than proposed by Menzies (1997) maximum socially acceptable value of 1 in 10^6 per annum.

7.2.3 Nominal probability of failure

The definition of the acceptable risk criteria is not an easy task as it was already discussed in previous subsection. However, the proper estimation of actual risk associated to the operation of any structure or a bridge is even more difficult.

The risk of any structural collapse is influenced by several uncertain factors. Despite load acting on the structural elements and its resistance these might include various environmental conditions, workmanships and human error, and prediction of future events (Melchers, 1999). In general all the uncertainties involved in the structural engineering problems can be divided to 'aleatory' (or intrinsic uncertainties) and 'epistemic'. The first refers to inherent uncertainties and the second to uncertainties which might be reduced with additional data, better modelling and better parameter estimation. There is also possible to breakdown all the uncertainties as follows (Melchers, 1999):

- Phenomenological uncertainty, which may arise whenever the form of construction or design technique extend the 'state of the art'.
- Decision uncertainty, which arises in connection with the decision as to whether a particular phenomena occurred.
- Modelling uncertainty, which is associated with simplified relationship used to describe real phenomenon.
- Prediction uncertainty, which is related to prediction of some future state of affairs.
- Physical uncertainty, which arises from inherent random nature of basic variables.
- Statistical uncertainty, which is associated with estimation of statistical parameters based on limited samples of the population.
- Uncertainty due to human factors, which arises from human involvement in the process (e.g. gross errors).

Generally it is very difficult to estimate most of the uncertainties mentioned above. Therefore in structural engineering it is common to neglect some of them (e.g. human errors, phenomenological and decision uncertainties, etc.). Moreover, very often in practical situations additional simplifications are made in the calculations. This cause that calculated probability of failure is a nominal one and does not reflect the actual failure rate of bridges.

Since the probabilities of failure calculated in the process of the safety assessment of bridges are usually the nominal (or notional) values it is necessary to compare these values with some target nominal values that are known to provide required overall safety and are consistent with risk acceptability criteria. The target nominal values of failure probabilities for bridges (expressed usually by the reliability index β) are usually established based on past performance criteria. In this criteria it is assumed that the average reliability of structures designed according to former rules is the required one. Therefore the target failure probabilities are generally close to an average of failure probabilities computed from a sample of past design.

7.2.4 Cost-benefit issues

According to Moses (2001) an optimum cost target safety level corresponds to a situation in which the marginal cost of further increasing the safety index is just balanced by marginal reductions in the risk-associated cost. The risk-associated cost can be defined as probability of failure times the cost of failure.

As is generally accepted, the cost of failure of an existing bridge should be the same as of a newly designed. Therefore, due to the fact that marginal costs of further increase the capacity in the case of existing structures are much higher than that corresponding to the newly designed structures, the target safety level for the assessment of existing bridges should be lower comparing to that used in the design. The reason that the marginal costs of safety increase for existing bridges are much higher is related to the fact that in the case of existing bridges the minor increase of safety requirements may lead to the strengthening or replacement while in newly design bridges it leads just to insignificant increase of section dimensions or reinforcement area.

The cost-benefit approach of choosing the required values of target reliabilities, described more detailed in JCSS (2001b), is conceptually very accurate and can be used for setting target values in some particular cases as for example assessment of large bridges. However, due to lack of data, regarding for example projected cost of failure, is rarely used in the bridge assessment practice and even in development of the design or evaluation codes.

7.2.5 Target reliabilities in codes and guidelines

As it was already stayed the nominal target reliabilities have to be established based on reliability analysis of many structures assumed to be sufficiently safe. Furthermore, the nominal target values have to take into account several other factors (e.g. failure type, associate risk and its costs, etc.). This is a quite comprehensive problem, therefore, it is normally handled by the specification bodies. In this section the target reliabilities for the design or assessment of existing bridges proposed in several codes and guidelines are resumed.

7.2.5.1 Target reliabilities for member level assessment

Eurocodes. Since the Eurocodes are the legal codes in most of the European countries the reliability levels stated there could give some idea on the required safety of bridges in Europe. The values of target reliability indices for Ultimate Limit State ULS, Serviceability Limit State SLS and for Fatigue presented in EC-0 (2002) are resumed in Table 7.2. Two sets of reliability indices are presented for different reference periods. Furthermore, in the case of ULS several values, corresponding to different reliability classes are defined. The reliability classes RC1, RC2 and RC3 correspond to the failure consequences, low, medium and high respectively. The consequences of failure are related to consequences for loss of human life and economic, social and environmental consequences.

Table 7.2: Target reliability index β (EC-0, 2002).

Limit State	Refer. period 1 year			Refer. period 50 years		
	RC-1	RC-2	RC-3	RC-1	RC-2	RC-3
Ultimate	4.2	4.7	5.2	3.3	3.8	4.3
Fatigue	—	—	—	—	1.5–3.8$^{(a)}$	—
Serviceability (irreversible)	—	2.9	—	—	1.5	—

Note:(a) depends on degree of inspectability, reparability and damage tolerance.

The values of the reliability index presented in Table 7.2 can give some indication to the evaluator on the required safety of bridges in Europe. However, using them as a target for the assessment of existing bridges can be over-conservative since they were proposed principally for bridge design.

Canadian CAN/CSA-S6-00 code. In CAN/CSA-S6-00 (2000) different values of the target reliability index for safety assessment of bridges are defined based on the system behaviour, the element behaviour and the inspection level. The proposed values for all traffic categories, except permit controlled, are presented in Table 7.3. In the case of traffic with permit controlled vehicles, the values in Table 7.3 may be decreased by 0.5. For structures that could affect the life safety of people or are essential to the local economy, or necessary for the movement of emergency vehicles, a value at least 0.25 greater than that given in Table 7.3 shall be used.

Table 7.3: Target reliability index β (CAN/CSA-S6-00, 2000).

System behaviour	Element behaviour (failure type)	Inspection level		
		INSP-1	INSP-2	INSP-3
S1 - Element failure leads to total collapse	E1 - sudden failure	4.00	3.75	3.75
	E2 - sudden with post-peak	3.75	3.50	3.25
	E3 - gradual failure	3.50	3.25	3.00
S2 - Element failure not lead to total collapse	E1 - sudden failure	3.75	3.50	3.50
	E2 - sudden with post-peak	3.50	3.25	3.00
	E3 - gradual failure	3.25	3.00	2.75
S3 - Element failure leads to local failure only	E1 - sudden failure	3.50	3.25	3.25
	E2 - sudden with post-peak	3.25	3.00	2.75
	E3 - gradual failure	3.00	2.75	2.50

Note:INSP-1 corresponds to not inspectable components; INSP-2 corresponds to situation when inspection is to the satisfaction of evaluator; INSP-3 corresponds to the case when inspection has been carried out by evaluator.

AASHTO LRFD and AASHTO LRFR codes. The minimum reliability index β=3.5 required for the design of bridges (AASHTO LRFD, 1994) in the

United States of America is based on average betas computed from a sample of past design. This value corresponds to the reliability of an individual member and the strength limit states. It was computed considering specific probabilistic models of loads, geometry and mechanical properties of materials. Therefore, if different probabilistic models were used different target reliability would be obtained for the same sample of past design. Moreover, the target value was computed considering an ADTT (Average Daily Truck Traffic) of 5000 trucks which is quite severe.

The evaluation code AASHTO LRFD (1994) proposes a value of the target reliability index for the strength assessment of bridge members, β=2.5, which was calibrated to corresponds to past AASHTO operating level load rating. This lower reliability for evaluation is justified by the fact that evaluation is performed for a much shorter exposure period, related to inspection every 2 to 5 years, consideration of site realities and the economic considerations of rating versus design. It does not take into account the structure redundancy as well.

Danish Reliability-Based Classification Guideline. In Vejdirectoratet (2004) the required safety index β for the verification of the ultimate limit state was adopted from NKB-36 (1978) for high safety class. Table 7.4 shows the recommended values corresponding to different failure tapes. It have to be noted, that the values presented in Table 7.4 should be used together with the probabilistic models based on which they were developed.

Table 7.4: Target reliability index β (NKB-36, 1978).

Consequences of failure	Failure type		
	Ductile with extra carrying capacity	Ductile, no extra carrying capacity	Brittle, no warning and capacity reserve
Less serious	3.1	3.7	4.2
Serious	3.7	4.2	4.7
Very serious	4.2	4.7	5.2

For the verification of serviceability limit state the guideline Vejdirectoratet (2004) recommends values proposed in EC-0 (2002) and ISO/CD 13822:1999

(1999), which range from 2.2–2.9, or that defined in NKB-36 (1978), which are 1.0 and 2.0 for reversible and irreversible limit states.

Probabilistic Model Code. Based on cost-benefit analysis performed for some representative structures, the Joint Committee of Structural Safety proposed a set of target reliabilities that are also compatible with calibration studies and statistical observations (JCSS, 2001). Table 7.5 shows the values recommended for serviceability as well as for ultimate limit state. In Table 7.5 different values are proposed for different relative costs of safety measures. Furthermore, similarly as in EC-0 (2002) the target reliabilities for ultimate limit state are differentiated according to consequences of failure: minor, moderate and large. However, in JCSS (2001) is stated that the failure consequences besides that described in previous paragraph depends also on type of failure, brittle and ductile with and without reserve strength.

Table 7.5: Target reliability index β (JCSS, 2001).

Relative cost of safety measure	Ultimate Limit State			Serviceability Limit State
	Minor failure consequences	Moderate fail. consequences	Large failure consequences	
Large	3.1	3.3	3.7	1.3
Normal	3.7	4.2	4.4	1.7
Small	4.2	4.4	4.7	2.3

Note: All the values correspond to 1 year reference period.

The values presented in Table 7.5 are intended to be used in design of structures. According to JCSS (2001), for existing structures the costs of achieving a higher reliability level are usually higher compared to structures under design and for this reason the target level should be lower.

Standard ISO 2394:1998. The choice of the target reliability index for assessment of existing structures in standard ISO 2394:1998 (1998) is related to the consequences of a structural failure as well as to the costs of a safety measure. The values proposed in that document are presented in Table 7.6. In the calibration of the proposed target reliability values the following distribution types were used: resistance - lognormal or Weibull; permanent loads - normal; time-varying loads - Gumbel.

Table 7.6: Target reliability index β (ISO 2394:1998, 1998).

Relative costs of safety measure	Consequences of failure			
	Small cons.	Some cons.	Moderate cons.	Great cons.
High	0	$1.5^{(a)}$	2.3	$3.1^{(b)}$
Moderate	1.3	2.3	3.1	$3.8^{(c)}$
Low	2.3	3.1	3.8	4.3

Note: (a) use β=0 for reversible SLS and *beta*=1.5 for irreversible SLS; (b) use β=2.3–3.1 for fatigue depending on possibility of inspection; (c) use β=3.1, 3.8 and 4.3 for ULS.

Standard ISO/CD 13822:1999. The target reliability for the assessment of existing structures, proposed in ISO/CD 13822:1999 (1999) and presented in Table 7.7, depends on the limit states analysed and related characteristics. For the ultimate limit state the main characteristics is the consequence of failure, for serviceability limit state the main characteristic is reversibility and finally for fatigue it is inspectability.

Table 7.7: Target reliability index β (ISO/CD 13822:1999, 1999).

Limit state	Conditions	Reliability index	Reference period
Serviceability	Reversible	0.0	Intended remaining life
	Irreversible	1.5	Intended remaining life
Fatigue	Inspectable	2.3	Intended remaining life
	Not inspectable	3.1	Intended remaining life
Ultimate	Very low fail. cons.	2.3	Min. stand. safety period
	Low fail. conseq.	3.1	Min. stand. safety period
	Medium fail. con.	3.8	Min. stand. safety period
	High fail. conseq.	4.3	Min. stand. safety period

Note: Minimum standard period of safety (e.g. 50 years).

7.2.5.2 Target reliabilities for system level assessment

The reliability of a bridge treated as a structural system is usually bigger than reliability of one of its members. According to Tabsh & Nowak (1991), the difference in the reliability indices for common types of bridge decks in United States is about 2, i.e. instead of β=3–4 for bridge member, for the bridge system β=5–6.

Traditional design or assessment methods did not consider this additional structure capacity in quantitative manner, however it was known that this additional over-strength exists and the requirements for the members can be chosen less conservative. Nowadays the assessment of existing structures can be performed at the member level as well as at the system level. Therefore, in order to these two different level assessment be consistent, the target reliabilities for the evaluation of existing bridges at the system level should be bigger than target reliabilities presented in the previous section.

Unfortunately, so far does not exist any code or guideline that clearly define target reliabilities for the assessment of bridges at the system level. Most of the codes are still member orientated and the research effort in last decades was to define the target safety for design or evaluation of structural members without accounting for redundancy and the system effect. However, in the current Canadian code CAN/CSA-S6-00 (2000) and in recent reports of Ghosn & Moses (1998) and Liu *et al.* (2001) some target values of reliability indices are proposed for the structural systems or at least for the members considering structural systems effect.

Canadian CAN/CSA-S6-00 code. From the specific clause of CAN/CSA-S6-00 (2000), regarding the evaluation of existing bridges, it could be concluded that the safety of structural system should be higher than the safety of the average member type by about 0.25. The target safety level expressed by β index, for the failure of the member which causes the total collapse of the structure, is fixed at a value between 4.0 and 3.0 depending of inspection level and ductility (see Table 7.3). The target safety indices for members which failures do not lead to the total collapse of the bridge or members of minor importance to the global safety are somehow lower (3.75–2.50). Since in the first case the member failure means the system failure (the total collapse) the target safety indices for the system can be taken the same as for target safety indices for members which failure lead to the system failure. Concluding, the target safety level for the systems expressed by β indices can be assumed as the same as in the first row block, S1, of the Table 7.3.

NCHRP Reports 406 and 458. In those reports Ghosn & Moses (1998) and Liu *et al.* (2001), besides the definition of target safety indices for the structural systems, they propose the procedure (see Section 7.3.3.2) which allowed to assess the redundancy of the structure and suggest how the structural redundancy may be considered in the definition of different safety margins concerning the behaviour of a bridge as a whole and in the adoption of the corresponding target system values of the reliability index.

According to Ghosn & Moses (1998), a bridge superstructure provides adequate levels of redundancy and system safety if all the following conditions are satisfied:

- The reliability index for a member is greater than the target value, e.g. β=3.5 (AASHTO LRFD, 1994);
- The difference between the system reliability index for the ultimate limit state and the reliability index for a member is greater than $\Delta\beta_{ult}$=0.85;
- The difference between the system reliability index for the functionality limit state and the reliability index for a member is greater than $\Delta\beta_{func}$=0.25;
- The difference between the system reliability index in damaged conditions and the reliability index for a member is greater than $\Delta\beta_{dam}$=-2.70

Therefore, the definition of the target values of the reliability level for the system should be always related to the target value assumed for the members (Ghosn & Moses, 1998). If the target value at a member level is β_{memb} the target system reliability indices can be defined by the following equations.
For ultimate limit state:

$$\beta_{ult} = \Delta\beta_{ult} + \beta_{memb} \tag{7.1}$$

For functionality limit state:

$$\beta_{func} = \Delta\beta_{func} + \beta_{memb} \tag{7.2}$$

For damaged condition limit state:

$$\beta_{dam} = \Delta\beta_{dam} + \beta_{memb} \tag{7.3}$$

As an example, if the target reliability index at a member level is set at a value β=3.5, than a bridge with an adequate redundancy will guarantee at least a value of β_{ult}=4.35, a β_{func}=3.75 and β_{dam}=0.8.

On the other side, according to Casas & Wiśniewski (2005), if the reliability index evaluated for a member is less than 3.5, this does not automatically send the bridge out of safety. In fact, if the superstructure presents a high level of redundancy, then even that β_{memb} is less than for example 3.5, the system reliability index β_{ult} may be higher than 4.35, β_{func} higher than 3.75 and the β_{dam} higher than 0.8, and, therefore, the bridge may be considered as safe. Following the same concept, if the structure is non-redundant it does not mean that it can not be safe enough. However the non-redundant structure must have higher member safety in order to satisfy the safety requirements of the structural system.

Similar requirements, as in the case of bridge superstructure, were also defined by Liu *et al.* (2001) for the bridge substructure. The requirements are as follows:

- The reliability index for a member is greater than the target value, e.g. β=3.5 (AASHTO LRFD, 1994);
- The difference between the system reliability index for the ultimate limit state and the reliability index for a member is greater than $\Delta\beta_{ult}$=0.50;
- The difference between the system reliability index for the functionality limit state and the reliability index for a member is greater than $\Delta\beta_{func}$=0.50;
- The difference between the system reliability index in damaged conditions and the reliability index for a member is greater than $\Delta\beta_{dam}$=-2.00

The important comment is that the results of target relative safety indices showed above were defined based on the analysis of typical highway multi-girder bridges and typical highway multi-pier bridge bents assumed to be adequately redundant. However according to Ghosn & Moses (1998) and Liu *et al.* (2001) a generalization can be made for other type of bridges. The generalization is based on the same assumption that was used to derive the target values for the calibration of safety factors in most design codes. The β values obtained for a set of actual bridges considered as safe by bridge engineers and representative of whole bridge population are used to define a target values that is finally accepted for all bridges (this is for instance the case of β_{target}=3.5 used in the calibration of the AASHTO LRFD (1994)).

7.3 Safety formats for assessment of bridges

7.3.1 General

The safety formats which are commonly used in bridge engineering for the purpose of design or safety assessment are based on the concept of limit states. According to Nowak & Collins (2000) the limit state is defined as the boundary between the desired and undesired performance of the structure and is mathematically represented by the so called limit state function or performance function $g(X_i)$. The safety format can be defined as the mathematical approach which allows to ensure that the performance (or limit state) function takes desired values.

In most of the bridge design codes permissible stresses format (single safety factor format) or partial safety factor format are traditionally used. Nevertheless, the permissible stresses format is quite archaic and can be extremely conservative for the purpose of the safety evaluation. However, the partial safety factor format as appears in the design codes may not be directly applicable to the assessment of existing bridges. It is due to the fact that the partial safety factors in the design codes are calibrated for the design purposes considering all the sources of uncertainty characteristic for the design of new structures.

On the other hand, the assessment of existing bridges often requires the use of advanced analytical models of the structural response (e.g. non-linear Finite

Element analysis, plastic analysis, etc.). The safety formats recommended in the design codes can not be used together with those kinds of structural analysis method without significant changes. Therefore, it can be stayed that in the process of assessment of existing bridges more advanced safety formats are required.

In general, enhanced safety formats can be divided into formats applicable to the member level assessment and to the system level assessment. The safety formats for member evaluation allow to assess safety of a individual member of the structure. However, the safety formats for system level evaluation allow to assess safety of a whole bridge considering its redundancy and robustness. Furthermore, for both member and system level assessment, three different groups of safety formats can be considered: deterministic or semi-probabilistic (partial or global safety factor methods), fully probabilistic and simplified probabilistic.

In the following sections a number of safety formats proposed by Casas & Wiśniewski (2005) for the assessment of existing bridges are presented. The methods were selected originally for the purpose of the assessment of existing railway bridges. However, they are general and can be applied to the assessment of all kind of bridges.

7.3.2 Safety formats for member level assessment

Semi-probabilistic formats. Partial Safety Factor Method is the most basic assessment method that can be used for the evaluation of existing bridges at the member level. The general form of the checking equation in this method is as follows:

$$\phi_R R_n \geq \gamma_{S1} S_{n1} + \ldots + \gamma_{Si} S_{ni} + \ldots + \gamma_{Sk} S_{nk} \tag{7.4}$$

where R_n is the nominal resistance of the section, S_{ni} is the nominal value of i-th action or action effect (dead load, live load, etc.), ϕ_R is the resistance factor (taking into account the uncertainty of mechanical and geometrical parameters describing the section resistance as well as the uncertainty of the resistance model itself) and γ_{Si} is the partial safety factor of load i-th (taking into account the uncertainty in the estimation of actions or actions effects).

Table 7.8: Partial safety factors for design of concrete bridges.

	Ultimate Limit State ULS		
	RSA, REBAP	EC-0, EC-2	PCSF
Permanent loads	1.5, 1.35$^{(a)}$ / 1.0	1.35 / 1.0	1.28, 1.22$^{(a)}$ / 1.0
Traffic loads	1.5 / 0.0	1.35, 1.45$^{(e)}$ / 0.0	—
Concrete resistance	1.5	1.5, 1.4$^{(a)}$–1.3$^{(c)}$	1.43
Steel resistance	1.15	1.15, 1.05$^{(b)}$	1.15, 1.09$^{(d)}$

Note: Values after slash are for favourable load effects; (a) corresponds to structures executed with enhanced quality; (b) corresponds to situation where measured geometrical data are used; (c) corresponds to situation when concrete strength is assessed based on cores retrieved from the structure; (d) applicable to the elements with depth below 250 mm; (d) applicable for railway traffic loads.

In Table 7.8 the partial coefficients for design of concrete bridges defined by Eurocodes (EC-0, 2002; EC-2, 2004; EC-2b, 2003) and Portuguese codes (REBAP, 1985; RSA, 1983) are summarized. Also the factors proposed in the report PCSF (2002) for design of precast concrete elements are showed. Factors corresponding to the resistance of materials, showed in Table 7.8, are the inverse of the factor ϕ_R from the Equation 7.4.

Due to different uncertainty related to modelling of the section resistance and actions of the existing bridges comparing to the new bridges, the partial safety factors used in assessment should be different from those used in the design. However, conservatively, the factors used for the design are normally used due to the lack of calibrated safety factors specific for existing structures.

Fully probabilistic format. Reliability analysis methods can be applied for the assessment of the bridge safety at the member level when calibrated partial safety factors for resistance and actions are not available or in case the bridge fails to pass assessment performed using partial safety factor method. The general form of the checking equation in the probabilistic methods is as follows:

$$\beta \geq \beta_{target} \tag{7.5}$$

where β is the reliability index as defined in Section 3.3.3 and β_{target} is the target reliability index that can be determined based on information presented in

Section 7.2. The reliability index β should be calculated using one of the existing reliability methods, FORM, SORM, Monte Carlo, discussed previously (see Section 3.4).

In order to perform the analysis using mentioned reliability methods the complete statistical information (mean value, standard deviation, type of distribution and correlations between variables) about basic variables is required. The probabilistic models of bridge permanent and variable loads, mechanical properties of materials, geometry and member resistance to bending and shear, necessary for assessment of precast concrete bridges, are discussed in further chapters.

Simplified probabilistic formats. Mean Load Method can be used to assess the bridge safety when all the basic variables are statistically independent and can be modelled by normal or lognormal probability distribution functions. The general form of the checking equation is the same as previously (Equation 7.5). However, in this case the reliability index can be computed analytically using one of the known equations.

In case of normally distributed and statistically independent random variables R and S the reliability index β can be calculated as follows:

$$\beta = \frac{\mu_R - \mu_S}{\sqrt{\sigma_R^2 + \sigma_S^2}} \tag{7.6}$$

where μ_R and μ_S are the mean values of the generalized resistance and the action respectively. σ_R and σ_S are the standard deviations of the generalized resistance and the action.

When the random variables R and S are lognormally distributed and statistically independent the reliability index β can be calculated as follows:

$$\beta = \frac{\ln \frac{\mu_R}{\mu_S}}{\sqrt{V_R^2 + V_S^2}} \tag{7.7}$$

where V_R and V_S are the coefficients of variation of the generalized resistance and the generalized action, and remaining parameters are as in Equation 7.6.

Since in the discussed methods all the variables are assumed to follow normal or lognormal distribution and are assumed to be statistically independent, limited statistical information is required to perform analysis (mean value, standard deviation or coefficient of variation).

7.3.3 Safety formats for system level assessment

All the safety formats presented in the previous section are applicable to the safety assessment of the structural members. However, bridges consist of a system of interconnected members where the failure of any single member may not necessarily cause the collapse of the whole structure. Therefore, the reliability of the member may not be representative of the reliability of the entire bridge.

The ability of a structural system, particularly a bridge system, to carry the loads after the failure of one of its members is called redundancy. Using different words the redundancy can be defined as the capability of the bridge to sustain the damage of some of its members without collapsing.

Several factors affect the reliability of structural systems. The most important is the composition type of the system, i.e. whether the system is formed by components in series or in parallel or in some mixed form. Another important factor is the level of ductility of the structural components. In addition, the correlation between the member capacities and/or the correlation between loads affects the reliability of the system as compared to the reliability of individual members.

The behaviour of some systems can be easily predicted intuitively without performing complicated analysis. This is usually the case of: some parallel systems, systems in series (the weakest link systems) and very simple mixed systems. In some cases the system behaviour can also be predictable based on some previous knowledge (results of analysis performed for similar structures). In all those cases the reliability assessment of the structure can be performed based just on the results of the member level analysis and the applicable safety formats are similar to those described in the previous section. However in many cases the behaviour of the bridge is unknown and difficult to predict, especially when dealing with existing, deteriorated structures. In all those cases the reliability assessment of the structure has to be performed based on the results of non-linear analysis.

7.3.3.1 System with known or predictable behaviour

Semi-probabilistic formats. Partial Safety Factor Method described previously (see Equation 7.4) could be adopted for the safety assessment of bridges at the system level. The American standards AASHTO LRFD (1994) and AASHTO LRFR (2003) outline the format explaining how bridge redundancy and other system response properties can be included in the design/assessment process using load or resistance factors modifiers. The checking equations take one of the following forms:

$$\phi_S \phi_R R_n \geq \gamma_{S1} S_{n1} + \ldots + \gamma_{Si} S_{ni} + \ldots + \gamma_{Sk} S_{nk} \tag{7.8}$$

$$\phi_R R_n \geq \eta(\gamma_{S1} S_{n1} + \ldots + \gamma_{Si} S_{ni} + \ldots + \gamma_{Sk} S_{nk}) \tag{7.9}$$

where ϕ_S is the resistance factor relating to the redundancy and ductility of the system and η is the load factor modifier related also to the redundancy and ductility of the system. Remaining symbols are the same as in Equation 7.4.

A system factor ϕ_S or η (where $\phi_S = 1/\eta$) is defined to give a measure of the level of redundancy of a bridge. If ϕ_S is less than 1.0, indicates that the bridge has a low level of redundancy. A system factor greater than 1.0 indicates that the level of redundancy is acceptable. Bridge superstructures that have a system factor greater than 1.0 may be rewarded by allowing that their live load margin be increased by a factor equal to ϕ_S.

AASHTO LRFD (1994) specification suggests to define system factors subjectively as a function of 'operational importance', the 'level of ductility' and the 'level of redundancy'. To include 'importance, ductility and redundancy' in the design process, to each one of those effects is assigned a factor of 0.95, 1.0, or 1.05. The total system factor for load η or for the resistance ϕ_S is the product of the individual factors.

Ghosn & Moses (1998) using reliability methods define the system redundancy factors ϕ_S for most common types of highway bridge superstructures in United States. Among all the others bridges constructed from AASHTO prestressed concrete I-beams were analysed. Table 7.9 shows the calibrated system factors for simple-span and continuous prestressed concrete I-beam bridges. Different values are suggested for various number of beams in the deck and various beams spacing. Also different values are suggested for ultimate limit state, functionality (serviceability) limit state and for damaged condition (the damaged condition is defined as the state after failure of one of the bridge main load carrying members).

Despite that the factors were calibrated for American traffic load condition and AASHTO I-beams, they can be adopted for other countries and other types of prestressed I-girders assuring that the load and resistance variabilities not vary significantly from that used in the calibration.

Table 7.9: System factors ϕ_S for prestressed concrete I-beam bridges (Ghosn & Moses, 1998).

Spacing [m]	Limit state	4 beams		6 beams		8 beams		10 beams	
		simp.	cont.	simp.	cont.	simp.	cont.	simp.	cont.
1.2	ultim.	0.87	0.93	1.04	1.08	1.08	1.10	1.08	1.10
	funct.	0.89	0.95	0.99	1.04	1.00	1.05	1.01	1.05
	damage	1.11	1.20	1.36	1.35	1.36	1.35	1.33	1.35
1.8	ultim.	0.98	1.04	1.06	1.08	1.06	1.08	1.06	1.08
	funct.	0.96	1.00	0.98	1.03	0.99	1.04	1.00	1.04
	damage	1.21	1.05	1.25	1.10	1.26	1.10	1.26	1.10
2.4	ultim.	1.04	1.04	1.07	1.05	1.07	1.05	1.07	1.05
	funct.	0.95	1.00	0.98	1.02	0.99	1.02	1.00	1.03
	damage	1.13	0.92	1.18	0.95	1.18	0.95	1.18	0.95
3.1	ultim.	1.06	1.02	1.06	1.03	1.06	1.03	—	—
	funct.	0.95	1.00	0.98	1.02	0.98	1.02	—	—
	damage	1.05	0.80	1.07	0.80	1.07	0.80	—	—
3.7	ultim.	1.01	1.00	1.02	1.01	—	—	—	—
	funct.	0.94	1.00	0.96	1.02	—	—	—	—
	damage	0.89	0.70	0.94	0.70	—	—	—	—

Note: For each configuration, use the lowest value from the ultimate limit state, functionality limit state and damaged condition. The values in table for the damaged condition shall be increased by 0.10 for bridges provided with a distributed set of diaphragms. A minimum value of 0.80 shall be used. A maximum value of 1.20 shall be used.

The system factors provided in Table 7.9 are intended for bending moment checks. According to Moses (2001) the system factor for shear should be considered as uniform value of $\phi_S = 1.0$. It is due to the fact that shear failures in members are often brittle, and their presence in a system of parallel members may not provide added shear capacity through redundancy. Bending failures are usually ductile, so redundancy does add to system bending capacity.

Fully probabilistic formats. The system reliability analysis methods may be applied for the assessment of existing bridges at the system level when there is a lack of calibrated partial safety factors including that accounting for redundancy and system behaviour. The general form of the checking equation in the fully probabilistic method for structural systems is equal to that defined previously (see Equation 7.5). However in this case, the target reliability index β_{target} has to be taken as the value required for structural system, usually bigger than one required for the member (see Section 7.2). Also, the calculated reliability index β has to correspond to the system failure and not just to the failure of one of its members. Unfortunately the calculation of the system reliability index is difficult and sometimes even impossible without performing non-linear structural analysis. Therefore, despite that exist analytical solution (Melchers, 1999; Thoft-Christensen & Murotsu, 1986) for several exceptional cases (some types of series, parallel and mixed systems) they are not really applicable for the assessment of existing bridges.

Simplified probabilistic formats. In many cases when the reliability index for the structural system can not be calculated analytically using methods described in the previous paragraph the Bounds Method can be used as the first estimation of the bridge system safety (Casas & Wiśniewski, 2005; Wiśniewski & Casas, 2006; Wiśniewski *et al.*, 2006a). The Bounds Method does not require complicated non-linear structural analysis. In this method the rough estimation of the behaviour of the structure and the system safety is performed by defining the lower bound due to the elastic analysis (where no redistribution between bridge elements is permitted), and the upper bound due to the plastic analysis (where complete redistribution between bridge members is assumed). In the practical application, the definition of the lower bound can be performed using e.g Mean Load Method presented in Section 7.3.2. The upper bound can be estimated by FORM, SORM or Monte Carlo analysis performed for the limit state function $g(X)$ assuming an ideal plastic behaviour.

For example, in a case of a continuous bridge and bending failures, in any critical i-th section, the limit state function $g(X)$ can be defined by the following expression:

$$g(X) = M_R^i - \lambda_{pl}^i(M_G^e + (M_Q^e) \tag{7.10}$$

where M_R^i is the ultimate resistance moment of the i-th section, M_G^e is the maximum bending moment due to permanent loads calculated for the equivalent simply supported beam, M_Q^e is the maximum bending moment due to traffic loads calculated also for the equivalent simply supported beam and λ_{pl}^i is the plastic moment redistribution factor for the analysed i-th section. The equivalent simply supported beam is defined as the simply supported beam with the span-length equal to the length of the analysed bridge span (see Figure 7.1).

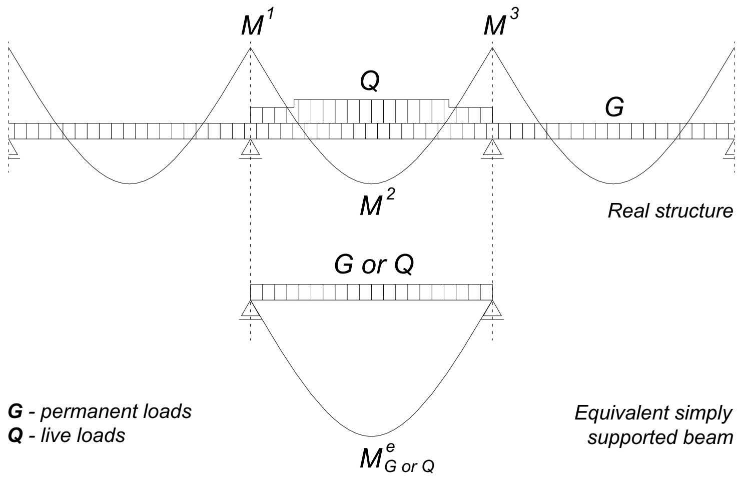

Figure 7.1: Bending moments in the equivalent simple supported beam obtained due to linear analysis.

In the plastic analysis, the assumption is that the redistribution of bending moments between critical sections (sections over the piers and the mid-span section) is complete. Therefore, all three cross-sections (mid-span section and sections over the piers) reach the ultimate bending moment (a plastic hinge is formed). Considering this fact, the moment redistribution factor can be defined as follows:

$$\lambda_{pl}^i = \frac{M_R^i}{\frac{M_R^1 + M_R^3}{2} + M_R^2} \tag{7.11}$$

where M_R^1, M_R^3 and M_R^2 are the ultimate bending resistance of the sections over the supports and at mid-span respectively, for the analysed span of the bridge, and M_R^i is the ultimate bending moment of the analysed section.

7.3.3.2 System that requires non-linear structural analysis

Semi-probabilistic formats. In the absence of calibrated system factors ϕ_S for bridge redundancy (see Equation 7.8) an alternative approach developed by Ghosn & Moses (1998) can be used in order to assess safety of existing bridges (Casas & Wiśniewski, 2005; Wiśniewski *et al.*, 2006b). This approach will be named furthermore in this thesis as Redundancy Factor Method.

According to Ghosn & Moses (1998), a bridge may be considered safe from a system point of view if it provides a reasonable safety level against first member failure, it does not produce large deformations under regular traffic conditions which would restrict the bridge's functionality, it does not reach its ultimate system capacity under extreme loading conditions and is able to carry some traffic loads after the brittle damage or the loss of a main load-carrying member. Thus, system safety is not only concerned with the ultimate system capacity, but also the deformation, and the post-damage capacity of the bridge structure. Based on this definition, four limit states should be checked to ensure adequate bridge system safety, namely: member failure limit state (this is the traditional check of individual member safety); functionality limit state (this is defined as a maximum live load displacement accounting for the non-linear behaviour of the bridge system); ultimate limit state (this is the ultimate capacity of the bridge system or the formation of a collapse mechanism) and damaged condition limit state (this is defined as the ultimate capacity of the bridge system after the complete removal of one main load carrying component from the structural model).

To be consistent with currently used structural assessment practice, the proposed method requires that individual member safety checks be performed via an appropriate available code using for example the partial safety factor method. In a second step, the system effect has to be taken into account to verify the functionality, ultimate and damaged condition limit states. The incorporation of system response into the safety assessment process is achieved using three redundancy ratios: r_f, r_u and r_d (for the serviceability, ultimate and damaged condition limit states respectively) which are actually the factors quantifying bridge robustness.

To assess the overall safety of any specific bridge at the system level, a redundancy factor ϕ_{red} can be determined. The following steps summarize the procedure required to define the redundancy factor to assess the overall safety of an existing bridge:

Step 1. Identify bridge members whose failure might be critical to the structural integrity of the bridge.

Step 2. Calculate required member capacity (R_{req}) using classical Partial Safety Factor Method and appropriate code (for example, Eurocode).

Step 3. Assess the actual capacity of the member (R) using appropriate strength models defined by the code (for example, Eurocode), considering actual (existing) member geometry and using best estimates of material strengths.

Step 4. Develop a structural model of the bridge using a finite element package that allows a static non-linear analysis of the structure. Consider real (existing) bridge dimensions and use a best estimate for material properties (usually mean values). Apply a best estimate of the unfactored permanent load (usually characteristic values should be appropriate). Do not include impact factor.

Step 5. Identify the loading position and the most critical load patterns (producing the most critical loading effect) for the critical member under consideration.

Step 6. Calculate the member reserve ratio r_1 defined by the following equation:

$$r_1 = \frac{LF_1}{LF_{1req}} \tag{7.12}$$

For this purpose the elastic linear structural analysis has to be performed with the load pattern defined in the previous steps. The required member load factor capacity LF_{1req} and actual member load factor capacity LF_1 are defined by the following equations:

$$LF_{1req} = \frac{R_{req} - D}{L_{TRUCK}} \tag{7.13}$$

$$LF_1 = \frac{R - D}{L_{TRUCK}} \tag{7.14}$$

where R is member capacity, D is the effect of the permanent load and L_{TRUCK} is the effect of the considered unfactored traffic load (e.g. Eurocode traffic Load Model 1 - TLM-1).

Step 7. Determine using non-linear analysis the load factor LF_f (see Figure 7.2) by which the applied unfactored traffic load (e.g. Eurocode TLM-1) has to be multiplied until a primary member reaches the functionality limit state . The functionality limit state is defined as allowable vertical deflection of primary member.

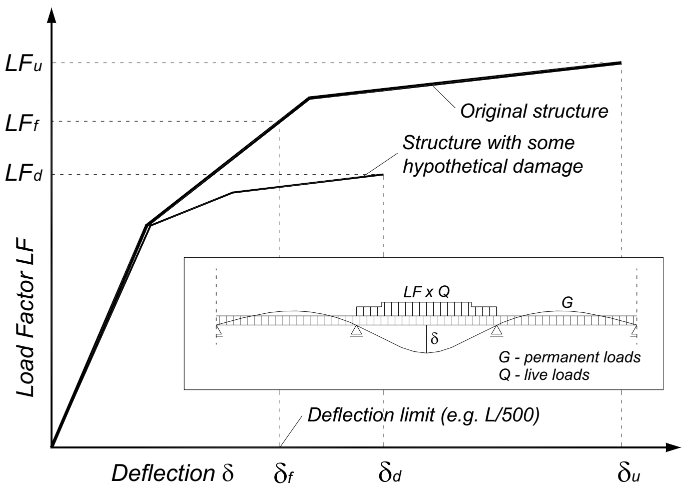

Figure 7.2: Load factor versus deflection curves obtained due to non-linear analysis for original structure and for the structure with some hypothetical damage.

Step 8. Calculate the system reserve ratio R_f (for the functionality limit state) using the following equation:

$$R_f = \frac{LF_f}{LF_1} \tag{7.15}$$

Step 9. Calculate the redundancy ratio r_f (for the functionality limit state) using the following equation:

$$r_f = \frac{R_f}{R_{f,target}} \tag{7.16}$$

where $R_{f,target}$, according to the results of reliability based calibration performed (Ghosn & Moses, 1998), can be considered equal to 1.1.

Step 10. Determine using non-linear analysis the load factor LF_u (see Figure 7.2) by which the considered unfactored traffic load (e.g. Eurocode TLM-1) has to be multiplied to reach the ultimate limit state.

Step 11. Calculate the system reserve ratio R_u (for the ultimate limit state) using the following equation:

$$R_u = \frac{LF_u}{LF_1} \tag{7.17}$$

Step 12. Calculate the redundancy ratio r_u (for the ultimate limit state) using the following equation:

$$r_u = \frac{R_u}{R_{u,target}} \tag{7.18}$$

where $R_{u,target}$, according to the results of reliability based calibration performed (Ghosn & Moses, 1998), can be considered equal to 1.3.

Step 13. Determine using non-linear analysis the load factor LF_d (see Figure 7.2) by which the considered unfactored traffic load (e.g. Eurocode TLM-1) has to be multiplied to reach the damaged condition limit state (for this purpose, a slightly different structural model has to be used, namely the model where one of the critical members identified in the first point is removed).

Step 14. Calculate the system reserve ratio R_d (for the damaged condition limit state) using the following equation:

$$R_d = \frac{LF_d}{LF_1} \tag{7.19}$$

Step 15. Calculate the redundancy ratio rd (for the damaged condition limit state) using the following equation:

$$r_d = \frac{R_d}{R_{d,target}} \tag{7.20}$$

where $R_{d,target}$, according to the results of reliability based calibration performed (Ghosn & Moses, 1998), can be considered equal to 0.5.

Step 16. Repeat the last three steps for damaged limit state by reintroducing the member previously removed and removing from the structural model another member whose failure might be critical for the structural integrity of the bridge until all members identified in step 1 have been removed one at a time. The final value of r_d will be the minimum for all critical members.

Step 17. After repeating all the previous steps to cover all critical load patterns, identify the minimum values of the redundancy ratios r_f, r_u and r_d.

Step 18. Determine the redundancy factor ϕ_{red} according to the following equation:

$$\phi_{red} = min(r_1 r_u; r_1 r_f; r_1 r_d) \tag{7.21}$$

where r_1, r_f, r_u and r_d are the values corresponding to the most critical loading patterns.

Step 19. Determine overall bridge safety: if the value of ϕ_{red} is less than 1, then the bridge may be considered as not safe; if ϕ_{red} is equal to or greater than 1, then the bridge may be considered as safe.

Fully probabilistic formats. Probabilistic non-linear analysis is the most conceptually complete and accurate method of safety assessment of bridges in the present state-of-the-art (Casas & Wiśniewski, 2005). This technique allows the assessment of the response at ultimate under given loading conditions considering the random nature of the basic variables and accounting for bridge redundancy. The general form of the checking equation in the fully probabilistic method for structural systems is equal to that defined previously (see Equation 7.5). Nevertheless, as it was already stated, the target reliability index β_{target} has to be taken as the value required for structural system (see Section 7.2). Also, the reliability index β has to correspond to the system failure and has to be calculated using one of the appropriate computational algorithms that allow to couple non-linear structural analysis using finite element methods and the reliability analysis. The allowable algorithms are presented in more detail in Section 3.6.

Simplified probabilistic formats. The application of the advanced methods of probabilistic non-linear analysis requires advanced knowledge of the structural reliability theory as well as significant computational effort as the non-linear analysis must be performed many times and may need specialized software packages which are not yet readily available. For these reasons, simplified probabilistic non-linear analysis methods, which only require a single non-linear analysis performed within common non-linear FEM packages can provide adequate alternatives when evaluating the safety of common type of bridges. This paragraph describes two simplified probabilistic non-linear analysis methods that were found to be sufficiently accurate for the purpose of assessing the safety of existing bridges.

Method of Ghosn and Moses. A simple way to take into account the non-linear behaviour of bridges (treated as a system) was proposed by Ghosn & Moses (1998) during the calibration of system factors ϕ_S (see Section 7.3.3.1) and system reserve ratios R_f, R_u and R_d (see previous paragraphs) for the design of bridges. The method is based on assessing the safety of individual bridge members while taking into consideration the structural system's performance expressed in terms of bridge redundancy. Structural redundancy is assessed through a non-linear structural analysis coupled with a simplified reliability analysis. Although the method was originally developed for evaluating the redundancy of highway bridges during the design process, the modifications proposed by Casas & Wiśniewski (2005) show that the method can be successfully applied to the capacity assessment of existing bridges.

As it was already stated, according to Ghosn & Moses (1998), a bridge may be considered safe from a system viewpoint if it provides a reasonable safety level against first member failure, it does not produce large deformations under high loads, it does not reach its ultimate system capacity under extreme loading conditions and it is able to carry some traffic loads after damage or the loss of a main load-carrying member. Thus, system safety is not only related to the ultimate system capacity, but also to the deformation, and post-damage capacity. Therefore, four limit sates should be checked to ensure adequate bridge system safety, namely: member failure limit state (this is the traditional check of individual member safety); functionality limit state (this is defined to limit maximum live load displacements accounting for the non-linear behaviour of the bridge system to ensure that the bridge remain functional after high load crossings); ultimate limit state (this is the ultimate capacity of the bridge system or the formation of a collapse mechanism) and damaged condition limit state (this is defined as the ultimate capacity of the bridge system after the complete removal of one main load carrying component from the structural model).

To be consistent with present assessment practices, the proposed method first requires checking the safety of individual members. In a second step, the system effect has to be taken into account and the verification of the functionality, ultimate and damaged condition limit states at the system level have to be carried out.

The incorporation of system behaviour during the safety assessment is done using the relative reliability indices $\Delta\beta_i$. For each of the three system limit states defined above, $\Delta\beta_i$ gives the difference between the safety indices for the system and the safety index for the member. In order to guarantee bridge safety, each of the relative reliability indices must be greater than an appropriate target value while at the same time member safety has to be assured by requiring that the member's reliability index remains above an acceptable level.

This method was proposed for the design of the new structures where the bridge members can be designed with appropriate level of safety. In existing structures where in some cases individual members may not meet the safety requirements, global system safety should be exclusively used as criteria as proposed by Casas & Wiśniewski (2005). In this case, the proposed safety format would take the form of following three inequalities.
For ultimate limit state:

$$\Delta\beta_{ult} + \beta_{memb} = \beta_{ult} \geq \Delta\beta_{ult,target} + \beta_{memb,target} = \beta_{ult,target} \tag{7.22}$$

For functionality limit state:

$$\Delta\beta_{func} + \beta_{memb} = \beta_{func} \geq \Delta\beta_{func,target} + \beta_{memb,target} = \beta_{func,target} \tag{7.23}$$

For damaged condition limit state:

$$\Delta\beta_{dam} + \beta_{memb} = \beta_{dam} \geq \Delta\beta_{dam,target} + \beta_{memb,target} = \beta_{dam,target} \tag{7.24}$$

The target values for the relative reliability indices and for member reliability index are presented in Section 7.2.

In this simplified approach, the reliability indices for individual members as well as the system can be calculated depending on the probability distribution types of two random variables, namely the generalized resistance, R, and the applied load, S. In Ghosn & Moses (1998) both variables were found to be reasonably well represented by lognormal distributions and for the calculation of the reliability indices β_i the lognormal format (see Equation 7.7) was found to be sufficiently accurate. However, in this section and for the sake of simplicity, the reliability indices β_i are presented using the normal format (see Equation 7.6).

Assuming that all the variables are Gaussian, the member reliability index for an existing bridge can be defined as:

$$\beta_{memb} = \frac{\overline{LF_1} - \overline{LL_{TRUCK}}}{\sqrt{\sigma_{LF}^2 + \sigma_{LL}^2}} \tag{7.25}$$

where $\overline{LF_1}$ is the mean value of the load factor that will cause the first member failure in the bridge assuming elastic analysis. $\overline{LL_{TRUCK}}$ is the mean value of the maximum expected lifetime traffic load (e.g. Eurocode traffic Load Model 1, TLM-1) including dynamic allowance effect expressed as a function of the design train load. σ_{LF} is the standard deviation of LF_1 while σ_{LL} is the standard deviation of the maximum expected live load LL_{TRUCK}.

The mean value of the load factor $\overline{LF_1}$ can be calculated using the following expression:

$$\overline{LF_1} = \frac{\overline{R} - \overline{D}}{L_{TRUCK}} \tag{7.26}$$

where $\overline{R}$ is the mean member capacity, $\overline{D}$ is the mean dead load effect and L_{TRUCK} is the effect of the design traffic load (e.g. Eurocode TLM-1) which is the original load that is incremented during the non-linear analysis.

The standard deviation σ_{LF} of the load factor LF_1 is expressed by:

$$\sigma_{LF} = \frac{\sqrt{\sigma_R^2 + \sigma_D^2}}{L_{TRUCK}} \tag{7.27}$$

where σ_R is the standard deviation of the member resistance, R, σ_D is the standard deviation of the mean dead load effects, D.

The system reliability index for the ultimate limit state is defined by:

$$\beta_{ult} = \frac{\overline{LF_u} - \overline{LL_{TRUCK}}}{\sqrt{\sigma_{LF}^2 + \sigma_{LL}^2}} \tag{7.28}$$

where $\overline{LF_u}$ (see Figure 7.2) is the mean value of the load factor corresponding to the ultimate limit state (the load factor by which the design load, has to be multiplied during the non-linear analysis for the ultimate limit state to be reached). The remaining parameters are the same as in the previous case.

The system reliability index for the functionality limit state is defined by the equation:

$$\beta_{func} = \frac{\overline{LF_f} - \overline{LL_{TRUCK}}}{\sqrt{\sigma_{LF}^2 + \sigma_{LL}^2}} \tag{7.29}$$

where $\overline{LF_f}$ (see Figure 7.2) is the mean value of the load factor corresponding to the functionality limit state. This is the load factor by which the design load has to be multiplied to reach the functionality limit state, normally represented by a maximum deflection allowance.

Finally the system reliability index for the damaged condition limit state is defined by the expression:

$$\beta_{dam} = \frac{\overline{LF_d} - \overline{LL_{truck}}}{\sqrt{\sigma_{LF}^2 + \sigma_{LL}^2}} \tag{7.30}$$

where $\overline{LF_d}$ (see Figure 7.2) is the mean value of the load factor corresponding to the damaged condition limit state. This is the load factor by which the design load has to be multiplied to cause the collapse of the damaged bridge. For this purpose, a slightly different structural model has to be used, namely the model where one of the critical bridge members is removed simulating a condition of severe bridge damage. $\overline{LL_{truck}}$ is the mean value of the maximum expected load (including dynamic allowance effect) corresponding to a low return period usually selected to correspond to the period of routine inspection. The remaining parameters are the same as in the previous cases. The exposure period is made to coincide with the routine inspection period to reflect the fact that severe damage to the bridge would be detected during the inspection and necessary repairs are made at that point.

Because of lack of data on the coefficients of variation associated with estimating the capacity of bridge systems, it is herein assumed that the load factors LF_u, LF_f and LF_d have the same coefficient of variation V_{LF} as that of the load factor LF_1 which can be expresses as:

$$V_{LF} = \frac{\sigma_{LF}}{\overline{LF_1}} \tag{7.31}$$

where σ_{LF} is as in Equation 7.27 and $\overline{LF_1}$ is determined by Equation 7.26. Also the bias factor which relates the mean values with the nominal values of LF_u, LF_f and LF_d is assumed to be equal to the bias calculated for LF_1. The bias factor λ_{LF} can be calculated according to the expression:

$$\lambda_{LF} = \frac{\overline{LF_1}}{LF_1} \tag{7.32}$$

The calculation of LF_1, LF_u, LF_f and LF_d requires the development of the structural model of the bridge being assessed and the use of a finite element package that can perform a static non-linear analysis of the structure. The input used for defining the structural model includes the best estimates of material properties, geometry and dead loads, identification of the bridge's most critical members and the identification of the loading positions and the most critical loading patterns for the critical members under consideration.

Method of Sobrino and Casas. Another simplified procedure for the reliability based assessment of existing bridges at the system level was proposed by Sobrino & Casas (1994). The method was originally used for the safety assessment of highway bridges and was subsequently adapted to railway bridges as shown by Casas & Wiśniewski (2005). The method takes into account the redundancy in bending about the longitudinal direction. It is most appropriate for continuous bridges. The general idea of the method is similar to the previous method in the sense that it uses information from sectional probabilistic analysis of individual members and combines it with the results of a deterministic non-linear analysis of the structural system to assess the structure's system reliability.

The proposed method requires the calculation of the probability of failure of the system (or safety index) and the comparison of the calculated value with the target value for the system. Therefore, the proposed safety format takes the form as defined by Equation 7.5 considering that both reliability indices, β and β_{target}, corresponds to reliability of the structural system.

To compute the reliability index, the first order reliability method (FORM) is recommended. However, any other reliability method such as SORM or Monte Carlo simulations can be used as well.

According to Sobrino & Casas (1994), the Limit State function $g(X)$ in bending for each critical section i situated over intermediate supports or at mid-span can be defined by:

$$g(X) = M_R^i - \lambda_{nla}^i(M_G^e + (M_Q^e) \tag{7.33}$$

where M_R^i is the ultimate resistance moment of the i-th section, M_G^e is the maximum bending moment due to permanent loads calculated for the equivalent simply supported beam, M_Q^e is the maximum bending moment due to traffic loads calculated also for the equivalent simply supported beam and λ_{nla}^i is the non-linear moment redistribution factor for the analysed i-th section. The equivalent simply supported beam is defined as the simply supported beam with the span-length equal to the length of the analysed bridge span (see Figure 7.1).

In Equation 7.33, λ_{nla}^i is the so-called moment redistribution factor for the i-th section defined as:

$$\lambda_{nla}^i = \frac{M_{nla}^i}{\frac{M_{nla}^1 + M_{nla}^3}{2} + M_{nla}^2} \tag{7.34}$$

where M_{nla}^i, M_{nla}^1, M_{nla}^3 and M_{nla}^2 (see Figure 7.3) are the bending moments at failure obtained in the non-linear analysis for the critical i-th section under consideration and the sections over the supports and at mid-span respectively, for the span where i-th section is located.

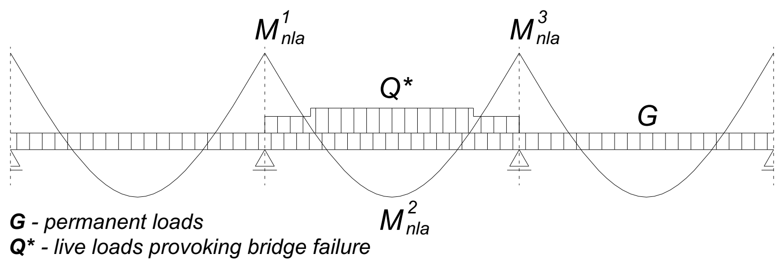

Figure 7.3: Bending moments at the failure state obtained due to non-linear analysis.

Sobrino & Casas (1994) verified that the variability in the mechanical properties and geometrical uncertainties do not change the failure mode of common type continuous bridge structures. Also, the coefficient of variation (COV) of the moment response for each section remains practically constant after yielding. Therefore, because at failure the values of M^i_{nla}, M^1_{nla}, M^3_{nla} and M^2_{nla} will be close to their ultimate values, it can be assumed that the COV of these variables is the same as the COV of the corresponding ultimate member bending capacity. The latter can be easily obtained for each section by simulation taking into consideration the random nature of the basic variables that control the bending capacity which are known to be the section's dimensions, as well as the concrete and steel strengths. The mean values of variables the M^i_{nla}, M^1_{nla}, M^3_{nla} and M^2_{nla} can be approximated by executing a non-linear analysis of the bridge members using as input the mean values of the basic variables.

As with the previous method, the procedure requires the development of a structural model of the bridge and the use of a finite element package allowing for the static non-linear analysis of structures. The best estimates of material properties, geometry and dead loads are used as input. The analysis requires the identification of the bridge critical sections and the identification of the loading position and the most critical loading patterns for the critical section under consideration. Only one non-linear analysis per failure mode or critical section is required.

Chapter 8

Practical comparison of various safety formats

8.1 Introduction

In this chapter several safety formats presented previously are applied to the reliability assessment of a reinforced concrete railway bridge in Brunna, Sweden. At first, the assessment is carried out for the intact bridge using various methods proposed. In the second stage, the significant damaged of the bridge is assumed in such a way that the bridge does not fulfil the safety requirements of the legal design code (EC-1, 2002; EC-1b, 2002; EC-2, 2004; EC-2b, 2003). However, the more sophisticated safety formats allow to proof that the safety margin present in the structure is higher than the required target value.

The evaluation of the bridge using the same basic material and geometrical parameters but different safety formats shows clearly advantages of using more sophisticated assessment methods in the process of bridge evaluation. Furthermore, it allows to compare practically safety formats proposed in the previous chapter.

The following example was developed partially within 'Sustainable Bridges' European Project and is also presented in Casas & Wiśniewski (2005). Furthermore, some parts of this study are discussed in Wiśniewski *et al.* (2006a,b), Wiśniewski & Casas (2006) and Wiśniewski *et al.* (2007).

8.2 Structure description

The 'Brunna Bridge' (see Figure 8.1) is a four-span continuous reinforced concrete structure constructed in 1969. The spans are 13.5 m, 15.0 m, 13.0 m and 11.0 m in length.

Figure 8.1: 'Brunna Bridge' - photo.

The superstructure consists of a U shaped girder with a web spacing of approximately 4.0 m. The girder's bottom flange is approximately 0.4 m thick and supports a single rail track. The total depth of the girder is 1.5 m and the webs are 0.8 m thick. Detailed dimensions of the cross-section are presented in Figure 8.2.

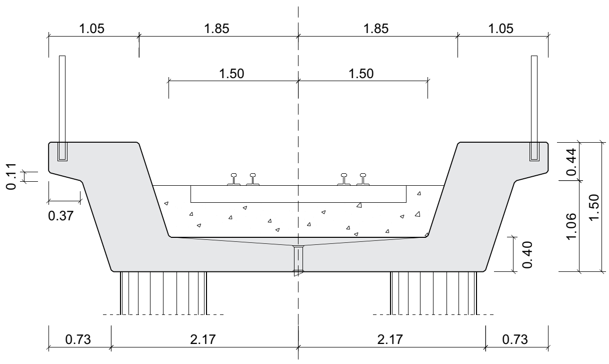

Figure 8.2: 'Brunna Bridge' - cross-section.

The 'Brunna Bridge' is a frame bridge, where the intermediate reinforced concrete circular columns (B, C and D in Figure 8.3) are rigidly connected to the deck and to the footing foundation. The end columns (A and E in Figure 8.3) are also circular in shape however they are designed as double pinned meant to transfer only the vertical reactions. The bridge has a skew of about 50 degrees. The connection of the superstructure to the abutment is designed by means of a cantilever nose with teeth immersed in the embankment.

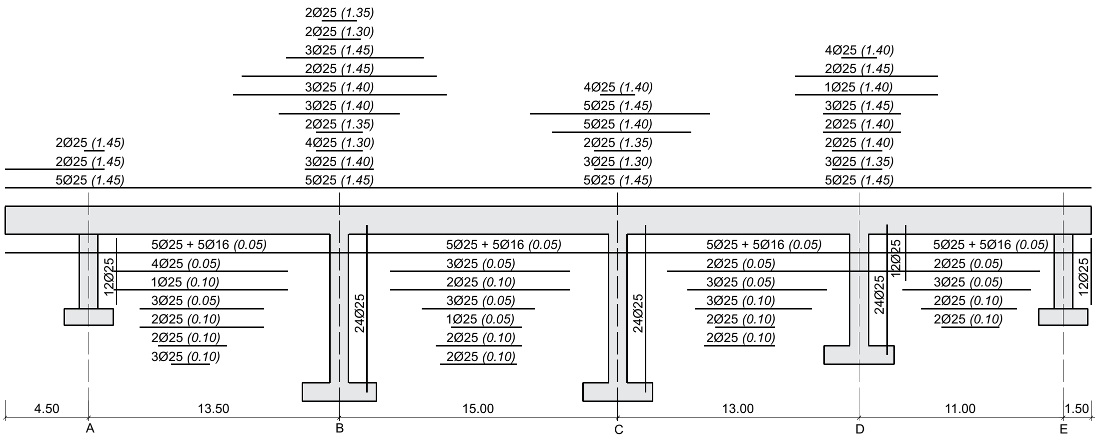

Figure 8.3: 'Brunna Bridge' - outline of the longitudinal reinforcement (values in parenthesis are vertical location of reinforcement measured from the bottom of the girder).

According to the design specifications, the concrete's characteristic compressive strength is 28MPa. The characteristic yielding strength of the reinforcing steel is 400MPa. The reinforcement of the main girders is composed of 25-mm bars. Up to twenty bars are provided in the mid-span sections, and 24 bars are placed over the piers. The outline of the longitudinal reinforcement is presented in Figure 8.3.

8.3 Finite element model

Some simplifications are made in the phase of bridge modelling. In a first approximation, the girder is modelled as two equal and parallel longitudinal beams coinciding with the webs. Only one of the beams is analysed assuming that no transverse redistribution of loads between the two webs is allowed and that the effect of the skew is negligible. Thus, the load is equally distributed to each beam, which ignores the random eccentricity in the transverse location of the load. Furthermore, the long-term changes in concrete and steel properties due to creep, shrinkage and ageing are neglected. This implies that the bending moment distribution due to dead loads is time invariant and the concrete behaviour throughout the design or effective life of the bridge remains as that obtained for the concrete at 28 days.

The special structural analysis software Plastd90 is used to modell the bridge. The software accounts for material non-linearity of structural steel and concrete. This program is based on the Finite Element Method (FEM) and uses the Timoshenko three node beam elements layered along the longitudinal beam's height. The methodology used by the program to model the non-linearity of concrete and steel, is described in Henriques (1998).

The non-linear FEM model consists of 67 beam elements. The elements representing the longitudinal beam comprise 15 layers of concrete and 6 layers of reinforcing steel. The piers are modelled by elements composed by 10 layers of concrete and 8 layers of mild reinforcement.

The boundary conditions between the main girder and the end piers (A and E of Figure 8.3) are assumed to be pinned supports since the connections were designed to only transfer the vertical reactions. Due to the fact that the interior reinforced concrete circular columns (B, C and D in Figure 8.3) were rigidly connected to the superstructure and to the footing, the model assumes a rigid frame connection between the columns and the longitudinal beams. The connections of the columns to the foundation are considered as fixed.

8.4 Geometry, mechanical properties and loads

The values of the most important variables describing the geometry and mechanical properties of the bridge considered during the analysis are presented in Table 8.1. In the table the inherent variability of the parameters is represented by the Coefficient of Variation (COV), which is defined as the ratio of the standard deviation to the mean value of each parameter. The COV's given in Table 8.1

were collected from the work of various researchers and presented in Chapters 4 and 5. Other material properties such as the elastic modulus of concrete and the concrete tensile strength are considered to be functions of the compression strength of concrete as defined in EC-2 (2004). All the other mechanical properties required as FEM input, which are not presented in the table, are also taken as defined in EC-2 (2004).

Table 8.1: Random variables considered in the analysis.

Random variable	Unit	Char. value	Mean value	COV	PDF
Concrete compressive strength, f_c	MPa	28.00	34.00	0.15	normal
Reinforcement yield strength, f_y	MPa	400.00	454.00	0.10	normal
Height of the girder, h_g	m	1.50	1.50	0.02	normal
Height of the slab, h_s	m	0.40	0.40	0.07	normal
Top Reinforcement area, A_{St}	m	nomin.	nomin.	0.02	normal
Bottom Reinforcement area, A_{Sb}	m	nomin.	nomin.	0.02	normal
Self weight of the structure, G_S	kN/m	47.53	47.53	0.08	normal
Permanent loads (ballast), G_{Ab}	kN/m	19.07	19.07	0.10	normal
Permanent loads (track), G_{At}	kN/m	2.00	2.00	0.10	normal
Railway traffic load (conc.), Q_c	kN/m	78.13	64.69	0.10	normal
Railway traffic load (distr.), Q_d	kN/m	40.00	31.70	0.10	normal
Impact factor, I	—	1.25	1.25	0.50	normal

The following loads were considered in the analysis (see Figure 8.4): Gs - Self-weight of the structure; Ga - Additional permanent loads; Q - Live load on the railway track (UIC train load model) as presented in Table 8.1 along with the COV of each load.

The values of railway traffic loads are obtained from the UIC train load model considering that the combined effect of the characteristic axle load (250kN) and distributed load (80kN/m) corresponds to the 98-th percentile of the PDF of the railway load assuming normal distribution. Considering this assumption, the mean value for the axle loads and distributed load are calculated to be respectively 207kN and 63.4kN/m. The values of the railway traffic load presented in

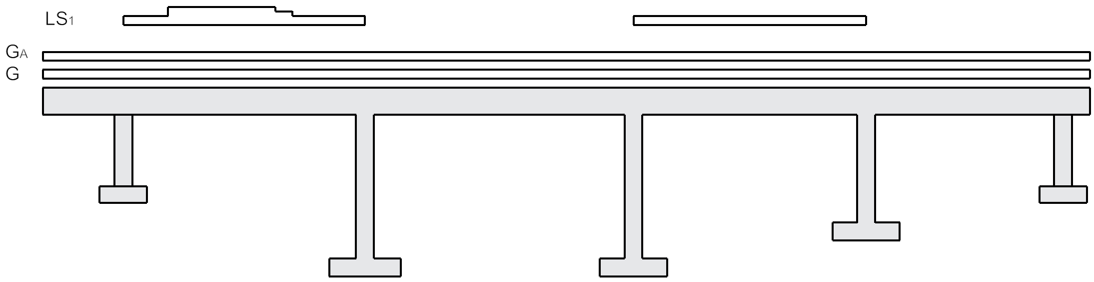

Figure 8.4: 'Brunna Bridge' - outline of loading configuration.

Table 8.1 are obtained by equally distributing the load to the two beam lines and distributing the concentrated load from the axles through the ballast (the distribution length was considered equal to 6.4m).

8.5 Loading scheme and condition states

To illustrate the analysis procedure, the analysis is performed for a single loading scheme designated as (LS_1) which causes the failure of the mid-span section of the first span (see Figure 8.4).

Furthermore, to show the benefits of using the simplified probabilistic non-linear analysis for the assessment of deteriorated structures, the analysis is performed for two condition states of the bridge. The first analysis is carried out for the original bridge where it is assumed that the structure is in perfect condition. The second analysis is performed assuming a serious level of deterioration where 50% of the bottom reinforcement of the section in the middle of the first span is assumed to be corroded and is removed from the model. The situation, where only one section of the bridge is subjected to such high level of deterioration while other sections remain intact is hypothetical and is only considered to illustrate the benefits of the proposed method for the safety assessment of existing bridges in case the standard member level assessment technique recommended by existing codes fails.

8.6 Structural analysis

8.6.1 Linear elastic analysis

The structural analysis of the bridge is performed at first considering the linear behaviour of the structure in order to define the elastic distribution of internal forces between the critical bridge sections. The bending moments for the middle span section (Sect.2) and the sections over the piers (Sect.1, Sect.3) of the first span, are listed in Table 8.2 for each of the loads obtained from the linear elastic analysis. The results in the first two rows correspond to the bending moments due to the permanent loads. Since the characteristic values of the permanent loads are equal to their mean values the corresponding bending moments are also equal. The last two rows correspond to the bending moments due to the mean value and the characteristic value of the railway traffic load respectively. The results were obtained for the load without impact.

Table 8.3 presents the results of the bending moments in the mid-span section (Sect.2) obtained for the equivalent simply supported beam, which is defined as the beam with a length equal to the length of the analysed span (13.5 m). The results in the first two rows correspond to the bending moments due to the mean values of the permanent loads. The last row corresponds to the bending moment due to the mean value of the railway traffic load without impact.

Table 8.2: Bending moments in the critical sections of the first span (13.5 m).

Load	Symbol	Unit	Bending moment		
			Sect. 1	Sect. 2	Sect. 3
Self weight of the structure	M_{Gs}	kNm	-481.19	415.60	-853.10
Additional permanent loads	M_{Ga}	kNm	-213.35	184.24	-378.25
UIC railway traffic load (mean)	M_Q	kNm	0	955.89	-579.91
UIC railway traffic load (char.)	M_{Qk}	kNm	0	1163.58	-705.72

8.6.2 Non-linear analysis for Ghosn and Moses methods

The load factors for the functionality, ultimate and damaged condition limit states obtained from the non-linear analysis are presented in Table 8.4. The ta-

Table 8.3: Bending moments in the equivalent simple supported beam (13.5 m).

Load	Symbol	Unit	Bending moment		
			Sect. 1	Sect. 2	Sect. 3
Self weight of the structure	M^e_{Gs}	kNm	0	1082.75	0
Additional permanent loads	M^e_{Ga}	kNm	0	480.04	0
UIC Railway traffic load (mean)	M^e_Q	kNm	0	1245.85	0

ble presents the results for the 'original bridge' and for the 'deteriorated bridge', where a significant percentage of the mid-span section reinforcement was removed from the model. The load factors LF_i are the factors by which the bridge traffic loads (UIC characteristic train load) have to be multiplied to reach the failure state. LF_f is the load factor for which the bridge reaches the functionality condition, which is defined as a maximum deflection equal to span length/500 which in the case of the 13.5m span is equal to 0.027m. LF_u is the load factor for which the whole structure fails and finally LF_d is the load factor for which the bridge after sustaining major damage (bridge without one of its main members) fails. Two major damage scenarios are assumed in this example. The first damage scenario consists of the formation of a hinge in the mid-span section. The second scenario assumes a hinge in the section over the pier B of the main girder (see Figure 8.3).

Table 8.4: Load factors for functionality, ultimate and damaged cond. limit state.

Condition state	Load factors			
	LF_f	LF_u	$LF_d^{(a)}$	$LF_d^{(b)}$
Original bridge (intact condition state)	3.93	5.80	1.66	2.00
Deteriorated bridge (reinforcement area A_{Sb} loss)	2.85	3.43	1.66	1.26

Note:$^{(a)}$ corresponds to the situation where a hinge is assumed in the mid-span section, $^{(b)}$ corresponds to the situation where a hinge is assumed over pier B.

8.6.3 Non-linear analysis for Sobrino and Casas method

The bending moments prior to the failure of the middle span section (Sect.2) and the sections over the piers (Sect.1, Sect.3) of the first span are obtained from a non-linear analysis and presented in Table 8.5. The results are obtained considering that all the variables describing structure geometry and material behaviour take their mean values (see Table 8.1). The dead loads and the railway traffic loads were also considered at their mean values. Table 8.5 presents the results for the original bridge and for the deteriorated bridge, where a significant percentage of the mid-span section reinforcement is removed from the model.

Table 8.5: Bending moments in the critical sections of the first span (13.5 m).

Bridge condition	Symbol	Unit	Bending moment		
			Sect. 1	Sect. 2	Sect. 3
Original bridge (intact cond.)	M_{nla}	kNm	-639.76	5751.30	-8073.67
Deteriorated bridge (A_{Sb} loss)	M_{nla}	kNm	-657.30	3010.65	-6321.26

8.7 Ultimate response of bridge sections

The bending resistance of each of the bridge's critical sections is obtained from the ultimate analysis of reinforced concrete sections subjected to a combination of loads (bending, shear and axial forces). The two previously defined condition states are considered, namely the original as built condition and the deteriorated condition that assumes a reduction in reinforcement area. At first, the sectional analyses are carried out for the characteristic values of the concrete compressive strength and steel yielding strength as defined in Table 8.1. These results are presented in Table 8.6 for the critical sections of the middle bridge span.

Table 8.6: Probabilistic ultimate response of critical sections.

Section	Symbol	Unit	Char. value	Mean value	COV	PDF
Section over the pier A	M_R^1	kNm	—	2228	0.10	normal
Mid-span section (original)	M_R^2	kNm	5164	5772	0.10	normal
Mid-span section (deterior.)	M_R^2	kNm	2742	3063	0.10	normal
Section over the pier B	M_R^3	kNm	—	8606	0.10	normal

Subsequently, simulations using the Latin Hypercube method (see Chapter 3) were performed to obtain the probabilistic resistance model of the sections subjected to bending. The analyses were carried as follows:

- At first a set of values of random variables are generated, using Latin Hypercube sampling method, for each of the parameters listed in Table 8.1.
- Sectional analyses are performed for each combination of generated variables (100 simulations).
- A statistical analysis of the results is performed to obtain the mean value, the standard deviation and the probability distribution type.

Figures 8.5 and 8.6 present the histograms of the calculated ultimate bending resistance of the mid-span section (Sec.2) for the original and deteriorated condition respectively. The normal curves plotted on the diagrams were determined based on the mean values and standard deviations of the results obtained from the simulation. The plots show a very good fit of the data using a normal distribution. The applicability of using a Normal distribution for the section's bending resistance is also confirmed by the K-S (Kolmogorov Smirnoff type) Lilliefors goodness of fit test. The results of the simulations for the mid-span section (Sec.2) and the sections over the piers (Sec.1 and Sec.3), for both the original and deteriorated conditions are summarized in Table 8.6.

In the present study, the probabilistic model for each section's resistance to bending is obtained by the Latin Hypercube simulations using appropriate software for sectional analysis. However, in practical applications, the probabilistic model of the resistance of typical railway bridge sections can be retrieved from the information presented in Chapter 6.

8.8 Safety assessment

8.8.1 Safety assessment at the member level

Semi-probabilistic format. In a first step, the safety of the main girder of the 'Brunna Bridge' in bending was checked using partial safety factor method

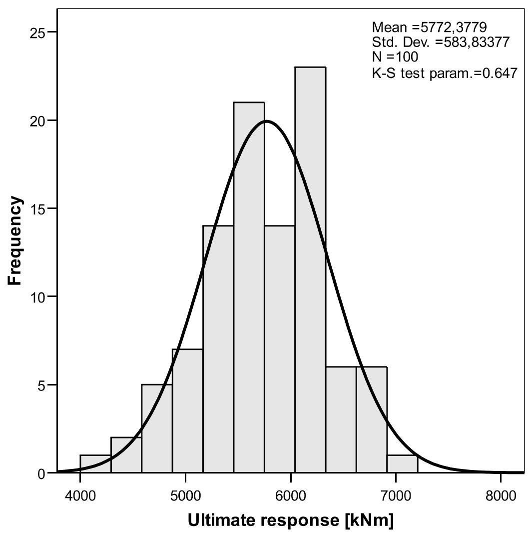

Figure 8.5: Histogram of mid-span section resistance - original bridge.

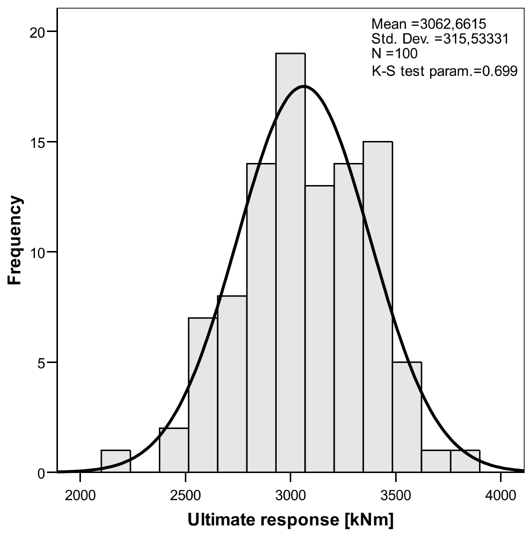

Figure 8.6: Histogram of mid-span section resistance - deteriorated bridge.

and linear elastic analysis. The safety check was performed for the middle span section of the first span considering the load scheme described in Section 8.5. The assessment was performed for the original bridge as well as for the deteriorated bridge using the following checking equation:

$$\phi_R M_{Rk} \geq \gamma_{Gs} M_{Gsk} + \gamma_{Ga} M_{Gak} + \gamma_G I M_{Qk} \tag{8.1}$$

where M_{Rk} is the characteristic moment capacity of the section; M_{Gsk} is the bending moment due to the characteristic value of the structure's self weight; M_{Gak} is the bending moment due to the characteristic value of the additional dead loads; M_{Qk} is the bending moment due to the characteristic value of the railway traffic loads; ϕ_R is the resistance factor; γ_{Gs} is the partial safety factor for the structure's self weight; γ_{Ga} is the partial safety factor for the additional dead loads; γ_Q is the partial safety factor for the railway traffic loads; and finally I is the impact factor.

Using the partial safety factors defined in the Eurocode and an impact factor equal to 1.25, the load effects as presented in Table 8.2 and the moment capacity as presented in Table 8.6, the checking equations for the original bridge takes the following form:

$$0.86 \cdot 5164 \gtreqless 1.35 \cdot 415.6 + 1.35 \cdot 184.24 + 1.45 \cdot 1.25 \cdot 1163.58$$

which after performing the calculations leads to the following inequality:

$$4441 \geq 2919 \text{ [kNm]}$$

As it can be seen, the safety is verified with a high margin. The high safety margin observed is the result of the overdesign of the section, which may be due to the application of different loads and/or the use of different safety codes during the actual design of the bridge.

Performing the same calculation for the deteriorated bridge and assuming that the ultimate capacity of the mid-span section is reduced down to 2742 kNm, the following inequality is obtained:

$$0.86 \cdot 2742 \gtreqless 1.35 \cdot 415.6 + 1.35 \cdot 184.24 + 1.45 \cdot 1.25 \cdot 1163.58$$

which simplifies to:

$$2358 \ngeq 2919 \text{ [kNm]}$$

As it can be seen using the partial safety factor method with the safety factors specified in the Eurocode, the mid-span section of the deteriorated bridge has an ultimate bending moment lower than the design moment. Therefore, based on the standard assessment method, the bridge should be declared as unsafe. The difference between the required and available member capacity is quite significant on the order of 25%.

Fully probabilistic format. The same section of the bridge as in the previous case was analyzed using fully probabilistic method. The safety was evaluated by means of the reliability index β. According to the procedure presented in the previous chapter the limit state function $g(X)$ was defined at first and then the reliability index β for the defined limit state function was calculated using FORM.

The limit sate function for the verification of the main girder section against bending is as follows:

$$g(X) = M_R - (M_{Gs} + M_{Ga} + I \cdot M_Q) \tag{8.2}$$

where M_R is the resistance of the analysed section against bending; M_{Gs} is the bending moment in the analysed section due to the self weight of the structure; M_{Ga} is the bending moment in the analysed section due to additional dead loads; M_Q is the bending moment in the analysed section due to the railway traffic loads and finally I is the impact factor.

Considering the information form Tables 8.1, 8.2 and 8.6, and assuming that the distribution types and COV's of load effects are equal to those of the corresponding loads the calculations were performed.

For the defined limit state function the reliability indices obtained using FORM are found to be β=6.61 and β=3.61 for original bridge and deteriorated bridge respectively. The FORM analyses were performed assuming statistical independence between all the variables. Comparing the obtained value of the reliability index β with the target values presented in the previous chapter it can be assumed that the bridge is sufficiently safe. However, the safety margin of the deteriorated bridge is relatively low.

Simplified probabilistic format. In order to compare results of the assessment using various safety formats the Mean Load Method was also used (see Equation 7.6). In the analysed case the generalized resistance R is the section resistance against bending and the generalized action S is composed by several components (bending moments in the section), hence Equation 7.6 takes a more complicated form:

$$\beta = \frac{\mu_{M_R} - (\mu_{M_{Gs}} + \mu_{M_{Ga}} + \mu_{I \cdot M_Q})}{\sqrt{\sigma^2_{M_R} + \sigma^2_{M_{Gs}} + \sigma^2_{M_{Ga}} + \sigma^2_{I \cdot M_Q}}} \tag{8.3}$$

where μ_{M_R} is the mean value of the resistance of the analysed section against bending; $\mu_{M_{Gs}}$ is the mean value of the bending moment in the analysed section due to the self weight of the structure; $\mu_{M_{Ga}}$ is the mean value of the bending moment in the analysed section due to additional dead loads; $\mu_{I \cdot M_Q}$ is the mean value of the bending moment due to the railway traffic loads including impact; σ_{M_R} is the standard deviation of the resistance of the analysed section against bending; $\sigma_{M_{Gs}}$ is the standard deviation of the bending moment in the analysed section due to the self weight of the structure; $\sigma_{M_{Ga}}$ is the standard deviation of the bending moment in the analysed section due to additional dead loads; $\sigma_{I \cdot M_Q}$ is the standard deviation of the bending moment in the analysed section due to the railway traffic loads including impact.

$$\beta = \frac{5772 - 415.6 - 184.24 - 1.25 \cdot 955.89}{\sqrt{(5772 \cdot 0.1)^2 + (415.6 \cdot 0.08)^2 + (184.24 \cdot 0.1)^2 + (1.25 \cdot 955.89 \cdot 0.14)^2}} = \\ = \frac{3977}{602} = 6.61$$

$$\beta = \frac{3063 - 415.6 - 184.24 - 1.25 \cdot 955.89}{\sqrt{(3063 \cdot 0.1)^2 + (415.6 \cdot 0.08)^2 + (184.24 \cdot 0.1)^2 + (1.25 \cdot 955.89 \cdot 0.14)^2}} = \\ = \frac{1268}{351} = 3.61$$

Considering the information form Tables 8.1, 8.2 and 8.6, and assuming that the distribution types and COV's of load effects are equal to those of the corresponding loads the calculations were performed. The mean value of the bending moment due to the railway traffic load including impact was considered to be equal to the product of their mean values. The COV of railway traffic load including impact was considered to be equal to 0.14. This value is the effect of the multiplication of the railway load with a COV equal to 0.10 by the impact factor with a COV equal to 0.50. The following equations show the performed calculation for the original bridge and deteriorated bridge respectively:

The evaluation performed using probabilistic member level assessment shows that the bridge is sufficiently safe even for the case of serious deterioration of the mid-span section assumed.

8.8.2 Safety assessment at the system level

8.8.2.1 Assessment considering simplified structural behaviour

Simplified probabilistic formats. In order to estimate the safety of the bridge at the system level the Bounds Method explained in previous chapter was used in a first step. The lower bounds were considered as calculated in the previous paragraph (β=6.61 and β=3.61 for original and deteriorated bridge respectively). The upper bounds were calculated using appropriate FORM analysis software. Considering a full redistribution (plastic analysis), the limit state function is defined by Equation 7.10 which in the cases under analysis can be rewritten as follows:

$$g(X) = M_R^2 - \frac{M_R^2}{\frac{M_R^1 + M_R^3}{2} + M_R^2}(M_{Gs}^e + M_{Ga}^e + I \cdot M_Q^e) \tag{8.4}$$

where M_R^1, M_R^3 and M_R^2 are the ultimate bending resistances of the sections over the supports and at mid-span (analysed section) respectively, for the first span of the bridge, M_{Gs}^e is the bending moment due to self weight calculated for the equivalent simply supported beam (span length equal to 13.5 m), M_{Ga}^e is the bending moment due to additional dead loads calculated for the equivalent simply supported beam, M_Q^e is the maximum bending moment due to traffic loads calculated also for the equivalent simply supported beam and I is the impact factor.

Considering probabilistic models of variables as presented in Tables 8.1, 8.3 and 8.6, and assuming that the distribution types and COV's of load effects are equal to those of the corresponding loads the FORM analysis performed leads to the reliability index β=10.00 and β=9.07 for original and deteriorated bridge respectively. FORM analysis was carried out considering statistical independence of all variables.

Analysing the results obtained with the elastic and plastic analysis it was concluded that the system safety of the 'Brunna Bridge' is very high. The actual reliability index for the original bridge is located somewhere between β=6.61 and β=10.00 and for the deteriorated bridge between β=3.61 and β=9.07.

8.8.2.2 Assessment considering non-linear structural behaviour

Semi-probabilistic formats. The reliability assessment of the 'Brunna Bridge' was also performed using the Redundancy Factor Method presented in the previous chapter. Since the application of the method is quite complex, the analysis was performed following the sequence of the step-by-step methodology proposed (see Section 7.3.3.2).

Step 1. In the present example only the safety of the mid-span section of the first span was decided to be analysed, hence the identification of the critical members of the bridge was simplified to the choice of that section.

Step 2. Calculation of the required member capacity was performed according to the Eurocode and the partial safety factor method. For bending the required member capacity is expressed by the following equation:

$$M_{Rk(req)} = \frac{\gamma_{Gs} M_{Gsk} + \gamma_{Ga} M_{Gak} + \gamma_Q I M_{Qk}}{\Phi_R} \tag{8.5}$$

where M_{Gsk}, M_{Gak} and M_{Qk} are the bending moments in the analysed section due to the characteristic values of the structure self weight, additional dead loads and the railway traffic loads respectively (considered as presented in Table 8.2); Φ_R is the resistance factor for the analysed section (considered equal to 0.86); γ_{Gs} , γ_{Ga} and γ_Q are the partial safety factor for the structure self weight, the additional dead loads and the railway traffic loads respectively (considered equal to 1.35; 1,35 and 1.50) and finally I is the impact factor (considered as showed in Table 8.1).

Performing the calculations the following value is obtained:

$$M_{Rk(req)} = \frac{1.35 \cdot 415.60 + 1.35 \cdot 184.24 + 1.5 \cdot 1.25 \cdot 1163.58}{0.86} = \frac{2992}{0.86} = 3478$$

Step 3. The actual member capacities for original and deteriorated condition state are shown in Table 8.6 (5164 kNm and 2742 kNm respectively).

Step 4. The non-linear FEM model of the 'Brunna Bridge' was developed as described in Section 8.3 of this chapter. The best estimates of material properties, structure geometry and loads were used (mostly mean values).

Step 5. In this example only the safety of the mid-span section of the first span was analysed, hence the identification of the loading position and the most critical load pattern was simplified to the longitudinal positioning of the railway traffic load (UIC train load model) to cause the maximum bending moment in the analysed section. The choice of the considered load position is explained in Section 8.5 of this chapter.

Step 6. In order to define the member reserve ratio r_1 the required member load factor capacity LF_{1req} and actual member load factor capacity LF_1 are determined according to the following equations:

$$LF_{1req} = \frac{M_{Rk(req)} - M_{Gs} - M_{Ga}}{M_{Qk}} \tag{8.6}$$

$$LF_1 = \frac{M_{Rk} - M_{Gs} - M_{Ga}}{M_{Qk}} \tag{8.7}$$

Considering the required and actual member bending resistance as defined in step 2 and 3, and considering the bending moments due to the mean dead loads and characteristic railway traffic loads as defined in Table 8.2 the required member load factor capacity is given as:

$$LF_{1req} = \frac{3478 - 415.60 - 184.24}{1163.58} = 2.47$$

The actual member load factor capacity for original and deteriorated bridge are calculated as:

$$LF_1 = \frac{5164 - 415.60 - 184.24}{1163.58} = 3.92 \quad ; \quad LF_1 = \frac{2742 - 415.60 - 184.24}{1163.58} = 1.84$$

The member reserve ratios for original and deteriorated bridge, defined in previous chapter by Equation 7.12, becomes:

$$r_1 = \frac{LF_1}{LF_{1req}} = \frac{3.92}{2.47} = 1.59 \;\; ; \;\; r_1 = \frac{LF_1}{LF_{1req}} = \frac{1.84}{2.47} = 0.75$$

Step 7. The load factors LF_f (see Table 8.4), for which the bridge reaches the functionality limit state defined as allowable deflection - L/500, were obtained via the non-linear analysis described in Section 8.6.2 of this chapter.

Step 8. The system reserve ratios R_f (for the functionality limit state) for original and deteriorated bridge are calculated using the *Equation* 7.15 as follows:

$$R_f = \frac{LF_f}{LF_1} = \frac{3.93}{3.92} = 1.00 \;\; ; \;\; R_f = \frac{LF_f}{LF_1} = \frac{2.85}{1.84} = 1.55$$

Step 9. The redundancy ratio r_f for the functionality limit state are obtained from the Equation 7.16. Considering $R_{f,target}$ equal to 1.1 they become for the original and deteriorated bridge as:

$$r_f = \frac{R_f}{R_{f,target}} = \frac{1.00}{1.10} = 0.91 \;\; ; \;\; r_f = \frac{R_f}{R_{f,target}} = \frac{1.55}{1.10} = 1.41$$

Step 10. The load factors LF_u (see Table 8.4), for which the bridge reaches the ultimate limit state, were obtained via the non-linear analysis described in Section 8.6.2 of this chapter.

Step 11. The system reserve ratios R_u (for the ultimate limit state) for original and deteriorated bridge are calculated using the Equation 7.17 as follows:

$$R_u = \frac{LF_u}{LF_1} = \frac{5.80}{3.92} = 1.48 \;\; ; \;\; R_u = \frac{LF_u}{LF_1} = \frac{3.43}{1.84} = 1.86$$

Step 12. The redundancy ratio r_u for the ultimate limit state are obtained from the Equation 7.18. Considering $R_{u,target}$ equal to 1.3 they become for the original and deteriorated bridge as:

$$r_u = \frac{R_u}{R_{u,target}} = \frac{1.48}{1.30} = 1.13 \;\; ; \;\; r_u = \frac{R_u}{R_{u,target}} = \frac{1.86}{1.30} = 1.43$$

Step 13. The load factors LF_u (see Table 8.4), for which the bridge reaches the damaged condition limit state, were obtained via the non-linear analysis described in Section 8.6.2 of this chapter. The assumed damage in this case was introduced in the model as the hinge in the main girder in the mid-span section.

Step 14. The system reserve ratios R_d (for the damaged condition limit state) for original and deteriorated bridge are calculated using the Equation 7.19 as follows:

$$R_d = \frac{LF_d}{LF_1} = \frac{1.66}{3.92} = 0.42 \;\; ; \;\; R_d = \frac{LF_d}{LF_1} = \frac{1.66}{1.84} = 0.90$$

Step 15. The redundancy ratio r_d for the damaged condition limit state are obtained from the Equation 7.20. Considering $R_{d,target}$ equal to 0.5 they become for the original and deteriorated bridge as:

$$r_d = \frac{R_d}{R_{d,target}} = \frac{0.42}{0.50} = 0.84 \;\; ; \;\; r_d = \frac{R_d}{R_{d,target}} = \frac{0.90}{0.50} = 1.80$$

Step 16. Calculation of the system reserve ratio and the redundancy ratio for the theoretical damaged condition is performed also assuming different damage scenario. The assumed damage in this case is introduced in the model as the hinge in the main girder in the section over pier B. The load factors LF_d obtained in the non-linear analysis for this case are presented in Table 8.4.

The following values of the system reserve ratio and the redundancy ratio are obtained for original and deteriorated bridge condition state:

$$R_d = \frac{LF_d}{LF_1} = \frac{2.00}{3.92} = 0.51 \;\; ; \;\; R_d = \frac{LF_d}{LF_1} = \frac{1.26}{1.84} = 0.68$$

$$r_d = \frac{R_d}{R_{d,target}} = \frac{0.51}{0.50} = 1.02 \;\; ; \;\; r_d = \frac{R_d}{R_{d,target}} = \frac{0.68}{0.50} = 1.36$$

The obtained value of redundancy ratio for original bridge is higher than the value obtained in step 15, therefore, the value previously calculated is considered as relevant. In case of deteriorated bridge the situation is opposite and the redundancy ration calculated in this step is considered relevant. The analysed two scenarios of possible damages are likely to be the most significant and relevant for the analysed case. Due to this fact the analysis are not repeated for any other scenarios.

Step 17. The analyses of all possible load patterns are omitted in this example due to the fact that just the safety of the mid-span section is analysed.

Hence, the minimum values of the redundancy ratios r_f, r_u and r_d are considered as those obtained in the steps 9, 12, 15 and 16.

Step 18. The redundancy factors ϕ_{red} for original and deteriorated bridge respectively are determined according to the Equation 7.21 as follows:

$$\phi_{red} = min(1.59 \cdot 0.91\ ;\ 1.59 \cdot 1.14\ ;\ 1.59 \cdot 0.84) = min(1.45\ ;\ 1.81\ ;\ 1.34) = 1.34$$

$$\phi_{red} = min(0.75 \cdot 1.41\ ;\ 0.75 \cdot 1.43\ ;\ 0.75 \cdot 1.36) = min(1.06\ ;\ 1.07\ ;\ 1.02) = 1.02$$

Step 19. Since the redundancy factor ϕ_{red} calculated in the previous step is greater than 1, the bridge may be considered as safe from the system point of view despite the fact, that in the case of deteriorated bridge the member check fails and the member reserve ratio is significantly smaller than 1. The fact that for original bridge condition state the redundancy factor is significantly higher than 1 means that actual safety margin in this case is expected to be very high.

Fully probabilistic formats. The safety assessment of the bridge at the system level is also performed using fully probabilistic methods. Two different algorithms are used, the Latin Hypercube simulation method and the Response Surface method, both described in more detail in Chapter 3. In the following paragraphs the results of the analysis are presented.

Latin Hypercube method. In this paragraph, the statistics of the bridge system capacity are evaluated using the Latin Hypercube Sampling (LHS) method. In a first step, a set of sample values is generated for each of the 9 random variables listed in Table 8.1 that control the bridge strength (i.e. without the live loads and impact). A non-linear structural analysis is performed for each combination of random variables for a total of 100 simulations. The loads applied correspond to the mean live load augmented by the mean impact factor. The strength capacity is thus expressed by the load factor by which the original mean load should be multiplied to cause the failure of the system. The means and standard deviations of the strength capacities of the original bridge system and the deteriorated bridge system are calculated and the histograms from the simulation's results are compared to those of Normal distributions.

Figures 8.7 and 8.8 present the histograms of the calculated load factors by which the nominal railway traffic loads have to be multiplied to cause the bridge failure, for the original and deteriorated bridges respectively.

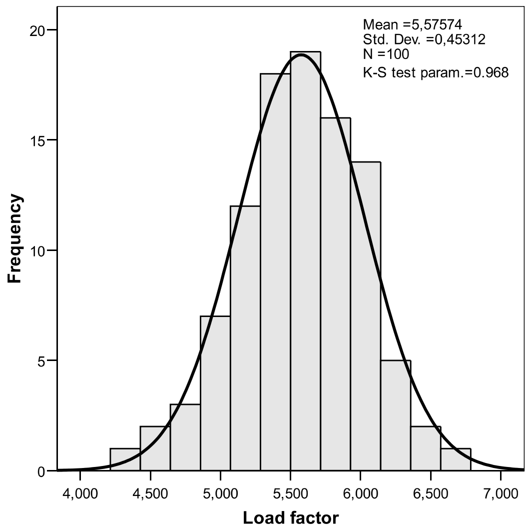

Figure 8.7: Histogram of the load factor at failure - original bridge system.

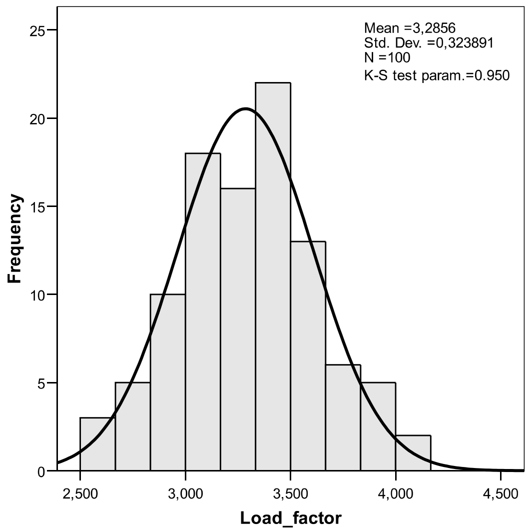

Figure 8.8: Histogram of the load factor at failure - deteriorated bridge system.

The normal curves plotted on the diagrams were determined based on mean values and standard deviations of the results obtained from simulation. For this example, the plots show a very good fit compared with the normal distribution, which is also confirmed using the K-S (Kolmogorov Smirnoff type) Lilliefors goodness of fit test.

The reliability index β for both the original and deteriorated states are calculated using the Mean Load Method. Due to the fact that both the system's structural resistance and the generalized applied loads follow normal distributions, the form of the Mean Load Method determined by Equation 7.6 is valid. In Equation 7.6 μ_R and μ_S are the mean values of the generalized resistance and the applied loads respectively. σ_R and σ_S are the standard deviations of the generalized resistance and loads. In this example, the resistance is modelled by the load factor by which the applied mean loads should be multiplied to cause the failure of the system. Thus, the mean value of the applied loads takes unit value. The standard deviation of the generalized action was considered to be equal to 0.14. This value is the effect of the multiplication of the railway load with a coefficient of variation equal to 10% by the impact factor with a coefficient of variation equal to 50%. Table 8.7 summarizes the results of the reliability index β for both condition states, namely original and deteriorated.

Table 8.7: Calculation of the reliability index.

Condition state	Resistance R		Action S		$R-S$		Safety index β
	Mean	St. dev.	Mean	St. dev.	Mean	St. dev.	
Original	5.576	0.453	1	0.14	4.576	0.474	9.65
Deteriorated	3.286	0.324	1	0.14	2.286	0.353	6.48

Response Surface method. In order to verify the quality of the results obtained by the Latin Hypercube method the reliability analysis is also performed using another fully probabilistic non-linear approach, namely the Response Surface method.

The following procedure is used during the analysis. In a first step, a sample set of input parameters for 19 analyses is initially prepared. The number of analyses (19) in a set is a sum of 1 analysis performed considering the mean values of all the structure related independent random variables (9 variables), and 18 analysis performed taking one of the 9 variables at its mean plus or minus 10% while the remaining variables are kept at their mean values. The results of the 19 analyses are then fitted in a linear polynomial function using a regression analysis. Subsequently, the reliability index β was calculated using FORM for the limit state function defined as the response function obtained in the previous step minus the live load, Q. The FORM algorithm also gives the coordinates of the design point for the calculated reliability index. The next step follows the same process, however, instead of the central (mean) values of the parameters, the coordinates of the design point obtained are used to define the polynomial fit. Also, the perturbation of the values is reduced to 5% for the second iteration and to 2.5% in the following ones. Furthermore, adjustments to the algorithm are made when the coordinates obtained in the FORM analysis are determined to be unreasonable (e.g. when negative values are obtained for the coefficients associated with the yield stress of steel reinforcement or concrete strength) or leads to unreasonable polynomial functions and consequently to doubtful reliability index values (e.g. reliability index out of range or significantly different from previous approximations). In such cases, instead of performing the analysis around the new design point obtained from the algorithm the analysis is performed for the set of variables located in the middle of the distance between the previous design point and the design point indicated by FORM. The process is repeated until convergence, which occurs when the reliability index β from two consecutive analyses is within 1%.

Equations 8.8 and 8.9 show the limit state functions obtained following the iterative procedure for the original and deteriorated condition states respectively.

$$\begin{aligned} g(X) = {} & 0.0000052326 \cdot f_c + 1.5205547862 \cdot h_g + 0.1484513209 \cdot h_s + \\ & + 0.0000092929 \cdot f_y + 0.7040553589 \cdot A_{Sb} + 0.9844101575 \cdot A_{St} + \\ & - 0.0101214575 \cdot G_S - 0.0092131489 \cdot G_{Ab} - 0.0098242475 \cdot G_{At} + \\ & - 3.9718007335 - Q \end{aligned} \tag{8.8}$$

$$\begin{aligned} g(X) = {} & 0.0000057766 \cdot f_c + 1.1547095388 \cdot h_g - 1.3725490196 \cdot h_s + \\ & + 0.0000147243 \cdot f_y + 0.6819640565 \cdot A_{Sb} + 1.2471336042 \cdot A_{St} + \end{aligned}$$

$$- 0.0050335570 \cdot G_S - 0.0101619433 \cdot G_{Ab} - 0.0100000000 \cdot G_{At} + - 3.4776301070 - Q \qquad (8.9)$$

The reliability indices calculated by FORM for the ultimate limit state functions for the intact and deteriorated bridge defined by Equations 8.8 and 8.9 are β=7.37 and β=6.17 respectively. The reliability indices were calculated assuming all the parameters as defined in Table 8.1. However, due to the fact that during the simulations the railway loads were applied as their mean value including impact and later incremented (by multiplying the mean load by the load factor) to reach the structure failure, the mean value of the generalized action Q is considered as unity. The standard deviation of the generalized action was considered to be equal to 0.14. As stated earlier, this value is the effect of the multiplication of the railway load with a coefficient of variation equal to 10% by the impact factor with a coefficient of variation equal to 50%. Similarly, the variability in the areas of the different reinforcement layers was considered to be fully dependent on the two random variables A_{sb} and A_{st} (for bottom and top reinforcement respectively). Thus, the variability of the reinforcement areas was accounted for by multiplying the characteristic area of each layer by a random variable with a mean value equal to unity and a coefficient of variation of 2%.

Simplified probabilistic formats. In this paragraph the safety assessment of the bridge at the system level is performed using simplified probabilistic formats. Two different methods are used, the method of Ghosn and Moses and the method of Sobrino and Casas, both described in more detail in the previous chapter. In the following paragraphs the results of the analysis are presented.

Method of Ghosn and Moses. In this paragraph,the reliability assessment of the 'Brunna Bridge' for the original and deteriorated condition states is performed using the simplified probabilistic method of Ghosn and Moses. The analysis necessary to obtain the load factors for functionality LF_f, ultimate LF_u and damaged condition LF_d limit states (see Table 8.4) were performed according to the methodology presented in previous chapter. After the determination of the load factors LF_i, the parameters necessary for the reliability analysis (bias factor and coefficient of variation) are determined by comparing the results of the analysis performed at the mean values of the input parameters and the results when the input parameters are taken at their nominal or characteristic values. Thus, the nominal and mean load factors for first member failure are obtained from:

$$LF_1 = \frac{M_R - M_{Gs} - M_{Ga}}{M_{Qk}} \tag{8.10}$$

$$\overline{LF_1} = \frac{\overline{M_R} - \overline{M_{Gs}} - \overline{M_{Ga}}}{M_{Qk}} \tag{8.11}$$

where M_R is the moment capacity of the section; M_{Gs} is the bending moment due to the structure self weight; M_{Ga} is the bending moment due to the additional dead loads and M_{Qk} is the bending moment due to the railway traffic load without impact. The line over each symbol indicate that it is the mean value.

Considering the moment capacity of the section as defined in Table 8.6 and considering the bending moments due to the dead loads and railway traffic load as defined in Table 8.2, the following values are obtained for the original bridge:

$$LF_1 = \frac{5164 - 415.60 - 184.24}{1163.58} = 3.92 \quad ; \quad \overline{LF_1} = \frac{5772 - 415.60 - 184.24}{1163.58} = 4.45$$

nominal and mean load factors for the deteriorated bridge are:

$$LF_1 = \frac{2742 - 415.60 - 184.24}{1163.58} = 1.84 \quad ; \quad \overline{LF_1} = \frac{3063 - 415.60 - 184.24}{1163.58} = 2.12$$

The bias factors for member capacity (expressed in terms of the load factor by which the characteristic value of the railway load has to be multiplied to reach the relevant member capacity) are obtained from:

$$\lambda_{LF} = \frac{\overline{LF_1}}{LF_1} \tag{8.12}$$

Thus, the following bias values are obtained for the original bridge and deteriorated bridge respectively:

$$\lambda_{LF} = \frac{4.45}{3.92} = 1.135 \quad ; \quad \lambda_{LF} = \frac{2.12}{1.85} = 1.152$$

The coefficients of variation of the member capacity are obtained from:

$$V_{LF} = \frac{\sqrt{\sigma^2_{M_R} + \sigma^2_{M_{Gs}} + \sigma^2_{M_{Ga}}}}{M_{Qk} \cdot \overline{LF_1}} \tag{8.13}$$

where M_{Qk} is the characteristic value of the bending moment due to the railway traffic loads without impact; σ_{M_R} is the standard deviation of the bending capacity of the analysed section; $\sigma_{M_{Gs}}$ is the standard deviation of the bending moment due to the self weight of the structure; $\sigma_{M_{Ga}}$ is the standard deviation of the bending moment due to additional dead loads and $\overline{LF_1}$ is mean value of the member capacity.

Considering the statistics of member resistances listed in Table 8.6, as well as the mean values of the self weigh and other dead load effects as defined in Table 8.2 and their corresponding coefficients of variation extracted from Table 8.1, the coefficient of variation for the load capacity of the original bridge is given as:

$$V_{LF} = \frac{\sqrt{(5772 \cdot 0.10)^2 + (415.60 \cdot 0.08)^2 + (184.24 \cdot 0.10)^2}}{1163.56 \cdot 4.45} = 0.112$$

and for the deteriorated bridge.

$$V_{LF} = \frac{\sqrt{(3063 \cdot 0.10)^2 + (415.60 \cdot 0.08)^2 + (184.24 \cdot 0.10)^2}}{1163.56 \cdot 2.12} = 0.125$$

The member reliability index is calculated assuming the normal distribution model from:

$$\beta_{memb} = \frac{\overline{LF_1} - \overline{LL_{TRAIN}}}{\sqrt{\sigma_{LF}^2 + \sigma_{LL}^2}} \tag{8.14}$$

where $\overline{LF_1}$ is the mean value of the load factor that will cause the first member failure in the bridge assuming elastic analysis. $\overline{LL_{TRAIN}}$ is the mean value of the load factor describing the maximum expected lifetime live load including dynamic allowance effect. σ_{LF} is the standard deviation of LF_1 while σ_{LL} is the standard deviation of the maximum expected live load LL_{TRAIN}.

The calculations are performed considering the mean value of the member capacity defined by Equation 8.11, the coefficient of variation of the member capacity as defined by Equation 8.13, the mean value of the maximum expected lifetime live load as the product of the impact factor (see Table 8.1) and the live load bias factor (the factor equal to 0.82 relating characteristic value of the railway traffic load effects to the mean value of the railway traffic load effects as presented in Table 8.2). The coefficient of variation for the live load with impact is calculated to be equal to 0.14. This value is the effect of the multiplication of the railway load with a coefficient of variation equal to 10% by the impact factor with a coefficient of variation equal to 50%. The following equations show the results of the calculations for the original bridge:

$$\beta_{memb} = \frac{4.45 - 1 \cdot 1.25 \cdot 0.82}{\sqrt{(4.45 \cdot 0.112)^2 + (1 \cdot 1.25 \cdot 0.82 \cdot 0.14)^2}} = \frac{3.425}{0.518} = 6.61$$

For the deteriorated bridge the member reliability index becomes:

$$\beta_{memb} = \frac{2.12 - 1 \cdot 1.25 \cdot 0.82}{\sqrt{(2.12 \cdot 0.125)^2 + (1 \cdot 1.25 \cdot 0.82 \cdot 0.14)^2}} = \frac{1.095}{0.301} = 3.64$$

To perform the calculations of the system reliability index for the ultimate, functionality and damaged condition limit state, the following assumptions are made: 1) the mean value of the load factors for the ultimate LF_u, functionality LF_f and damaged condition LF_d limit states are assumed to have a bias factor equal to that obtained for the load factor describing the member capacity LF_1. 2) the coefficients of variation of the system's load factors are also assumed to be equal to the coefficient of variation obtained for the load factor describing the member capacity. Thus, the system reliability index for the serviceability limit state (defined as the allowable deformation equal to span lenght/500) is calculated assuming normally distributed variables:

$$\beta_{func} = \frac{\overline{LF_f} - \overline{LL_{TRAIN}}}{\sqrt{\sigma_{LF}^2 + \sigma_{LL}^2}} \tag{8.15}$$

where $\overline{LF_f}$ is the mean value of the load factor corresponding to the load level for which the deformation of the mid-span section reach the limit defined as span lenght/500=0.027m. The remaining parameters are the same as those in Equation 8.14. The reliability index for the functionality limit state obtained for the original bridge is given as:

$$\beta_{func} = \frac{1.135 \cdot 3.92 - 1 \cdot 1.25 \cdot 0.82}{\sqrt{(1.135 \cdot 3.92 \cdot 0.112)^2 + (1 \cdot 1.25 \cdot 0.82 \cdot 0.14)^2}} = \frac{3.424}{0.519} = 6.60$$

The deteriorated bridge's reliability index for the functionality limit state becomes:

$$\beta_{func} = \frac{1.152 \cdot 2.85 - 1 \cdot 1.25 \cdot 0.82}{\sqrt{(1.152 \cdot 2.85 \cdot 0.125)^2 + (1 \cdot 1.25 \cdot 0.82 \cdot 0.14)^2}} = \frac{2.258}{0.435} = 5.19$$

The system reliability index for the ultimate limit state is calculated according to the expression:

$$\beta_{ult} = \frac{\overline{LF_u} - \overline{LL_{TRAIN}}}{\sqrt{\sigma_{LF}^2 + \sigma_{LL}^2}} \tag{8.16}$$

where $\overline{LF_u}$ is the mean value of the load factor corresponding to the ultimate limit state. Considering the characteristic value of the load factor LF_u from Table 8.4, the reliability indices for the ultimate limit state are calculated for the original and deteriorated bridge as:

$$\beta_{ult} = \frac{1.135 \cdot 5.80 - 1 \cdot 1.25 \cdot 0.82}{\sqrt{(1.135 \cdot 5.80 \cdot 0.112)^2 + (1 \cdot 1.25 \cdot 0.82 \cdot 0.14)^2}} = \frac{5.558}{0.751} = 7.40$$

$$\beta_{ult} = \frac{1.152 \cdot 3.43 - 1 \cdot 1.25 \cdot 0.82}{\sqrt{(1.152 \cdot 3.43 \cdot 0.125)^2 + (1 \cdot 1.25 \cdot 0.82 \cdot 0.14)^2}} = \frac{2.926}{0.514} = 5.69$$

The system reliability index for the damage condition limit state is calculated using the equation:

$$\beta_{dam} = \frac{\overline{LF_d} - \overline{LL_{TRAIN}}}{\sqrt{\sigma_{LF}^2 + \sigma_{LL}^2}} \tag{8.17}$$

where $\overline{LF_d}$ is the mean value of the load factor corresponding to the damage condition limit state. Considering the characteristic value of the load factor LF_d given in Table 8.4, the reliability indices for the damage condition limit state were determined as follows for the original and deteriorated bridges:

$$\beta_{dam} = \frac{1.135 \cdot 1.66 - 1 \cdot 1.25 \cdot 0.82}{\sqrt{(1.135 \cdot 1.66 \cdot 0.112)^2 + (1 \cdot 1.25 \cdot 0.82 \cdot 0.14)^2}} = \frac{0.859}{0.225} = 3.37$$

$$\beta_{dam} = \frac{1.152 \cdot 1.26 - 1 \cdot 1.25 \cdot 0.82}{\sqrt{(1.152 \cdot 1.26 \cdot 0.125)^2 + (1 \cdot 1.25 \cdot 0.82 \cdot 0.14)^2}} = \frac{0.427}{0.231} = 1.85$$

All the calculated reliability indices are higher than the target values defined in previous chapter. Thus, the structure can be considered to be safe.

To check the level of inherent redundancy of the bridge, the relative reliability indices are calculated as:

$$\Delta\beta_{func} = \beta_{func} - \beta_{memb} \tag{8.18}$$

$$\Delta\beta_{ult} = \beta_{ult} - \beta_{memb} \tag{8.19}$$

$$\Delta\beta_{dam} = \beta_{dam} - \beta_{memb} \tag{8.20}$$

The values obtained in the calculations for the 'intact bridge' and for the 'damaged bridge' respectively are:

$$\Delta\beta_{func} = 6.60 - 6.61 = -0.01$$
$$\Delta\beta_{ult} = 7.40 - 6.61 = 0.79$$
$$\Delta\beta_{dam} = 3.37 - 6.61 = -3.24$$

$$\Delta\beta_{func} = 5.19 - 3.64 = 1.55$$
$$\Delta\beta_{ult} = 5.69 - 3.64 = 2.05$$
$$\Delta\beta_{dam} = 1.85 - 3.64 = -1.79$$

Comparing the relative reliability indices with the target values presented in previous chapter it is concluded, that the bridge in its original condition is not sufficiently redundant. However it is considered to be safe due to the fact that the member safety is high. For the deteriorated condition the redundancy is already sufficiently high allowing to consider the bridge safe even though the member safety is violated.

Method of Sobrino and Casas. The reliability assessment of the 'Brunna Bridge' for both condition states (original and deteriorated) is also performed using the simplified probabilistic non-linear analysis method of Sobrino and Casas. The safety of the bridge's continuous main girder is evaluated by means of the reliability index β. According to the procedure presented in previous chapter in this method the limit state function is defined by Equation 7.33 which in the cases under analysis can be rewritten as follows:

$$g(X) = M_R^2 - \frac{M_{nla}^2}{\frac{M_{nla}^1 + M_{nla}^3}{2} + M_{nla}^2}(M_{Gs}^e + M_{Ga}^e + I \cdot M_Q^e) \quad (8.21)$$

where M_{nla}^1, M_{nla}^3 and M_{nla}^2 are the bending moments at failure obtained due to the non-linear analysis for the sections over the supports and at mid-span (analysed section) respectively, for the first span of the bridge, M_{Gs}^e is the bending moment due to self weight calculated for the equivalent simply supported beam (span length equal to 13.5 m), M_{Ga}^e is the bending moment due to additional dead loads calculated for the equivalent simply supported beam, M_Q^e is the maximum bending moment due to traffic loads calculated also for the equivalent simply supported beam and I is the impact factor.

The reliability analysis is executed using FORM, which requires the complete statistical information about all the random variables. In this case the distribution types and statistical parameters of the impact factor are considered as defined in Table 8.1. The mean value of the load effect in the equivalent simply supported beam is obtained from Table 8.3. The distribution types and coefficient of variations of the load effects are considered equal to those of the corresponding loads (see Table 8.1). The statistical definition of the member capacity is considered as defined in Table 8.6. The mean values of the bending moments at failure for the section over the piers and in the mid-span are considered as presented in Table 8.5. The distribution types for the bending moments at failure are assumed to be normal and the coefficient of variation are taken equal to the coefficient of variation of the moment capacity of the corresponding sections presented in Table 8.6.

For the defined limit state function the reliability indices obtained using FORM are found to be β=6.61 and β=4.67 for original bridge and deteriorated bridge respectively. The FORM analysis was performed assuming statistical independence between all the variables. When the correlation between the bending moment at failure in the mid-span section M_{nla}^2 and moment capacity of the mid-span section M_R^2 was assumed, the reliability index increases to β=7.16 and β=9.21 for the correlation coefficients C=0.5 and C=0.99 respectively when analysing the original bridge. When analysing the deteriorated bridge, the reliability index increases to the values β=5.28 and β=6.84 for the correlation coefficient C=0.5 and C=0.99 respectively. The effect of the statistical correlation between these two variables was studied due to the significant likelihood of their mutual dependency since they essentially represent the moments at the same section.

Due to the fact that the calculated values of the reliability index β are higher than the target values defined in previous chapter, the structure can be rated as safe. Comparing the calculated reliability indices with the values obtained from the Latin Hypercube Method (β=9.65 and β=6.48 for the original bridge and deteriorated bridge) or from the Response Surface Method (β=7.37 and β=6.17) it can be concluded that this method is also sufficiently accurate.

8.9 Analysis of results

The safety assessment of this bridge performed using several member level and system level assessment methods shows that the 'Brunna Bridge' is sufficiently safe (see Table 8.8). This is found to be true for both the original (as constructed) and the deteriorated conditions. The latter assumes that 50% of the mid-span reinforcement has corroded which would have meant that the bridge would have failed the standard safety check using code-specified partial safety factors and linear elastic analysis.

Table 8.8: Results of the assessment of the 'Brunna Bridge'.

	Safety format	Result of the safety assessment	
		Original bridge	Deterior. bridge
Member	Partial safety factor method	safe	unsafe
	Fully probabilistic method	β=6.61	β=3.64
	Mean load method	β=6.61	β=3.64
System	Bounds method	$6.61 \leq \beta \leq 10.00$	$3.61 \leq \beta \leq 9.07$
	Redundancy factor method	safe	safe
	Latin Hypercube method	β=9.65	β=6.48
	Response Surface method	β=7.37	β=6.17
	Ghosn and Moses method	β=7.40	β=5.69
	Sobrino and Casas method	β=6.61 (7.16$^{(a)}$;9.21$^{(b)}$)	β=4.67 (5.28$^{(a)}$;6.84$^{(b)}$)

Note:$^{(a)}$,$^{(b)}$ for correlations between M^2_{nla} and M^2_R C=0.5 and C=0.99 respectively.

As presented in Table 8.8 the fully probabilistic analysis at the member level leads to the reliability indices β=6.61 and β=3.64 for original and deteriorated bridge respectively. Comparing that values with the target values defined in legal codes and guidelines and presented in previous chapter it may be concluded that the bridge could be considered as safe. However, the safety index β obtained for deteriorated bridge is close to the limits defined by some more liberal recommendations and even below the limits defined by more conservative codes. The fact that the reliability index obtained using FORM is close to the target value and at the same time the member safety check using partial safety factor method fails significantly, shows that the partial safety factors in the Eurocode are rather calibrated for highway than for railway bridges. The coefficient of variation of the traffic load is significantly smaller for railway traffic than for highway traffic, this leads to the higher safety of railway bridges when considering the same partial safety factor in the checking equation.

Comparing the results, showed in Table 8.8, of the simplified probabilistic assessment performed using Mean Load method with results obtained using fully probabilistic format it can be observed that the reliability indices found by both methods are exactly the same. This happens due to the fact that all the variables describing limit state function are considered to be normally distributed and the limit state function is linear. In other situation, when some of the variables are not normal or/and the limit state function is non-linear the reliability indices would be different and those obtained by fully probabilistic method would be more rigorous.

Regarding the results of the assessment of the bridge at the system level, resumed also in Table 8.8, the upper bound estimates of the reliability indices β obtained for the bridge system due to a plastic probabilistic analysis using Bounds Method are found to be equal to 10.0 and 9.07 for the original and deteriorated bridge respectively. The reliability indices calculated for the member considering elastic analysis (the lower bound estimates) are equal to 6.61 and 3.64. The difference between the reliability indices from plastic analysis compared to those from elastic analysis demonstrate the large reserve strength provided by the system even for the case when large levels of deterioration are observed in critical bridge members. Observe that despite the very large decrease in the member reliability index due to member deterioration, the corresponding decrease in the upper bound estimate of the system reliability index is much less pronounced. This is due to the ability of the system to redistribute the load from the deteriorated member to the other intact members.

Similar observations can be made analysing results of the assessment performed using Redundancy Factor method. The values of the redundancy factors obtained are equal to 1,34 and 1,02 for the original and deteriorated bridge respectively. For both condition states, the redundancy factor is greater than 1, which means that the structure is safe from the system point of view even though the member check fails for the case of the deteriorated bridge.

Regarding fully probabilistic formats for system level assessment, the results in Table 8.8 show that the reliability index values obtained from the Response Surface Method (RSM) and the Latin Hypercube Simulation (LHS) are somewhat different. This lack of conformity can be explained by the fact, that the Latin Hypercube Method is not sufficiently accurate for such high reliability levels. In the case of LHM the reliability index is calculated based on the results of sampling performed in the region relatively close to the mean values of all the variables. However, for high reliability levels such as those observed in this analysis, the design point (failure region) is located far away from the region of mean values and the sampling performed there may not describe the failure region appropriately. In the case of the Response Surface Method used in this study, sampling is performed iteratively close to the design point (failure region). Due to the iterative procedure, the polynomial function determined by the regression analysis gives a fairly accurate representation of the tangent to the failure surface near the most likely failure point and the reliability index obtained by means of this method is more exact. It is noted however, that the analysis performed using the RSM was designed to concentrate on the ultimate moment capacity and ignore other numerically possible failure modes. Specifically, in certain cases of the numerical analysis (certain iterations), it was found that the cracking capacity may be higher than the ultimate capacity (capacity prior to failure). But, in order to guarantee convergence to the same mode observed in the other methods (both approximate and the LHS) the results of the non-linear analysis corresponding to ultimate capacity were considered for definition of the Response Surface rather than at results corresponding to the maximum capacity (which in some cases would be cracking capacity). On the other hand, the cracking capacity of the reinforced concrete bridge is normally not critical as it is usually reached in service condition states without necessarily affecting the bridge's overall safety and when analysing ultimate states the bridge should be assumed to have already cracked. It is also noted that during the RSM analysis, all the variables are considered to follow Normal distributions including those related to the concrete strength and yielding stress of steel. This assumption probably led to smaller values of the design point coordinates corresponding to steel yielding and concrete compressive strengths that would have been obtained if Lognormal distributions are assumed as usually recommended. Normal distributions for all the variables were assumed in order to compare results of analysis with the simplified methods. The consideration of normal distribution for resistance of steel and concrete does not affect significantly the results of LHM due to the fact that sampling is performed near the mean value, where both distribution functions are nearly the same. However, in the case of the RSM, the iterative algorithm is executed at the coordinates of the design point where for very high reliability levels the difference between the Normal and Lognormal results may be significant.

In the case of the deteriorated bridge, the reliability level is significantly lower compared to the original bridge and the reliability index obtained by the LHM and RSM are closer than those of the intact bridge.

The reliability index values calculated using the simplified method of Ghosn and Moses is generally lower than that obtained from the more advanced methods (except for the results obtained by RSM for the original bridge where the results are very close). This occurs because the simplified method of Ghosn and Moses implicitly assumes full correlation between all the members' strengths and that the COV's of the system is equal to the COV of the most critical member. On the other hand, although the fully probabilistic non-linear analysis approaches (RSM and LHS) lead to some level of correlation between the member strengths since the basic parameters that control each member's strength are the same (see Table 8.1), the various sizes, shapes and reinforcing details of each member would lead to slightly lower correlations in the member strengths, leading to slightly higher overall system reliability levels. Furthermore, the simplified reliability analysis of Ghosn and Moses assumes that the overall COV is the same as that of the most critical member. This assumption would lead to a higher overall COV than the one obtained from the fully-probabilistic non-linear system analysis. The justification for using the higher COV in the Ghosn and Moses method is that the uncertainties in the modelling of the non-linear system effects must be at least as high as those for the modelling of the individual member effects. It is well known that the non-linear finite element analysis of structural systems is not exactly accurate due to difficulties in modelling the material behaviour at high loads as well as the variations in the bridge boundary conditions and secondary member effects. Thus, the method of Ghosn and Moses is generally more conservative than the more exact simulation methods when the latter do not explicitly consider the modelling uncertainties associated with the reliability analysis of the structural system.

In the case of the Sobrino and Casas method, the reliability index calculated assuming no correlation between the bending moment at failure in the mid-span section M^2_{nla} and moment capacity of the mid-span section M^2_R, is significantly lower than that obtained from the more advanced methods. When assuming partial correlation between these two parameters the reliability index obtained is closer to the exact values. It is herein recommended to include, a partial correlation between the bending moment at failure in the mid-span section M^2_{nla} and the moment capacity of the mid-span section M^2_R since the response of the same section at ultimate and the response very close to ultimate are expected to be correlated. Notwithstanding the above-mentioned observations, the results of Table 8.8 show that the reliability indices for both the original and deteriorated condition states obtained applying the simplified probabilistic non-linear methods are sufficiently high and very similar to those calculated by means of the full probabilistic non-linear analysis. Due to the fact that the simplified probabilistic non-linear analyses require considerably lower computational effort than the fully probabilistic methods while providing sufficient accuracy, they seem to be adequate methods for wider use in bridge assessment practice when bridge redundancy and structural system reserve strengths are important factors that contribute to overall bridge safety.

8.10 Conclusions drawn from the analysis

The detailed safety analysis, performed using several safety formats discussed previously, shows how a bridge that would have been rated as deficient using traditional semi-probabilistic member safety analysis methods may in actuality have extremely high system reliability levels thus eliminating the need for its replacement or rehabilitation. This is due to the ability of the bridge system to redistribute the load from the weak member to the other stronger members. This is a significant structural property that should reinforce the importance of performing the safety assessment of bridges at the system level in order to take full advantage of the redundancy of the bridge. Furthermore, even neglecting bridge redundancy but performing probabilistic analysis and thus considering real variabilities of all the parameters affecting bridge member capacity may be sufficient to proof required bridge safety.

The various approaches illustrated in previous sections vary in the level of complexity. However, the example shows how the simplified probabilistic methods for the safety assessment at the member level (Mean Load method), and the system level (method of Ghosn and Moses and method of Sobrino and Casas) are sufficiently accurate while only requiring a basic level of knowledge of structural reliability techniques. Furthermore, the Redundancy Factor method also seems to be an adequate and efficient technique for the safety assessment of existing bridges especially when the evaluator is not familiar with the reliability theory.

Chapter 9

Case studies

9.1 Introduction

In this chapter two examples that demonstrate how practically perform the assessment of existing concrete bridges are presented. The first example shows how to assess a bridge using the 'step-level' methodology proposed in Section 2.4. During this 'step-level' assessment several relatively simple safety formats, discussed in Chapters 7 and 8, are applied. Some models of bridge traffic loads and models of shear and bending resistance, presented respectively in Chapters 5 and 6, are also used. Furthermore, the effects of applying more adequate model of bridge traffic loads in the assessment are analysed. The bridge analysed in this example is a one span simply supported precast prestressed concrete I girder bridge.

The second example illustrates how to perform the assessment of a bridge using the most advanced assessment methodology based on probabilistic non-linear analysis. In this analysis the probabilistic models of loads, material properties and bridge geometry, presented in Chapters 4 and 5, are applied. Besides the assessment of the ultimate limit states, the assessment of serviceability limit states is performed. The serviceability assessment is not the subject of this thesis, however, it is performed to show the potentials of the probabilistic methods in the assessment of other limit states than ultimate. The bridge analysed in this example is a continuous two span concrete overpass constructed from precast prestressed U shape girders.

9.2 Assessment of the 'Barrela Bridge'

9.2.1 General information

The 'Barrela Bridge' is a 14 m long bridge located in 'Santa Maria da Feira', north of Portugal. The bridge deck is nearly 10 m wide and is supporting two traffic lines, 3.5 m each, and two 1.49 m wide sidewalks. The bridge is located within the local road and is carrying the two directions traffic characteristic for the suburbs of the mid-size town.

The bridge has been constructed in 2003 and it has been designed according to Portuguese codes RSA (1983) and REBAP (1985) for the 'vehicle class I'. Generally, the bridge is in a very good condition and does not require any intervention. However, it has been selected for this study to check if it can carry the traffic loads defined in EC-1b (2002). The verification is performed just for the critical sections of the main girders.

9.2.2 Geometry and material data

The 'Barrela Bridge' is a simple supported structure with a span of 13.3 m. The cross-section of the deck comprises five precast prestressed I shape 0.75 m deep beams spaced by 2.28 m and cast-in-place 0.20 m thick reinforced concrete slab supported during concreting by 0.05 m thick precast concrete panels. The basic dimensions of the bridge are presented in Figures 9.1 and 9.2.

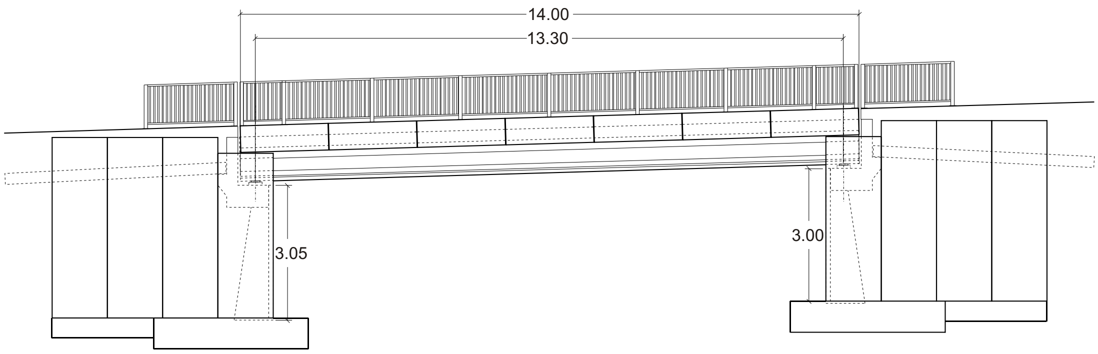

Figure 9.1: Side view of the 'Barrela Bridge'.

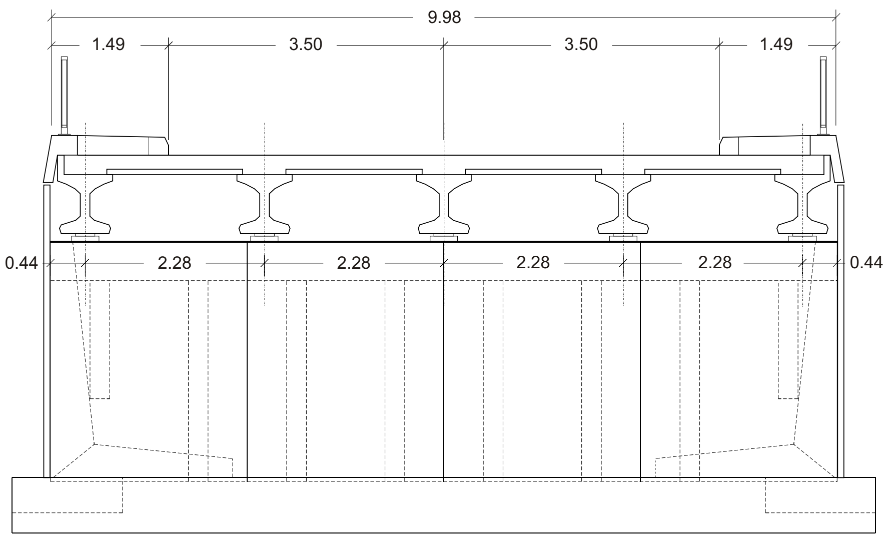

Figure 9.2: Cross-section of the 'Barrela Bridge'.

The materials used for girders fabrication and construction of cast-in-place element are as follows: concrete of precast girders - C45/55, concrete of cast-in-place elements - C25/30, reinforcing steel - S500, prestressing steel - S1680/1860.

The prestressing of the precast girders is composed of 10 strands 0.6" at the bottom flange of the girder. The longitudinal mild reinforcement of the girders comprises of 14 bars $\phi10$ and has just constructional character. The transverse reinforcement comprises of closed stirrups with diameters varying along the girder length ($\phi16$ - 0.7 m, $\phi12$ - 2.0 m, $\phi10$ - 2.2 m and $\phi8$ on remaining length). The stirrups are spaced by 0.20 m besides the girders ends (0.70 m lenght) where they are spaced by 0.05 m to help in transferring prestressing force. The reinforcement of the concrete slab in the longitudinal direction, parallel to the girders axes, is composed of $\phi8$ bars spaced by 0.25m. In transverse direction, the slab is reinforced with $\phi16$ bars spaced by 0.20 m.

9.2.3 Safety assessment

The safety assessment of the bridge is performed according to the 'step-level' procedure proposed in Section 2.4. The critical sections of the bridge most loaded girder, selected for the evaluation, are the mid-span section in bending and the section near the support (1.0 m from the axis of the support) in shear.

Loads considered in the assessment. The bridge permanent loads have been determined based on the bridge geometry and the characteristic densities of the construction materials. The bridge geometry has been assumed according to the construction drawings. The values of the permanent loads considered in the assessment are listed bellow:

- Self weight of the beam - 6.295 kN/m
- Self weight of the slab - 6.250 kN/m^2
- Asphalt wearing surface - 1.6 kN/m^2
- Parapet, railing, sidewalk - 7.5 kN/m^2

From bridge variable loads, just that due to vehicular traffic are considered in the assessment. The traffic load are assumed according to EC-1b (2002). The characteristic values of the load intensities are as follows (for details see Section 5.4.3):

- Lane 1 - 9 kN/m^2 and two axles 300 kN each
- Lane 2 - 2.5 kN/m^2 and two axles 200 kN each

1-st level assessment. In the first step the assessment of the bridge is performed using strength and load models as defined in codes EC-1b (2002), EC-2 (2004) and EC-2b (2003). Simplified calculation models are used and the safety is checked using partial safety factors method and the partial factors as defined in EC-0 (2002), EC-2 (2004) and EC-2b (2003).

Performing simple calculation it can be determined that the maximum bending moment in the most loaded girder (the second girder from the bridge edge) due to permanent loads is equal to 535 kNm. The maximum shear force in the critical section (1.0 m from the axis of the support) of the same girder is 149 kN. These values has been obtained considering that the girder carry just the loads directly applied on it (2.28 m wide area of the top flange).

The maximum bending moment in the analysed girder due to traffic loads is equal to 1537 kNm. The maximum shear force in the critical section of this girder is 436 kN. These values has been obtained considering that all traffic load is distributed just to three girders directly supporting carriageway in the proportion 40%, 30% and 30%.

The characteristic resistance of the mid-span section in bending, determined using the simplest model (strands capacity times lever arm) is 2125 kNm. The characteristic shear resistance of the critical section determined according to EC-2 (2004) formula is 846 kN. The shear resistance has been calculated assuming the inclination of concrete struts equal to 30 degree (this inclination is usual for prestressed elements). If the effect of prestress was neglected (the inclination of struts 45 degree) the characteristic resistance of the section would be 488 kN. Both values of the section capacity has been obtained using simplified models of steel and concrete behaviour (elasto-plastic).

The assessment is performed using the checking Equation 7.4 defined in Section 7.3.2. Using the partial safety factors defined in the Annex A2 (for bridges) of EC-1b (2002) and the load effects and the section capacities as presented above, the checking equations for the bending verification takes the following form:

$$\frac{2125}{1.15} \gtreqless 1.35 \cdot 535 + 1.35 \cdot 1537$$

which after performing the calculations leads to the following inequality:

$$1848 \ngeq 2797 \text{ [kNm]}$$

Performing the same calculation for shear, the following inequality is obtained:

$$\frac{846}{1.15} \gtreqless 1.35 \cdot 149 + 1.35 \cdot 436$$

which simplifies to:

$$736 \ngeq 790 \text{ [kN]}$$

As it can be seen, using the simplest models for the determination of load effects and the resistance, and using partial safety factors specified in the Eurocode, the bridge fails the evaluation. Therefore, the bridge has to be reassessed using more refined methods. The partial factor for the resistance has been considered equal to 1.15 due to the fact that the steel is the parameter governing the capacity (for both cases, shear and bending).

2-nd level assessment. In the second step more accurate models are used to calculate section resistances. The redistribution of load to the girders is obtained from the finite element model. The material parameters, load model and the assessment methodology remain the same.

Performing structural analysis using finite element method and the grillage type model of the bridge, the following values of the internal forces in the critical sections have been obtained: the maximum bending moment in the most loaded girder (the second girder from the bridge edge) due to permanent loads - 572 kNm; the maximum shear force in the critical section (1.0 m from the axis of the support) of the same girder - 147 kN; the maximum bending moment due to traffic loads - 1347 kNm; the maximum shear force in the critical section of this girder - 439 kN.

The characteristic resistance of the mid-span section in bending calculated using non-linear sectional analysis software 'Seccao' (Henriques, 2002) is 2438 kNm. The characteristic shear resistance of the critical section determined using Modified Compression Field Theory (Vecchio & Collins, 1986) and the software 'Response 2000' (Bentz, 2000) is 1027 kN. These values of ultimate capacity are obtained considering stress-strain relationships for steel and concrete similar to these presented in Figures 6.7 and 6.8.

Performing assessment using the same methodology as previously, the following form of the checking equations for the bending verification can be obtained:

$$\frac{2438}{1.15} \gtreqless 1.35 \cdot 572 + 1.35 \cdot 1347$$

which after performing the calculations leads to the following inequality:

$$2120 \ngeq 2591 \text{ [kNm]}$$

Performing calculation for shear, the following inequality is obtained:

$$\frac{1027}{1.15} \gtreqless 1.35 \cdot 147 + 1.35 \cdot 439$$

which simplifies to:

$$893 > 791 \text{ [kN]}$$

As it can be seen, using more advanced resistance models and more accurate structural analysis method it can be proved that the shear capacity of the girder is sufficient to carry current traffic loads (Eurocode LM1 model) which are higher than those for which the bridge has been designed (RSA vehicle). Nevertheless, the bridge still fails the bending assessment. Therefore, the next level assessment has to be performed.

3-rd level assessment. In the third level of assessment, the material properties and loads can be updated on the basis of tests and observations. In the analysed case, due to the lack of test data, the material properties are considered as in previous steps. However, based on the observation, the traffic loads are considered to have lower intensity than previously assumed. The calculation models and assessment methodology remain the same as in the second level of assessment.

In the previous levels of assessment the traffic load intensity has been assumed according to EC-1b (2002) without taking into account the characteristics of real traffic in the bridge location. As it has been already discussed in Section 5.4.3, the traffic load model LM1 defined in EC-1b (2002) allows for using the adjustment factors α that take into account traffic characteristics in the specific countries and should be specified on the national level. Unfortunately, the national factors are so far not defined in Portugal. Nevertheless, EC-1b (2002) recommends the minimum value of this factor as 0.8. Furthermore, EC-1b (2002) says that the basic intensity of load in the traffic load model LM1 corresponds to heavy industrial traffic. For more common traffic on usual highways and motorways it recommends a moderate reduction (10 to 20%) of α factors applied to tandem system and the uniformly distributed loads on Lane 1. Considering the fact that the 'Barrela Bridge' is located within the local road, characterized by rather limited traffic of heavy vehicles, the reduction of 20% of load intensity on the Lane 1 seems to be reasonable.

Performing structural analysis using finite element method and the grillage type model of the bridge, and considering reduced intensity of traffic loads as explained above, the following values of the internal forces in the critical sections have been obtained: the maximum bending moment in the most loaded girder (the second girder from the bridge edge) due to traffic loads - 1076 kNm; the maximum shear force in the critical section of this girder - 341 kN.

Performing assessment using the same safety format as in previous step, the following form of the checking equations for the bending verification can be obtained:

$$\frac{2438}{1.15} \gtreqless 1.35 \cdot 572 + 1.35 \cdot 1076$$

which simplifies to:

$$2120 \ngeq 2225 \text{ [kNm]}$$

As it can be seen, the reduction of the traffic load intensity do not change the assessment results sufficiently and the bridge still fails the bending capacity evaluation. Thus, the next level assessment has to be performed.

Considering the fact, that the shear capacity of the bridge girders, in the previous assessment step, has been proved to be sufficient, the shear verification in this assessment level is already unnecessary. However, it is also performed to show the differences in the evaluation on different levels of assessment.

$$\frac{1027}{1.15} \gtreqless 1.35 \cdot 147 + 1.35 \cdot 341$$

$$893 > 659 \text{ [kN]}$$

4-th level assessment. In this assessment level the modified partial safety factors are used. The modified factors take into account bridge redundancy and the fact that the main girders of the bridge (precast prestressed I beams) are executed with enhanced quality (factory made members). The strength, the load and the calculation models remain the same as in the previous assessment level. Furthermore, the general assessment methodology remains also the same (just the partial factors are adjusted).

According to information presented in Table 7.8, the partial safety factors for permanent loads of factory made members executed with enhanced quality can be considered as 1.22 (in the analysed case reduced factor applies just to the part of permanent load corresponding to the self weight of I beam). Furthermore, according to the information presented in Table 7.9 and using linear interpolation, the redundancy factor (see Equation 7.8) for bending verification of bridge member at the ultimate limit state can be considered equal to 1.05 (for shear the redundancy factor is 1.0). This value corresponds to simple supported bridge deck composed of 5 I girders spaced by 2.28 m.

Performing assessment using above discussed adjustment in the safety format, the following form of the checking equations for the bending verification can be obtained:

$$1.05 \cdot \frac{2438}{1.15} \gtreqless 1.22 \cdot 139 + 1.35 \cdot 433 + 1.35 \cdot 1076$$

which after performing the calculations leads to the following inequality:

$$2226 > 2207 \text{ [kNm]}$$

As it can be seen, the adjustment in the safety factor for permanent load (due to self weight of the factory made members) and the consideration of the bridge redundancy factor allow to prove that the bridge is safe for considered level of traffic loads. The factored bending moments applied to the member are smaller than the factored bending capacity of the member.

The shear safety has already been proved in the second level of assessment. However, the calculations are also presented for this level in order to show the differences in the results that may come from using different safety factors.

$$1.00 \cdot \frac{1027}{1.15} \gtreqless 1.22 \cdot 39 + 1.35 \cdot 108 + 1.35 \cdot 341$$

$$893 > 654 \text{ [kN]}$$

5-th level assessment. Besides the fact that the bridge 'Ponte de Berrela' has already proved to be sufficiently safe to carry the actual traffic loads, in this section it is evaluated using most advanced assessment method in order to show its advantages.

In this level of assessment the safety of the bridge is checked using probabilistic methods. From several available probabilistic methods of assessment, described in Section 7.3, the Mean Load Method is selected to be used in this case as the simplest and sufficiently accurate for practical applications. In the Mean Load Method the checking equation is defined by the inequality 7.5. Assuming that all the variables are normally distributed and statistically independent, the reliability index β may be computed using Equation 7.6.

In order to perform analysis using probabilistic methods, all load and resistances variables have to be defined by their probability distribution functions. Table 9.1 resumes the parameters of the distributions for loads and resistances used in the analysed case. The mean value and the coefficient of variation for shear and bending resistance are assumed according to Tables 6.13 and 6.20. The parameters of the distribution corresponding to the effects of permanent loads are assumed according to the information presented in Section 5.3. For the purpose of simplicity, all permanent loads are considered to have the same distribution parameters and the selected relatively high coefficient of variation aims to cover also the model uncertainty. The parameters of the distribution corresponding to the effects of highway traffic loads are calculated assuming that the characteristic load intensities in the load model LM1 defined in EC-1b (2002) correspond to 95-th percentile of the PDF of the traffic load, which is presumed to be normally distributed random variable with coefficient of variation of 15%. This relatively high coefficient of variation for traffic loads aims to cover the variability not just due to load itself but also due to dynamic amplification, girder distribution and load modelling.

Table 9.1: Random variables considered in the analysis.

Random variable	Unit	Char. value	Mean value	COV	PDF
Bending resistance, mid-span, M_R	kNm	2438	2560	0.07	normal
Shear resistance, support, V_R	kN	1027	1212	0.11	normal
Moment - permanent loads, M_G	kNm	572	572	0.10	normal
Shear - permanent loads, V_G	kN	147	147	0.10	normal
Moment - traffic loads, M_Q	kNm	1076	861	0.15	normal
Shear - traffic loads, V_Q	kN	341	273	0.15	normal

Using Equation 7.6 and data from the Table 9.1 the reliability index corresponding to bending failure is obtained as follows:

$$\beta = \frac{2560 - 572 - 861}{\sqrt{(2560 \cdot 0.07)^2 + (572 \cdot 0.10)^2 + (861 \cdot 0.15)^2}} = \frac{1127}{228} = 4.9$$

For shear, the following reliability index is obtained:

$$\beta = \frac{1212 - 147 - 273}{\sqrt{(1212 \cdot 0.11)^2 + (147 \cdot 0.10)^2 + (273 \cdot 0.15)^2}} = \frac{792}{140} = 5.7$$

Comparing the obtained values of the reliability indices with the target values for the member level assessment presented in Section 7.2.5.1 it can be concluded that the safety is verified with considerable high safety margin. It has to be mentioned that the reliability indices obtained correspond to the reference period of 100 years (the reference period characteristic for the LM1 load model from Eurocode) and to the traffic load with reduced intensity on the Lane 1. When the standard load intensity is considered for tandem and uniformly distributed load on the Lane 1, the reliability indices calculated are 3.7 and 5.0 for bending and shear. These values are also sufficiently high to considered the bridge safe. Therefore, even when the bridge would be localized within a highway characterized by high volume of very heavy traffic, in this level of assessment it could be rated as safe regardless the fact that it would fail the assessment on the lower levels.

9.2.4 Real bridge loads and their effects on the assessment

In previous section the assessment of the bridge has been performed considering the traffic load model according to EC-1b (2002) and assuming somehow arbitrary the scatter of the distribution of the load effects produced by this model as 15%. As it has already been discussed, the traffic load model in EC-1b (2002) is representative for the heavy traffic characteristic for busy highways close to the industrial regions and may not be appropriate for the assessment of bridges localized on the roads of minor importance. Even the reduction of the load intensity of the tandem and the distributed load on the Lane 1 by 20% (as suggested in the Eurocode for normal roads) may not be sufficient and will lead to the higher calculated load effects than the actual one. Furthermore, the traffic load model in EC-1b (2002) is expected to produce the load effects that the bridge is going to experience during its lifetime, assumed for the new bridges as 100 years. When assessing the existing bridge the reference period (or projection period) can be significantly reduced for example to 5 or 10 years after which the bridge is going to be inspected and again reassessed.

In this section the load effects in the bridge main members, produced by the traffic loads, are calculated according to one of the models presented in Section 5.4.6. The model of Flint and Neill Partnership (FNP) is selected due to the fact that does not require any additional data about traffic besides traffic intensity and the projection period. The model of Moses and Ghosn, presented also in Section 5.4.6, requires data from Weigh-in-Motion (WIM) measurements, regarding gross vehicle weight and the geometry of the most common truck which may produce the maximum load effects (in this case would be 3 or 4 axles rigid truck). The WIM data are not available for the location of the bridge 'Ponte de Barella'. In such situation, the model of Moses and Ghosn could be used with data presented in Section 5.4.6, which are representative for United States condition. Nevertheless, the results obtained assuming these data might be incorrect basically due to different truck characteristics in United States (comparing to Europe). Therefore, the model of Flint and Neill Partnership is assumed to be a better alternative in the analysed case, even though it is not exactly representative for Portuguese traffic. In the case where WIM data are available for a specific bridge site the model of Moses and Ghosn might be more adequate.

According to the FNP model presented in Section 5.4.6, the load effects in critical sections of bridge main girders, produced by the traffic load moving over the bridge, can be modelled by the probability distribution function which is a product of three variables: M_{Qdet} or V_{Qdet}, G_{dist} and I.

The first variable, M_{Qdet} or V_{Qdet}, is a deterministic variable describing the load effect in the bridge member in question. It can be bending moment or shear obtained due to structural analysis of the bridge (e.g. using FEM) considering the load model similar to that defined in EC-1b (2002) (for details see Section 5.4.6). In the analysed case of the maximum bending moment in the mid-span section of the most loaded girder produced by this load model is equal to 1251 kNm. The maximum shear in the section near the support of the same girder produced by this load model is equal to 424 kN.

The second variable, G_{dist}, is a random variable described by the type I extreme value distribution (Gumbel distribution), defined by Equations 5.8 and 5.9, with the distribution parameters defined in Tables 5.11 and 5.12. In the analysed case of the bridge with 13.3 m span, the distribution parameters have been defined according to Table 5.12 (characteristic for bridges with more than one traffic lane) using linear interpolation and considering the traffic intensity 2000 trucks per day per direction (characteristic for minor roads). The parameters U and α defined for bending are 0.296 and 55 respectively. However, for shear U and α are 0.296 and 57. Above defined parameters U correspond to annual maxima. The distribution parameters U calculated using Equation 5.11 for 100 years projection period are 0.380 and 0.377 for bending and shear respectively.

The third variable, I, is a normally distributed random variable describing the dynamic amplification of the static loads. The distribution parameters for this variable are defined in Table 5.13. In the analysed case, assuming medium/poor quality of the pavement, the mean value of the dynamic amplification factor is equal to 1.13 and the corresponding standard deviation is 0.10.

Performing the reliability analysis using FORM (see Section 3.4) for the below defined limit state functions:

$$g(X) = M_R - M_G - M_{Qdet} G_{dist} I \tag{9.1}$$

$$g(X) = V_R - V_G - V_{Qdet} G_{dist} I \tag{9.2}$$

and assuming the probabilistic models of the variables as defined above (see also Table 9.1), the following results are obtained. For one year reference period, the reliability index β for bending is equal to 7.71 and for shear is 6.80. For the reference period of 100 years the reliability indices β are 7.11 and 6.50. In both cases the reliability indices are higher than the required values defined in Section 7.2.5.1.

Comparing the β values obtained using FNP load model, for the reference period of 100 years, with the results obtained in previous section (5-th level of assessment) it can be concluded that the FNP load model is generally less conservative and gives significantly higher β. Furthermore, due to the fact that the FNP load model assumes higher variability for shear than for bending the index β for shear is lower than for bending. In the analysis performed in the previous section the situation is opposite. Comparing the results obtained in previous section with the results obtained in this section, one have to keep in mind that the results have been obtained considering different distributions for traffic loads

(Normal vs. product of Gumbel and Normal) which makes impossible quantitative comparison of reliability indices β. However, the qualitative comparison is possible.

9.2.5 Conclusions drawn from the assessment

Results presented in the previous sections show that the structure satisfies the ultimate limit states of bending and shear in the critical sections of the main bridge girder. The ultimate limit states are satisfied even though the traffic loads considered in the assessment are significantly higher than the one used to design the bridge. The initial assessment performed using traditional methods gives somehow different results (structure fails the assessment). Nevertheless, more refined analyses applied according to the 'step-level' assessment methodology allow to prove that the structure is able to carry higher loads. The probabilistic assessment performed using specific traffic load model, which is probably more representative for the location of the 'Barrela Bridge' than the EC-1b (2002) load model, shows very high safety margin for both analysed failure scenarios.

9.3 Assessment of the overpass 'PS12'

9.3.1 General information

The 'PS12' is a 50 m long overpass over highway A11 connecting Guimarães and Braga, north of Portugal. The bridge deck is 7.6 m wide and is supporting two traffic lines, 2.5 m each, and two 1.30 m wide sidewalks. The bridge is located within the low importance local road and is carrying mostly light traffic.

The bridge has been constructed in 2002 and it has been designed according to Portuguese codes RSA (1983) and REBAP (1985) for the 'vehicle class I'. Generally, the bridge is in a very good condition and it has been selected for this study just to show the applicability of one of the fully probabilistic safety assessment methods presented in this thesis, namely Monte Carlo simulation technique (see Section 3.4).

The verification is performed for one of the Ultimate Limit State (ULS) and for the Serviceability Limit States (SLS). The Serviceability Limit States are not a subject of this thesis, however, they are assessed in this example to show the potentials of the probabilistic methods in the assessment of other limit states than ultimate. From the Ultimate Limit States just the limit state of bending is selected to be checked in two critical sections of the bridge, mid-span and over-pier. The results showed in the following sections are also presented in Wiśniewski *et al.* (2004d,e,f,g) and Henriques *et al.* (2004).

9.3.2 Geometry and material data

The bridge is composed of two 25 m long spans supported by cast-in-place reinforced concrete pier in the middle of the total length and by elastomer bearings at the abutments. The structure is designed in the final stage as continuous and integral with the pier. The cross-section of the deck is comprised of one precast U shape beam and the slab composed by precast concrete panels and cast-in place topping. The basic dimensions of the described overpass are presented in Figures 9.3 and 9.4.

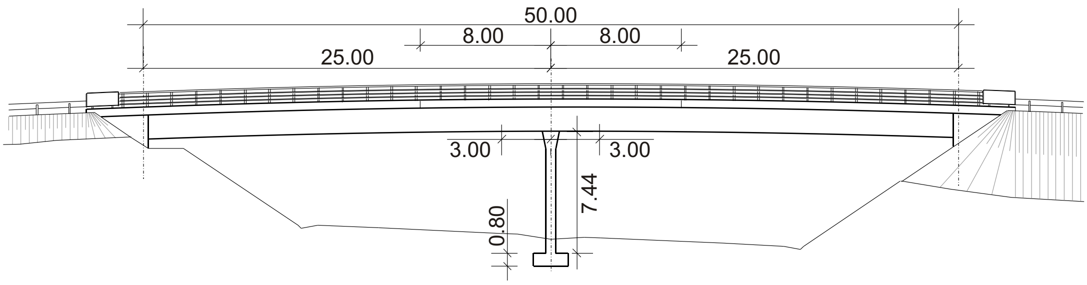

Figure 9.3: Side view of the overpass 'PS12'.

The materials used for girders fabrication and construction of cast-in-place elements are: concrete of precast girders - C60/70, concrete of cast-in-place elements - C30/37, reinforcing steel - S500, prestressing steel - S1680/1860 and S950/1050.

The prestressing of the precast girders is composed of two layers of strands at the bottom slab of the girder and one layer of strands at the top of the girder. The continuity prestress consists of post-tensioning bars between the girders faces over the pier and straight cables at the cast-in-place slab over the pier.

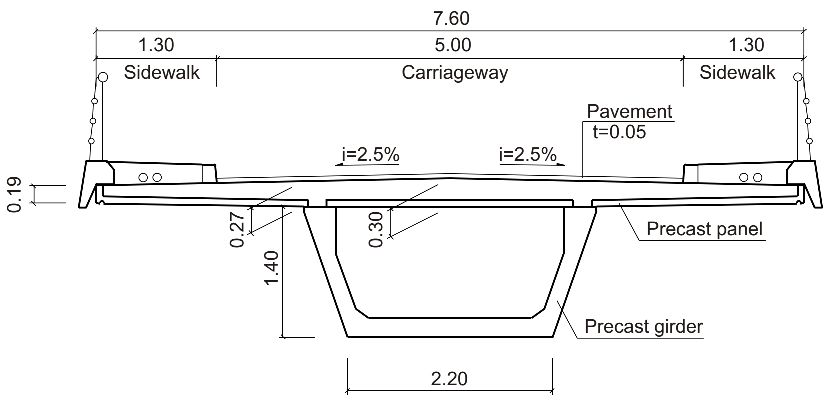

Figure 9.4: Cross-section of the overpass 'PS12'.

The structure was designed as erected in several constructional phases. Since the evolution of the structure has significant influence for the development of stresses in the sections of the structural elements, the construction sequence is described below:

- 3 days - application of prestress to the precast girders;
- 28 days - erection of the girders and precast panels, concreting of the joint girders-pier;
- 29 days - prestressing of the cast joint;
- 30 days - concreting of part of the cast-in-place slab;
- 33 days - application of prestress to the executed slab;
- 34 days - concreting of the remaining part of the cast-in-place slab;
- 42 days - application of additional dead loads (equipment, pavement, etc.).

9.3.3 Numerical model of the structure

The special numerical code 'Plastd90' (Henriques, 1998) is used to model the analysed bridge. The software allows to model constructional phases and considers non-linearity of steel and concrete. Also influence of time dependency of material properties (creep, shrinkage, ageing of concrete and relaxation of prestressing steel) can be taken into account.

The non-linear FEM model consists of 50 beam elements. The elements modelling girder are comprised of 15 layers of concrete and 5 layers of reinforcing steel. The pier is modelled by elements composed by 8 layers of concrete and 2 layers of mild reinforcement. The system of prestress is represented by 9 cable elements. Six of them are modelling three layers of prestressing strands in the precast girders (three cables for each precast girder). Additional three cable elements are representing the continuity post-tensioning bars between the faces of the girders over the pier and the layer of post-tensioning cables in the deck slab over the pier (16 meters).

The boundary conditions are modelled as follows: the connection of the pier with the foundation is considered as fixed, the connection between the girders and the abutments is assumed to be free for rotations and horizontal displacements.

The numerical model described above has been verified against the measured data obtained due to diagnostic load test of the bridge performed by the Structural Division of the University of Minho (Cruz *et al.*, 2003; Wiśniewski *et al.*, 2004b,c). After minor calibration the model gives the results matching very well the values measured on the bridge.

9.3.4 Loads and load combinations

The following loads are considered in the analysis:

- G - self weight of the structure (modelled separately for precast and cast-in-place elements);
- P - prestressing (modelled separately for each layer of strands, bars and cables);
- G_A - additional permanent loads (modelled separately for precast elements, cast-in-place elements and for asphalt wearing surface;
- $Q_{1/2}$ - vehicular traffic load on the notional lines (considered as specified in RSA (1983));

- Q_S - pedestrian traffic load on the sidewalk (considered as specified in RSA (1983));
- $T_{S/W}$ - non-linear gradient of temperature along the height of the deck (considered separately for winter and summer);

The simulations are carried out for several loads combinations, presented in Table 9.2, and for different load configurations. Two diverse traffic load models , 'Vehicle' and 'Knife' (RSA, 1983), are used to assess the stresses in the middle-span section and in the section over the pier. Also two configurations of differential temperature are used, namely for winter and summer.

Table 9.2: Load combinations.

Combination	Identification	Combination factors
ULS - basic	$B1_{S/W}$; $B2_{S/W}$	$G + P + \kappa Q_{1/2} + 0.6Q_S + 0.6T_{S/W}$
SLS - quasi perm.	$QP1_{S/W}$; $QP2_{S/W}$	$G + P + 0.2Q_{1/2} + 0.2Q_S + 0.3T_{S/W}$
SLS - frequent	$F1_{S/W}$; $F2_{S/W}$	$G + P + 0.4Q_{1/2} + 0.2Q_S + 0.3T_{S/W}$
SLS - rare	$R1_{S/W}$; $R2_{S/W}$	$G + P + Q_{1/2} + 0.4Q_S + 0.5T_{S/W}$

Due to huge importance of construction sequence for development of stresses in the structural elements, the loading up to 42-nd day is modelled according to the chronology described in Section 9.3.2. After all constructional stages (equal for all cases) four different load histories are considered. For quasi permanent (QP) combination the QP values of live loads are applied at 70-th day and maintain up to 1000-th day. For frequent (F) combination the QP values of live loads are applied at 70-th day, at 100-th day the live load rise to the F value and it remains constant till 1000-th day. For rare (R) combination the sequence up to 100-th day is equal to F combination. Later in 190-th day the live load rises to rare (R) value and that load level maintain also up to 1000-th day.

For basic (B) combination the sequence is equal up to 1000-th day as for rare combination. Later the live and temperature loads rise to the values defined in Table 9.2 considering κ equal to 1.0. After that the traffic load is increased up to the structure failure (κ factor rise up to the ultimate value). It is assumed that influence of creep and shrinkage after 1000 days is negligible. The κ factor is defined as a safety margin.

9.3.5 Variability of parameters

Trying to reduce the necessary time of simulations the pre-selection of the variables is performed by using the 'so called' screening procedure. The influence of each variable is assessed by comparing the numerical results obtained considering all variables with their mean value, with the results when the value of 'tested' variable is changed (mean +/- standard deviation). The remaining variables continued to be as previously. Performing such analysis for each variable the importance of each one of them is accessed in terms of percentage change.

In the analysed example the screening procedure allows to eliminate all the variables that describe the geometry and material properties of the pier. Also the variability of such parameters as elasticity modulus and ultimate strain of prestressing and reinforcing steel are found to be insignificant. Other variables, like position and area of the passive girder reinforcement, concrete elasticity modulus, have a low importance, however they are considered as random in the further simulations. The distribution types and coefficients of variation of parameters considered random in the analysis are presented in Table 9.3. The remaining parameters (which are not presented in the table) are assumed to be deterministic.

The parameters for concrete compressive strength are obtained by analysis of data provided by precasters and the general contractor of the bridge. The parameters for remaining concrete properties are established according to results presented in Section 4.2. The statistical parameters of time dependent characteristics of concrete are adopted from Tsubaki (1988). The probabilistic models of the area and the mechanical properties of the reinforcing and prestressing steel are considered according to the information presented in Sections 4.3 and 4.4. The models of variability for the dimensions of concrete members are generally assumed as presented in Section 4.5. The models of permanent loads used in the analysis are considered as discussed in Section 5.3. The variable load models are taken from the code RSA (1983) and their distribution parameters are assumed as presented in Henriques (1998). The variability in prestressing force of precast elements has been obtained by statistical evaluation of the results provided by the girders fabricator.

Table 9.3: Basic random variables.

Random variable	Distr. type	Bias factor	Coef. of variation or deviation
Concrete compressive strength	Normal	0.81 (0.81)*	8% (6%)
Concrete tensile strength	Normal	(A)	15% (15%)
Concrete elasticity modulus	Normal	(B)	8% (8%)
Creep coefficient	Normal	1.0	20%
Shrinkage strain	Normal	1.0	30%
Steel yield limit	Normal	1.2 (1.04)	8% (2.5%)
Area of bars strands and cables	Normal	1.0 (1.0)	2.5% (1.5%)
Section height	Normal	1.0 (1.01)	3.5% (0.5%)
Tendons coordinates	Uniform	1. 0 (1.0)	± 20 (5) mm
Reinforcement coordinates	Uniform	1. 0 (1.0)	± 20 (20) mm
Prestressing force	Normal	1.0 (1.0)	6% (1.5%)
Self weight	Normal	1.05 (1.03)	10% (8%)
Self weight of the pavement	Normal	1.0	25%
Traffic loads	Gumbel	1.0	11%
Temperature	Gumbel	1.0	8%

Note: values in brackets apply for precast girders; in case of steel parameters the values in brackets apply for prestressing steel; (A) correlated with compression strength of concrete, correl. coef. = 0.7; (B) correlated with compression strength of concrete, correl. coef. = 0.9; (*) 0.81=0.95x0.85 bias factor times the factor taking in the consideration different behaviour of concrete in the specimens and real constructional element.

9.3.6 Assessment of the ultimate limit state of bending

Prior to the probabilistic failure assessment of the studied bridge some deterministic analyses are performed using all variables as their mean or nominal values. The objectives of these analyses is to choose the most appropriate loading approach and to compare behaviour of the structure due to different load models.

Deterministic non-linear failure analysis. Some results of the deterministic failure analysis of the bridge are presented bellow. Figure 9.5 shows the loading scheme LS1 (scheme chosen to obtain the maximum moment in the middle of the span - the traffic loads applied just on the one span) and the load-displacement curves. The two curves on the diagram represent two diverse situations of differential temperature namely for summer and winter. Figure 9.6 shows the load scheme LS2 (scheme chosen to obtain the maximum moment over the pier - the traffic loads applied on both spans) and load-deformation curves also for summer and winter.

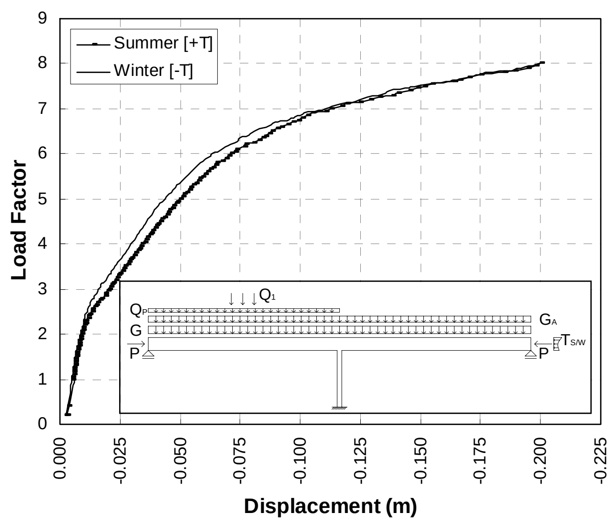

Figure 9.5: Load-displacement curve - loading scheme LS1.

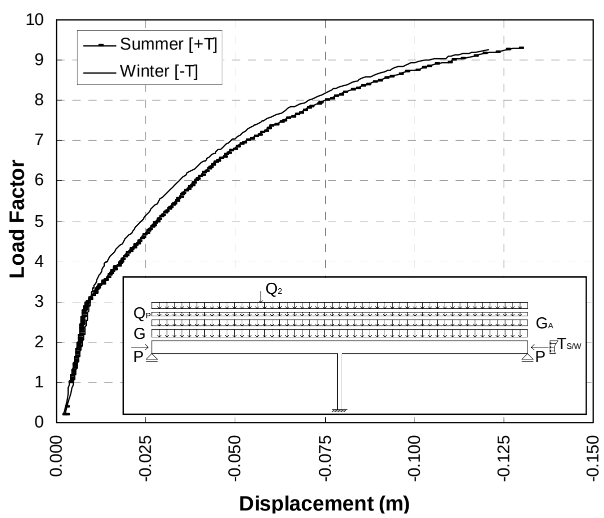

Figure 9.6: Load-displacement curve - loading scheme LS2.

Probabilistic non-linear failure analysis. The safety assessment of the bridge is performed according to the following methodology: the random variables are generated according to the parameters presented in Table 9.3 using Monte Carlo sampling; the structural analyses are performed for each combination of generated variables (≈1000 simulations); the results of the analyses are evaluated statistically and the probability of failure is calculated for load schemes LS1 and LS2.

Figure 9.7 presents the histogram of the calculated load factor κ defined in Table 9.2 for the load scheme LS1. The normal curve plotted on the diagram is determined based on mean values and standard deviations of the results obtained from simulation.

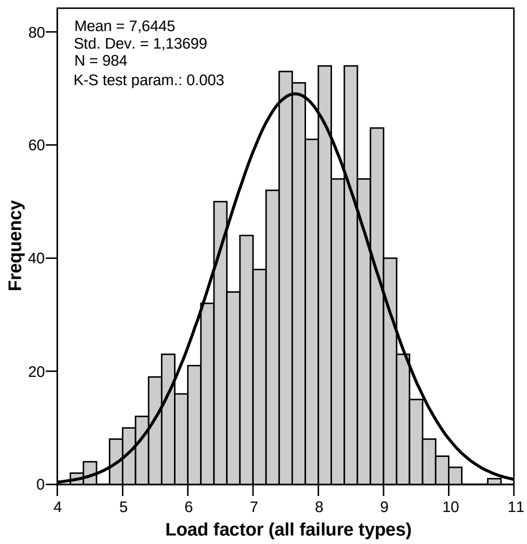

Figure 9.7: Histogram of calculated load factor κ for the load scheme LS1.

In the presented example the plot shows a significant deviation of the obtained results from the normal distribution. It is because of two different failure patterns which take place. Most common failure is by yielding of bottom layer of prestressing strands in the middle-span section. However, some failures are due to crushing of bottom layer of concrete in the section over the pier. Dividing the results for two groups corresponding to different failures, the normal curves are obtained as presented in Figures 9.8 and 9.9.

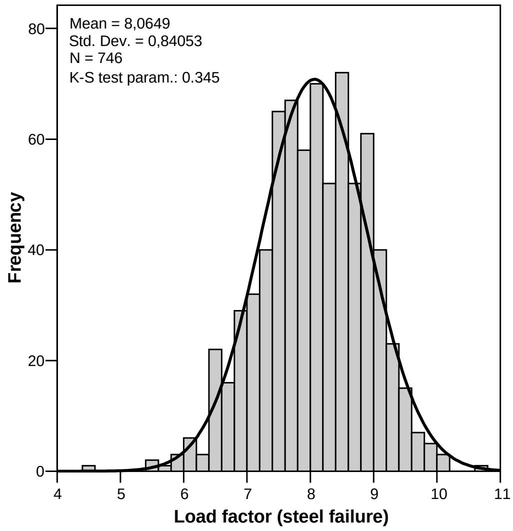

Figure 9.8: Histogram of κ for the load scheme LS1 - failure by steel.

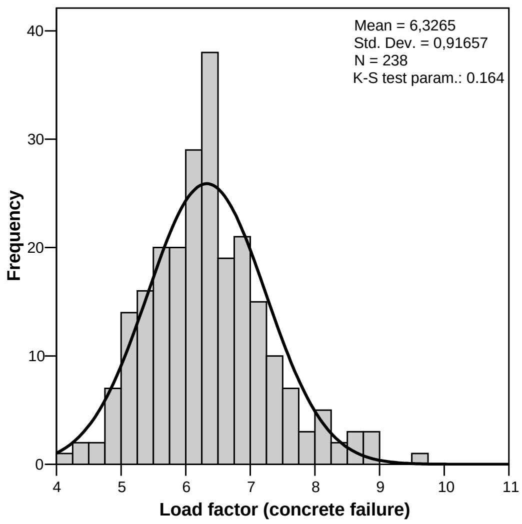

Figure 9.9: Histogram of κ for the load scheme LS1 - failure by concrete.

The probability of failure of the structure corresponding to the load scheme LS1 and LS2 is calculated using Equation 9.3. The safety index β corresponding to this probability of failure is calculated according to Equation 3.48.

$$P_f = \max\left\{P_f^{(A)}; P_f^{(B)}\right\} = \max\left\{z^{(A)} \cdot \phi\left(\frac{1-\mu^{(A)}}{\sigma^{(A)}}\right); z^{(B)} \cdot \phi\left(\frac{1-\mu^{(B)}}{\sigma^{(B)}}\right)\right\} \quad (9.3)$$

The results of this calculation as well as the results for remaining loading schemes are presented in Table 9.4. In case of loading scheme LS2 it is necessary to split the results for three failure modes corresponding to steel failure and concrete failures in two different zones.

Table 9.4: Statistical parameters of load factor κ.

Load scheme	Failure mode	Freq. of occurence	Mean value	Stand. dev.	Distr. type	Index β	Global β
$LS1_{+T}$	Ductile	0.76	8.06	0.840	Normal	8.41	6.04
	Fragile	0.24	6.33	0.916	Normal	5.81	
$LS1_{+T}$	Ductile	0.74	8.13	0.835	Normal	8.51	5.50
	Fragile	0.26	6.27	1.000	Normal	5.27	
$LS1_{+T}$	Ductile	0.04	9.66	0.680	Normal	12.74	7.28
	Fragile 1	0.11	6.67	0.814	Normal	6.97	
	Fragile 2	0.85	9.65	0.971	Normal	8.91	
$LS1_{+T}$	Ductile	0.04	9.63	0.769	Normal	11.21	7.87
	Fragile 1	0.11	6.29	0.697	Normal	7.58	
	Fragile 2	0.85	9.64	0.845	Normal	10.23	

9.3.7 Assessment of the serviceability limit states

The serviceability assessment of the bridge is performed according to the following methodology: the random variables are generated according to the parameters presented in Table 9.3 using Monte Carlo sampling; the structural analyses are performed for each combination of generated variables; the results of the analyses are evaluated statistically and the characteristic value of the response and the safety index are calculated.

Limit state of deformation. The limit state of deformation defined by Eurocode for bridges is expressed as follows:

$$y = \frac{L + 40}{2000} = \frac{25 + 40}{2000} = 0.0325m = 3.25cm \tag{9.4}$$

The comparison of allowable value of deformation with the characteristic value and with the value associated to probability considered as adequate for SLS verification, presented in Table 9.5, leads to conclusions that the limit state is verified with huge reserve. The existing safety margin, described by β index, in this case is equal to 8.8.

Table 9.5: Statistical parameters of structure deformation.

Combin. of loads	Mean value	Standard deviation	Distrib. type	Characteristic value 95%	Value corresp. to p_f=10^{-2}
$QP1_S$	0.18 cm	0.35 cm	Normal	0.75 cm	1.00 cm

Note: Characteristic value 95% ($\beta \approx 1.64$); (W) Value Associated to p_f=10^{-2} ($\beta \approx 2.33$).

Limit state of cracking. In Table 9.6 the results for the girder bottom fibres of middle span section are presented. The section over the pier is less decompressed and the results for that section are omitted. As it is easy to see the results in the last two columns are significantly far from the limit equal to 3.19 MPa. The limit is fixed in this case as the 5-th percentile of concrete tensile strength defined by statistical parameters presented in Table 9.3. The mean value is calculated according to CEB-FIP (1991) as a function of compressive strength. The parameters assumed for girders concrete tensile strength are the following: Mean = 4.32 MPa and St.Dev. = 0.69 MPa. The β index calculated for this case is equal to 6.0.

Table 9.6: Statistical parameters of stresses for cracking assessment.

Combin. of loads	Mean value	Standard deviation	Distrib. type	Characteristic value 95%	Value corresp. to p_f=10^{-2}
$F1_S$	-1.47 MPa	0.67 MPa	Normal	-0.37 MPa	0.09 MPa

Note: Characteristic value 95% ($\beta \approx 1.64$); (W) Value Associated to p_f=10^{-2} ($\beta \approx 2.33$).

Limit state of decompression. Results presented in Table 9.7 correspond to the bottom fibres of the section at the middle span. This section has been chosen as more relevant despite the fact that initially (on the 70-th day) the decompression at the section over the pier was found more probable. However the analysis in time shows that, due to redistribution caused by creep and shrinkage, stresses at the middle span section are more important. The analysis of results shows again that the limit state is verified with huge reserve. The safety margin assessed in terms of β index is equal to 4.27.

Table 9.7: Statistical parameters of stresses for decompression assessment.

Combin. of loads	Mean value	Standard deviation	Distrib. type	Characteristic value 95%	Value corresp. to p_f=10^{-2}
$QP1_S$	-2.65 MPa	0.62 MPa	Normal	-1.63 MPa	-1.20 MPa

Note: Characteristic value 95% ($\beta \approx 1.64$); (W) Value Associated to p_f=10^{-2} ($\beta \approx 2.33$).

Limit state of tensile stresses in prestressing-steel. The limitations of tensile stresses in prestressing steel is defined differently in CEB-FIP (1991), EC-2b (2003) and in REBAP (1985). In first case the limit is defined as $0.75f_{pk}$ for rare combination and in second case the limit is defined as $0.65f_{pk}$ for quasi permanent combination. Due to this fact two rows in Table 9.8 are found corresponding to different load combinations. The verification presented is made for the bottom layer of the strands at the middle span section. This section again has been found more exposed to the limit state violation. Since the mechanical properties of steel used in analysis are considered deterministic with values adopted from codes, the comparison is made with deterministically defined allowable limits fixed as 1395 MPa and 1209 MPa for the first and the second case respectively. As it could be seen, the values presented in last two columns of the table are reasonably higher than the limit for QP combination and slightly higher than the limit for R combination. The significant exceeding of the limit in the first case could be explained by the fact that this limit does not exist in REBAP (1985). However the slight surpassing of the limit in the second case probably would not happened if real properties of prestressing steel were considered.

Table 9.8: Statistical parameters of maximum tensile stresses in prestressing steel.

Combin. of loads	Mean value	Standard deviation	Distrib. type	Characteristic value 95%	Value corresp. to p_f=10^{-2}
$QP1_S$	1348 MPa	25 MPa	Normal	1389 MPa	1406 MPa
$R1_S$	1371 MPa	25 MPa	Normal	1412 MPa	1429 MPa

Note: Characteristic value 95% ($\beta \approx 1.64$); (W) Value Associated to p_f=10^{-2} ($\beta \approx 2.33$).

Limit state of compression in concrete. The limit values of compression in concrete defined in EC-2 (2004) and EC-2b (2003) are the following: $0.45 f_{ck}(t)$ for quasi permanent combination of loads and $0.60 f_{ck}$ for rare combination. The values proposed in REBAP (1985) are quite similar. Table 9.9 presents the results of maximum compression in concrete obtained during simulations. In the first row the results for girder top fibres at the middle span for QP combination are presented and in the second row the results for slab top fibres also at the middle span section are showed. It is important to notice, that results for verification of the first limit are taken for age of concrete equal to 70 days. This is due to the fact that this verification is to ensure validity of assumption of linear creep. The second limit is verified for age of concrete equal to 1000 days.

Table 9.9: Statistical parameters of maximum compressive stresses in concrete.

Combin. of loads	Mean value	Standard deviation	Distrib. type	Characteristic value 95%	Value corresp. to p_f=10^{-2}
$QP1_S$	-9.19 MPa	0.71 MPa	Normal	-10.35 MPa	-10.84 MPa
$R1_S$	-4.49 MPa	0.36 MPa	Normal	-5.08 MPa	-5.33 MPa

Note: Characteristic value 95% ($\beta \approx 1.64$); (W) Value Associated to p_f=10^{-2} ($\beta \approx 2.33$).

In this case the limit values is fixed as a percentage of characteristic value (5-th percentile) of concrete compressive strength, defined by statistical parameters presented in Table 9.3. The limit for first case is equal to -20.09 MPa and for second is -16.32 MPa which is significantly far from the obtained results. The β index calculated is equal to 4.73 and 10.0 for the first and the second case respectively.

9.3.8 Conclusions drawn from the assessment

Results presented in the previous sections show that the structure satisfies the ultimate limit state of bending and the serviceability limits except in one case: the limit of tensile stresses in prestressing tendons. The safety margin, assessed in terms of β index, is significantly large for most of the situations. Keeping in mind that the bridge has been designed and assessed considering the same permanent and variable loads, and assuming that it has been appropriately designed (without excessive strength reserves), it can be concluded that the applied fully probabilistic non-linear assessment method shows the potentials of 'extracting' strength reserves present in the structure which can not be evaluated using traditional methods. Therefore, this method, as well as other fully probabilistic non-linear assessment methods, can be successfully used in the assessment of existing bridges which fails traditional evaluation of the ultimate limit states as well as the serviceability limit states.

Chapter 10

Conclusions

10.1 Summary and general conclusions

This thesis deals with different topics related to the load capacity evaluation of existing concrete bridges. At first, the currently recommended procedures and methodologies for the assessment of existing bridges are presented and discussed. Then, several probabilistic models of bridge geometry and mechanical properties of materials, used in the construction of concrete bridges, are demonstrated. Some new models, developed within the program of this thesis, are also shown. Subsequently, the problem of bridge loading is discussed. Several probabilistic models of bridge permanent loads are presented. However, the major focus is placed on bridge traffic loads. Afterwards, several probabilistic models of bending and shear resistance of concrete bridge elements are demonstrated. Also, some new models developed within the program of this thesis are shown. After the load and the resistance models, the safety requirements and safety formats applicable to bridge assessment are presented and compared.

The information presented in this thesis form a solid framework that can be practically used in the process of assessment of existing concrete bridges in Portugal. This has been verified by applying the selected assessment procedure, several proposed safety formats, developed resistance models and presented load models in the assessment of three concrete bridges, one reinforced concrete railway bridge and two precast prestressed concrete highway bridges.

The detailed safety analysis of the reinforced concrete continuous railway bridge 'Brunna Bridge', performed using several safety formats discussed in this thesis, shows how the bridge that would have been rated as deficient using traditional semi-probabilistic member safety analysis methods may in actuality have extremely high system reliability levels, thus eliminating the need for its replacement or rehabilitation. This is due to the ability of the bridge system to redistribute the load from weak members to other stronger members. This is a significant structural property that should reinforce the importance of performing the safety assessment of bridges at the system level in order to take full advantage of the redundancy of the bridge. Furthermore, even neglecting bridge redundancy but performing probabilistic analysis, and thus considering real variabilities of all the parameters affecting bridge member capacity, may be sufficient to prove required bridge safety.

The assessment of the precast prestressed concrete I girder bridge 'Barrela Bridge', curried out using 'step-level' assessment procedure proposed in this thesis for assessment of bridges in Portugal, shows that the structure can be considered safe even though the traffic loads used in the assessment are significantly higher than those applied to design the bridge. The initial assessment performed using traditional methods gives somewhat different results (structure fails the assessment). Nevertheless, more refined analyses applied according to the 'step-level' assessment methodology proves that the structure is able to carry higher loads. The further evaluation of 'Barrela Bridge' performed using selected simplified probabilistic traffic load model, which is assumed to be more representative in this case than the EC-1b (2002) load model, shows significant increase in the safety margin when comparing to lower level assessment. The main conclusion drawn from this analysis is that the appropriate modelling of traffic loads in the process of assessment of existing bridges may save many bridges from unnecessary rehabilitation, strengthening or replacement.

The reliability evaluation of the precast prestressed concrete overpass 'PS12', performed using fully probabilistic non-linear analysis, shows that the structure satisfies the analysed ultimate and serviceability limit states with a significant safety margin (except the limit of tensile stresses in prestressing tendons). The general conclusions drawn from this example are similar to those obtained in the analysis of the 'Brunna Bridge', namely that the probabilistic non-linear assessment methods show the potentials of 'extracting' strength reserves present in the structure which can not be evaluated using traditional methods. Therefore, these methods can be successfully used in the assessment of existing bridges which fails the traditional evaluation of the ultimate limit states. Furthermore, as it has been proved in this example, they also can be used in the assessment of the serviceability limit states.

10.2 Conclusions regarding some specific topics presented in the thesis

Besides the general conclusions regarding presented framework for the assessment of existing concrete bridges in Portugal and its applications to the real structures, some conclusions related to specific topics discussed in selected chapters of this thesis are also drawn.

Conclusions regarding assessment procedures. The main conclusion drawn from the review of the assessment procedures, presented in Chapter 2, is that efficient structural assessment strategies have to be based on the application of new and increasingly sophisticated analysis levels, where the highest level combines load redistribution analysis (non-linear analysis) with a probabilistic analysis. Therefore, the procedure, which is selected in this thesis for using in load capacity evaluation of bridges in Portugal, is comprised of five levels of assessment with increasing levels of complexity. The recommendation to go forward to the next level is made only if the bridge fails to pass the previous assessment level. The procedure systematize the use of several load capacity evaluation methods, starting with the simplest deterministic evaluation, based on the current design code, and finishing with fully probabilistic assessment, based on the reliability theory.

Conclusions regarding models of material properties and geometry. The main observation from the review of the existing models and the models developed based on Portuguese data, performed in Chapter 4, is that the variability of mechanical properties of materials used in bridge construction and the geometry of bridge members is similar in most of the countries and is more dependent on the production or execution quality rather than other factors. Also, due to increase of the quality of production of concretes and reinforcing steels, the variability of strength properties of these materials is currently lower than some years or decades ago. This has to be considered when assessing existing bridges. Furthermore, due to the higher execution quality, the precast elements are generally characterized by lower variability in element geometry and in the mechanical properties of concrete than elements cast in-situ.

Conclusions regarding bridge load models. The load models used in the process of assessment of existing bridges should reflect the actual loads acting on the bridge and the loads that the bridge may experience during its remaining life. The conclusion drawn from the Chapter 5, regarding bridge loads, is that the bridge traffic load models defined in RSA (1983) and EC-1b (2002) are, due to different reasons, not the most adequate models for the assessment of existing bridges in Portugal. The load models from RSA (1983) are quite obsolete and do not reflect the actual heavy traffic. However, the load model from EC-1b (2002) is very conservative and overestimate the loads that existing bridges may experience during their remaining life. Therefore, some alternative models should be used in the assessment of existing bridges in Portugal. The simplified probabilistic load models presented in this thesis might be recommended where there is a lack of better models. Nevertheless, the use of proposed models should be preceded by measurements of real traffic using Weigh-in-Motion systems and by the calibration of some of the parameters of the models.

Conclusions regarding bending and shear resistance models. The review of existing bending resistance models and the models developed within the program of this, which are presented in Chapter 5, leads to the general conclusion that the statistics of the bending capacity of typical concrete bridge members are very similar to the statistics of the steel strength governing the capacity of the member (e.g. reinforcing or prestressing steel). Therefore, when assessing the existing bridge the information regarding the properties of steel used for the construction of this bridge is very much appreciated. Quite similar conclusions to this above made for bending can be drawn for the shear resistance of the members with sufficient amount of reinforcement. However, the shear failure mechanism is much more complicated than the mechanism of bending failure. Thus, due to several possible failure modes this general observation may not be true, especially when there is not enough longitudinal reinforcement, the member is prestressed, or there is too much shear reinforcement leading to failure by compression of concrete struts. From analysis of the models of shear capacity of the reinforced concrete members without shear reinforcement, it may be concluded that the governing variable is the tensile strength of concrete. Therefore, when assessing the existing bridge where the main members do not have shear reinforcement the information regarding the actual condition of concrete in the structure and its tensile strength capacity is very welcome.

Conclusions regarding safety formats for assessment. The main conclusion that comes from the review of several safety formats and assessment methods, presented in Chapter 7 and compared in Chapter 8, is that the probabilistic methods are likely to show the safety reserves in the structure which might not be evident when performing deterministic assessment. Therefore, they should be used in the assessment of existing bridges that fails traditional deterministic evaluation. Comparing several presented probabilistic methods, characterized by different level of complexity and accuracy, it can be concluded that the simplified probabilistic methods for the member level evaluation (Mean Load method), and at the system level evaluation (method of Ghosn and Moses and method of Sobrino and Casas) are sufficiently accurate while only requiring a basic level of knowledge of structural reliability techniques. The combination of accuracy and simplicity would make these methods more likely to be used by engineering practitioners for the safety assessment of existing bridges. Furthermore, the Redundancy Factor method also seems to be an adequate and efficient technique for the safety assessment of existing bridges especially when the bridge evaluator is not familiar with the reliability theory. A more accurate method, as Response Surface method or Latin Hypercube simulation method, due to their complexity, might be used just as a last resort to save a bridge from unnecessary rehabilitation, strengthening or replacement.

10.3 Suggestions for further research

Whilst performing the several assessments and analysis presented in this dissertation, and also during the writing of the literature review for some chapters of this thesis, several areas that require further research have been identified.

The first area that evidently need investigation in Portugal is the area of bridge traffic loads. The bridge load model defined in RSA (1983), which is used presently to design and assess the bridges in Portugal, is rather obsolete. However, the bridge load model defined in EC-1b (2002) is very conservative which might be good in the design of new bridges but evidently is disqualifying it from the assessment of existing bridges. Therefore, there is a need to perform a campaign of the measurements of real traffic and to perform the calibration of bridge load model from EC-1b (2002) for the purpose of the design of new bridges and the assessment of existing bridges in Portugal.

The second area that need further investigation is the area related to the definition of modelling uncertainties. In the assessment of existing bridges by means of probabilistic methods, in order to obtain quantitatively accurate results, the difference between the prediction of the bridge response, obtained from the analysis, and the actual response of the structure, have to be considered in the assessment by introducing modelling variable. Some models proposed for this variable can be found in the available literature. Nevertheless, these models are questionable and generally correspond to simplified models of analysis rather than to currently common global non-linear structural analysis, where advanced response models and constitutive relationships are used. Therefore, there is a need to define the modelling uncertainty for different levels of structural analysis and different constitutive relationships.

The third area that evidently need further development is the area of systematization and unification of the methods of probabilistic analysis and the input parameters used for these analysis. Generally, the probabilistic methods are very sensitive to the parameters used in the analysis. It is commonly known that adjusting the parameters used for the probabilistic analysis one may get almost any required results, which evidently may not be correct. Also, when performing more and more refined reliability analysis (e.g. considering system behaviour, load redistribution, etc.) almost any required level of reliability, expressed by the reliability index β, can be obtained. Therefore, there is a need to establish general rules for the probabilistic modelling of the input parameters. Some rules are already defined in JCSS (2001), and also in this thesis, however, they are not exhaustive. Furthermore, there is a need to establish rules for the use of different level of the reliability analysis and to define the corresponding required reliability level for each of the analysis level. In this field there is also some work done (Ghosn & Moses, 1998) that is reported in this thesis, however, it is not sufficient.

Of course there is also a possibility to research further into the variation in the properties of materials used in bridge construction and to develop models of shear and bending resistance for other bridge types. Nevertheless, it probably will not lead to any significant progress or improvements of the existing models. Therefore, as soon as the uncertainties in the mechanical properties of materials or in bridge geometry and the uncertainties in the prediction of section capacities will not change significantly, the models developed and presented in this thesis are rather sufficient.

Bibliography

AASHTO LRFD (1994). *Load and Resistance Factor Bridge Design Specification*. American Association of State Highways Transportation Officials, DC, Washington. 2.3.3, 5.4.5, 7.2.5.1, 7.2.5.2, 7.2.5.2, 7.3.3.1, 7.3.3.1

AASHTO LRFR (2003). *Manual for Condition Evaluation and Load and Resistance Factor Rating of Highway Bridges*. American Association of State Highways Transportation Officials, DC, Washington. 2.3.1, 2.3.3, 7.3.3.1

Bartlett, F.M. & MacGregor, J.G. (1996). Statistical Analysis of Compressive Strength of Concrete in Structures. *ACI Materials Journal*, **93**, 158–168. 4.2.3, 4.2.3, 4.2.3, 4.3, 4.4, 4.2.3, 4.5, 4.2.5

BD21/01 (2001). *The Assessment of Highway Bridges and Structures.* Design Manual for Roads and Bridges. Vol.3, Section 4, Part 3.. HMSO, London. 2.3.3

BD44/95 (1995). *The Assessment of Concrete Highway Bridges and Structures.* Design Manual for Roads and Bridges. Vol.3, Section 4, Part 14.. HMSO, London. 2.3.3

Bell, B. (2004). *European Railway Bridge Demography - Deliverable D1.2, WP1-02-T-040531-R-D1.2*. Sustainable Bridges - VI Framework Programme, Brussels. 1.1

Bentz, E.C. (2000). *Sectional Analysis of Reinforced Concrete Members*. Ph.D. thesis, University of Toronto, Graduate Department of Civil Engineering. 6.2.3, 6.4.4, 9.2.3

Bez, R. & Hirt, M.A. (1991). Probability-Based Load Models of Highway Traffic. *Structural Engineering International*, 37–42. 5.4.5

Bohigas, A.C. (2002). *Shear Design of Reinforced High-Strength Concrete Beams*. Ph.D. thesis, Technical University of Catalonia, Department of Construction Engineering. 6.2.3, 6.1

BRIME (2001). *Bridge Management in Europe - Final Report D14*. IV Framework program, Brussels, (http://www.trl.co.uk/brime). 1.1, 2.2.2, 2.3.1, 2.3.2, 2.3.3, 2.4

CAN/CSA-S6-00 (2000). *Canadian Highway Bridge Design Code*. Canadian Standards Association, Toronto. 2.3.1, 2.3.3, 5.4.5, 7.2.5.1, 7.3, 7.2.5.2, 7.2.5.2

Carlson, F. (2006). *Modelling of Traffic Loads on Bridges. Based on Measurements of Real Traffic Loads in Sweden*. Ph.D. thesis, Lund University, Division of Structural Engineering. 5.4.2, 5.4.5

Casas, J.R. (1999). Evaluation of Existing Concrete Bridges in Spain. *ACI Concrete International*, **21**, 48–53. 1.1

Casas, J.R. (2005). *Probabilistic Modelling - Background Document WP4-G-R-02*. Sustainable Bridges - VI Framework Programme, Brussels. 6.2.2, 6.3.2, 6.4, 6.3.2, 6.5, 6.3.3, 6.4.2, 6.15, 6.4.2, 6.4.3

Casas, J.R. & Wiśniewski, D.F. (2005). *Safety Formats and Required Safety Levels - Background Document WP4-G-R-01*. Sustainable Bridges - VI Framework Programme, Brussels. 7.1, 7.2.1, 7.2.5.2, 7.3.1, 7.3.3.1, 7.3.3.2, 7.3.3.2, 7.3.3.2, 7.3.3.2, 8.1

Casas, J.R., Wiśniewski, D.F., Cervenka, J. & Plos, M. (2005). *Probabilistic Nonlinear Analysis - Background Document WP4-G-R-03*. Sustainable Bridges - VI Framework Programme, Brussels. 3.6.1

CEB-FIP (1991). *Model Code 1990 - Design Code*. Comite Euro-International du Beton, Lausanne. 9.3.7, 9.3.7

Cooper, D.I. (1997). *Development of Short Span Bridge-specific Assessment Live Loading*. Thomas Telford, London, 'Safety of Bridges' edited by P. C. Das. 5.4.6, 5.4.6, 5.11, 5.12, 5.13

COST323 (1997). *Collection and Analysis of Needs and Requirements as Regards Weighing vehicles in Motion*. Cooperation in the Field of Scientific and Technical Research, Brussels, (http://cost323.zag.si). 5.4.2, 5.4.2, 5.4, 5.5

COST345 (2004). *Procedures Required for the Assessment of Highway Structures. Numerical Techniques for Safety and Serviceability Assessment - Report of the Working Groups 4 and 5*. Cooperation in the Field of Scientific and Technical Research, Brussels, (http://cost345.zag.si). 1.1, 2.3.1, 2.3.2, 2.4

Crespo, C. (1996). *A Reliability Based Methodology to Define the Limit State of Decompression in Prestressed Concrete Bridges*. Ph.D. thesis, Technical University of Catalonia, Department of Construction Engineering. 3.6.2, 5.4.5

Cruz, P.J.S. & Wiśniewski, D.F. (2004). Ave River Bridge - A Major Precast Prestressed Concrete U-Girder Bridge in Portugal. *PCI Journal*, **49**, 72–86. 6.3.3

Cruz, P.J.S., Wiśniewski, D.F. & Valente, I. (2003). *Relatório de Prova de Carga - Passagem Superior 12 - Relatório 03-DEC/E-17*. University of Minho, Department of Civil Engineering. 9.3.3

Devalapura, R.K. & Tadros, M.K. (1992). Critical Assessment of ACI 318 Eq. (18-3) for Prestressing Steel Stress at Ultimate Flexure. *ACI Structural Journal*, **89**, 538–546. 4.4.3, 4.18

EC-0 (2002). *EN1990: Eurocode - Basis of Structural Design*. CEN, Brussels, final version. 7.2.5.1, 7.2, 7.2.5.1, 7.2.5.1, 7.3.2, 9.2.3

EC-1 (2002). *EN1991-1-1: Eurocode 1: Action on Structures - Part 1-1: General Actions - Densities, Self-weight, Imposed Loads for Buildings*. CEN, Brussels, final version. 8.1

EC-1B (2002). *prEN1991-2: Eurocode 1: Action on Structures - Part 2: Traffic Loads on Bridges*. CEN, Brussels, final draft. 5.4.3, 5.4.3, 5.4.3, 5.4.3, 5.4.4, 5.4.4, 5.4.5, 5.4.6, 8.1, 9.2.1, 9.2.3, 9.2.3, 9.2.3, 9.2.3, 9.2.4, 9.2.5, 10.1, 10.2, 10.3

EC-2 (2004). *EN1992-1-1: Eurocode 2: Design of Concrete Structures. Part 1: General Rules and Rules for Buildings*. CEN, Brussels, final version. 4.2.3, 4.2.3, 6.3.4, 6.3.4, 6.4.4, 7.3.2, 8.1, 8.4, 9.2.3, 9.3.7

EC-2B (2003). *prEN1992-2: Eurocode 2: Design of Concrete Structures. Part 2: Concrete bridges. Design and Detailing Rules*. CEN, Brussels, stage 34. 7.3.2, 8.1, 9.2.3, 9.3.7, 9.3.7

ENEVOLDSEN, I. (2001). Experience with Probabilistic-based Assessment of Bridges. *Structural Engineering International*, **11**, 251–260. 1.1

FABER, M.H., VAL, D.V. & STEWART, M.G. (2000). Proof Load Testing for Bridge Assessment and Upgrading. *Engineering Structures*, 1677–1689. 2.2.4, 2.2.4

FLORIAN, A. (1992). An Efficient Sampling Scheme: Updated Latin Hypercube Sampling. *Probabilistic Engineering Mechanics*, **7**, 123–120. 3.6.2

GETACHEW, A. (2003). *Traffic Load Effects on Bridges. Statistical Analysis of Collected and Monte Carlo Simulated Vehicle Data*. Ph.D. thesis, Royal Institute of Technology, Stockholm. 5.4.5

GHOSN, M. (1999). *Modelling of Bridge Dead and Live Loads*. ASCE, Reston, Virginia, chapter 2 in 'Bridge Safety and Reliability' edited by D. Frangopol. 5.2.1, 5.2.2, 5.3.1, 5.4.1, 5.4.5, 5.4.6

GHOSN, M. & FRANGOPOL, D.M. (1999). *Bridge Reliability: Components and Systems*. ASCE, Reston, Virginia, chapter 4 in 'Bridge Safety and Reliability' edited by D. Frangopol. 3.6.3

GHOSN, M. & MOSES, F. (1985). Markov Renewal Model for Maximum Bridge Loading. *Journal of Engineering Mechanics*, **111**, 1093–1105. 5.4.5

Ghosn, M. & Moses, F. (1998). *Redundancy in Highway Bridge Superstructures - NCHRP Report N. 406*. Transportation Research Board, DC, Washington. 7.2.5.2, 7.2.5.2, 7.2.5.2, 7.3.3.1, 7.9, 7.3.3.2, 7.3.3.2, 7.3.3.2, 7.3.3.2, 7.3.3.2, 7.3.3.2, 10.3

Gonçalves, A.F. (1987). *Resistência do Betão nas Estruturas*. Ph.D. thesis, Civil Engineering National Laboratory (LNEC), Lisbon. 4.2.3, 4.5

Haldar, A. & Mahadevan, S. (2000a). *Probability, Reliability and Statistical Methods in Engineering Design*. John Wiley & Sons, New York. 2.1, 3.1, 3.1, 3.2.1, 3.6.1

Haldar, A. & Mahadevan, S. (2000b). *Reliability Assessment Using Stochastic Finite Element Analysis*. John Wiley & Sons, New York. 3.6.2, 3.6.3, 3.6.4

Henriques, A.A. (1998). *Aplicação de Novos Conceitos de Segurança no Dimensionamento do Betão Estrutural*. Ph.D. thesis, Faculty of Engineering of the University of Porto, Department of Civil Engineering. 4.2.3, 4.3, 4.10, 8.3, 9.3.3, 9.3.5

Henriques, A.A., Wiśniewski, D.F. & Cruz, P.J.S. (2004). *Aferição Probabilística de Segurança Estrutural de Pontes de Betão Pré-fabricado*. Lisbon, Congresso de Métodos Computacionais em Engenharia. 9.3.1

Henriques, A.A.R. (2002). *Estruturas Pré-esforçadas. Programa de Análise à Rotura de Secções de Betão Armado Sujeitas à Flexão*. Faculdade de Engenharia, Universidade do Porto, Porto. 6.3.4, 9.2.3

Iman, R.L. & Conover, W.J. (1982). A Distribution-Free Approach to Inducing Rank Correlation Among Input Variables. *Communication Statistics*, **B11**, 311–334. 3.6.2

ISO 2394:1998 (1998). *Basis for Design of Structures - General Principles on Reliability of Structures*. International Organization for Standardization, Geneva. 7.2.5.1, 7.6

ISO/CD 13822:1999 (1999). *Basis for Design of Structures - Assessment of Existing Structures*. International Organization for Standardization, Geneva. 7.2.5.1, 7.2.5.1, 7.7

James, G. (2003). *Analysis of Traffic Load Effects on Railway Bridges*. Ph.D. thesis, Royal Institute of Technology, Stockholm. 5.4.5

JCSS (2001). *Probabilistic Model Code*. Joint Committe on Structural Safety, http://www.jcss.ethz.ch, 12-th draft. 4.2.2, 4.1, 4.2, 4.3.2, 4.3.2, 4.8, 4.9, 4.4.2, 4.4.2, 4.16, 4.17, 4.5.2, 4.23, 5.1, 5.3.2, 5.3.2, 5.3.2, 5.3, 6.2.3, 6.2.3, 7.2.5.1, 7.5, 7.2.5.1, 10.3

JCSS (2001b). *Probabilistic Assessment of Existing Structures*. The publishing Company of RILEM, Cachan Cedex France, edited by D. Diamantidis. 2.3.1, 7.2.4

Jeppsson, J. (2003). *Reliability-based Assessment Procedures for Existing Concrete Structures*. Ph.D. thesis, Lund University, Division of Structural Engineering. 1.1

Kaymaz, I. (2005). Application of Kriging Method to Structural Reliability Problems. *Structural Safety*, **27**, 133–151. 3.6.3

Lauridsen, J. (2004). *Bridge Owner's Benefits from Probabilistic Approaches - Experiences and Future Challenges*. Balkema, Roterdam, iABMAS'04 - Bridge Maintenance, Safety, Management and Cost , E. Watanabe, D.M. Frangopol & T. Utsunomiya (eds). 1.1

Liu, W., Neuenhoffer, A., Ghosn, M. & Moses, F. (2001). *Redundancy in Highway Bridge Substructures - NCHRP Report N. 458*. Transportation Research Board, DC, Washington. 7.2.5.2, 7.2.5.2, 7.2.5.2

Lopes, P.J.A. & Wiśniewski, D.F. (2004). *Modern Precast Solutions for Short and Medium Span Bridges*. Proceedings of the 5th Conference on Small and Medium Span Bridges, Małe Mosty 2004, Wrocław, Poland. 6.3.3

Melchers, R.E. (1999). *Structural Reliability Analysis and Prediction*. John Wiley & Sons, Chichester, 2nd edn. 3.1, 3.2.1, 3.2, 3.3, 3.6, 3.9, 3.4.1, 3.4.2, 3.6.2, 4.2.1, 4.5.3, 5.2.1, 5.3.1, 5.4.5, 6.1, 6.2.2, 6.2.3, 6.2.3, 6.2.3, 7.2.2, 7.2.2, 7.1, 7.2.3, 7.3.3.1

Menzies, J.B. (1997). *Bridge Failures, Hazard and Societal Risk*. Thomas Telford, London, Safety of Bridges edited by P.C. Frangopol. 7.2.2, 7.2.2

Mirza, S.A. & MacGregor, J.G. (1979a). Variability of Mechanical Properties of Reinforcing Bars. *Journal of the Structural Division, ASCE*, **105**, 921–937. 4.3.3, 4.10, 4.3.3, 4.3.3

Mirza, S.A. & MacGregor, J.G. (1979b). Variation in Dimensions of Reinforced Concrete Members. *Journal of the Structural Division, ASCE*, **105**, 751–766. 4.5.1, 4.5.3, 4.24, 4.25, 4.26, 4.5.3

Mirza, S.A., Hatzinikolas, M. & MacGregor, J.G. (1979). Statistical Descriptions of Strength of Concrete. *Journal of the Structural Division, ASCE*, **105**, 1021–1037. 4.2.3, 4.2.3, 4.2.3, 4.2.3, 4.2.3, 4.3, 4.2.3, 4.5, 4.2.3, 4.2.3

Mirza, S.A., Kikuchi, D.K. & MacGregor, J.G. (1980). Flexural Strength Reduction Factor for Bonded Prestressed Concrete Beam. *ACI Journal*, **77**, 237–246. 4.4.3, 4.18, 4.4.3, 5.3.2

Moses, F. (2001). *Calibration of Load Factors for LRFR Bridge Evaluation - NCHRP Report N. 454*. Transportation Research Board, DC, Washington. 7.2.4, 7.3.3.1

Moses, F. & Ghosn, M. (1985). *A Comprehensive Study of Bridge Loads and Reliability - Report FHWA/OH-85/005*. Case Western Reserve University, Cleveland. 5.4.5, 5.4.6, 5.4.6, 5.9, 5.10, 5.4.6, 5.4.6

NKB-36 (1978). *Recommendation for Loading and Safety Regulations for Structural Design - Publication 36*. Nordic Committee for Building Regulations. 7.2.5.1, 7.4, 7.2.5.1

NOWAK, A.S. (1999). *Calibration of LRFD Bridge Design Code - NCHRP Report N. 368*. Transportation Research Board, DC, Washington. 5.4.6, 6.2.3, 6.2.3, 6.3.2, 6.2, 6.3.2, 6.4.2, 6.14, 6.4.2

NOWAK, A.S. & COLLINS, K.R. (2000). *Reliability of Structures*. McGraw-Hill, New York. 3.1, 3.2.1, 3.3.1, 3.4.1, 3.6.2, 5.2.2, 5.3.1, 5.4.1, 6.2.1, 7.3.1

NOWAK, A.S. & HONG, Y.K. (1991). Bridge Live Load Models. *Journal of Structural Engineering, ASCE*, **117**, 2757–2767. 5.4.5

NOWAK, A.S. & SZERSZEN, M.M. (1998). Bridge Load and Resistance Models. *Engineering Structures*, **20**, 985–990. 5.3.1, 5.2

NOWAK, A.S. & SZERSZEN, M.M. (2003). Calibration of Design Code for Buildings (ACI 318): Part1 - Statistical Models for Resistance. *ACI Structural Journal*, **100**, 377–382. 4.2.3, 4.3, 4.4, 4.3.3, 4.10, 4.3.3, 4.4.3, 4.18, 4.4.3

NOWAK, A.S., YAMANI, A.S. & TABSH, S.W. (1994). Probabilistic Models for Resistance of Concrete Bridge Girders. *ACI Structural Journal*, **91**, 269–276. 6.2.2, 6.2.3, 6.2.3, 6.3.2, 6.3.2, 6.3.2, 6.3.3, 6.4.2, 6.4.2, 6.4.3

O'BRIEN, E.J. & O'CONNOR, A.J. (1998). *Eurocode for Traffic Loads on Road Bridges (EC1.3) - Calibration of Irish Conditions - Report No. 98-001*. Department of Civil Engineering, Trinity College, Dublin. 5.4.2, 5.4.4, 5.4.4

O'CONNOR, A.J. (2001). *Probabilistic Traffic Load Modelling for Highway Bridges*. Ph.D. thesis, University of Dublin, Trinity College. 5.4.4, 5.4.5

O'CONNOR, A.J., JACOB, B., O'BRIEN, E.J. & PRAT, M. (1998). *Effects of Traffic Loads on Road Bridges - Preliminary Studies for the Re-assessment of the Traffic Load Model for Eurocode 1, Part 3*. Lisbon, Portugal, Proceedings of the 2-nd European Conference on Weigh in Motion of Road Vehicles. 5.4.2

PCSF (2002). *Precast Concrete Safety Factors - Final Report*. European Research, Contract SMT4 CT98 2267. 4.2.3, 4.4, 4.2.3, 4.5, 4.5.3, 4.29, 5.3.1, 7.3.2

PIPA, M.J. (1995). *Ductilidade de Elementos de Betão Armado Sujeitos a Acções Cíclicas. Influência das Características Mecânicas das Armaduras*. Ph.D. thesis, School of Engineering of the Technical University of Lisbon, Department of Civil Engineering. 4.3.3, 4.10, 4.3.3, 4.12, 4.13, 4.3.3

PORTARIA N.1092/97 (1997). *Portaria n.1092/97 - Regulamenta os Limites de Peso e Dimensão dos Veículos*. Ministério da Adiministração Interna, Lisboa. 5.4.2, 5.5

RAJASHEKHAR, M.R. & ELLINGWOOD, B.R. (1993). New Look at the Response Approach for Reliability Analysis. *Structural Safety*, **12**, 205–220. 3.6.3

REBAP (1985). *Regulamento de Estruturas de Betão Armado e Pré-Esforçado*. Ministério da Habitação, Obras Públicas e Transportes, Lisboa. 6.3.3, 6.4.3, 7.3.2, 9.2.1, 9.3.1, 9.3.7, 9.3.7

RSA (1983). *Regulamento de Segurança e Acções para Estruturas de Edifícios e Pontes*. Ministério da Habitação, Obras Públicas e Transportes, Lisboa. 1.1, 5.4.3, 5.4.3, 5.4.3, 5.4.3, 5.4.4, 5.4.4, 6.3.3, 6.4.3, 7.3.2, 9.2.1, 9.3.1, 9.3.4, 9.3.5, 10.2, 10.3

RSEP (1961). *Regulamento de Solicitações em Edifícios e Pontes*. Ministério das Obras Públicas, Lisboa. 1.1, 5.4.3, 5.4.4

RYALL, M.J. (2001). *Bridge Management*. Butterworth-Heinemann, Oxford. 2.2.4

SAMARIS (2005). *State of the Art Report on Assessment of Structures in Selected EEA and CE Countries - Deliverable D19*. Sustainable and Advanced Materials for Road Infrastructure - V Framework program, Brussels, (http://samaris.zag.si). 1.1, 2.3.1, 2.3.3, 5.4.2, 5.4.2

SCHNEIDER, J. (1997). *Introduction to Safety and Reliability of Structures*. IABSE, Zürich. 2.3.1, 2.3, 3.1, 3.2.1, 3.7, 3.8, 3.10, 3.14, 6.2.1, 6.2.3

SCHUEREMANS, L. & VAN GEMERT, D. (2005). Benefit of Splines and Neural Networks in Simulation Based Structural Reliability Analysis. *Structural Safety*, **27**, 246–261. 3.6.3

SIA 462 (1994). *Evaluation de la Sécurite Structurale des Ouvrages Existants*. Société Suisse des Ingénieurs et des Architectes, Zürich. 2.3.3

Siriaksorn, A. (1980). *Serviceability and Reliability Analysis of Partially Prestressed Concrete Beams*. Ph.D. thesis, University of Illinois at Chicago Circle. 4.5.3

Sobrino, J.A. (1993). *Evaluación del Comportamiento Funcional y de la Seguridad Estructural de Puentes Existentes de Hormigón Armado y Pretensado*. Ph.D. thesis, Technical University of Catalonia, Department of Construction Engineering. 1.1, 4.2.3, 4.3, 4.4, 4.3.1, 4.3.3, 4.10, 4.3.3, 4.3.3, 4.11, 4.3.3, 4.4.3, 4.18, 4.4.3, 4.4.3, 4.19, 4.20, 4.4.3, 4.5.1, 4.5.3, 4.27, 4.28, 6.3.2, 6.3, 6.3.2, 6.3.3, 6.4.2

Sobrino, J.A. & Casas, J.R. (1994). *Random System Response of Reinforced and Prestressed Concrete Bridges*. Balkema, Roterdam, iCOSSAR'93 - International Conference on Structural Safety and Reliability, Schueller, Shinozuka and Yao (eds). 7.3.3.2, 7.3.3.2

Spaethe, G. (1992). *Die Sicherheit Tragender Baukonstruktionen, Zweite Neubearbeitete Auflage*. Springer - Verlag, Wien, New York. 4.2.3, 4.2.3

Stewart, M.G. (1995). Workmanship and Its Influence on Probabilistic Models of Concrete Compressive Strength. *ACI Materials Journal*, **92**, 361–372. 4.2.3, 4.2.3

Strauss, A. (2003). *Stochastische Modellierung und Zuverlässigkeit von Betonkonstruktionen*. Ph.D. thesis, University of Applied Science and Natural Resources, Vienna, Department of Civil Engineering and Natural Hazards. 1.1, 4.3, 4.3.3, 4.10, 4.3.3, 4.4.3, 4.18, 4.4.3, 4.4.3

Sustainable Bridges (2006). *Guideline for Load and Resistance Assessment of Existing European Railway Bridges*. Sustainable Bridges - VI Framework Programme, Brussels. 2.3.2, 5.3.1

Tabsh, S.W. & Nowak, A.S. (1991). Reliability of Highway Girder Bridges. *Journal of Structural Engineering ASCE*, **117**, 2372–2373. 6.2.2, 6.3.2, 6.3.2, 7.2.5.2

Teigen, J.G., Frangopol, D.M., Sture, S. & Felippa, C. (1991). Probabilistic FEM for Nonlinear Concrete Structures. I: Theory. *Journal of Structural Engineering ASCE*, **117**, 2674–2689. 3.6.4

Thelandersson, S. (2004). *Assessment of Material Property Data for Structural Analysis of Nuclear Containments - Rapport TVBK-3051*. Lund University, Department of Structural Engineering. 4.3

Thoft-Christensen, P. & Murotsu, Y. (1986). *Application of Structural Systems Reliability Theory*. Springer-Verlag, Berlin. 7.3.3.1

Tsubaki, T. (1988). *Probabilistic Models*. John Wiley and Sons, chapter 5 in 'Mathematical Modelling of Creep and Shrinkage of Concrete' edited by Z.P Bazant. 9.3.5

Val, D., Bljuger, F. & Yankelevsky, D. (1996). Optimization Problem Solution in Reliability of Reinforced Concrete Structures. *Computers and Structures*, **60**, 351–355. 3.6.4

Val, D., Bljuger, F. & Yankelevsky, D. (1997). Reliability Evaluation in Nonlinear Analysis of Reinforced Concrete Structures. *Structural Safety*, **19**, 203–217. 3.6.4

Vecchio, F.J. & Collins, M.P. (1986). The Modified Compression-Field Theory for Reinforced Concrete Elements Subjected to Shear. *ACI Journal*, **83**, 219–231. 6.2.3, 6.4.2, 6.4.4, 9.2.3

Vejdirectoratet (1996). *Rules for Determination of the Load Carrying Capacity of Existing Bridges*. Road Directorate, Ministry of Transport - Denmark. 2.3.3

Vejdirectoratet (2004). *Reliability-Based Classification of the Load Carrying Capacity of Existing Bridges - Report 291*. Road Directorate, Ministry of Transport - Denmark. 2.3.3, 5.2.2, 5.3.1, 5.4.5, 7.2.5.1, 7.2.5.1

WAARTS, P.H. (2000). *Structural Reliability Using Finite Element Analysis. An Appraisal of DARS: Directional Adaptive Response Surface Sampling*. Ph.D. thesis, Delft University Press. 3.6.3

WIŚNIEWSKI, D.F. & CASAS, J.R. (2006). *Probabilistic Methods in the Safety Assessment of Existing Bridges: A Step-by-Step Process*. CSCE, Montreal, proceedings of the 7-th International Conference on Short and Medium Span Bridges. 7.1, 7.3.3.1, 8.1

WIŚNIEWSKI, D.F., BILISZCZUK, J. & CRUZ, P.J.S. (2004a). Mosty z Prefabrykatów z Betonu Spreżonego w Portugalii. *Inżynieria i Budownictwo*, **4/2004**, 188–193. 6.3.3

WIŚNIEWSKI, D.F., CRUZ, P.J.S. & HENRIQUES, A.A. (2004b). *Avaliação Probabilística dos Limites de Deformação de Pontes em Provas de Carga*. FEUP, Porto, Encontro Nacional, Betão Estrutural 2004. 9.3.3

WIŚNIEWSKI, D.F., CRUZ, P.J.S. & HENRIQUES, A.A. (2004c). *Probability Based Assessment of Acceptable Precast Girders Deflections for Proof Load Testing*. Balkema, Leiden, proceedings of the 2-nd International Conference on Bridge Maintenance Safety and Management, IABMAS´04. 9.3.3

WIŚNIEWSKI, D.F., HENRIQUES, A.A. & CRUZ, P.J.S. (2004d). *Avaliação da Segurança de Pontes de Betão Pré-fabricado*. FEUP, Porto, Encontro Nacional, Betão Estrutural 2004. 9.3.1

WIŚNIEWSKI, D.F., HENRIQUES, A.A. & CRUZ, P.J.S. (2004e). *Failure Analysis of Precast Concrete Highway Bridges*. Proceedings of the 1st International Conference on Engineering Failure Analysis, ICEFA-I 2004, Lisbon, Portugal. 9.3.1

WIŚNIEWSKI, D.F., HENRIQUES, A.A. & CRUZ, P.J.S. (2004f). *Probability Based Assessment of Serviceability Limit States in Precast Concrete Bridges*. Proceedings of the IABSE Symposium 'Metropolitan Habitants and Infrastructure', Shanghai, China. 9.3.1

Wiśniewski, D.F., Henriques, A.A. & Cruz, P.J.S. (2004g). *Safety and Serviceability of Precast Prestressed Concrete Bridges*. Proceedings of the 5th Conference on Small and Medium Span Bridges, Małe Mosty 2004, Wrocław, Poland. 9.3.1

Wiśniewski, D.F., Biliszczuk, J., Cruz, P.J.S. & Lopes, P.J.A. (2005). Prefabrykowane Elementy żelbetowe do Budowy Małych Mostów, Przepustów i Tuneli pod Nasypami w Portugalii. *Inżynieria i Budownictwo*, **4/2005**, 215–221. 6.3.3

Wiśniewski, D.F., Casas, J.R. & Bien, J. (2006a). Metody Oceny Niezawodności Eksploatowanych Mostów Kolejowych. *Inżynieria i Budownictwo*, **7-8/2006**, 378–384. 7.1, 7.3.3.1, 8.1

Wiśniewski, D.F., Casas, J.R. & Ghosn, M. (2006b). Load Capacity Evaluation of Existing Railway Bridges based on Robustness Quantification. *Structural Engineering International*, **16**, 161–166. 7.1, 7.3.3.2, 8.1

Wiśniewski, D.F., Ferreira, R.M. & Cruz, P.J.S. (2006c). *Properties of Ready-Mixed Concretes - Report 06-DEC/E-11*. University of Minho, Department of Civil Engineering. 4.2.4

Wiśniewski, D.F., Casas, J.R. & Ghosn, M. (2007). Simplified Probabilistic Non-linear Assessment of Existing Railway Bridges. *Structure and Infrastructure Engineering*, (submitted for publication). 7.1, 8.1

Appendix A

Variability of the properties of ready-mixed concretes

A.1 Introduction

In this appendix the results of statistical analysis of data of basic concrete properties are presented. The analysed data was collected and made available for this study by the concrete quality control laboratories of the two biggest precast concrete companies in Portugal - Civibral and Maprel, and one of the biggest civil engineering contractor - Mota-Engil. The data provided by Civibral corresponds to the company production of plant-cast concrete bridge girders manufactured during the years 2000 and 2001. The data provided by Maprel corresponds to the company production of plant-cast concrete elements manufactured during the years 2000 and 2001. However, data provided by Mota-Engil corresponds to the production of ready-mixed site-cast concrete used on the construction of bridges and culverts on the A11 highway connecting Braga and Guimarães on the north of Portugal. All the collected data regarding compressive strength of concrete at different ages (16 hours, 1 day, 3 days, 7 days and 28 days) and the volume weight of concrete were obtained during the ordinary tests performed for conformity purpose. The tests were realized on the concrete cube specimens with the dimensions, 15cm x 15cm x 15cm, according to the current standard (EN 206 Concrete: Specification, performance, production and conformity).

A.2 Experimental data

The following section resumes the results of statistical evaluation of data. In Tables A.1, A.3 and A.5 the minimum value X_{min}, maximum value X_{max}, mean value X_{mean}, and coefficient of variation CV of concrete compressive strength at different ages corresponding to concrete of different classes are presented. Furthermore, the numbers of samples N_{sampl} used in the analysis are showed.

The skewness and kurtosis of the distribution of analysed data are presented in Tables A.2, A.4 and A.6. Skewness characterizes the degree of asymmetry of a distribution around its mean (positive/negative skewness - distribution with an asymmetric tail extending toward more positive/negative values). Kurtosis characterizes the relative peakedness or flatness of a distribution compared with the normal distribution (positive/negative kurtosis - relatively peaked/flat distribution). Moreover, in Tables A.2, A.4 and A.6 the results of K-S Lilliefors goodness-of-fit test are showed. The parameters presented in tables are the significance interval for accepting or rejecting the null hypothesis saying that the observed distribution is not significantly different from a theoretical, normal or lognormal distribution (significance interval bigger than 0.05 means that the null hypothesis can not be rejected). In the last column of Tables A.2, A.4 and A.6 the correlation coefficient between the concrete compressive strength at different age and that at 28 days is also showed. The correlation coefficient is a dimensionless index, ranging from -1 to 1, that reflects the extent of a linear relationship between two parameters (-1/1 represent perfect negative/positive correlation, 0 represents lack of correlation).

Besides the K-S Lilliefors goodness-of-fit test the choice of the appropriate probability distribution function describing the best the concrete compressive strength was also confirmed by the histograms and P-P plots presented also in this section in Figures A.1 to A.16. Histograms show the frequency of occurrence of the results in specified intervals. P-P plots show the correspondence of the experimental results to the theoretical distribution function.

The basic statistics and characteristics of distribution described above for the case of concrete compressive strength were also obtained for concrete volume weight. The results are resumed in Tables A.7, A.8 and Figures A.17, A.18.

Compressive strength of concrete. Plant-cast concrete - Civibral.

Table A.1: Basic statistics of the concrete compressive strength.

Concrete class	Concr. age	Numb. N_{sampl}	Min. val. X_{min}	Max. val. X_{max}	Mean val. X_{mean}	Var. coef. CV
C35/45	16 hours	349	21.5	38.0	27.3	8.6
	3 days	390	28.0	47.6	35.8	9.1
	28 days	412	44.9	58.9	48.6	4.7
C40/50	16 hours	58	26.5	39.1	32.8	7.8
	3 days	126	36.5	47.3	41.3	5.3
	28 days	158	49.2	60.6	54.1	4.5
C45/55	16 hours	63	26.5	41.7	33.8	10.8
	3 days	99	33.6	45.1	41.3	5.7
	28 days	108	50.2	59.1	54.9	3.9

Note: In the table values of X_{min}, X_{max} and X_{mean} are in [MPa]; values of CV are in [%]

Table A.2: Distribution characteristics, goodness-of-fit test and correlations

Concrete class	Concrete age	Skew-ness	Kurto-sis	K-S test of normal.	K-S test of log-norm.	Correlation with f_{c28}
C35/45	16 hours	1.33	3.47	0.0000	0.0027	0.2269
	3 days	0.43	0.56	0.6703	0.7755	0.6338
	28 days	1.22	2.35	0.0096	0.0359	1.0000
C40/50	16 hours	0.47	0.24	0.1500	0.2293	0.3580
	3 days	0.42	0.07	0.6109	0.7915	0.4507
	28 days	0.37	-0.20	0.8173	0.8998	1.0000
C45/55	16 hours	0.37	-0.54	0.5436	0.7655	-0.1284
	3 days	-1.25	1.73	0.1294	0.0634	0.5177
	28 days	-0.63	-0.56	0.0012	0.0000	1.0000

Compressive strength at 28 days. Concrete C35/45 - Civibral.

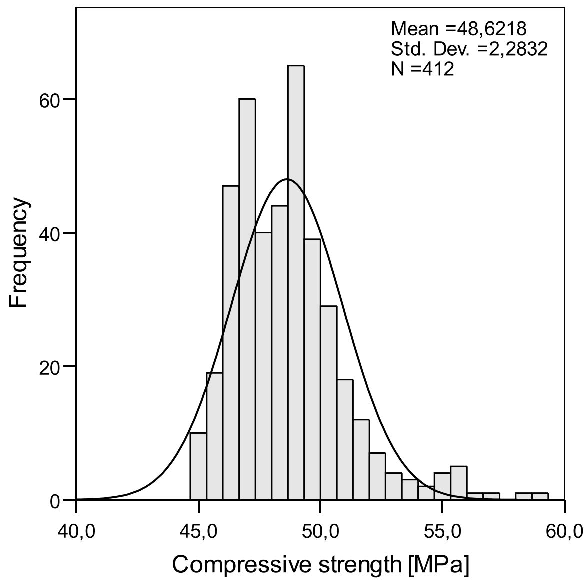

Figure A.1: Histogram of experimental data and Normal PDF.

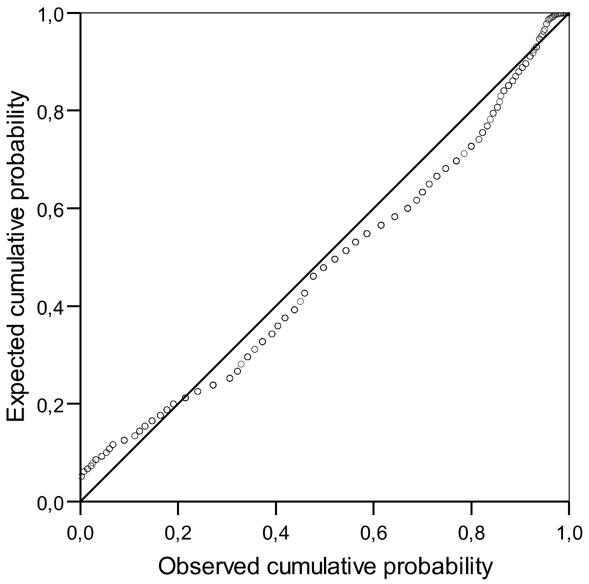

Figure A.2: Normal P-P plot (experimental vs. theoretical CDF).

Compressive strength at 28 days. Concrete C40/50 - Civibral.

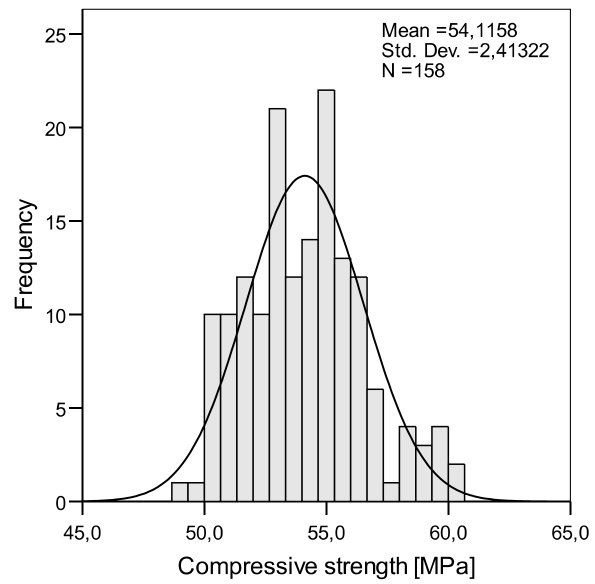

Figure A.3: Histogram of experimental data and Normal PDF.

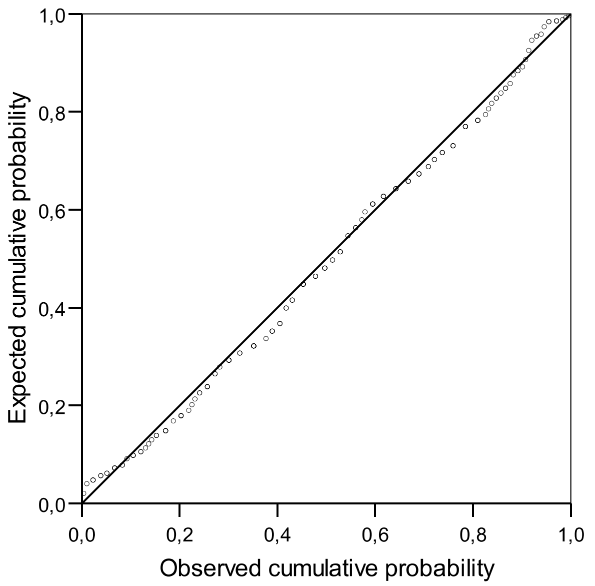

Figure A.4: Normal P-P plot (experimental vs. theoretical CDF).

Compressive strength at 28 days. Concrete C45/55 - Civibral.

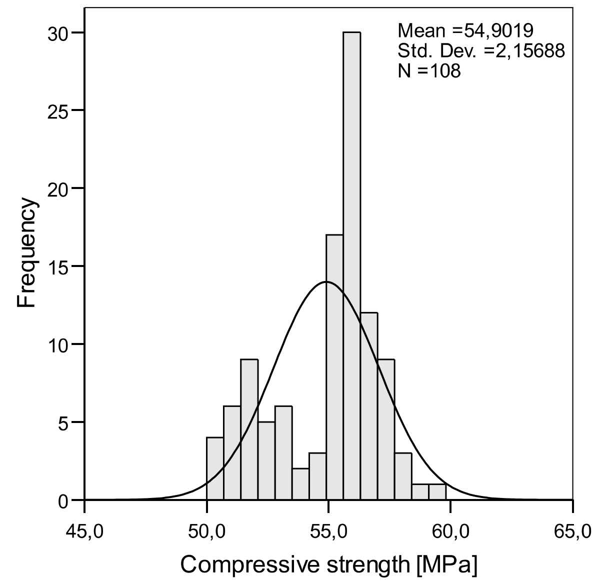

Figure A.5: Histogram of experimental data and Normal PDF.

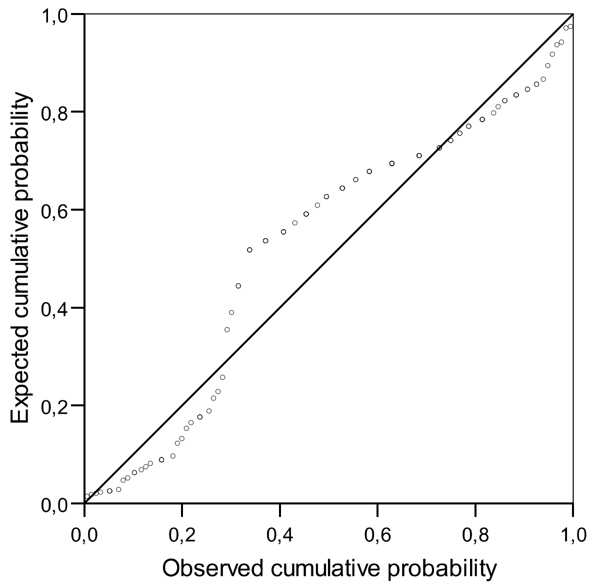

Figure A.6: Normal P-P plot (experimental vs. theoretical CDF).

Compressive strength of concrete. Plant-cast concrete - Maprel.

Table A.3: Basic statistics of the concrete compressive strength.

Concrete class	Concr. age	Numb. N_{sampl}	Min. val. X_{min}	Max. val. X_{max}	Mean val. X_{mean}	Var. coef. CV
C30/37	1 day	615	1.2	50.3	16.0	47.7
	3 days	130	19.2	45.9	31.1	13.5
	7 days	647	25.6	50.7	39.3	10.7
	28 days	1337	37.1	58.4	45.4	8.8
C45/55	1 day	385	13.1	49.8	37.4	13.1
	3 days	262	31.1	53.6	42.7	11.1
	7 days	209	38.4	63.0	49.4	8.1
	28 days	478	50.2	66.5	56.3	5.2

Note: In the table values of X_{min}, X_{max} and X_{mean} are in [MPa]; values of CV are in [%]

Table A.4: Distribution characteristics, goodness-of-fit test and correlations

Concrete class	Concrete age	Skew-ness	Kurto-sis	K-S test of normal.	K-S test of log-norm.	Correlation with f_{c28}
C30/37	1 day	2.03	4.65	0.0000	0.0000	0.2077
	3 days	0.53	1.49	0.9752	0.9971	0.4513
	7 days	0.25	-0.33	0.0612	0.5407	0.8232
	28 days	0.57	-0.21	0.0000	0.0029	1.0000
C45/55	1 day	-1.00	3.28	0.1459	0.0014	0.2339
	3 days	0.18	-0.56	0.7507	0.9268	0.3063
	7 days	0.38	0.40	0.5021	0.8696	0.6460
	28 days	0.63	0.86	0.0412	0.1330	1.0000

Compressive strength at 28 days. Concrete C30/37 - Maprel.

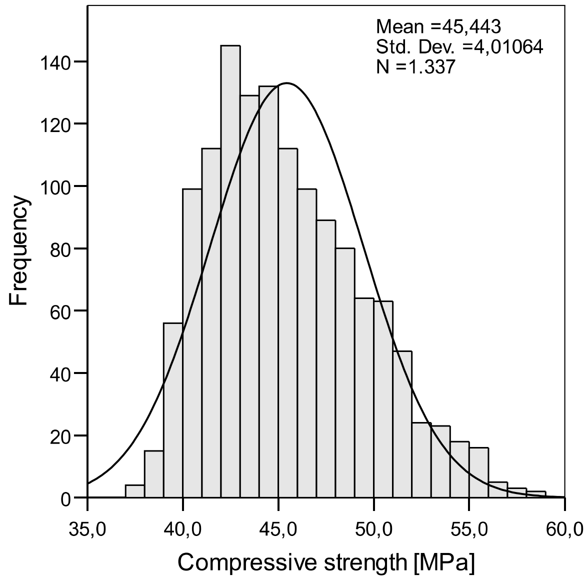

Figure A.7: Histogram of experimental data and Normal PDF.

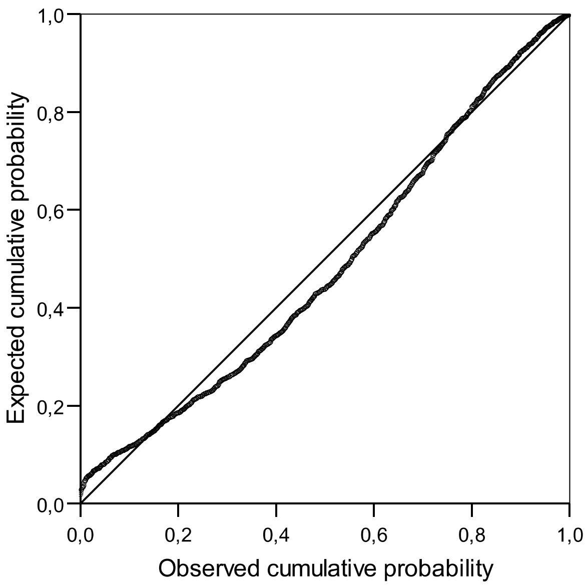

Figure A.8: Normal P-P plot (experimental vs. theoretical CDF).

Compressive strength at 28 days. Concrete C45/55 - Maprel.

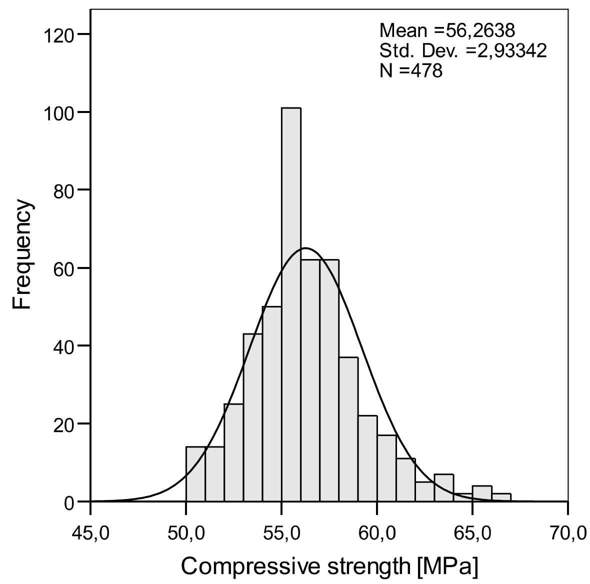

Figure A.9: Histogram of experimental data and Normal PDF.

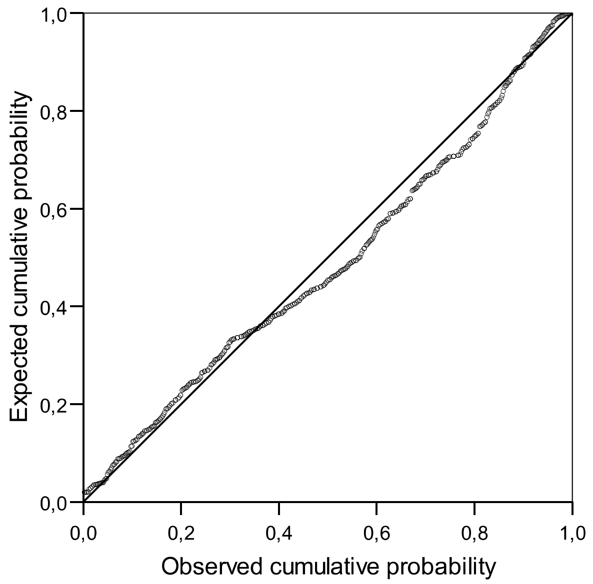

Figure A.10: Normal P-P plot (experimental vs. theoretical CDF).

Compressive strength of concrete. Site-cast concrete - Mota-Engil.

Table A.5: Basic statistics of the concrete compressive strength.

Concrete class	Concr. age	Numb. N_{sampl}	Min. val. X_{min}	Max. val. X_{max}	Mean val. X_{mean}	Var. coef. CV
C25/30	7 days	243	24.2	38.3	29.7	9.3
	28 days	486	32.1	45.6	37.8	7.7
C30/37	7 days	444	32.1	46.7	36.6	5.9
	28 days	892	37.4	58.8	43.8	7.5
C40/50	7 days	265	39.2	61.4	51.0	7.6
	28 days	534	52.2	68.4	59.2	5.8

Note: In the table values of X_{min}, X_{max} and X_{mean} are in [MPa]; values of CV are in [%]

Table A.6: Distribution characteristics, goodness-of-fit test and correlations

Concrete class	Concrete age	Skew-ness	Kurto-sis	K-S test of normal.	K-S test of log-norm.	Correlation with f_{c28}
C25/30	7 days	0.59	-0.39	0.1201	0.2062	0.5966
	28 days	0.30	-0.60	0.0773	0.2634	1.0000
C30/37	7 days	0.68	1.38	0.2835	0.6469	0.7943
	28 days	0.89	1.12	0.0000	0.0022	1.0000
C40/50	7 days	0.37	-0.15	0.6073	0.5779	0.7256
	28 days	0.41	-0.35	0.1561	0.3660	1.0000

Compressive strength at 28 days. Concrete C25/30 - Mota-Engil.

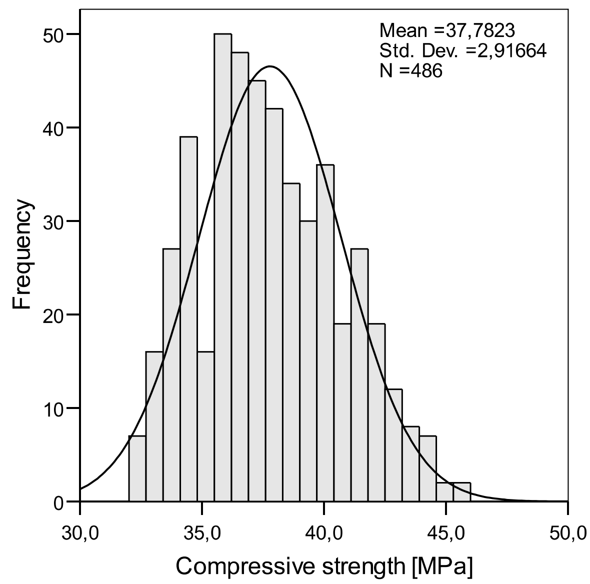

Figure A.11: Histogram of experimental data and Normal PDF.

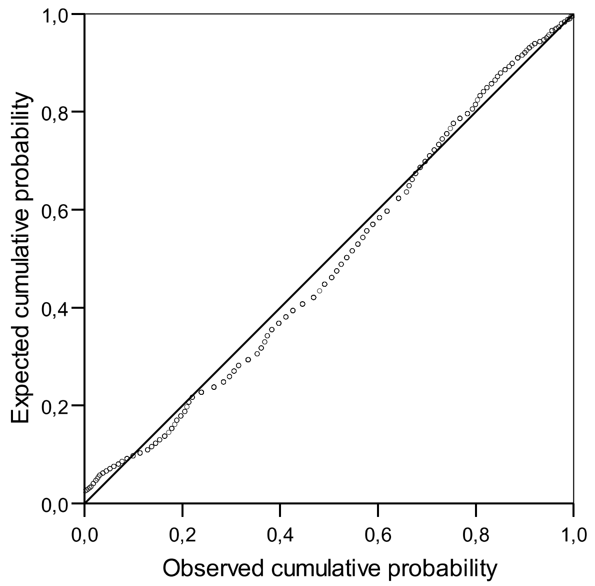

Figure A.12: Normal P-P plot (experimental vs. theoretical CDF).

Compressive strength at 28 days. Concrete C30/37 - Mota-Engil.

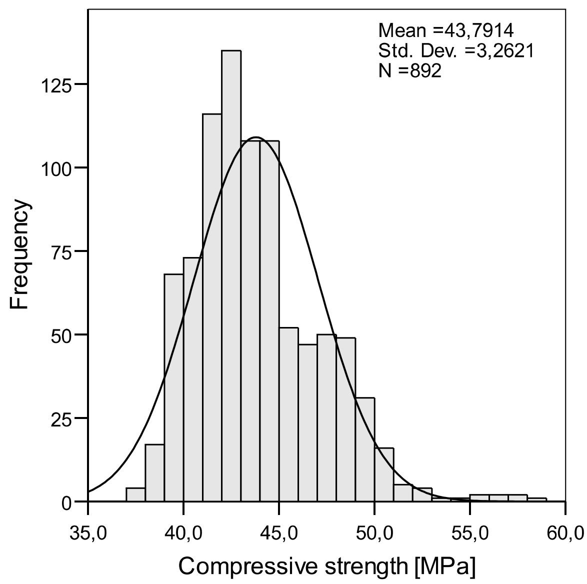

Figure A.13: Histogram of experimental data and Normal PDF.

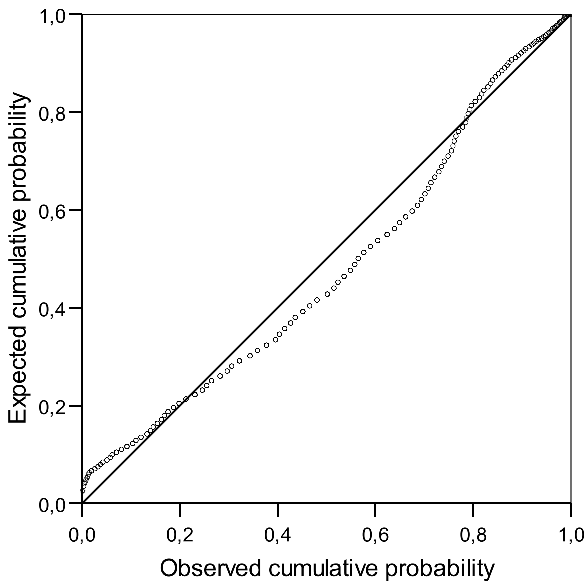

Figure A.14: Normal P-P plot (experimental vs. theoretical CDF).

Compressive strength at 28 days. Concrete C40/45 - Mota-Engil.

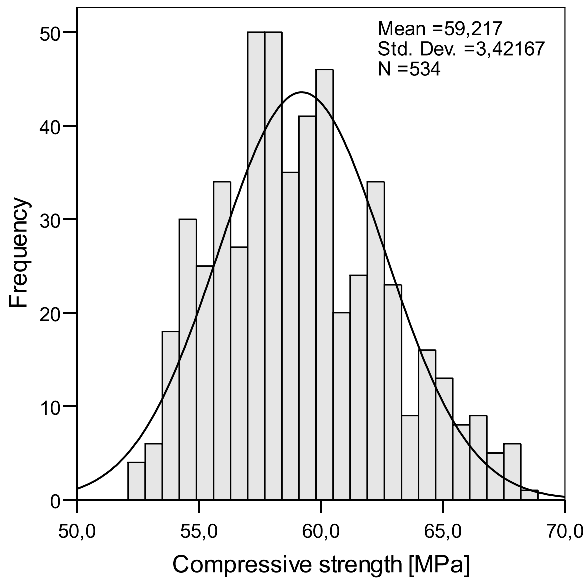

Figure A.15: Histogram of experimental data and Normal PDF.

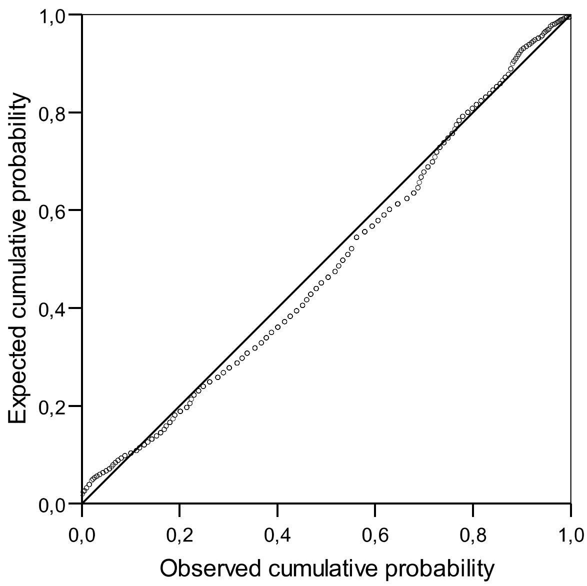

Figure A.16: Normal P-P plot (experimental vs. theoretical CDF).

Volume weight of concrete. Ready-mixed plant-cats and site-cast concretes.

Table A.7: Basic statistics of the concrete volume weight.

Concrete producer	Concr. class	Numb. N_{sampl}	Min. val. X_{min}	Max. val. X_{max}	Mean val. X_{mean}	Var. coef. CV
Civibral	C35/45	1166	2367	2507	2434	1.0
	C40/50	354	2381	2504	2428	0.9
	C45/55	282	2356	2462	2399	0.8
Maprel	C30/37	2729	2289	2485	2388	0.9
	C45/55	1430	2356	2483	2424	0.8
Engil	C25/30	729	2323	2486	2413	1.1
	C30/37	1368	2308	2519	2422	1.1
	C40/50	904	2370	2521	2464	0.9
All prod.	All clas.	8962	2289	2521	2417	1.3

Note: In the table values of X_{min}, X_{max} and X_{mean} are in [kg/m^3]; values of CV are in [%]

Table A.8: Distribution characteristics, goodness-of-fit test and correlations

Concrete producer	Concrete class	Skew-ness	Kurto-sis	K-S test of normal.	K-S test of log-norm.	Correlation with f_{c28}
Civibral	C35/45	-0.24	-0.16	0.0023	0.0017	0.1788
	C40/50	0.40	-0.45	0.0171	0.0176	0.1243
	C45/55	0.43	-0.02	0.0581	0.0627	0.1593
Maprel	C30/37	0.21	1.31	0.0000	0.0000	0.3810
	C45/55	0.16	-0.01	0.0050	0.0076	0.1450
Engil	C25/30	-0.56	0.65	0.0000	0.0000	0.3771
	C30/37	-0.45	1.14	0.0000	0.0000	0.2695
	C40/50	-0.34	0.54	0.0041	0.0029	0.2765
All prod.	All clas.	0.16	-0.24	0.0000	0.0000	0.4842

Volume weight of concrete. Ready-mixed plant-cats and site-cast concretes.

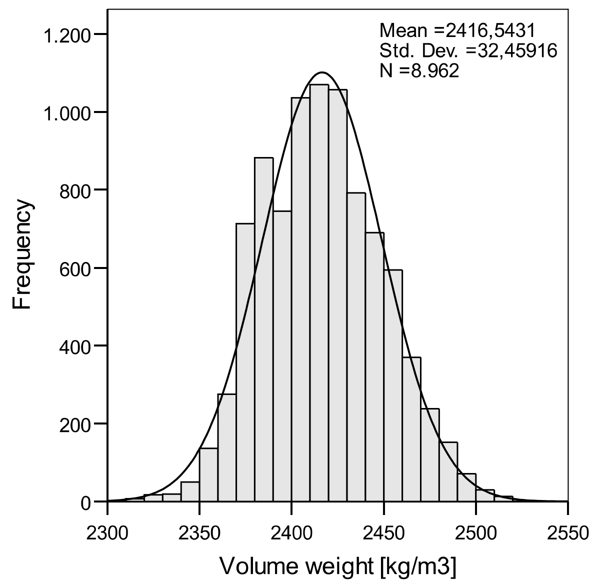

Figure A.17: Histogram of experimental data and Normal PDF.

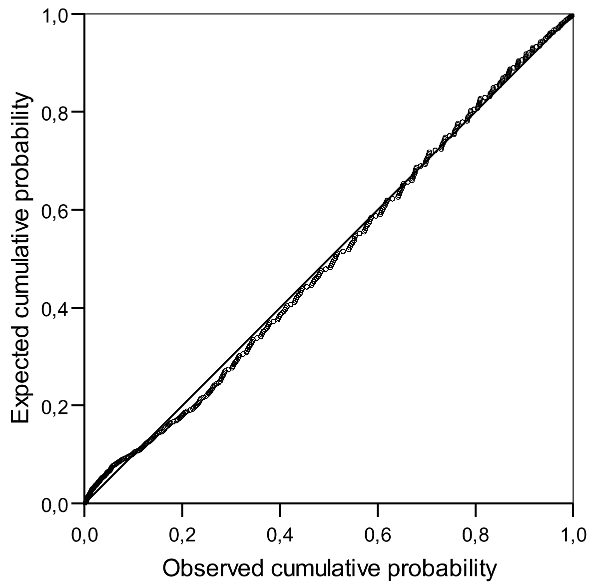

Figure A.18: Normal P-P plot (experimental vs. theoretical CDF).

A.3 Conclusions

The analysis of results of statistical evaluation of data regarding concrete compressive strength at various ages and concrete volume weight, presented in previous section, leads to the following conclusions:

- The mean value of concrete compressive strength at 28 days is close to expected for all concrete classes. However, for concrete C45/55 the mean compressive concrete strength is a bit smaller than expected. This is probably due to the lack of correspondence between concrete class C45/55 defined by the Eurocode and the class B50 defined in Portuguese code.
- The variation of results obtained during the compression tests for each concrete class is very small. The coefficient of variation of concrete compressive strength at 28 days is always smaller than 10% and usually oscillates around 5-7%.
- The variability of concrete compressive strength is smaller for concretes of higher classes.
- Easy to notice is the expected bigger variability of strength properties of younger concretes.
- The coefficient of variation of concrete compression strength at certain concrete age for younger concretes depends probably more on curing conditions and/or concrete composition than on concrete class.
- The variability of compressive strength of plant-cast concrete is usually slightly smaller than that of site-cast concrete.
- The lognormal distribution function usually better approximate the observed distribution of concrete compressive strength. However the normal distribution function was also found appropriate for modelling the distribution of that concrete property.
- The correlation between concretes in different ages is easier to notice for concretes at 3 days (or 7 days) and 28 days. The correlation between concrete at 16 hours (or 1 day) and 28 days is negligible.

- The mean value of concrete volume weight obtained in the analysis of all the data is equal to 2417 kg/m^3.
- The variation of results of concrete volume weight measured by coefficient of variation is equal to 1.3%.
- The mean value and the coefficient of variation of concrete volume weight depend probably more on the concrete aggregate composition than on other factors (class, age or producer).
- The normal distribution function seems appropriate to model the probability distribution of concrete volume weight.
- The correlation between the concrete volume weight and the concrete compressive strength at 28 days is negligible.

Appendix B

Variability of the properties of reinforcing steel bars

B.1 Introduction

In this appendix the results of statistical evaluation of data from standard quality test of steel reinforcing bars are presented. The data used in the statistical analysis was collected by the Department of Civil Engineering of the University of Coimbra during several years on some bridge construction sites in the neighbourhood of Coimbra. The collected data represents the properties of ordinary steel reinforcing bars of several batches and several bars from the same batch. Most probably it corresponds also to different producers and producing units. The tests were performed in the Laboratory of Testing of Materials and Structures of University of Coimbra according to the current standards (E450-1998 Varões de aço A500 NR para armaduras de betão armado, caracteristìcas, ensaios e marcação; E460-2002 Varões de aço A500 NR de ductilidade especial para armaduras de betão armado, caracteristìcas, ensaios e marcação).

B.2 Experimental data

The following section resumes results of statistical evaluation of data performed regarding mechanical parameters of reinforcing bars of normal (NR) and special (NRSD) ductility S500 grade steel. The data corresponds to bars of various diameters starting from 10 mm up to 32 mm. The analysed characteristic parameters are: yield strength f_{sy}, ultimate tensile strength f_{su}, ratio f_{sy}/f_{su}, modulus of elasticity E_s, strain at ultimate load ϵ_{su}, cross-sectional area A_s and ratio $A_{s,real}/A_{s,nominal}$.

In Tables B.1 and B.2 mean values and standard deviations of most of the above-mentioned characteristic parameters are presented, respectively for different steel ductility types and different bar diameters. As it can be seen the bar diameter does not show any influence on the basic statistics of steel properties. Therefore, in further statistical analysis the data corresponding to different bar diameters are evaluated together. Despite the fact that the steel ductility type does not also show clear influence on the steel properties, the data corresponding to steels of normal and special ductility are evaluated separately.

In Tables B.3 and B.5 the minimum value X_{min}, maximum value X_{max}, mean value X_{mean}, and coefficient of variation CV of characteristic parameters of steels S500 NR and S500 NRSD are presented. Furthermore, the numbers of samples N_{sampl} used in the statistical analysis are showed.

The skewness and kurtosis of the distribution of analysed data are presented in Tables B.4 and B.6. Skewness characterizes the degree of asymmetry of a distribution around its mean (positive/negative skewness - distribution with an asymmetric tail extending toward more positive/negative values). Kurtosis characterizes the relative peakedness or flatness of a distribution compared with the normal distribution (positive/negative kurtosis - relatively peaked/flat distribution). Moreover, in Tables B.4 and B.6 the results of K-S Lilliefors goodness-of-fit test are showed. The parameters presented in tables are the significance interval for accepting or rejecting the null hypothesis saying that the observed distribution is not significantly different from a theoretical, normal or lognormal distribution (significance interval bigger than 0.05 means that the null hypothesis can not be rejected). In the last column of Tables B.4 and B.6 the correlation coefficient between several properties of steel reinforcing bars and theirs yield strength is also showed. The correlation coefficient is a dimensionless index, ranging from -1 to 1, that reflects the extent of a linear relationship between two parameters (-1/1 represent perfect negative/positive correlation, 0 represents lack of correlation).

Besides the K-S Lilliefors goodness-of-fit test the choice of the appropriate probability distribution function describing the best the reinforcing steel properties was also confirmed by the histograms and P-P plots presented also in this section in Figures B.1–B.12 and B.14–B.25. Histograms show the frequency of occurrence of the results in specified intervals. P-P plots show the correspondence of the experimental results to the theoretical distribution function.

The correlation plots showing correlations between various steel properties and steel yielding strength are presented in Figures B.13 and B.26

B. Variability of the properties of reinforcing steel bars

Properties of reinforcing bars. Grade S500 NR - All diameters.

Table B.1: Basic statistics of the properties of reinforcing bars.

Steel Property	Distr. param.	Bar diameter 10	12	16	20	25	32
Yield strength f_{sy} [MPa]	Mean	592	606	601	594	610	620
	St. dev.	38	37	35	31	37	30
Ultimate strength f_{su} [MPa]	Mean	676	698	704	697	711	751
	St. dev.	46	42	41	31	36	26
Elasticity modulus E_s [GPa]	Mean	200	206	207	203	204	200
	St. dev.	7	11	12	7	9	2
Ultimate strain ϵ_s [%]	Mean	13.2	13.0	12.8	14.8	14.0	15.0
	St. dev.	2.0	3.1	3.1	3.8	3.4	4.0
Area A_s [mm^2]	Mean	70	103	183	296	464	726
	St. dev.	2	4	8	9	14	31

Properties of reinforcing bars. Grade S500 NR SD - All diameters.

Table B.2: Basic statistics of the properties of reinforcing bars.

Steel Property	Distr. param.	Bar diameter 10	12	16	20	25	32
Yield strength f_{sy} [MPa]	Mean	—	562	589	592	568	586
	St. dev.	—	32	40	23	22	27
Ultimate strength f_{su} [MPa]	Mean	—	674	699	691	685	712
	St. dev.	—	26	51	14	21	27
Elasticity modulus E_s [GPa]	Mean	—	201	201	201	200	200
	St. dev.	—	2	1	3	2	2
Ultimate strain ϵ_s [%]	Mean	—	15.1	11.6	10.9	14.6	11.2
	St. dev.	—	1.7	0.9	1.0	2.8	1.1
Area A_s [mm^2]	Mean	—	103	184	302	475	774
	St. dev.	—	3	11	5	7	20

Properties of reinforcing bars. Grade S500 NR - All diameters.

Table B.3: Basic statistics of the properties of reinforcing bars.

Steel Property	Numb. N_{sampl}	Min. val. X_{min}	Max. val. X_{max}	Mean val. X_{mean}	COV CV
Yield strength f_{sy}	398	507 MPa	723 MPa	603 MPa	6.0 %
Ultimate strength f_{su}	398	573 MPa	822 MPa	703 MPa	5.9 %
Ratio f_{su}/f_{sy}	398	1.00	1.32	1.17	3.3 %
Elasticity modulus E_s	290	179 GPa	237 GPa	205 GPa	4.9 %
Ultimate strain ϵ_s	380	6.2 %	26.0 %	13.5 %	24.5 %
Ratio $A_{s,real}/A_{s,nominal}$	398	0.82	1.00	0.92	4.3 %

Table B.4: Distribution characteristics, goodness-of-fit test and correlations

Steel Property	Skew-ness	Kur-tosis	K-S test of normal.	K-S test of log-norm.	Correlation with f_{sy}
Yield strength f_{sy}	0.25	-0.02	0.4653	0.8222	1.0000
Ultimate strength f_{su}	0.10	-0.23	0.3006	0.2410	0.8504
Ratio f_{su}/f_{sy}	0.61	1.98	0.0557	0.1069	-0.2884
Elasticity modulus E_s	1.50	2.03	0.0000	0.0000	0.0703
Ultimate strain ϵ_s	0.83	0.96	0.0767	0.9698	0.0761
Ratio $A_{s,real}/A_{s,nominal}$	-0.18	-0.68	0.5368	0.4311	-0.4076

Steel grade S500 NR - All bar diameters. Yield strength.

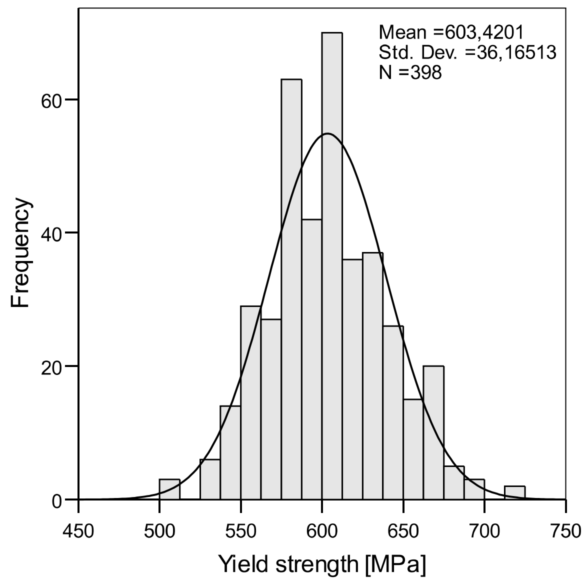

Figure B.1: Histogram of experimental data and Normal PDF.

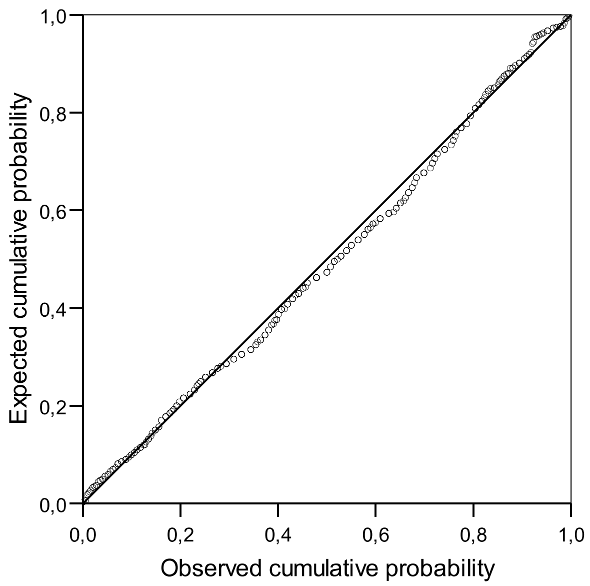

Figure B.2: Normal P-P plot (experimental vs. theoretical CDF).

Steel grade S500 NR - All bar diameters. Ultimate strength.

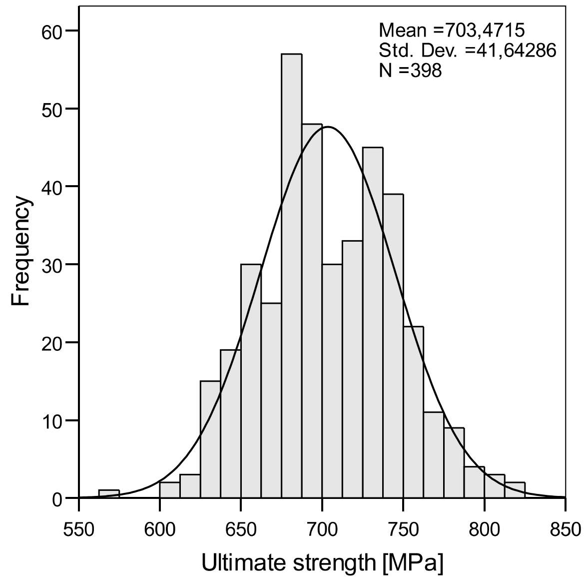

Figure B.3: Histogram of experimental data and Normal PDF.

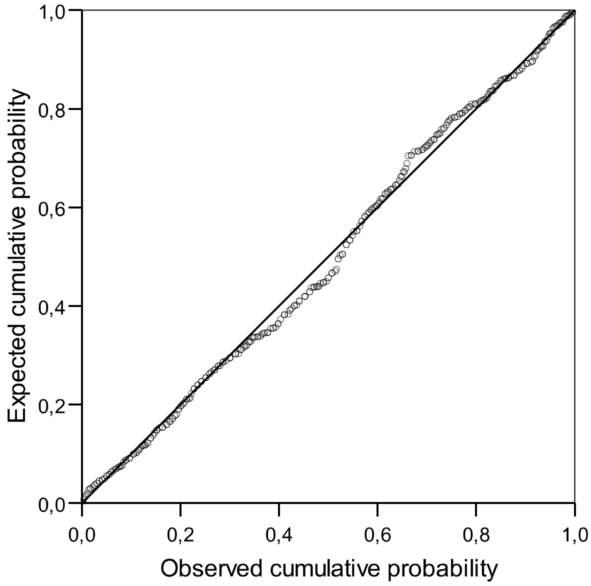

Figure B.4: Normal P-P plot (experimental vs. theoretical CDF).

Steel grade S500 NR - All bar diameters. Ratio ultimate/yield strengths.

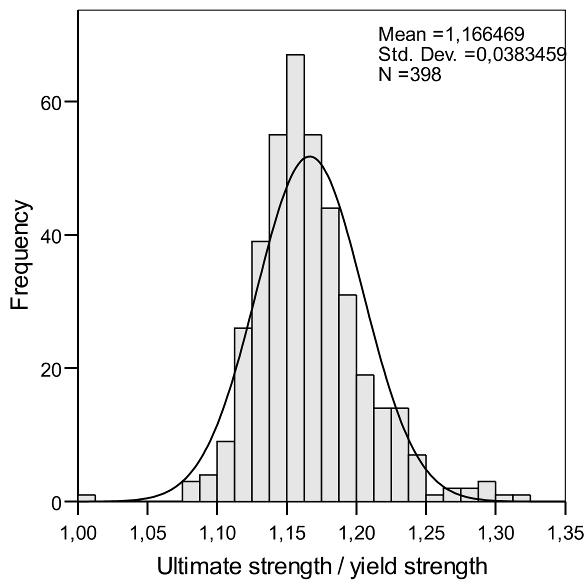

Figure B.5: Histogram of experimental data and Normal PDF.

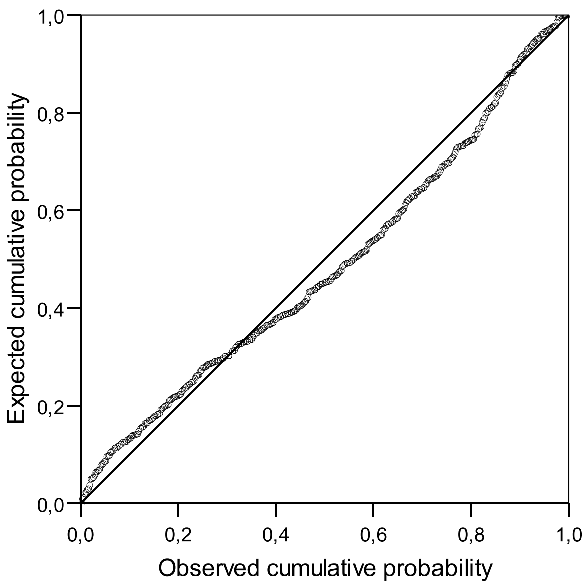

Figure B.6: Normal P-P plot (experimental vs. theoretical CDF).

Steel grade S500 NR - All bar diameters. Elasticity modulus.

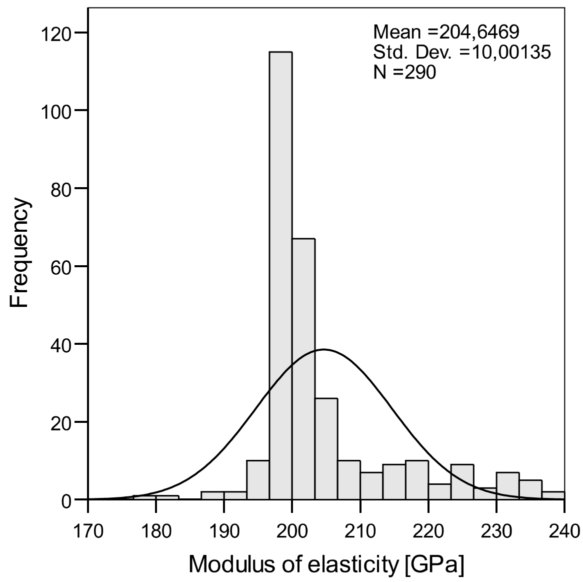

Figure B.7: Histogram of experimental data and Normal PDF.

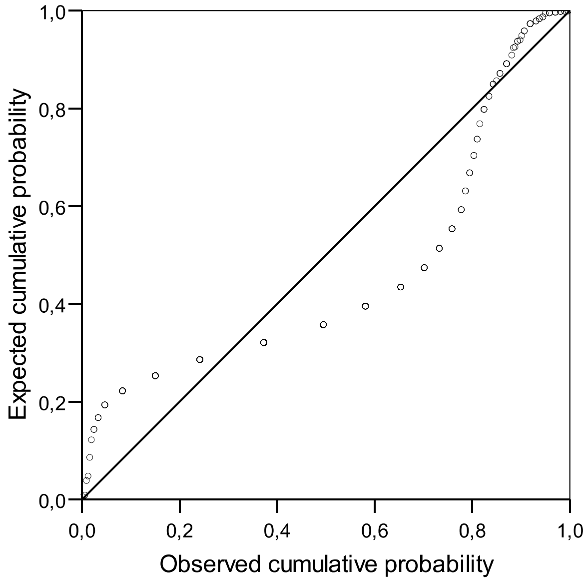

Figure B.8: Normal P-P plot (experimental vs. theoretical CDF).

Steel grade S500 NR - All bar diameters. Strain at ultimate load.

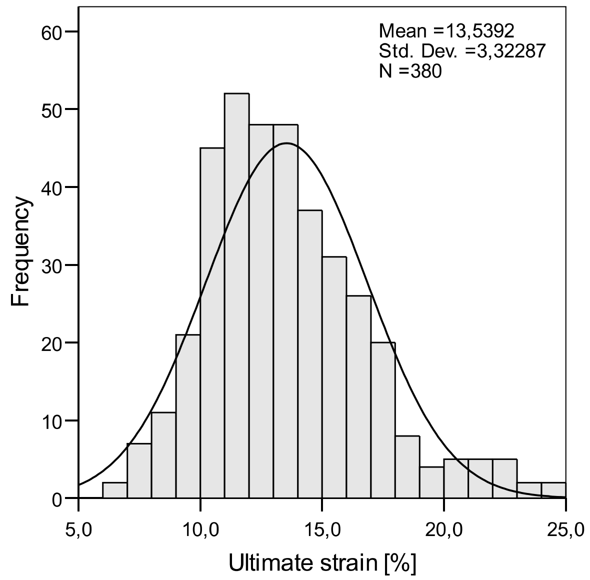

Figure B.9: Histogram of experimental data and Normal PDF.

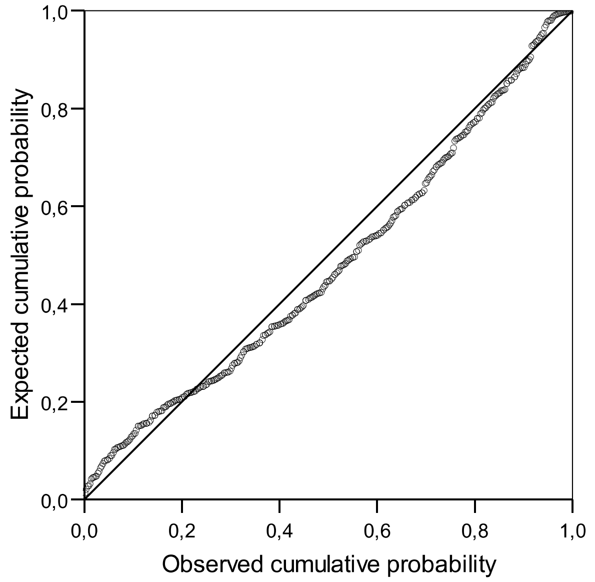

Figure B.10: Normal P-P plot (experimental vs. theoretical CDF).

Steel grade S500 NR - All bar diameters. Real/nominal area.

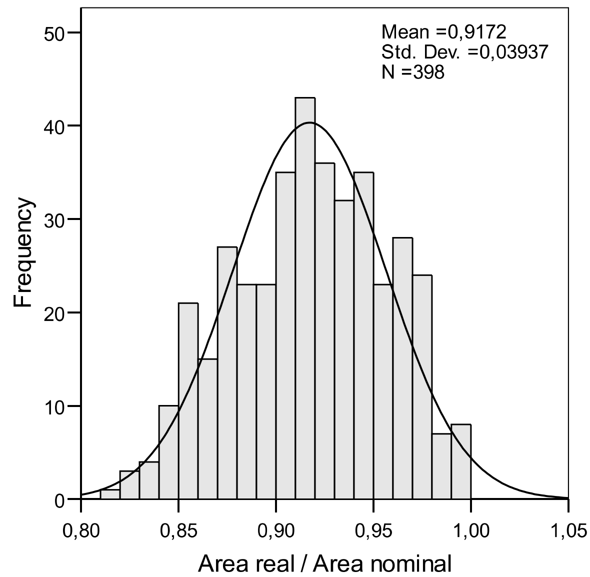

Figure B.11: Histogram of experimental data and Normal PDF.

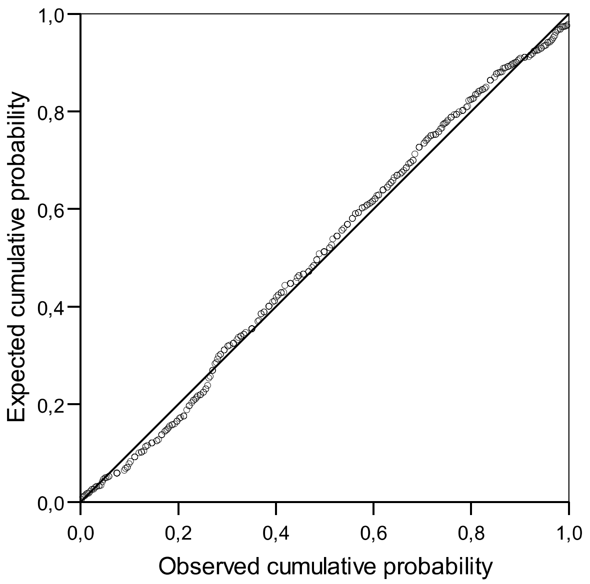

Figure B.12: Normal P-P plot (experimental vs. theoretical CDF).

Steel grade S500 NR - All bar diameters. Correlations.

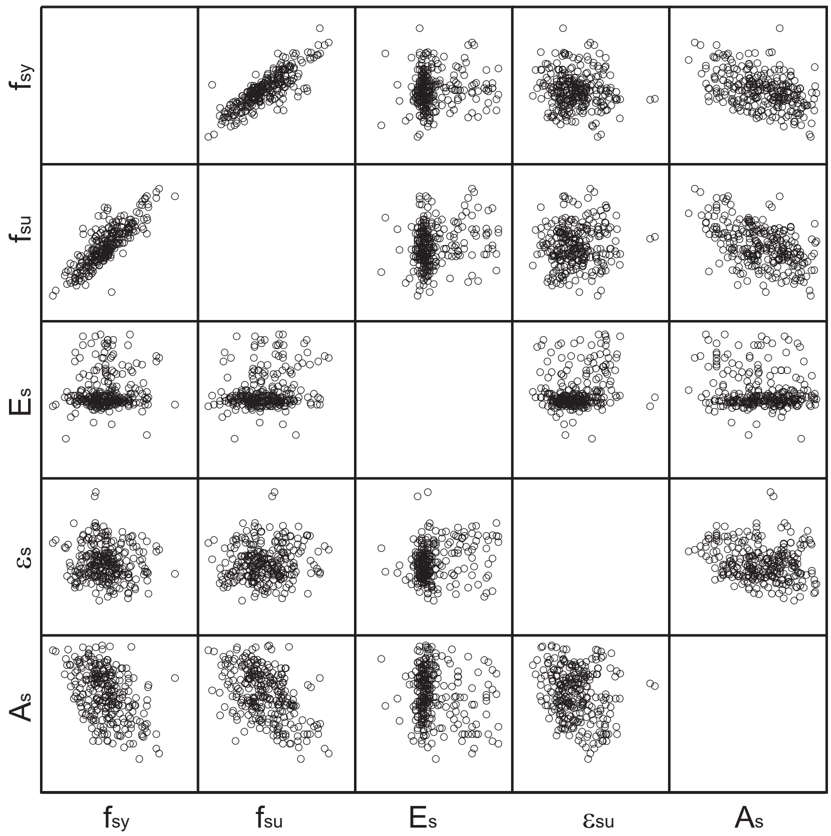

Figure B.13: Correlation matrix.

Properties of reinforcing bars. Grade S500 NR SD - All diameters.

Table B.5: Basic statistics of the properties of reinforcing bars.

Steel Property	Numb. N_{sampl}	Min. val. X_{min}	Max. val. X_{max}	Mean val. X_{mean}	COV CV
Yield strength f_{sy}	70	507 MPa	667 MPa	578 MPa	5.5 %
Ultimate strength f_{su}	70	622 MPa	795 MPa	691 MPa	4.9 %
Ratio f_{su}/f_{sy}	70	1.13	1.28	1.20	2.8 %
Elasticity modulus E_s	62	195 GPa	208 GPa	201 GPa	1.0 %
Ultimate strain ϵ_s	66	9.6 %	19.9 %	13.1 %	19.2 %
Ratio $A_{s,real}/A_{s,nominal}$	70	0.83	0.99	0.94	4.4 %

Table B.6: Distribution characteristics, goodness-of-fit test and correlations

Steel Property	Skew-ness	Kur-tosis	K-S test of normal.	K-S test of log-norm.	Correlation with f_{sy}
Yield strength f_{sy}	0.11	0.18	0.9496	0.9640	1.0000
Ultimate strength f_{su}	0.45	0.67	0.6618	0.7786	0.8638
Ratio f_{su}/f_{sy}	0.37	-0.05	0.1622	0.2005	-0.4906
Elasticity modulus E_s	0.75	4.12	0.0045	0.0043	0.2724
Ultimate strain ϵ_s	0.77	-0.37	0.0454	0.1228	-0.4240
Ratio $A_{s,real}/A_{s,nominal}$	-0.85	-0.18	0.0906	0.0848	-0.4035

Steel grade S500 NR SD - All bar diameters. Yield strength.

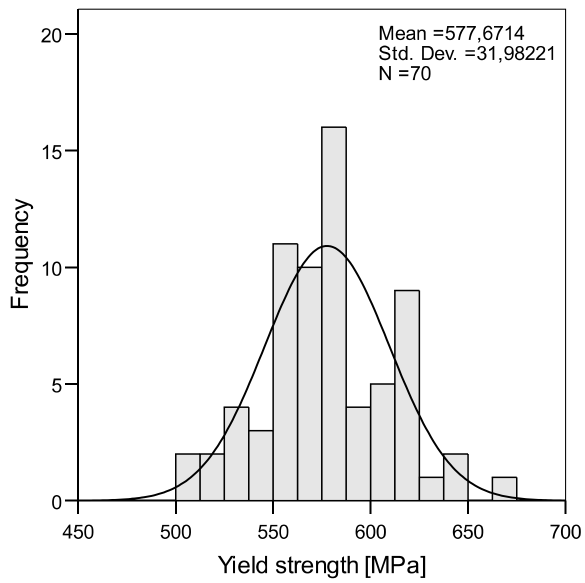

Figure B.14: Histogram of experimental data and Normal PDF.

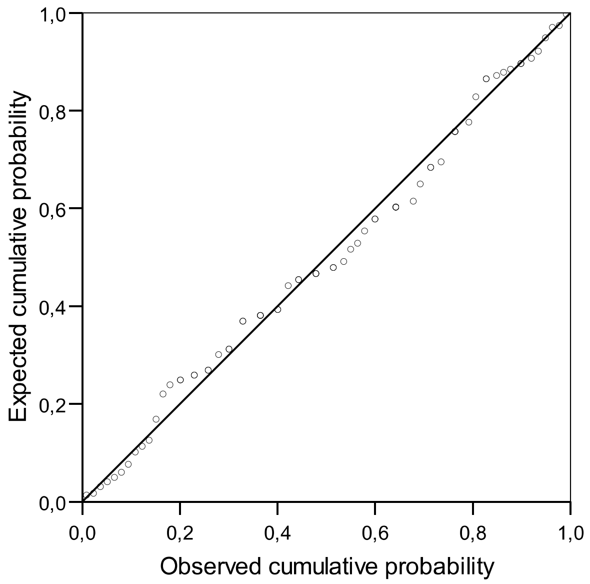

Figure B.15: Normal P-P plot (experimental vs. theoretical CDF).

Steel grade S500 NR SD - All bar diameters. Ultimate strength.

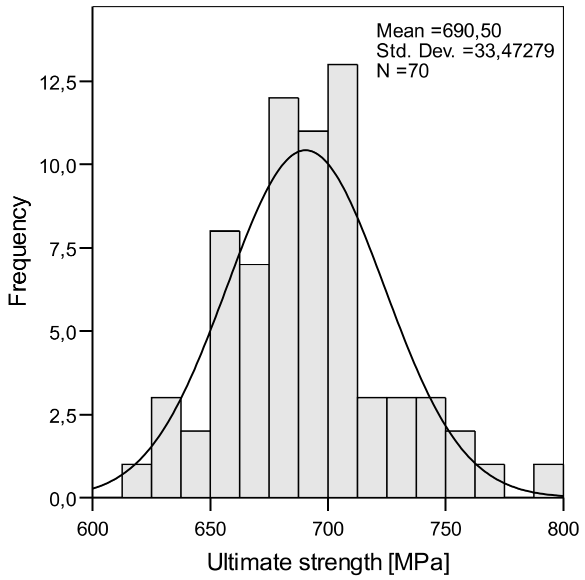

Figure B.16: Histogram of experimental data and Normal PDF.

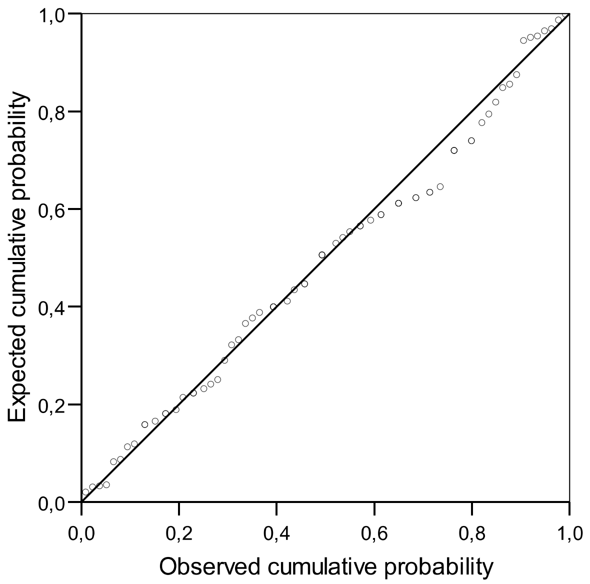

Figure B.17: Normal P-P plot (experimental vs. theoretical CDF).

Steel grade S500 NR SD - All bar diameters. Ratio ultimate/yield strengths.

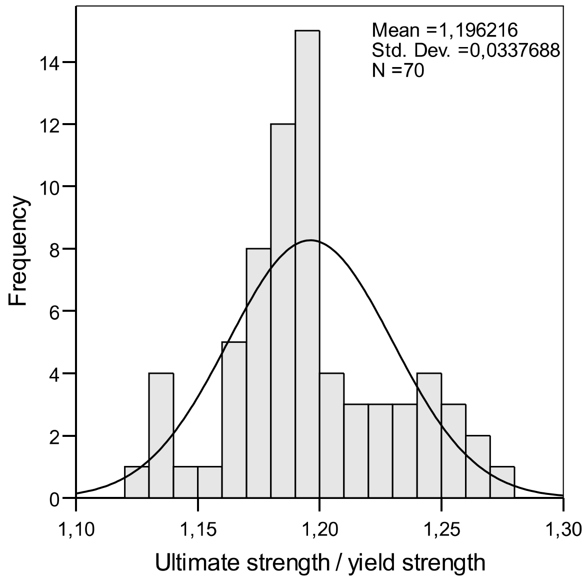

Figure B.18: Histogram of experimental data and Normal PDF.

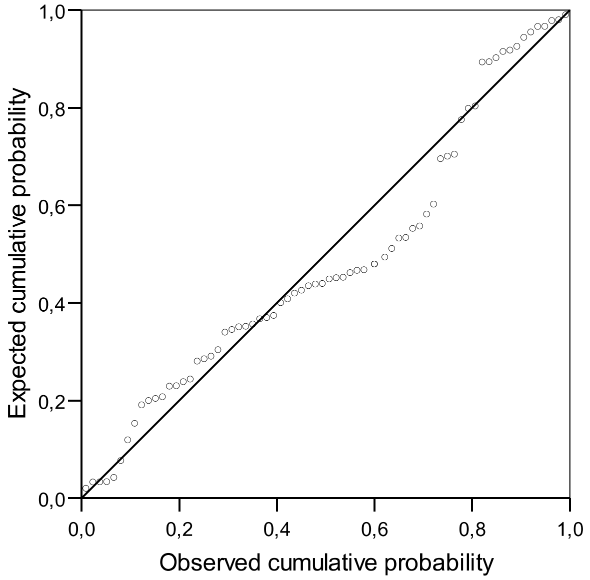

Figure B.19: Normal P-P plot (experimental vs. theoretical CDF).

Steel grade S500 NR SD - All bar diameters. Elasticity modulus.

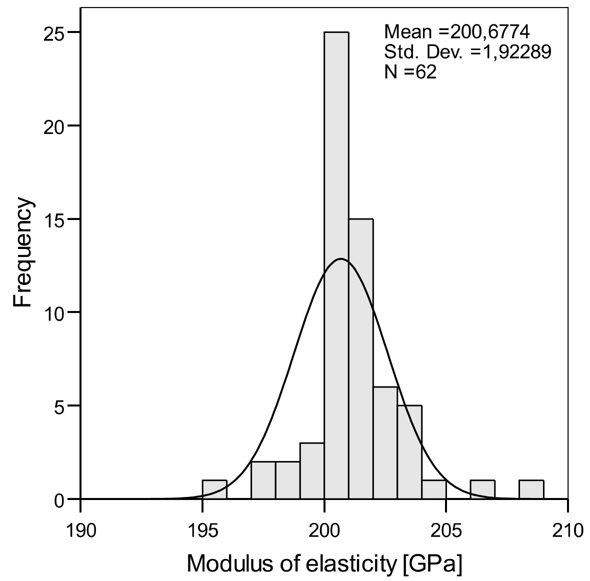

Figure B.20: Histogram of experimental data and Normal PDF.

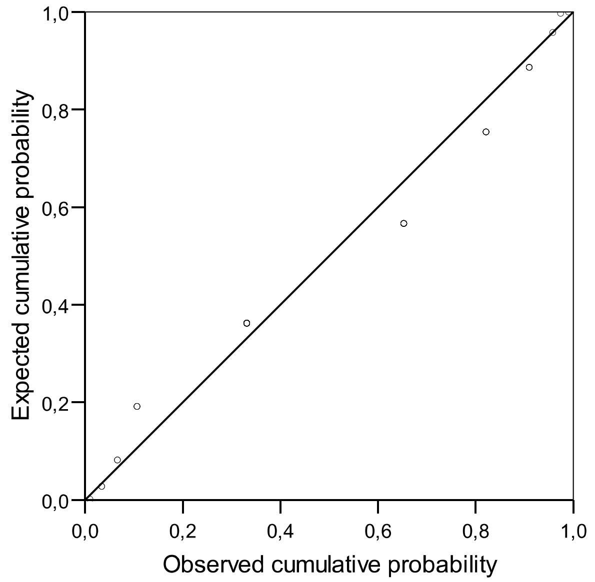

Figure B.21: Normal P-P plot (experimental vs. theoretical CDF).

Steel grade S500 NR SD - All bar diameters. Strain at ultimate load.

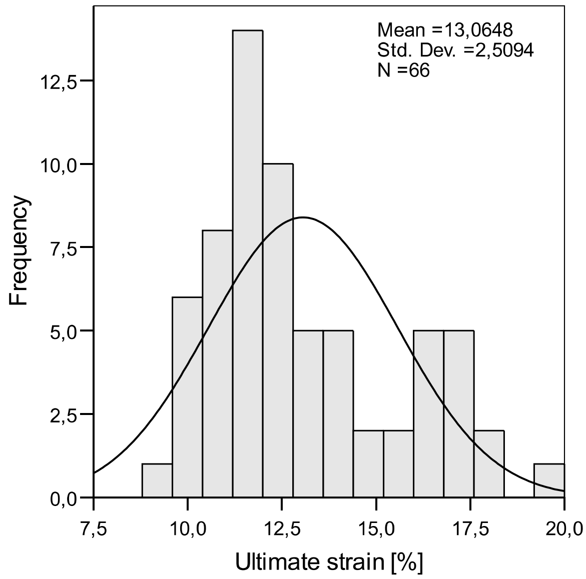

Figure B.22: Histogram of experimental data and Normal PDF.

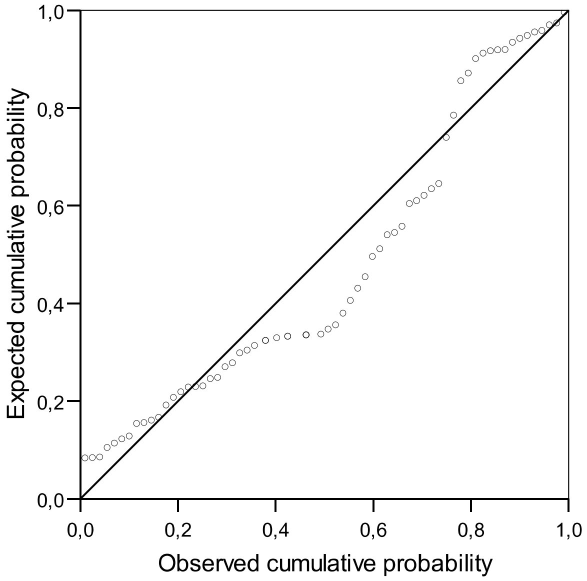

Figure B.23: Normal P-P plot (experimental vs. theoretical CDF).

Steel grade S500 NR SD - All bar diameters. Real/nominal area.

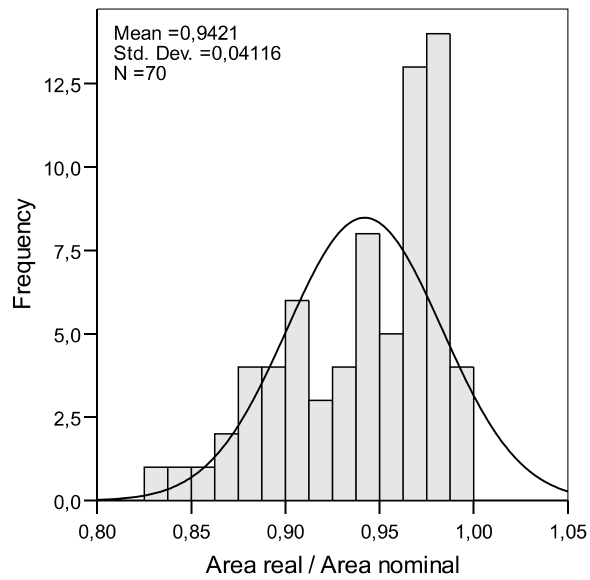

Figure B.24: Histogram of experimental data and Normal PDF.

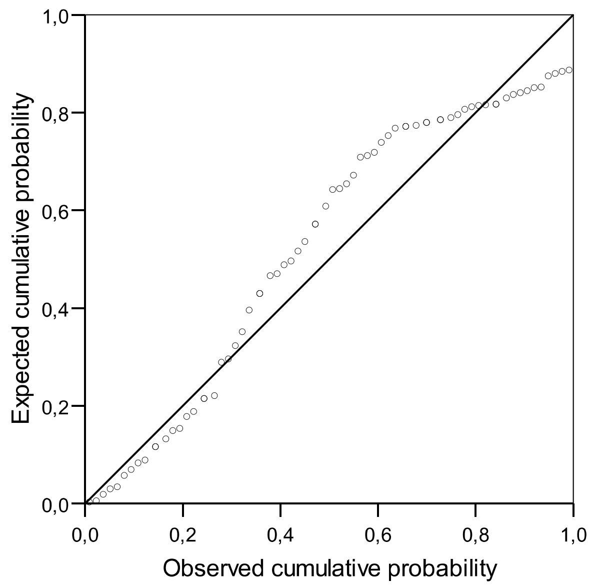

Figure B.25: Normal P-P plot (experimental vs. theoretical CDF).

Steel grade S500 NR SD - All bar diameters. Correlations.

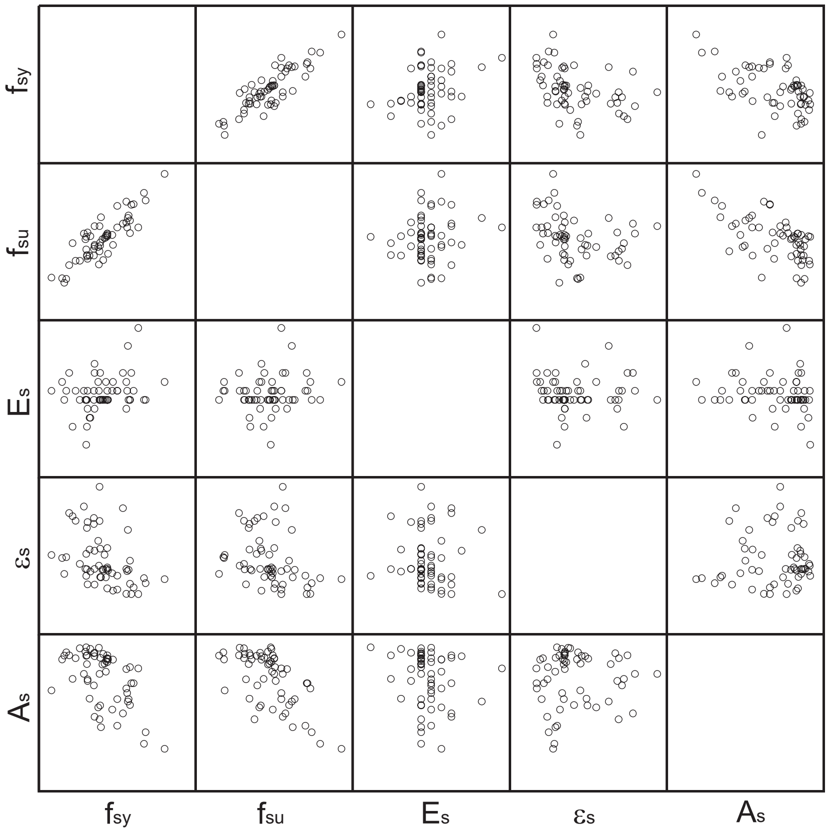

Figure B.26: Correlation matrix.

B.3 Conclusions

The analysis of results of statistical evaluation of data regarding properties of reinforcing steel bars, presented in previous section, leads to the following conclusions:

- The mean value of the yield strength of tested reinforcing steels is significantly higher than the expected value defining the steel grade. The bias factor relating the mean with the characteristic value of this steel property is oscillating between 1.16–1.21. The characteristic value is defined as a quantile of 5%.
- The variation of results obtained during the tensile test for each steel grade is quite small. The coefficient of variation of steel yield strength oscillates between 5.5–6.0%.
- The mean value of the ultimate strength is also higher than the expected value. The bias factor relating the mean with the characteristic value of this steel property is equal to 1.28 and 1.20 for steel of normal and special ductility respectively. The characteristic value is defined as a quantile of 5% and 10% for steels of normal and special ductility respectively.
- The observed variability of ultimate tensile strength is slightly smaller than the variability of yield strength. The coefficient of variation of this steel property oscillates between 4.9–5.9%.
- The mean value of the ratio ultimate/yield strength for normal and special ductility steel bars is 1.17 and 1.20 respectively.
- The corresponding coefficients of variation are 3.3% and 2.8% respectively for steels of normal and special ductility.
- The mean value of the elasticity modulus of tested reinforcing bars is higher than the expected value and takes values between 201 GPa and 205 GPa.
- The variation of results regarding elasticity modulus obtained during the tests is relatively small. The corresponding coefficient of variation lays between 1.0–4.9%.

- The mean value of strain at the ultimate load takes values 13.5% and 13.1% for steels of normal and special ductility respectively.
- The coefficient of variation, describing variability of the ultimate strain of tested reinforcing bars is relatively high and takes values between 19.2–24.5%.
- The mean value of the ratio real/nominal cross-sectional area of tested bars oscillates between 0.92–0.94.
- The coefficient of variation of the ratio real/nominal area of tested bars is oscillating between 4.3–4.4%
- All the analysed properties of reinforcing steel bars fits well to the normal or lognormal distribution functions. The exception is the ultimate strain, elasticity modulus and in some cases real/nominal bar area. However they also can be reasonably well approximated by normal or lognormal distribution.
- The correlations between the steel properties are visible only for the yield strength and the ultimate strength. This allows to define close form relation between these properties.
- The correlations between other steel properties are negleglible.

Appendix C

Variability of the properties of prestressing strands

C.1 Introduction

In this appendix the results of statistical evaluation of data from standard quality test of prestressing steel strands are presented. The data used in the statistical analysis was collected by the Department of Civil Engineering of the University of Coimbra during several years (2000–2006) corresponding mostly to the construction of The Europe Bridge but also to some other bridges in the neighbourhood of Coimbra. The collected data represents the properties of prestressing strands of several producers and producing units, several batches and several rolls from the same batch. The tests were performed in the Laboratory of Testing of Materials and Structures of University of Coimbra according to the current standards (ASTM A416/A416m-99 Standard specification for Steel Strand, Uncoated Seven-Wire for Prestressed Concrete; EN10138-3 Prestressing Steels, Part 3, Strand; E453-2002 Cordões de aço para pré-esforço, caracteristìcas e ensaios.)

C.2 Experimental data

The following section resumes results of statistical evaluation of data performed regarding prestressing strands of 1770 and 1860 grade and diameters of 16 mm and

15.2 mm. The analysed characteristic parameters are: stress at 0.1% offset, $f_{p0.1}$, stress corresponding to total strain of 1%, ultimate tensile strength f_{pu}, modulus of elasticity E_p, ultimate strain ϵ_{pu} and cross-sectional area A_p. In Tables C.1, C.3 and C.5 the minimum value X_{min}, maximum value X_{max}, mean value X_{mean}, and coefficient of variation CV of above mentioned characteristic parameters are presented. Furthermore, the numbers of samples N_{sampl} used in the statistical analysis are showed.

The skewness and kurtosis of the distribution of analysed data are presented in Tables C.2, C.4 and C.6. Skewness characterizes the degree of asymmetry of a distribution around its mean (positive/negative skewness - distribution with an asymmetric tail extending toward more positive/negative values). Kurtosis characterizes the relative peakedness or flatness of a distribution compared with the normal distribution (positive/negative kurtosis - relatively peaked/flat distribution). Moreover, in Tables C.2, C.4 and C.6 the results of K-S Lilliefors goodness-of-fit test are showed. The parameters presented in tables are the significance interval for accepting or rejecting the null hypothesis saying that the observed distribution is not significantly different from a theoretical, normal or lognormal distribution (significance interval bigger than 0.05 means that the null hypothesis can not be rejected). In the last column of Tables C.2, C.4 and C.6 the correlation coefficient between several properties of prestressing strands and theirs ultimate tensile strength is also showed. The correlation coefficient is a dimensionless index, ranging from -1 to 1, that reflects the extent of a linear relationship between two parameters (-1/1 represent perfect negative/positive correlation, 0 represents lack of correlation).

Besides the K-S Lilliefors goodness-of-fit test the choice of the appropriate probability distribution function describing the best the strands properties was also confirmed by the histograms and P-P plots presented also in this section in Figures C.1–C.12, C.14–C.25 and C.27–C.38. Histograms show the frequency of occurrence of the results in specified intervals. P-P plots show the correspondence of the experimental results to the theoretical distribution function. The correlation plots showing correlations between various strands properties are showed in Figures C.13, C.26 and C.39

Properties of prestressing strands. Grade 1770 - Diameter 16.0 mm.

Table C.1: Basic statistics of the properties of prestressing strands.

Steel Property	Numb. N_{sampl}	Min. val. X_{min}	Max. val. X_{max}	Mean val. X_{mean}	COV CV
0.1% proof stress $f_{p0.1}$	90	1499 MPa	1628 MPa	1556 MPa	1.7 %
1% proof stress f_{py}	90	1508 MPa	1650 MPa	1592 MPa	1.7 %
Ultimate strength f_{pu}	90	1738 MPa	1842 MPa	1800 MPa	1.2 %
Elasticity modulus E_p	90	180 GPa	202 GPa	195 GPa	2.0 %
Ultimate strain ϵ_p	90	3.07 %	5.20 %	4.15 %	8.7 %
Area A_p	90	149 mm^2	153 mm^2	151 mm^2	0.4 %

Note: All the stresses were calculated from forces registered by the testing machine considering the real area of strand determined based on measured specimen weight

Table C.2: Distribution characteristics, goodness-of-fit test and correlations

Steel Property	Skew-ness	Kur-tosis	K-S test of normal.	K-S test of log-norm.	Correlation with f_{pu}
0.1% proof stress $f_{p0.1}$	0.42	-0.19	0.5953	0.6188	0.5681
1% proof stress f_{py}	-0.24	0.11	0.9392	0.9631	0.6389
Ultimate strength f_{pu}	-0.57	0.19	0.7397	0.7153	1.0000
Elasticity modulus E_p	-0.89	1.57	0.3326	0.2884	0.1522
Ultimate strain ϵ_p	0.45	1.20	0.0064	0.0191	0.0334
Area A_p	1.07	2.79	0.0377	0.0393	-0.1177

Steel grade 1770 - Strands diameter 16.0 mm. 0.1% proof stress.

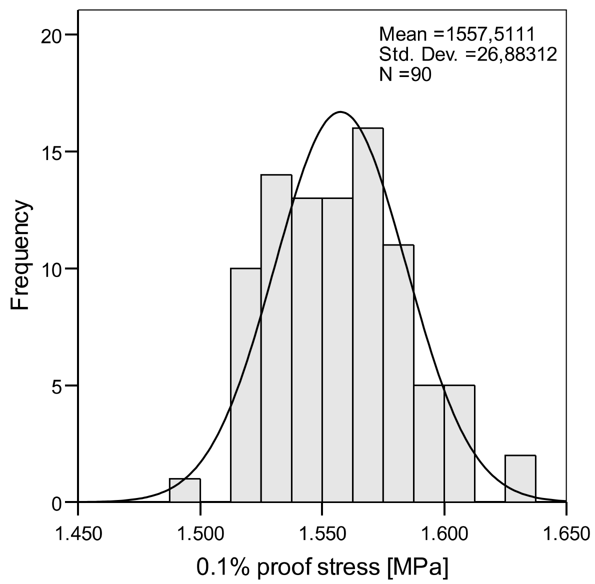

Figure C.1: Histogram of experimental data and Normal PDF.

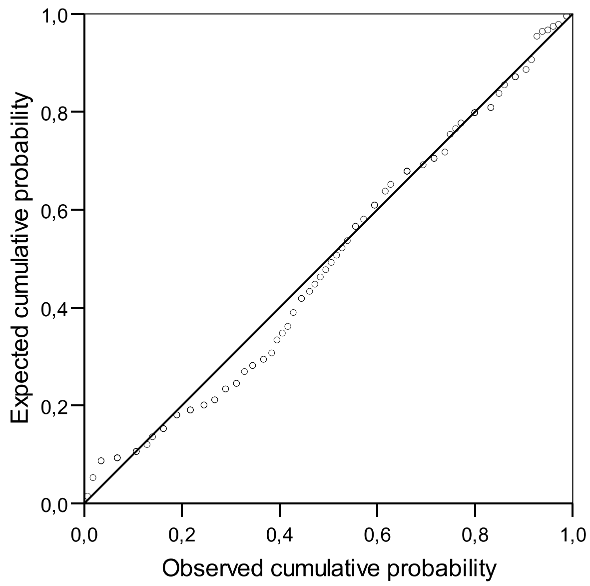

Figure C.2: Normal P-P plot (experimental vs. theoretical CDF).

Steel grade 1770 - Strands diameter 16.0 mm. 1% proof stress.

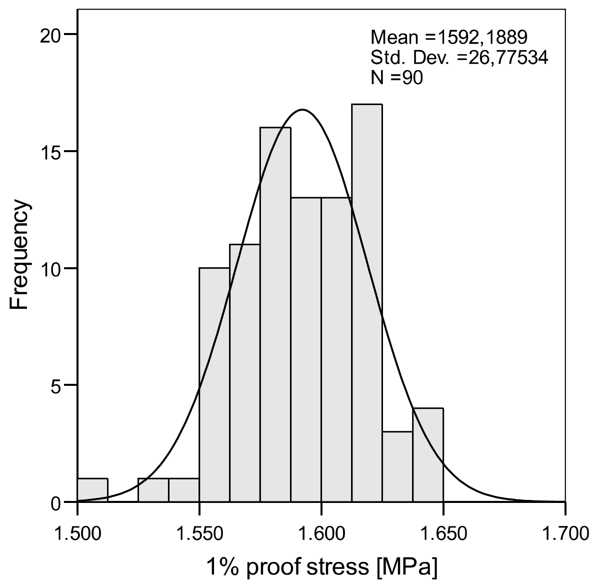

Figure C.3: Histogram of experimental data and Normal PDF.

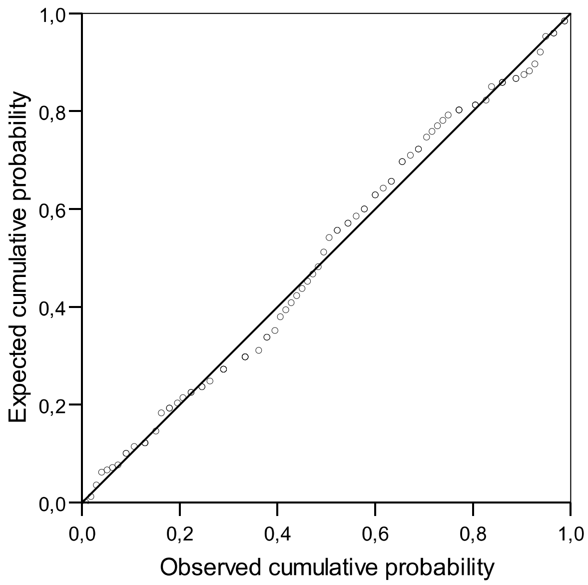

Figure C.4: Normal P-P plot (experimental vs. theoretical CDF).

Steel grade 1770 - Strands diameter 16.0 mm. Ultimate strength.

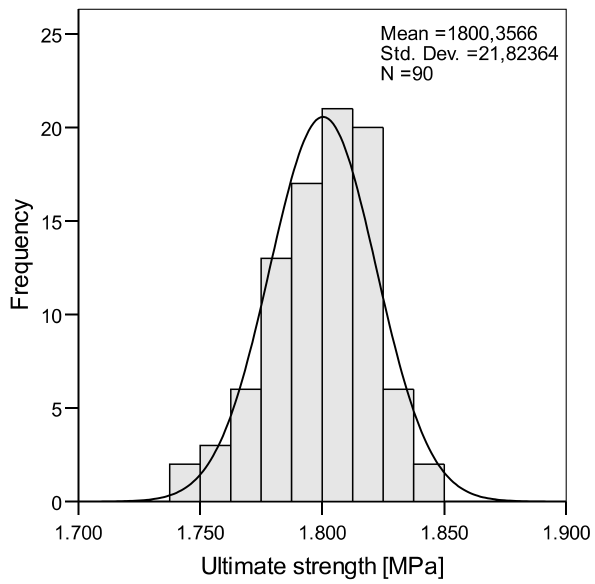

Figure C.5: Histogram of experimental data and Normal PDF.

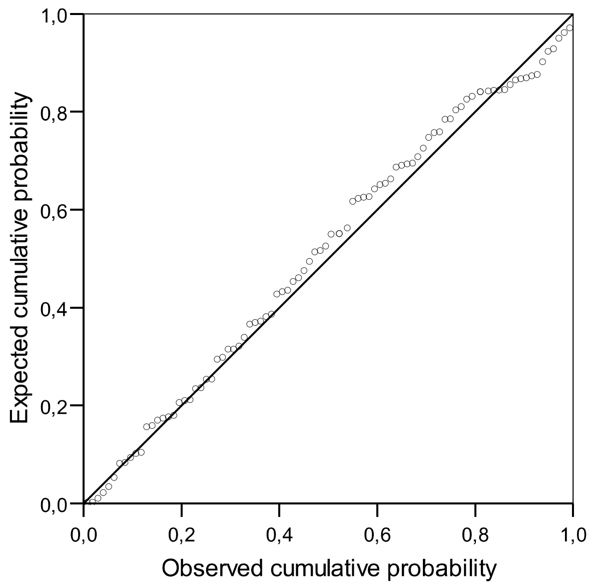

Figure C.6: Normal P-P plot (experimental vs. theoretical CDF).

Steel grade 1770 - Strands diameter 16.0 mm. Elasticity modulus.

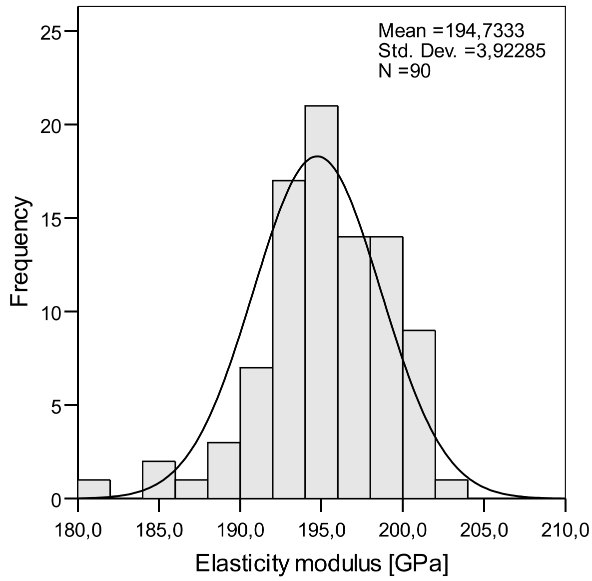

Figure C.7: Histogram of experimental data and Normal PDF.

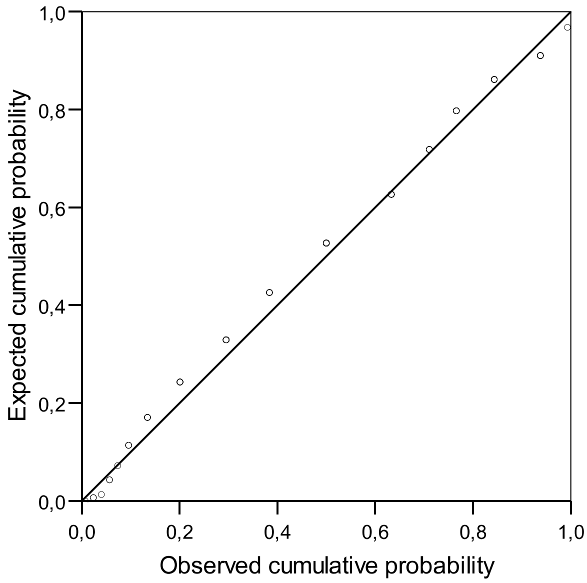

Figure C.8: Normal P-P plot (experimental vs. theoretical CDF).

Steel grade 1770 - Strands diameter 16.0 mm. Ultimate strain.

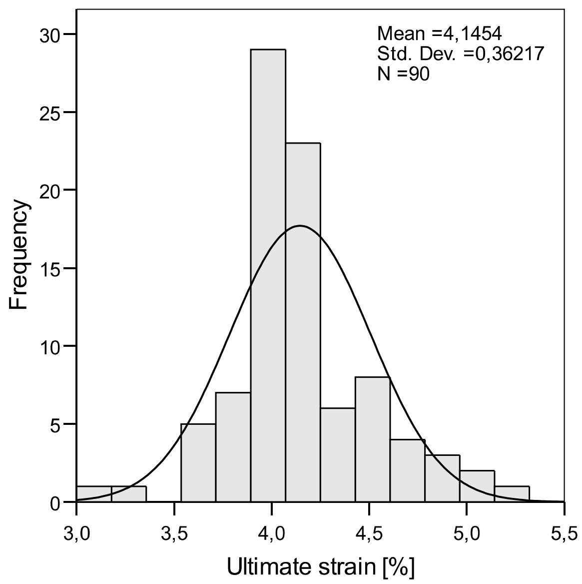

Figure C.9: Histogram of experimental data and Normal PDF.

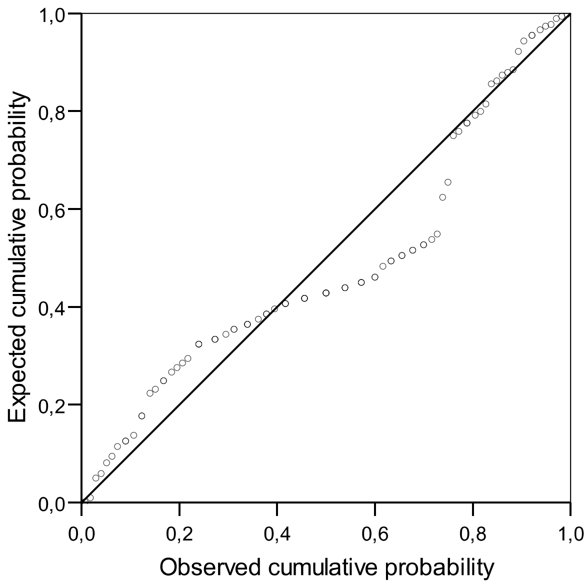

Figure C.10: Normal P-P plot (experimental vs. theoretical CDF).

Steel grade 1770 - Strands diameter 16.0 mm. Cross-sectional area.

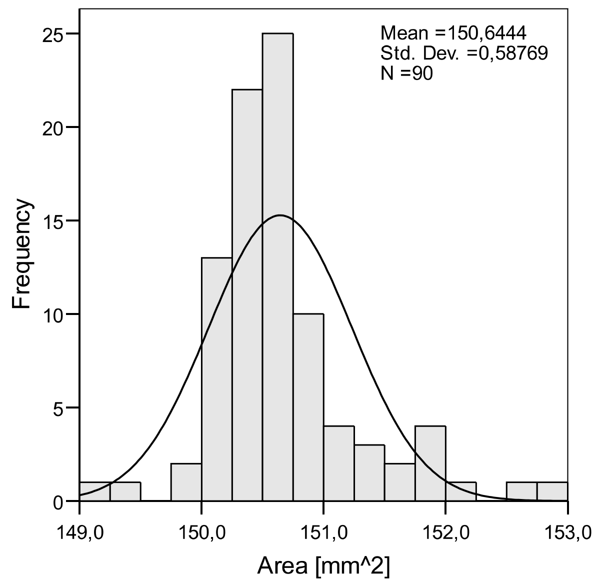

Figure C.11: Histogram of experimental data and Normal PDF.

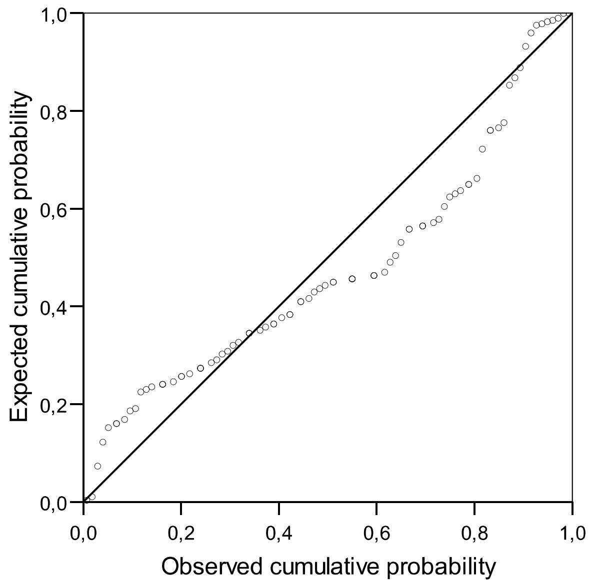

Figure C.12: Normal P-P plot (experimental vs. theoretical CDF).

Steel grade 1770 - Strands diameter 16.0 mm. Correlations.

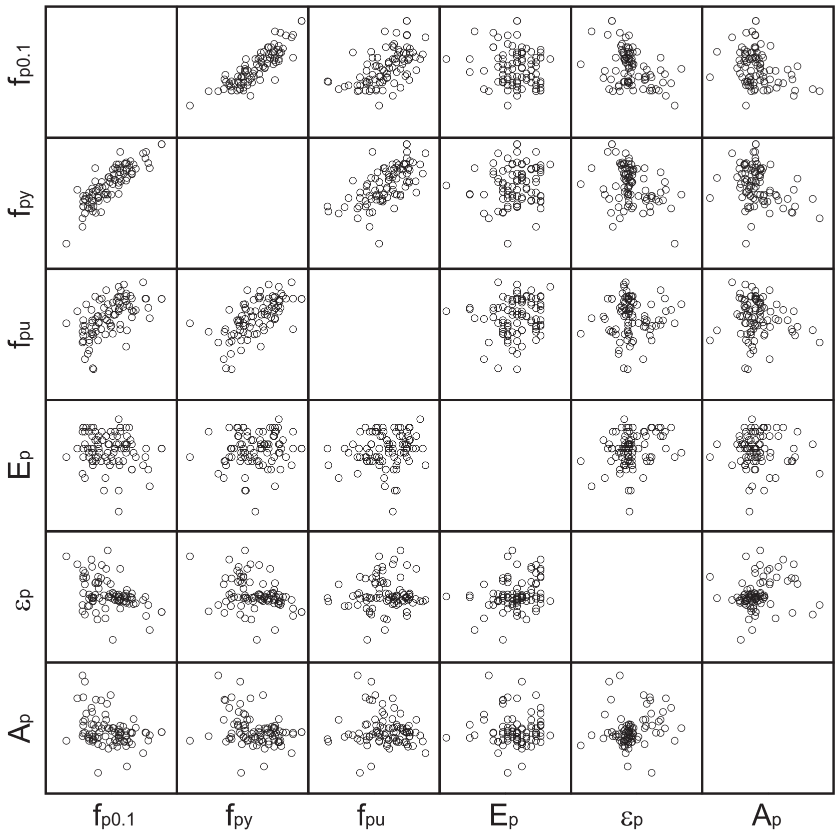

Figure C.13: Correlation matrix.

Properties of prestressing strands. Grade 1860 - Diameter 15.2 mm.

Table C.3: Basic statistics of the properties of prestressing strands.

Steel Property	Numb. N_{sampl}	Min. val. X_{min}	Max. val. X_{max}	Mean val. X_{mean}	COV CV
0.1% proof stress $f_{p0.1}$	35	1634 MPa	1800 MPa	1718 MPa	2.3 %
1% proof stress f_{py}	140	1590 MPa	1902 MPa	1741 MPa	2.9 %
Ultimate strength f_{pu}	140	1849 MPa	2045 MPa	1934 MPa	2.2 %
Elasticity modulus E_p	140	186 GPa	214 GPa	199 GPa	2.1 %
Ultimate strain ϵ_p	140	2.85 %	6.41 %	3.99 %	13.8 %
Area A_p	140	135 mm^2	144 mm^2	140 mm^2	1.3 %

Note: All the stresses were calculated from forces registered by the testing machine considering the real area of strand determined based on measured specimen weight

Table C.4: Distribution characteristics, goodness-of-fit test and correlations

Steel Property	Skew-ness	Kur-tosis	K-S test of normal.	K-S test of log-norm.	Correlation with f_{pu}
0.1% proof stress $f_{p0.1}$	0.05	-0.18	1.0000	1.0000	0.7692
1% proof stress f_{py}	0.19	0.53	0.9896	0.9778	0.7306
Ultimate strength f_{pu}	0.35	-0.54	0.2543	0.2741	1.0000
Elasticity modulus E_p	0.42	1.58	0.0658	0.0861	-0.0843
Ultimate strain ϵ_p	0.86	2.32	0.1000	0.3293	-0.1338
Area A_p	-0.62	0.57	0.0194	0.0161	-0.5408

Steel grade 1860 - Strands diameter 15.2 mm. 0.1% proof stress.

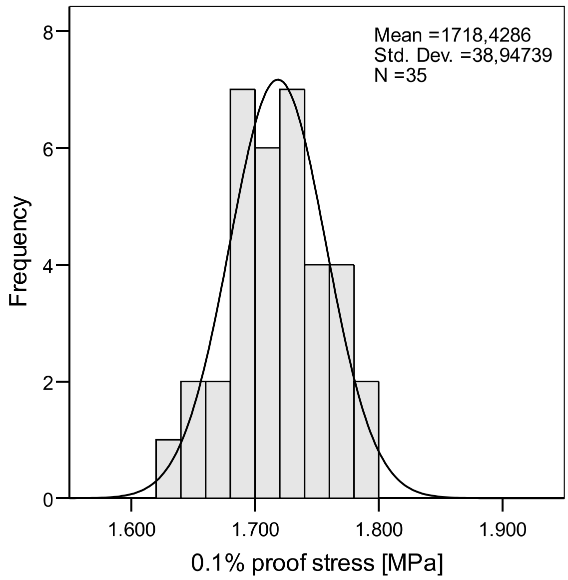

Figure C.14: Histogram of experimental data and Normal PDF.

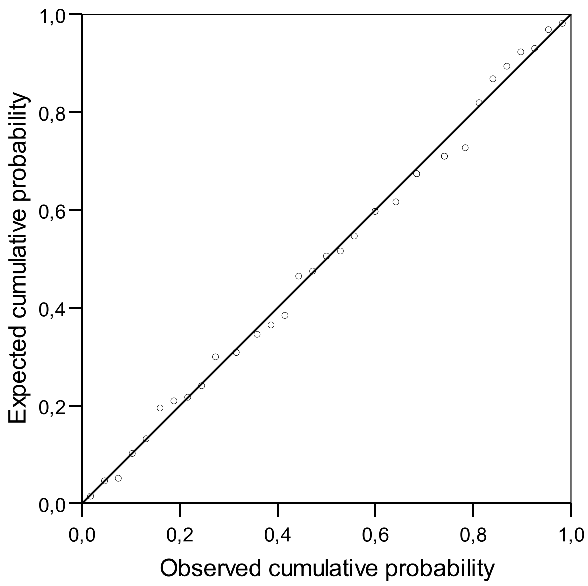

Figure C.15: Normal P-P plot (experimental vs. theoretical CDF).

Steel grade 1860 - Strands diameter 15.2 mm. 1% proof stress.

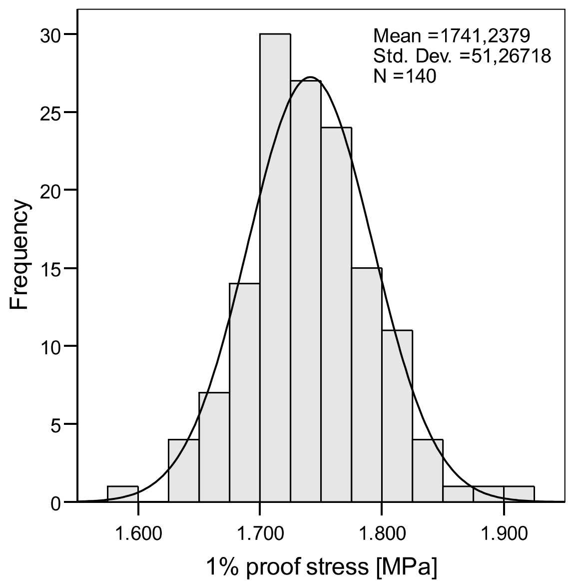

Figure C.16: Histogram of experimental data and Normal PDF.

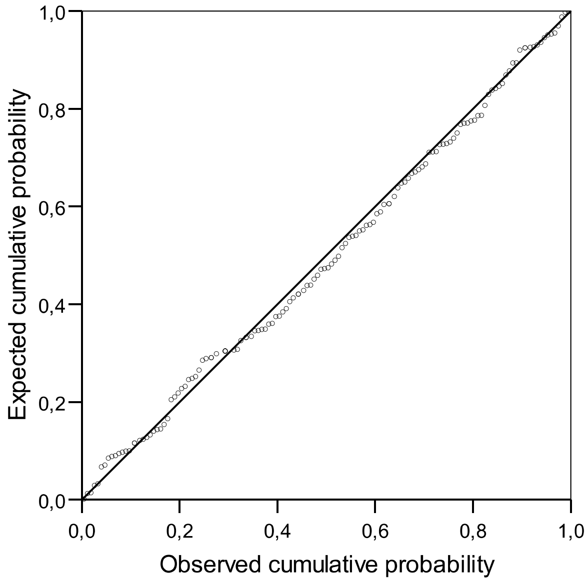

Figure C.17: Normal P-P plot (experimental vs. theoretical CDF).

Steel grade 1860 - Strands diameter 15.2 mm. Ultimate strength.

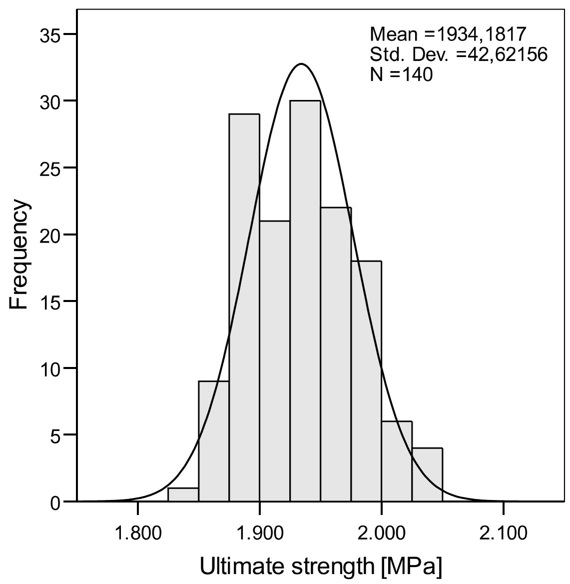

Figure C.18: Histogram of experimental data and Normal PDF.

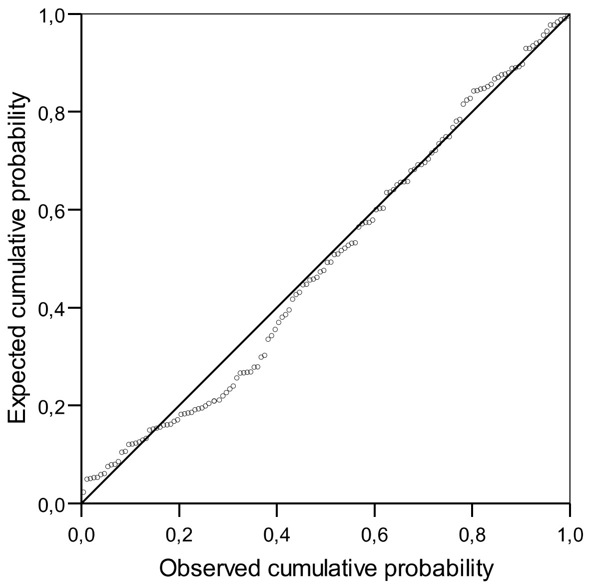

Figure C.19: Normal P-P plot (experimental vs. theoretical CDF).

Steel grade 1860 - Strands diameter 15.2 mm. Elasticity modulus.

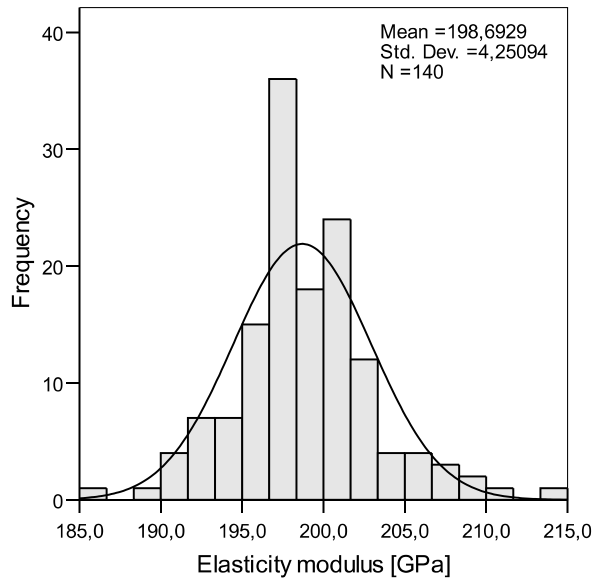

Figure C.20: Histogram of experimental data and Normal PDF.

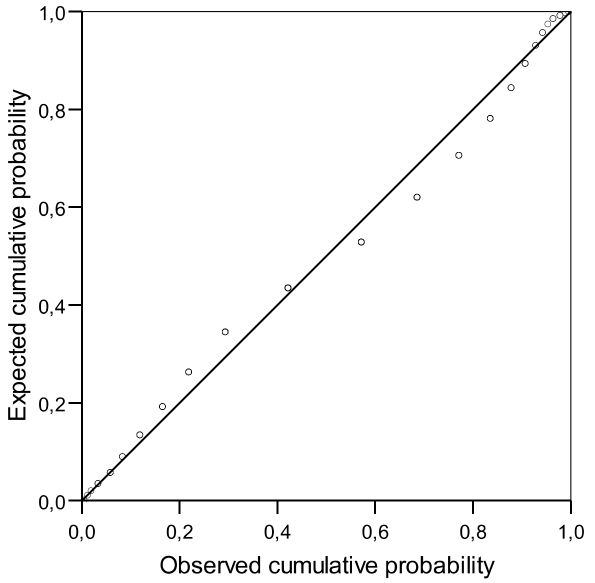

Figure C.21: Normal P-P plot (experimental vs. theoretical CDF).

Steel grade 1860 - Strands diameter 15.2 mm. Ultimate strain.

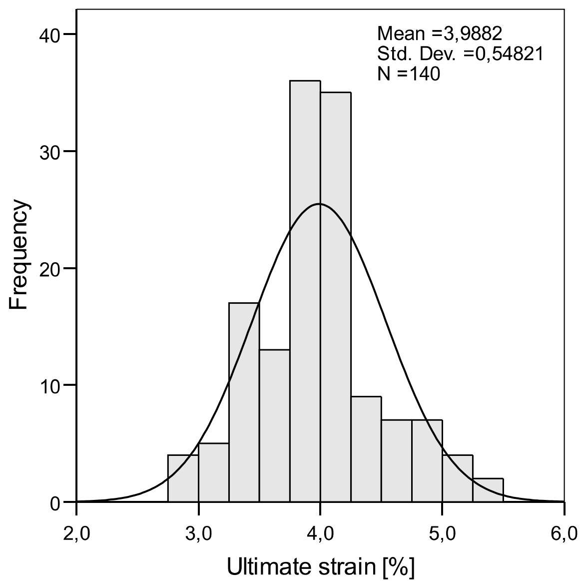

Figure C.22: Histogram of experimental data and Normal PDF.

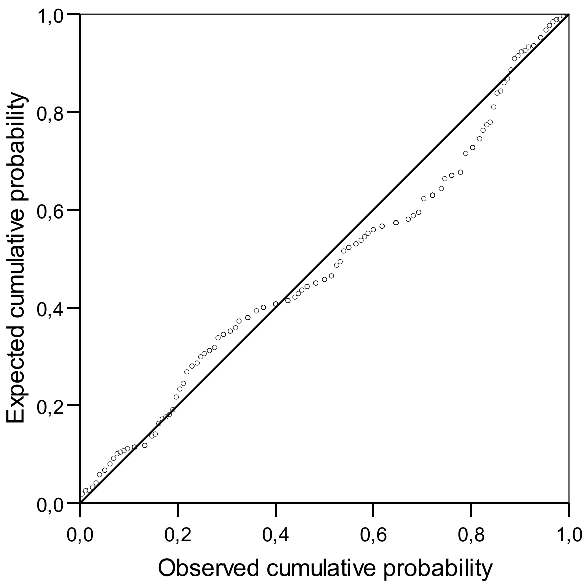

Figure C.23: Normal P-P plot (experimental vs. theoretical CDF).

Steel grade 1860 - Strands diameter 15.2 mm. Cross-sectional area.

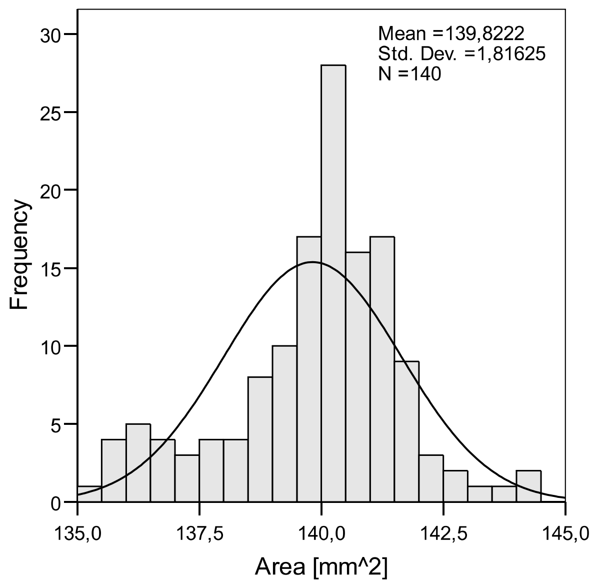

Figure C.24: Histogram of experimental data and Normal PDF.

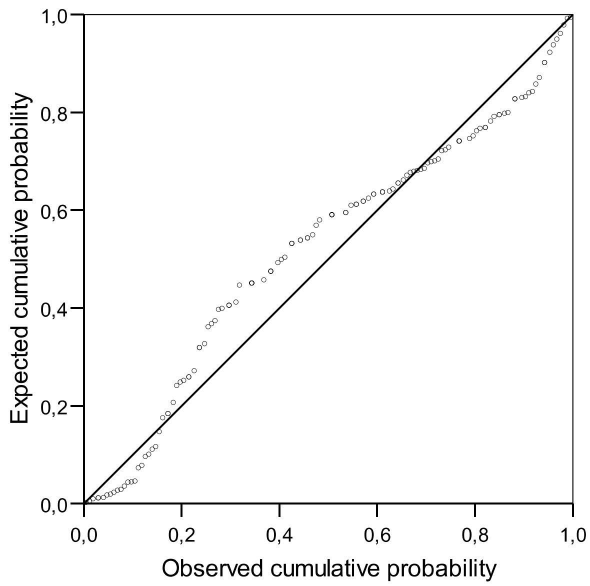

Figure C.25: Normal P-P plot (experimental vs. theoretical CDF).

Steel grade 1860 - Strands diameter 15.2 mm. Correlations.

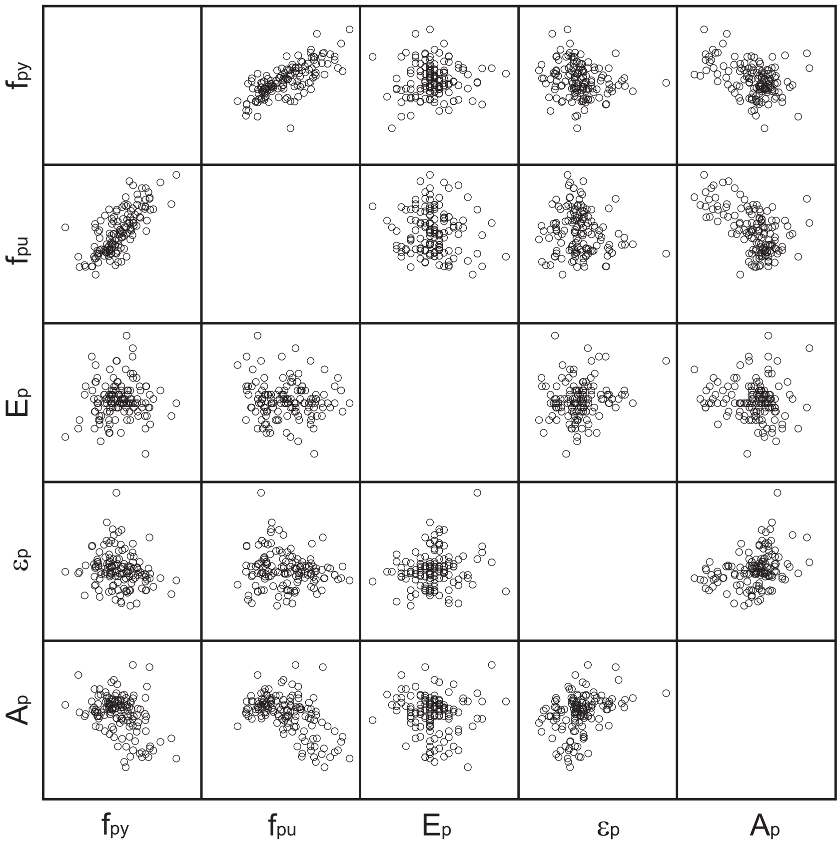

Figure C.26: Correlation matrix.

Properties of prestressing strands. Grade 1860 - Diameter 16.0 mm.

Table C.5: Basic statistics of the properties of prestressing strands.

Steel Property	Numb. N_{sampl}	Min. val. X_{min}	Max. val. X_{max}	Mean val. X_{mean}	COV CV
0.1% proof stress $f_{p0.1}$	21	1601 MPa	1790 MPa	1697 MPa	3.1 %
1% proof stress f_{py}	178	1617 MPa	1853 MPa	1728 MPa	2.6 %
Ultimate strength f_{pu}	178	1803 MPa	2051 MPa	1925 MPa	2.3 %
Elasticity modulus E_p	178	186 GPa	206 GPa	198 GPa	1.7 %
Ultimate strain ϵ_p	178	2.73 %	5.38 %	3.84 %	10.5 %
Area A_p	178	144 mm^2	155 mm^2	150 mm^2	1.3 %

Note: All the stresses were calculated from forces registered by the testing machine considering the real area of strand determined based on measured specimen weight

Table C.6: Distribution characteristics, goodness-of-fit test and correlations

Steel Property	Skew-ness	Kur-tosis	K-S test of normal.	K-S test of log-norm.	Correlation with f_{pu}
0.1% proof stress $f_{p0.1}$	0.12	-0.77	0.9773	0.9847	0.8103
1% proof stress f_{py}	0.12	0.16	0.7800	0.7713	0.7780
Ultimate strength f_{pu}	0.14	-0.15	0.8617	0.8402	1.0000
Elasticity modulus E_p	-0.63	0.78	0.0332	0.0240	0.2412
Ultimate strain ϵ_p	-0.07	2.59	0.0000	0.0000	0.2233
Area A_p	-0.22	0.35	0.8724	0.8251	-0.5681

Steel grade 1860 - Strands diameter 16.0 mm. 0.1% proof stress.

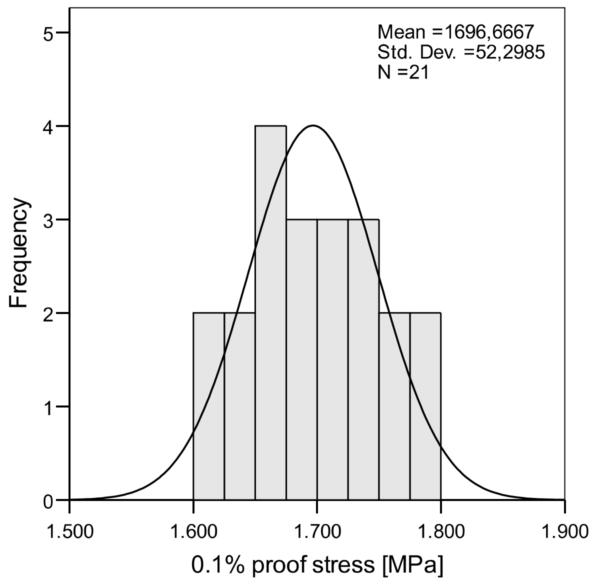

Figure C.27: Histogram of experimental data and Normal PDF.

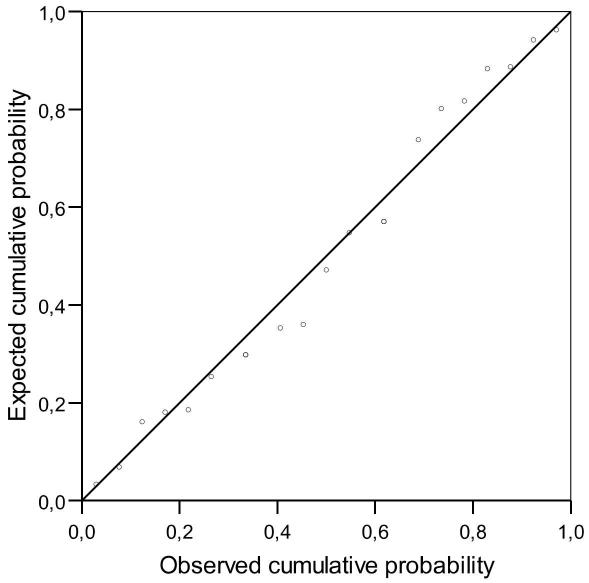

Figure C.28: Normal P-P plot (experimental vs. theoretical CDF).

Steel grade 1860 - Strands diameter 16.0 mm. 1% proof stress.

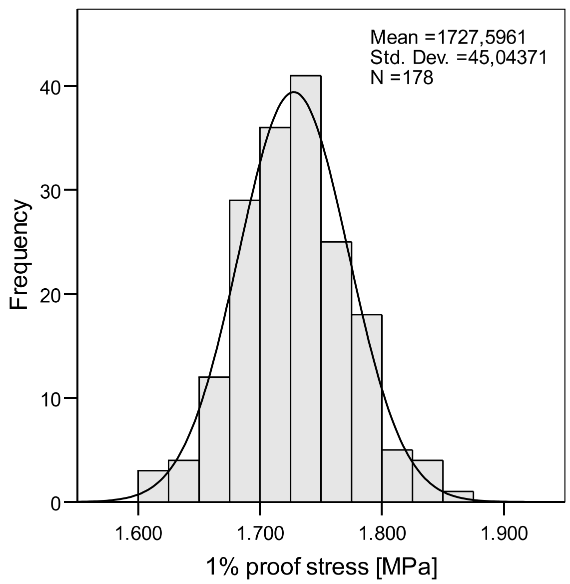

Figure C.29: Histogram of experimental data and Normal PDF.

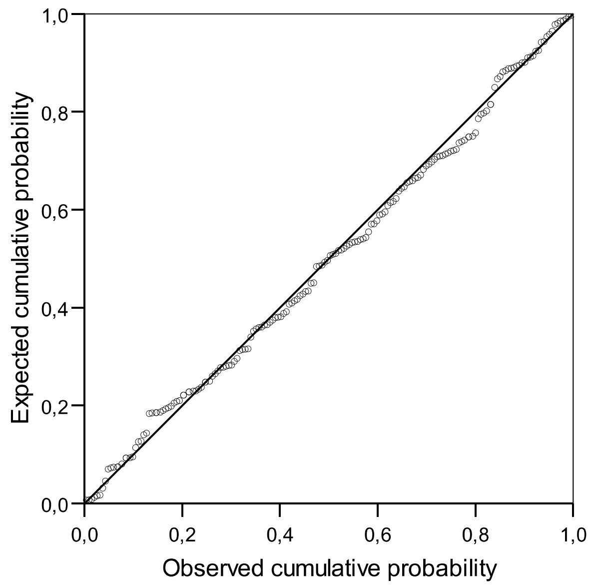

Figure C.30: Normal P-P plot (experimental vs. theoretical CDF).

Steel grade 1860 - Strands diameter 16.0 mm. Ultimate strength.

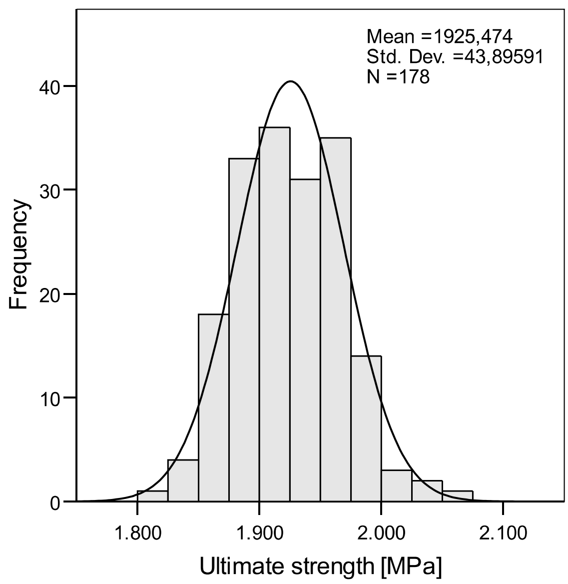

Figure C.31: Histogram of experimental data and Normal PDF.

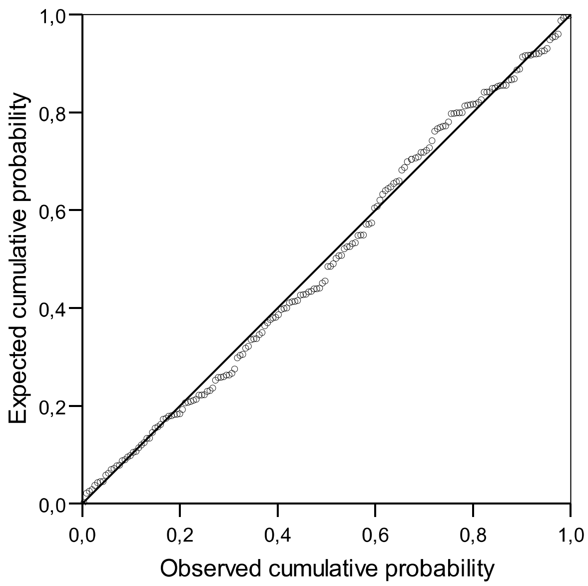

Figure C.32: Normal P-P plot (experimental vs. theoretical CDF).

Steel grade 1860 - Strands diameter 16.0 mm. Elasticity modulus.

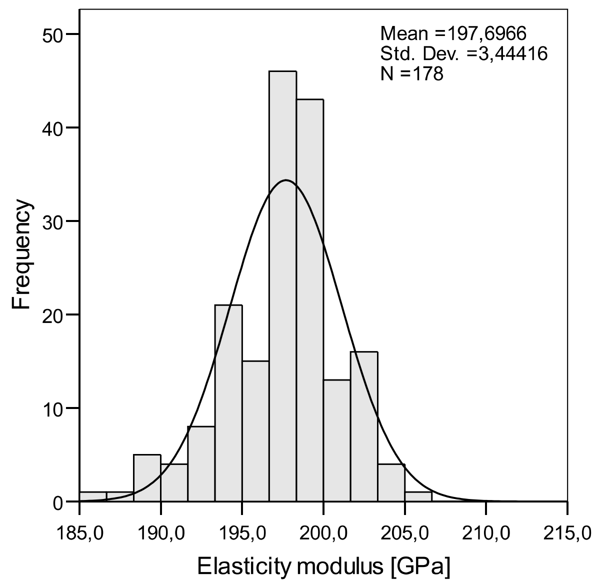

Figure C.33: Histogram of experimental data and Normal PDF.

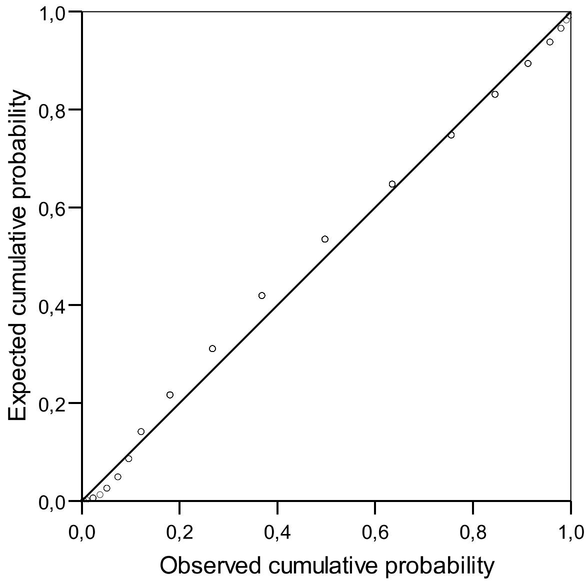

Figure C.34: Normal P-P plot (experimental vs. theoretical CDF).

Steel grade 1860 - Strands diameter 16.0 mm. Ultimate strain.

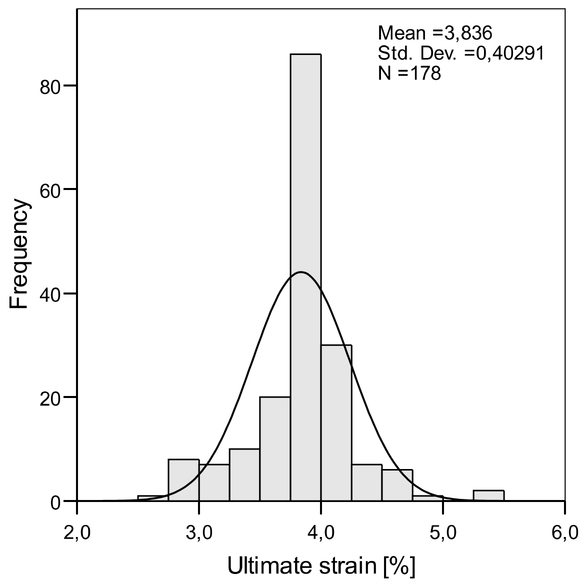

Figure C.35: Histogram of experimental data and Normal PDF.

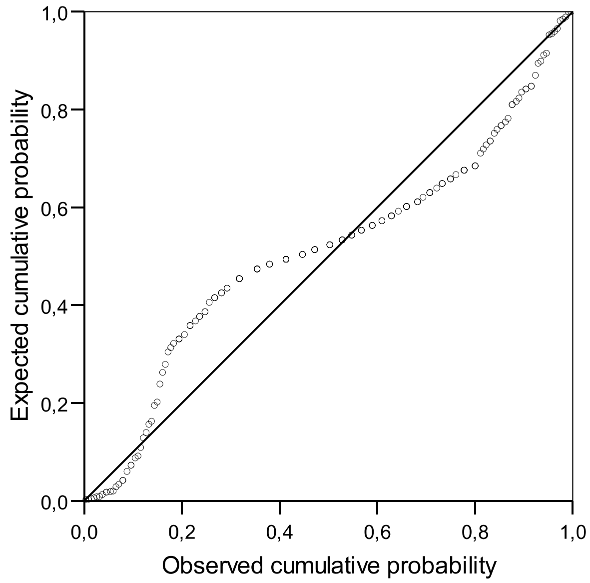

Figure C.36: Normal P-P plot (experimental vs. theoretical CDF).

Steel grade 1860 - Strands diameter 16.0 mm. Cross-sectional area.

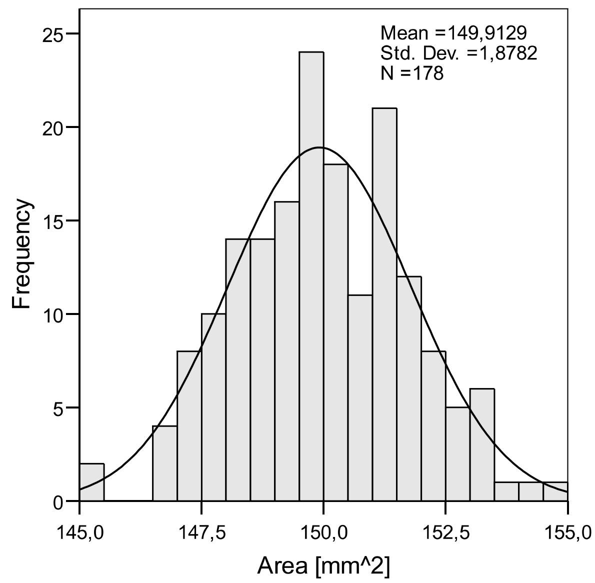

Figure C.37: Histogram of experimental data and Normal PDF.

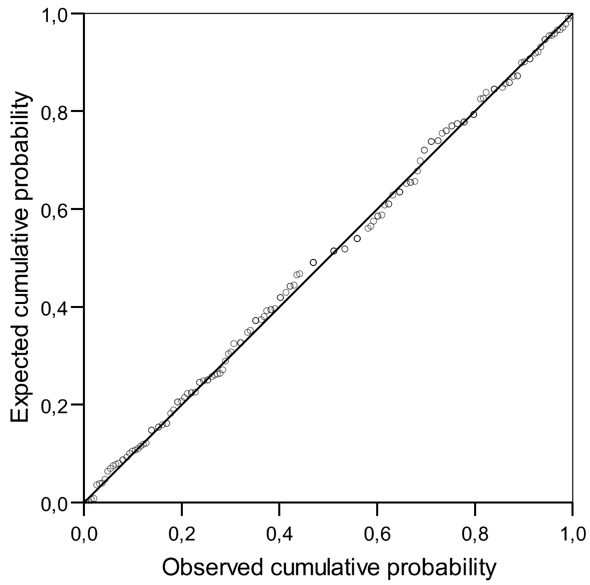

Figure C.38: Normal P-P plot (experimental vs. theoretical CDF).

Steel grade 1860 - Strands diameter 16.0 mm. Correlations.

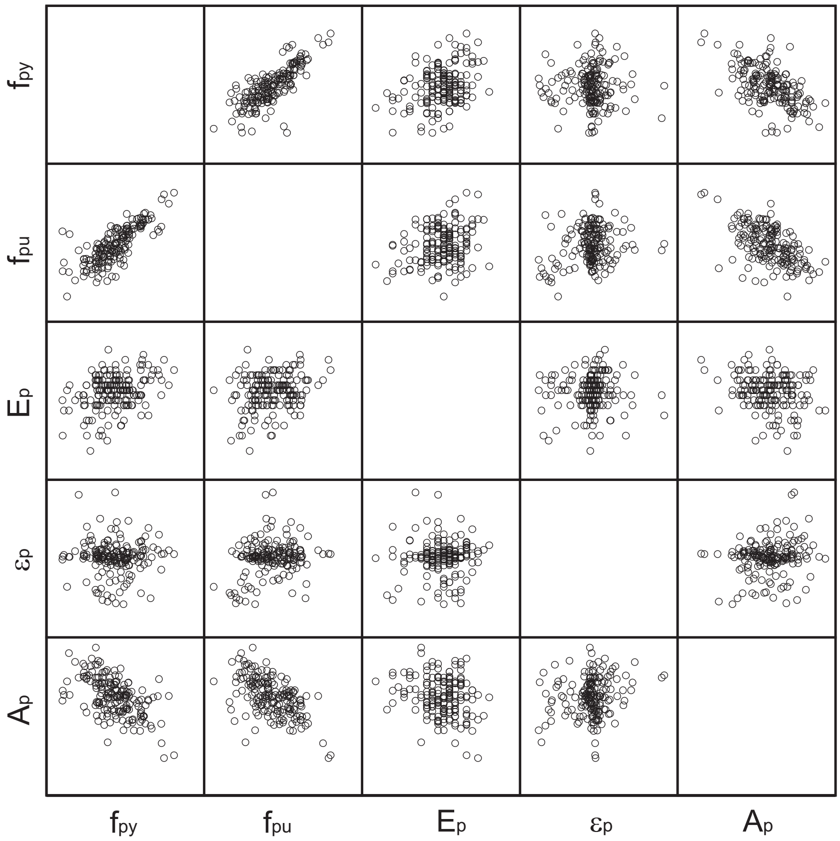

Figure C.39: Correlation matrix.

C.3 Conclusions

The analysis of results of statistical evaluation of data regarding properties of common types prestressins strands, presented in previous section, leads to the following conclusions:

- The mean value of the ultimate tensile strength of tested prestressing steels is slightly higher than the expected value defining the steel grade. The bias factor relating the mean with the nominal value of this steel property is oscillating between 1.02–1.04.
- The variation of results obtained during the tensile test for each steel grade is very small. The coefficient of variation of ultimate tensile strength is always smaller than 2.5% and for the analysed data it oscilates between 1.2–2.3%.
- The mean value of the theoretical yielding limit defined as proof stress at 0.1% offset or stress corresponding to 1% total strain is also sligthly higher than the expeceted value.
- The observed variability of 0.1% and 1% proof stresses is also very small, however, it is bigger than the variability of ultimate tensile strength. The coefficients of variation of those steel properties oscilate between 1.7–3.1%.
- The mean value of the elasticity modulus of tested strands is higher than the expected value and depending on steel grade and diameter takes values between 195 GPa and 199 GPa.
- The variation of results regarding elasticity modulus obtained during the tests is very small. The corresponding coefficient of variation lays between 1.7–2.1%.
- The mean value of the ultimate strain takes values around 4%, more specifically 3.84–4.15%.
- The coefficient of variation, describing variability of the ultimate strain of tested prestressing strands is relatively high and takes values between 8.7–13.8%.

- The mean value of the cross-sectional area of tested strands is equal or almost equal to the expected.
- The coefficient of variation of the area of tested strands is oscillating between 0.4–1.3%
- All the analysed properties of prestressing strands fits well into the normal or lognormal distribution functions. The exception is the ultimate strain and in some cases the elasticity modulus and strand area. However they can also be reasonably well approximated by normal or lognormal distribution.
- The correlations between the steel properties are visible only for the stress parameters like 0.1% proof stress, 1% proof stress and ultimate tensile stress. This allows to define close form relation between those properties.
- The correlations between other steel properties are negleglible.

Appendix D

Tolerances in precast concrete bridge elements

D.1 Introduction

In this appendix the results of statistical analysis of data regarding dimensions of common precast prestressed bridge girders are presented. Some of the analysed data weas collected and made available for this study by the quality control division of one of the biggest precast concrete company in Portugal - Maprel. Other data was collected during the campaign of measurements performed at the starting period of this thesis on the casting plant of other Portuguese precast bridge girder producer - Civibral. The data provided by Maprel corresponds to all the company production of precast prestressed concrete U-shape bridge girders manufactured between November 2002 and September 2003. They were obtained during measurements performed for conformity purposes. For each manufactured beam just one section was measured. The data collected in Civibral corresponds to the randomly chosen precast prestressed concrete I-shape bridge girders elements manufactured during the spring of 2003. They were collected especially for the purpose of this study. The main objective was to check the variations in dimensions of the girder cross-section along girder's length and between several girders of the same type. Also the variation comparing to the nominal (projected) dimensions was studied. In this case several sections along the length of ten randomly selected beams were measured.

D.2 Experimental data

The following section resumes results of statistical evaluation of data performed. In Tables D.1–D.4, D.6 and D.7 the minimum value X_{min}, maximum value X_{max}, mean value X_{mean}, and standard deviations σ_X of dimensions of various types of precast bridge girders (see Figures D.1 and D.2) are presented. Furthermore, the numbers of samples N_{sampl} are showed. In Tables D.6 and D.7 for each girder dimension two set of measurements can be found. First corresponds to the measurements performed on several cross-section of selected beam, second corresponds to all measurements performed on all the beams. Moreover, in Tables D.5 and D.8 the results corresponding to all girders height are resumed. In order to be comparable X_{min}, X_{max} and X_{mean}, are presented as dimensionless factors of measured to nominal value. CV_λ is the coefficient of variation.

Dimensions of precast bridge girders. U-shape - Maprel.

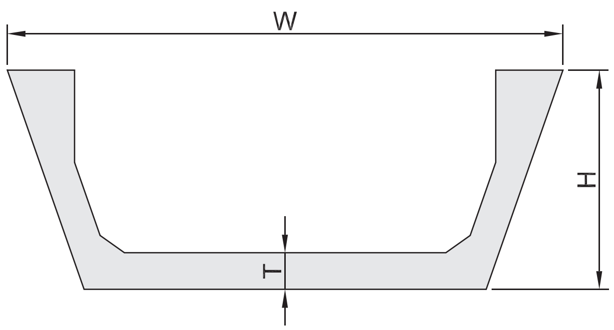

Figure D.1: Cross-section of the girder.

Table D.1: Basic statistics of the dimensions of precast girders U90.

Girder dimen.	Numb. N_{sampl}	Nom. val X_{nom}	Min. val. X_{min}	Max. val. X_{max}	Mean val. X_{mean}	St. dev. σ_X
H	7	900	890	910	915	6.9
W	7	2820	2820	2830	2826	5.3
T	7	200	200	210	206	5.3

All parameters except N_{sampl} are in [mm].

Table D.2: Basic statistics of the dimensions of precast girders U120.

Girder dimen.	Numb. N_{sampl}	Nom. val X_{nom}	Min. val. X_{min}	Max. val. X_{max}	Mean val. X_{mean}	St. dev. σ_X
H	8	1200	1210	1220	1214	5.2
W	8	3058	3057	3058	3057	0.5
T	8	200	200	220	211	6.4

All parameters except N_{sampl} are in [mm].

Table D.3: Basic statistics of the dimensions of precast girders U160.

Girder dimen.	Numb. N_{sampl}	Nom. val X_{nom}	Min. val. X_{min}	Max. val. X_{max}	Mean val. X_{mean}	St. dev. σ_X
H	14	1600	1610	1620	1618	4.3
W	14	3320	3320	3320	3320	0.0
T	14	200	200	230	217	9.1

All parameters except N_{sampl} are in [mm].

Table D.4: Basic statistics of the dimensions of precast girders U190.

Girder dimen.	Numb. N_{sampl}	Nom. val X_{nom}	Min. val. X_{min}	Max. val. X_{max}	Mean val. X_{mean}	St. dev. σ_X
H	8	1900	1910	1920	1914	5.0
W	8	3530	3510	3530	3520	8.0
T	8	200	200	250	222	14.1

All parameters except N_{sampl} are in [mm].

Table D.5: Basic statistics of the dimensions of precast U-shape girders.

Girder dimen.	Numb. N_{sampl}	Nom. range X_{nom} [mm]	Min. val. λ_{min}	Max. val. λ_{max}	Mean val. λ_{mean}	Var. coef. CV_λ [%]
H	55	900-1900	0.989	1.017	1.008	0.55
W	55	2800-3500	0.994	1.003	0.999	0.20
T	55	200	1.000	1.250	1.061	4.69

Dimensions of precast bridge girders. I-shape - Civibral.

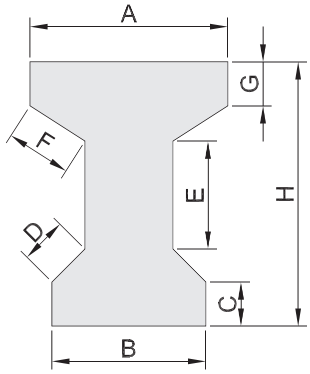

Figure D.2: Cross-section of the girder.

Table D.6: Basic statistics of the dimensions of precast girders I60.

Girder dimen.	Numb. N_{sampl}	Nom. val X_{nom}	Min. val. X_{min}	Max. val. X_{max}	Mean val. X_{mean}	St. dev. σ_X
A	$15^{(a)}$	450	445	455	451.1	2.6
	$75^{(b)}$	450	445	459	451.3	2.5
B	$10^{(a)}$	350	350	360	355.5	2.8
	$50^{(b)}$	350	350	360	354.6	3.3
C	$10^{(a)}$	100	100	105	101.5	2.4
	$50^{(b)}$	100	95	105	100.6	2.2
D	$9^{(a)}$	110	100	105	102.2	2.6
	$45^{(b)}$	110	100	105	101.7	2.4
E	$9^{(a)}$	260	240	245	243.9	2.2
	$45^{(b)}$	260	240	250	244.9	2.0
F	$9^{(a)}$	139	145	145	145.0	0.0
	$45^{(b)}$	139	140	145	143.6	2.3
G	$11^{(a)}$	100	100	105	101.4	2.1
	$55^{(b)}$	100	95	105	99.5	2.0
H	$15^{(a)}$	600	587	603	598.2	5.3
	$75^{(b)}$	600	583	608	599.0	4.2

Dimensions in [mm]; $^{(a)}$ corresponds to selected beam; $^{(b)}$ corresponds to all the beams.

Table D.7: Basic statistics of the dimensions of precast girders I120.

Girder dimen.	Numb. N_{sampl}	Nom. val X_{nom}	Min. val. X_{min}	Max. val. X_{max}	Mean val. X_{mean}	St. dev. σ_X
A	$15^{(a)}$	800	798	802	800.0	1.3
	$105^{(b)}$	800	796	804	800.4	1.6
B	$15^{(a)}$	440	440	450	442.6	3.1
	$78^{(b)}$	440	430	450	441.0	4.4
C	$15^{(a)}$	150	155	160	157.9	2.5
	$85^{(b)}$	150	155	160	158.0	2.4
D	$15^{(a)}$	160	158	160	159.9	0.5
	$75^{(b)}$	160	155	165	160.0	0.9
E	$15^{(a)}$	725	715	720	719.3	1.8
	$75^{(b)}$	725	715	725	719.0	2.3
F	$15^{(a)}$	335	330	335	332.0	2.5
	$75^{(b)}$	335	330	335	331.7	2.4
G	$15^{(a)}$	75	74	82	77.4	2.0
	$105^{(b)}$	75	70	82	76.3	2.0
H	$15^{(a)}$	1200	1206	1221	1211.2	4.2
	$105^{(b)}$	1200	1206	1226	1211.9	3.4

Dimensions in [mm]; $^{(a)}$ corresponds to selected beam; $^{(b)}$ corresponds to all the beams.

Table D.8: Basic statistics of the dimensions of precast I-shape girders.

Girder dimen.	Numb. N_{sampl}	Nom. range X_{nom} [mm]	Min. val. λ_{min}	Max. val. λ_{max}	Mean val. λ_{mean}	Var. coef. CV_λ [%]
A	180	450-800	0.989	1.020	1.002	0.56
B	128	350-440	0.977	1.029	1.007	0.95
C	135	100-150	0.950	1.067	1.036	2.10
D	120	110-160	0.909	1.031	0.972	2.23
E	120	260-725	0.923	1.000	0.973	0.79
F	120	139-335	0.985	1.043	1.006	1.64
G	160	75-100	0.933	1.093	1.009	1.98
H	180	600-1200	0.971	1.021	1.005	0.69

D.3 Conclusions

The analysis of results of statistical evaluation of data regarding dimensions of precast concrete bridge girders, presented in previous section, leads to the following conclusions:

- The mean values of the dimensions of precast bridge girders are usually slightly bigger than the expected. However, the observed difference is usually lower than 1% except the case of the thickness of U-shape girder's bottom slab, where the observed diference is around 6% and some dimmensions of I beams, where the difference is around 3%.
- The girder depth, the most important dimension from the point of view of the girder's capacity, is usually 0.5–0.8% bigger than expected. This correspond to 15–22 mm for the range of dimmensions considered.
- The coefficient of variation of precast concrete bridge girders' dimensions is on the level of 2% or lower which corresponds to the standard deviation lower than 2.5 mm. The exception is the case of the thickness of U-shape girders bottom slab, where it is on order of 5% which coressponds to 5–15 mm.
- The coefficient of variation of the girder's depth is lower than 1%. This correspond to the standard deviation of 3.5–5.0 mm for the range of dimmensions considered.